

Exploratory Photochemistry: Pushing the Boundaries of the
***p*-Hydroxyphenacyl Photoremovable Protecting Group**

By

Chamani Perera

Submitted to the Department of Chemistry and
the Faculty of the Graduate School of the University of Kansas
in partial fulfillment of the requirements for the degree of
Doctor of Philosophy

Richard S. Givens Chairperson

Robert G. Carlson Committee Member

David R. Benson Committee Member

Paul R. Hanson Committee Member

Jennifer S. Laurence Committee Member

Date defended:-----

The Dissertation Committee for Chamani Perera Certifies
That this is the approved version of the following dissertation:

**Exploratory Photochemistry: Pushing the Boundaries of the
p-Hydroxyphenacyl Photoremovable Protecting Group**

Richard S. Givens Chairperson

Date defended:-----

Abstract

Exploratory Photochemistry: Pushing the Boundaries of the *p*-Hydroxyphenacyl Photoremovable Protecting Group

- A. Exploratory and Mechanistic Photochemistry**
- B. Novel Applications of the *p*-Hydroxyphenacyl Photoremovable Protecting Group**

By

Chamani Perera, Ph.D.
Department of Chemistry, November 2009
University of Kansas

The *p*-hydroxyphenacyl (pHP) chromophore is an attractive addition to the family of photoremovable protecting groups in chemistry and biology. Substituent effects on the pHP moiety were explored using cyano substituent at *ortho* and *para* positions, employing GABA and acetate leaving groups. The quantum yield for GABA release from 3-cyano pHP GABA in water was substantially higher (0.42) than that for the parent.

Two novel applications of pHP photochemistry were demonstrated. A light sensitive release of a fluorophore from an almost non-fluorescent pHP fluorophore quencher ensembles resulted in regenerated fluorescence upon exposure to ultraviolet radiation. Carbazole as the quencher leaving group drove the photorelease toward an electron-transfer, radical mechanism. A second application demonstrated that fluorophilic pHP derivatives obtained by attaching a fluorous chain, could be employed to separate the products, often in 95-100% yield, after photorelease from the cage by using fluorous solid phase extraction and fluorous liquid-liquid extraction separation technology.

TO MY DAD

Acknowledgment

I owe my deepest gratitude to several people. Their help and inspiration greatly contributed to the successful completion of this work. First I would like to extend my most heartfelt appreciation to Dr. Givens. He is an exceptional teacher and a mentor. His encouragement, guidance and support led to my better understanding of the subject, while his kindness and thoughtfulness made my graduate life endurable. It is also a pleasure to extend my gratitude to the Givens family for their kind hospitality.

I gratefully acknowledge the members of my committee, Dr. R. Carlson, Dr. D. Benson Jr., Dr. P. Hanson and Dr. J. Lawrence, for their constructive comments and willingness to be on my committee in the midst of their busy schedules.

I would like to thank Todd Williams and Bob Drake for their help with UPLC analyses; Gerald Lushington for conducting computational studies; and David VanderVelde and Sarah Neuenswander for assistance with NMR analyses. I am also grateful to Victor Day for performing the crystallographic analyses.

It is a pleasure to thank past and present members of the Givens Group. The contributions of each individual to the group dynamics made the past several years an adventure.

Words fail me on how to express my appreciation to my family. I am forever indebted to them. I thank my brother and sister for their support and encouragement. The gratitude that I feel for my parents, (the late) Rev. Oswald Perera and Sita Perera, is immense. They have been and are the ultimate role models and their unconditional love made me the person I am today. I also would like to thank my in-laws for welcoming me into their families. I offer my deepest gratitude to my husband Nalin for his love, support and patience, and finally I thank my daughter Nethni for making my life complete. Without them, I would be nothing.

Table of Contents

Abstract	iii
Acknowledgment	v
List of Figures	viii
List of Tabela	xi
List of Schemes	xiii
Chapter One: Exploratory and Mechanistic Photochemistry	
Introduction	
1.0 Effect of Cyano Substituent on the Photophysical and Photochemical Properties of the <i>p</i> -Hydroxyphenacyl (pHP) Photoremovable Protecting Group	02
2.0 A Comparison of the Ground State, Base-activated and Photoactivated Favorskii Rearrangement, a Mechanistic Study	27
1.1 Statement of the Problem	51
2.1 Statement of the Problem	53
Results	
1.2 Effect of Cyano Substituent on the Photophysical and Photochemical Properties of the <i>p</i> -Hydroxyphenacyl (pHP) Photoremovable Protecting Group	54
2.2 A Comparison of the Ground State, Base-activated and Photoactivated Favorskii Rearrangement, a Mechanistic Study	64
Discussion	
1.3 Effect of Cyano Substituent on the Photophysical and Photochemical Properties of the <i>p</i> -Hydroxyphenacyl (pHP) Photoremovable Protecting Group	72
1.4 Conclusions	86
2.3 A Comparison of the Ground State, Base-activated and Photoactivated Favorskii Rearrangement, a Mechanistic Study	87
2.4 Conclusions	95
Experimental	96
References	112

Chapter Two: Novel Applications of the *p*-Hydroxyphenacyl Photoremovable Protecting Group

3.0 Instant Fluorescence from Release of Quencher-Fluorescent Dye Bifunctional Phototriggers: Photorelease Reactions, Synthesis, and Proof of Concept

Introduction	117
Statement of the Problem	136
Results	138
Discussion	158
Conclusions	168
Experimental	169
References	182

4.0 Applications of pHP Photochemistry as a Fluorous Separation Technique, A Method of Separation for Product Isolation; a Proof-of-Concept Investigation

Introduction	185
Statement of the Problem	202
Results	204
Discussion	216
Conclusions	223
Experimental	224
References	231

List of Figures

Figure 1-1. (a) Kerr gated time-resolved fluorescence contour of <i>p</i> -hydroxyphenacyl acetate (b) Normalized fluorescence decay at 330 nm and 440 nm.	16
Figure 1-2. Picosecond Kerr gated time-resolved resonance Raman spectra of 1.23	18
Figure 1-3. Temporal dependence of the triplet $\sim 1600\text{ cm}^{-1}$ band areas for 1.23	18
Figure 1-4. Triplet decay kinetics observed for 1.23 by transient absorption measurements in water/MeCN mixed solvent varying water concentration	21
Figure 1-5. Pump-probe spectroscopy of 1.23 in 87% aqueous CH ₃ CN	23
Figure 2-1. Possible transition states for the formation of the zwitterion or Cyclopropanone intermediates	37
Figure 2-2. (a) Representation of stationary points for semibenzilic acid mechanism (b) Schematic potential energy diagram with relative energies of stationary points for semibenzilic acid mechanism.	44
Figure 2-3. (a) Representation of stationary points for cyclopropanone mechanism (b) Schematic potential energy diagram with relative energies of stationary points for cyclopropanone mechanism.	45
Figure 2-4. The inversion and retention transition state structures for the enolate of 2.36 .	47
Figure 2-5. Cyclopropanone ring formation as a function of C-Cl bond distance.	48
Figure 2-6. Concerted proton relays in MeOH addition to the cyclopropanone transition state.	49
Figure 1-6. a) Crystal structure of 2-bromo-5-(phenylmethoxy) benzonitrile(1.29b), b) 2,6-dibromo-5-(phenylmethoxy) benzonitrile (1.37).	56
Figure 1-7. Titration curve of 5-acetyl-2-hydroxybenzonitrile (1.8) against 0.0461 M NaOH	58
Figure 1-8. UV-Vis Spectrum of 3-cyano pHP GABA (1.33a) in ammonium acetate buffer a) pH 7.05 (concn. 4.33×10^{-4}), b) pH 3.70 (concn. 6.02×10^{-4}).	59
Figure 1-9. ¹ H NMR spectra of the photolysis of 1.33a in D ₂ O	60
Figure 1-10. The Stern-Volmer plot of sorbate quenching of the photoreaction of 3-cyano pHP GABA (1.33a) at 3000 Å in water	61
Figure 1-11. ¹ H NMR spectra of photolysis of 1.40b in 20% D ₂ O/CD ₃ CN	63

Figure 1-12. Plot of Φ_{dis} vs. concentration of salt for 3- cyano pHP GABA	64
Figure 2-7. pHP derivatives tested for possible base activated Favorskii rearrangements	65
Figure 2-8. Potential base-catalyzed Favorskii and hydrolysis products from the pHP derivatives in Figure 2-7.	65
Figure 2-9. A plot of $\ln[\text{pHP OPO(OEt)}_2]$ vs. time for pHP OPO(OEt) ₂ .	70
Figure 1-13. Resonance structures of enol ether 1.44	73
Figure 1-14. A plot of Φ of phenylacetic acid appearance (Φ_p) at different pH conditions for pHP OAc (triangles) and 3,5-di- ^t butyl pHP OAc (circles)	76
Figure 1-15. Brønsted Linear Free Energy Relationship. LFER between $\log(\Phi_{dis}/\tau^3)$ and the pK _a values of the acids released during photolysis of pHP esters	81
Figure 3-1. Structure of subunit C of PKA.	120
Figure 3-2. Caged fluoresceins	123
Figure 3-3. 5-aminofluorecein based caged fluorophores	127
Figure 3-4. Fluorescence imaging of HeLa cells loaded with a caged and cell permeable coumarin 3.18 .	130
Figure 3-5. Structures of caged coumarins employed in HeLa cell and human fibroblast studies	130
Figure 3-6 Bioconjugates of caged probes. (a) Schematic showing photolysis of conventional bioconjugates. (b) Schematic diagram showing photolysis of novel bioconjugates.	131
Figure 3-7. (a) Fluorescein structure divided into two parts, the benzene moiety and the fluorophore. ⁴² (b) structure of fluorescein derivative 3.21 .	132
Figure 3-8. Photos of the fluorescence of fluorescein derivatives	133
Figure 3-9. UV-vis spectra of the three components of pHP ensemble at different pHs	145
Figure 3-10. H ¹ NMR spectra of the photolysis 3.35 in 20% D ₂ O/CD ₃ CN	147
Figure 3-11. H ¹ NMR spectra of carbazole-9H-acetic acid (3.32) in 20% D ₂ O/CD ₃ CN	151

Figure 3-12. (a) Fluorescence spectra recorded during photolysis of 3.35 . (b) A photograph illustrating the increase of fluorescence with time during photolysis of 3.35	154
Figure 3-13. Fluorescence spectra recorded during photolysis of 3.39 .	155
Figure 3-14. Possible π -stacked confirmations of 3.35 .	156
Figure 3-15. a) Π -stacked and b) extended conformations of 3.39 . (c) Structure of 3.39 .	157
Figure 3-16. Structures of novel pHP-based fluorophore quencher ensembles.	158
Figure 3-17. A schematic representation of electron movement in Dexter mechanism	159
Figure 3-18. Acceptor emission and quencher absorption with large spectral overlap.	160
Figure 3-19. A schematic representation of Förster mechanism.	160
Figure 4-1. Illustration of a three phase liquid-liquid extraction	187
Figure 4-2. Solid phase extraction over fluoruous reverse phase silica gel	189
Figure 4-3. An HPLC trace illustrating a separation based on the fluorine content.	190
Figure 4-4. An example of a strategy for fluoruous triphasic reaction with separation.	200
Figure 4-5. Schematic representation of synthesis of photocleavable surface and subsequent photodeprotection	201
Figure 4-6. Molecular structures of the photoactive reagents used for masking the SAM surface.	201
Figure 4-7. ^1H NMR spectra of the photolysis of 4.28b in 10% $\text{D}_2\text{O}:\text{CD}_3\text{CN}$.	211
Figure 4-8. Fluorescence spectra of the fluorescence emission from samples of 4.28a subjected to photolysis in EtOAc/buffer	213
Figure 4-9. Fluorescence spectra of the fluorophobic and fluorophilic fractions obtained from the separation of the photolysis mixture of 4.28c using F-SPE	215
Figure 4-10. Fluorescence spectra of the fluorophobic and fluorophilic layers obtained from the separation of the photolysis mixture of 4.28c using liquid-liquid extraction	215

List of Tables

Table 1-1. Quantum Yields of Phosphate Ester Disappearance and Product Appearance for Para Substituted Phenacyl Phosphates	9
Table 1-2. Ground State and Excited State pK _a s for Substituted pHP Derivatives	15
Table 1-3. Time Constants of the Triplet Decay Dynamics and the Rearrangement Reaction of pHP derivatives in H ₂ O/CH ₃ CN Mixed Solvent	19
Table 2-1. Rates of Halide Ion Release from α-Halocyclohexanones	32
Table 2-2. Rates of Chloride Ion Release in the Reactions of <i>meta</i> and <i>para</i> Substituted Derivatives of 2.19	35
Table 1-4. UV Data of 3-cyano pHP GABA in Water and Varying pH Levels	58
Table 1-5. Quantum Yield Studies of 3-cyano pHP GABA (1.33a) at various pH's	61
Table 1-6. Stern-Volmer Quenching Data of 1.33a	61
Table 1-7. Quantum Yields for the Disappearance of Cyano Substituted pHP Acetates in 20% H ₂ O/CH ₃ CN and 20% H ₂ O/ DMSO at 3000 Å	63
Table 1-8. Φ _{Dis} of 2-cyano pHP GABA (1.33a) and pHP OAc (1.40c) as a Function of Concentration of LiClO ₄ or NaClO ₄	64
Table 2-3. Rate Constants for the Disappearance of pHP Derivatives	71
Table 2-4. Stability of pHP derivatives in 0.1M HClO ₄ acid	71
Table 2-5. Concentration of pHP OPO(OEt) ₂ in 0.05M NaOMe/MeOH at Reflux at Different Time Intervals	110
Table 2-6. Concentration of pHP OAc in 0.05M NaOMe/MeOH at Reflux at Different Time Intervals	110
Table 2-7. Concentration of pHP Br in 0.05M NaOMe/MeOH at Reflux at Different Time Intervals	111
Table 2-8. Concentration of pHP OTs in 0.05M NaOMe/MeOH at Reflux at Different Time Intervals	111
Table 3-1. Practical Considerations for Different Fluorophores.	125

Table 3-2. Fluorescent and Photochemical Properties of Caged Coumarins	128
Table 3-3. UV-vis data of 3-[5-aminoFL(OPv) ₁] pHP Carbazole-9-acetic acid (3.35), 5-aminofluorescein(3.23) and carbazole-9-acetic acid (3.32)	146
Table 3-4. Quantum Yields for the Disappearance of 3.35 , 3.43 and 3.44 . in 16% pH 7.50 Tris Buffer/MeOH	152
Table 4-1. Some Representative Fluorous Solvents	186
Table 4-2. Partition Coefficients (<i>p</i>) for Triphenylphosphine and Perfluorotriphenylphosphine in Various Fluorous/Organic Solvent Systems	188
Table 4-3. Some Fluorous Tin Reagents, Their Applications, and Mode of Purification	196
Table 4-4. Percentage of Leaving Group Recovered After Separating from OtherPhoto- products Employing F-SPE and Liquid-Liquid Extraction Following Photolysis	214

List of Schemes

Scheme 1.1	7
Scheme 1.2	12
Scheme 1.3	13
Scheme 1.4	14
Scheme 1.5	22
Scheme 1.6	26
Scheme 2.1	28
Scheme 2.2	28
Scheme 2.3	29
Scheme 2.4	29
Scheme 2.5	30
Scheme 2.6	31
Scheme 2.7	31
Scheme 2.8	32
Scheme 2.9	34
Scheme 2.10	36
Scheme 2.11	38
Scheme 2.12	39
Scheme 2.13	40
Scheme 2.14	41
Scheme 2.15	42

Scheme 2.16	50
Scheme 1.7	54
Scheme 1.8	55
Scheme 1.9	55
Scheme 1.10	56
Scheme 1.11	57
Scheme 2.17	66
Scheme 2.18	67
Scheme 2.19	68
Scheme 2.20	69
Scheme 1.12	77
Scheme 1.13	78
Scheme 1.14	82
Scheme 1.15	83
Scheme 2.21	87
Scheme 2.22	88
Scheme 2.23	89
Scheme 2.24	90
Scheme 2.25	93
Scheme 3.1	126
Scheme 3.2	139
Scheme 3.3	139
Scheme 3.4	140

Scheme 3.5	140
Scheme 3.6	141
Scheme 3.7	142
Scheme 3.8	143
Scheme 3.9	143
Scheme 3.10	144
Scheme 3.11	148
Scheme 3.12	149
Scheme 3.13	150
Scheme 3.14	165
Scheme 3.15	166
Scheme 4.1	193
Scheme 4.2	197
Scheme 4.3	198
Scheme 4.4	199
Scheme 4.5	206
Scheme 4.6	208
Scheme 4.7	209
Scheme 4.8	210
Scheme 4.9	212
Scheme 4.10	220
Scheme 4.11	221

Chapter One: Exploratory and Mechanistic Photochemistry

1.0 Effect of Cyano Substituent on the Photophysical and Photochemical Properties of the *p*-Hydroxyphenacyl (pHP) Photoremovable Protecting Group

2.0 A Comparison of the Ground State, Base-activated and Photoactivated Favorskii Rearrangement, a Mechanistic Study

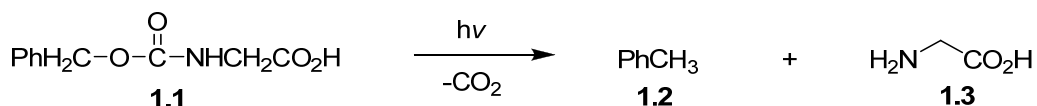
Introduction

1.0 Effect of Cyano Substituent on the Photophysical and Photochemical Properties of the *p*-Hydroxyphenacyl (pHP) Photoremovable Protecting Group

Protecting groups have become an indispensable necessity in organic synthesis as well as in biological studies. A protecting group inhibits the action of a functionality, generally by making a covalent linkage. The functionality can be reactivated by the removal of the protecting group. In organic synthesis, protecting groups are extensively used to block the activity of a functional group that can interfere with an imminent reaction sequence and then are removed at the end or as necessary depending on the synthetic route. In biological studies, the activity of a certain functionality is blocked by the protecting group and then reactivated at a desired time and location. The applicability of a protecting group in both organic synthesis and physiological studies is often dictated, from among several considerations, by the methods of removal. The usual deprotection techniques involve use of either an acid or a base, which are sometimes undesirable, as these conditions might not be tolerated by the other functional groups present in the system. In biological studies this becomes even more problematic as the addition of acid or base will affect the entire environment rendering the pH change incompatible with or deleterious to the natural conditions. Moreover the rate of deprotection, usually by hydrolysis, is not fast enough when studying the rates of very rapid biochemical processes.

It is in this light that the concept of photoremovable protecting groups (PPGs), groups that block the activity of functionalities and then reactivate the functionalities when exposed to light, becomes very attractive in both synthetic organic chemistry and biological studies. The PPGs are either connected via a covalent linkage or, in the case of ions, by electrostatic and

hydrogen bonded associations.¹ The process is sometimes referred to as “traceless reagent delivery” as there is no “residue” from light, the deprotecting reagent, in the reaction media. Compounds having a PPG are also referred to as caged compounds.² One of the first recorded examples of PPGs was by Barltop *et al.*,³ where they demonstrated the release of glycine by photolysis of N-benzyloxycarbonyl glycine (Equation 1.1)



Eq. 1.1

Since then much research has gone into developing good photoremovable protecting groups and their applicability in many fields had been demonstrated. Caged compounds have great potential for probing biological phenomena in cellular media. In conventional tools used to study biological processes the researchers loses the control of the agent (inhibitor, activator, etc..) once in the cell.⁴ Using a PPG to deactivate the agent allows the researcher to regain control even within the cell as release of the agent can be accomplished with spatial, temporal and concentration control.⁴ In very general terms, basic steps in studying biological phenomena using PPGs would include defining the active site of the agent of interest, attaching it to a PPG via a covalent linkage, thereby silencing the biological activity, transporting the caged compound into the desired biological system, then, and only then, releasing the agent from the caged compound via exposure to light regenerating the activity in the intended biological study.⁴

Biologically important molecule such as ATP, amino acids, neurotransmitters, steroids, second messengers, sugars, and lipids have been caged and then used for the analysis of various biological phenomena.⁵ Among these, caged ATP is the most commonly caged molecule as it can be used to probe many processes that are triggered by ATP as the energy source for the

biological action.^{6,7} *o*-Nitrobenzyl (ONB), a popular PPG (see below), caged ATP is commercially available and has been used extensively. As an example, Mantel *et al.* employed caged ATP to study the activity of Ca²⁺ATPase.⁸ Controlled release of ATP triggered the catalytic cycle of ATPase enabling the authors' investigation of the molecular processes like ATP hydrolysis and formation of the phosphorylated enzyme during the catalytic cycle employing Fourier transform IR (FTIR) spectroscopy.⁸

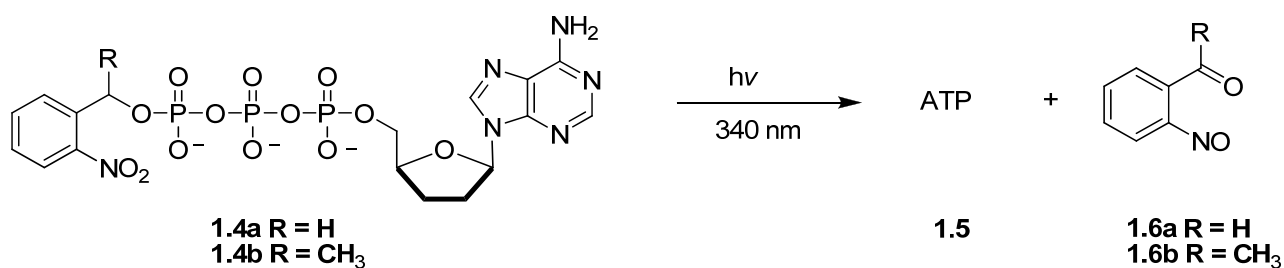
Several neurotransmitters like glutamate, GABA (γ aminobutyric acid), dopamine, and carbamoylcholine have also been caged.^{9,10} ONB caged glutamate, widely used to study the kinetics of neuronal signaling, is also commercially available. Shao and Dudeck¹¹ employed ONB caged glutamate to analyze the localization of the excitatory synaptic input in pyramidal cells. By selectively photolyzing different regions of subicular neurons containing ONB caged glutamate, the generation of a postsynaptic current after pyramidal cell stimulation could be assigned to the somatodendritic region.¹²

The criteria for a viable PPG for biological applications, as outlined by Sheehan¹³ and by Lester,¹⁴ can be summarized as:

1. Good aqueous solubility of the PPG-substrate derivative and the resultant photo products,
2. Efficient photochemical release of the caged substrate,
3. Rapid photorelease of the caged substrate, i.e., direct release from the excited state of the caging chromophore by a primary photochemical cleavage of the covalent bond,
4. Photoproducts stable to the surrounding media,
5. Excitation wavelengths ≥ 300 nm,
6. High absorptivity of the chromophore,

7. Inert caged compounds and photoproducts to the media and to other reagents, and
8. Generally high yielding synthetic methods for the assembly of the caged compound.

Although there has been much interest in the concept of PPGs over the past three decades, only a handful of compounds have been developed as good PPGs, e. g., the *o*-nitrobenzyl (ONB)², benzoin¹⁵, coumarylmethyl¹⁶ and *p*-methoxyphenacyl groups.^{13,17} Among these, the *o*-nitrobenzyl has been by far the most popular and widely used PPG. The first report of an *o*-nitrobenzyl group as a PPG was published by Barltrop, *et al.*¹⁸ in 1966 for the release of carboxylic acids. Then in 1977, Engels and Schlaeger¹⁹ demonstrated the photorelease of cAMP and AMP from the *o*-nitrobenzyl (ONB) ester. This was rapidly followed by the work of Kaplan and coworkers² and, together, these publications elevated *o*-nitrobenzyl into the first and eventually the most popular PPG. Kaplan reported the synthesis and the release of ATP from two *o*-nitrobenzyl ATP esters, 2-nitrobenzyl (ONB, **1.4a**) and 1-(2-nitrophenyl)ethyl (NPE, **1.4b**) (Equation 1.2).

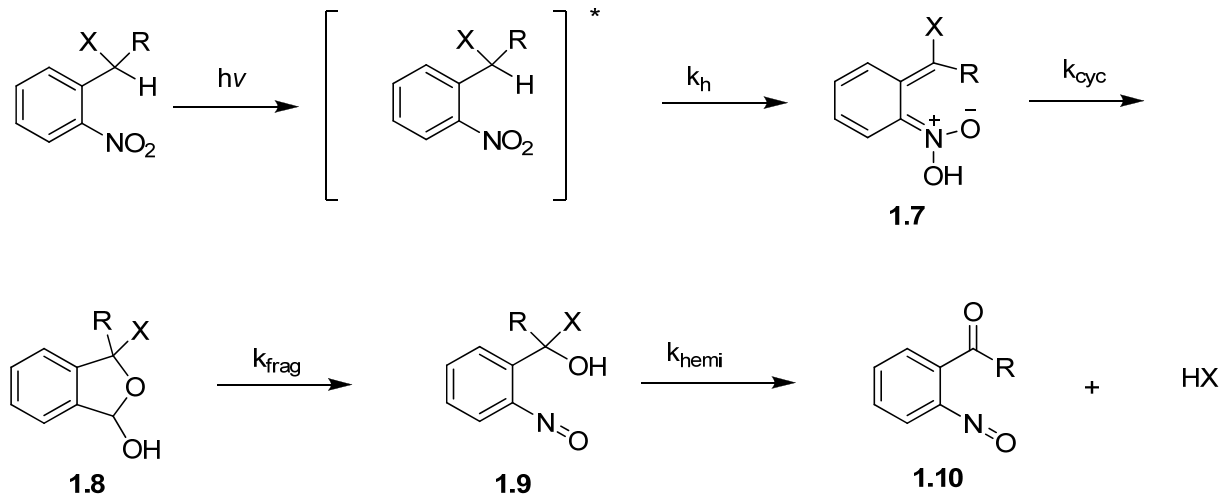


Eq. 1.2

The yields for the released ATP from the two *o*-nitrobenzyl derivatives were different: 80% of the ATP was released from NPE caged ATP in less than 60 seconds while only 25% was released in 60 seconds from ONB caged ATP. This study indicated that substituted *o*-nitrobenzyl esters may be better candidates for photoremovable protecting groups. Since then several

variants of the parent ONB group, such as 4,5-dimethoxy,^{20a} 4,5-dimethoxy 1-(2-nitrophenacyl) ethyl^{20b} and α -carboxy-2-nitrobenzyl,^{20c} have been developed. Over the years the ONB group has been successfully used to cage a wide variety of groups including nucleotides,²¹ peptides and proteins,²² carboxylic acids,²³ amines and amides,²⁴ alcohols,²⁵ phosphates,²⁶ calcium ions,²⁷ and a number of fluorophores.²⁸

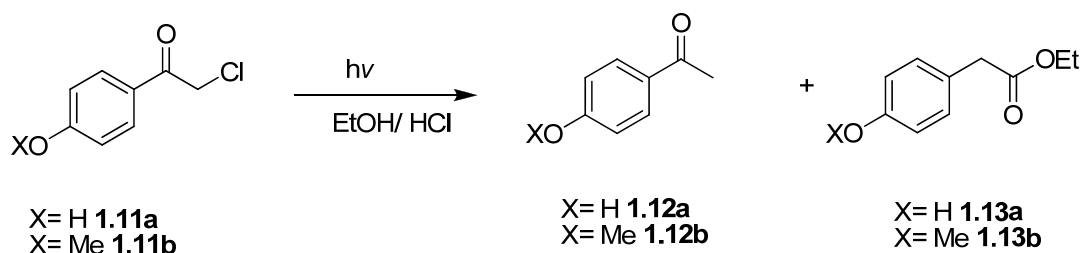
The mechanistic aspects of photorelease of caged compounds from ONB cages have been explored by many groups²⁹, most prominently by Wirz, *et al.*,³¹ and are believed to occur through an initial intramolecular photoredox reaction. A general scheme for the reaction mechanism is shown in Scheme 1.1. Initial excitation of the chromophore leads to an intramolecular hydrogen atom abstraction of the benzylic hydrogen by the excited nitro group resulting in the formation of *aci*-nitro intermediate **1.7**. Cyclization of **1.7** gives rise to an isoxazole intermediate **1.8**; fragmentation of **1.8** generates hemiacetal **1.9**; and the final collapse of the hemiacetal results in the release of the caged species with formation of the nitroso product **1.10**. Work by Walker³⁰ and Corrie²¹ identified the decay of the *aci*-nitro species (**1.7**) by the decay of its UV absorption as rate limiting. However, Wirz *et al.*³¹ later reported that the decay of the hemiacetal intermediate was the rate determining step in the release of methoxide (X = MeO in **1.9**), a poorer leaving group, suggesting that the rate defining step may be either the oxazole or hemiacetal hydrolyses. Both the oxazole and hemiacetal are UV silent under the reaction conditions.

Scheme 1.1

Although the ONB group has been widely used, there are inherent disadvantages. The main disadvantages are due to undesirable properties of the photoproduct of the reaction, the nitroso ketone **1.10**.³² It is toxic to cell viability and reactive toward nucleophiles present in the medium. It also contains a strong absorbing chromophore that increasingly competes for light as the reaction progresses, lowering the efficiency of the photorelease. The finding that the rate determining step of the reaction is the hydrolysis of the hemiacetal for all but the best leaving groups also limits the applicability of the chromophore to the study of slow kinetic processes in mechanistic studies in biological media.

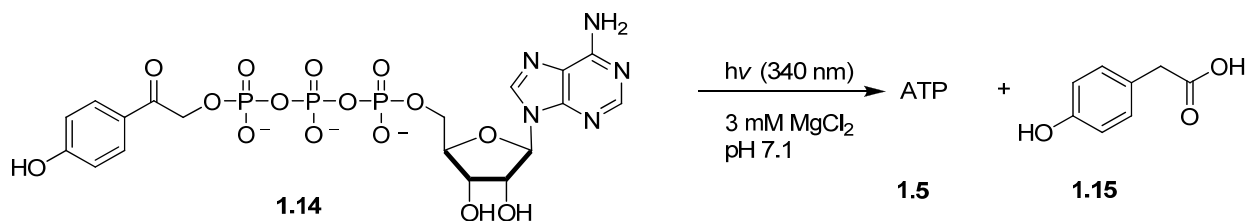
These drawbacks in the ONB group have created interest in the scientific community toward developing better candidates for photoremovable protecting groups. One of the most recent and promising PPG is the *p*-hydroxyphenacyl (pHP) group.³³ *p*-Hydroxyphenacyl as a photo-activated group for the release of chloride ion was first reported by Anderson and Reese in 1962³⁴ when they revealed the release of chloride from *p*-hydroxyphenacyl chloride (**1.11a**) as well as from *o*- and *p*-methoxyphenacyl chlorides (**1.11b**) in ethanol. The product of the chromophore was a modest yield of the corresponding ethyl phenylacetate (Equation. 1.3). A

decade later in 1973, Sheehan and Umezawa⁴ reported the efficacy of a closely related methoxy analog for the release of glycine derivatives from the *p*-methoxyphenacyl group.



Eq. 1.3

However, the *p*-hydroxyphenacyl group attracted little attention, until its rediscovery by Givens and coworkers several decades later.^{33,35} The release of caged phosphates and ATP in aqueous solvents and the exclusive formation of *p*-hydroxyphenylacetic acid (**1.15**) as the only photoproduct of the chromophore were reported in 1996.³⁵ Release of ATP from the pHP group is shown in Equation 1.4.



Eq. 1.4

Several other derivatives of *para* substituted phenacyl chromophores were explored as potential PPGs and compared with the *p*-hydroxy derivative (Table 1.1).³³ Among the ones studied, the acetamido and carbamoyl derivatives photoreleased efficiently but resulted in a large number of byproducts that discouraged further exploration. The methoxy derivative showed two products, *p*-hydroxyacetophenone and methyl or *t*-butyl *p*-methoxyphenylacetate depending on the alcohol solvent.

Table 1-1. Quantum Yields of Phosphate Ester Disappearance and Product Appearance for Para Substituted Phenacyl Phosphates in pH 7.2 Tris Buffer at 300 nm³³

<i>p</i> -substituent	$\Phi_{\text{dis}}^{\text{a}}$	$\Phi_{\text{pX-PA}}^{\text{b}}$	$\Phi_{\text{pX-A}}^{\text{c}}$	other products
-NH ₂	<0.05	0.0	<0.05	na
CH ₃ CONH-	0.38	0.0	0.11	Dimers
CH ₃ OCONH	0.34	0.0	nd	unknowns
CH ₃ O- ^d	0.42	0.20	0.07	na
-OH ^e	0.38	0.12 ^f	0.0	none

^a Φ for phosphate ester disappearance. ^b Φ for appearance of phenylacetate. ^c Φ for appearance of acetophenone. ^dSolvent was MeOH and diethyl phosphate was the leaving group. ^e10 % aq. CH₃CN was added to the solvent. ^fValue is an estimate, related more recent examples are nearly the value of the Φ_{dis}

The *p*-hydroxyphenacyl phototrigger satisfies many of the conditions that were listed as prerequisites for a PPG. It is highly water soluble; photorelease is relatively efficient and fast; the pHP caged compounds and photoproducts are biologically benign; the photorelease occurs through a primary photochemical process and; caging of a desired functionality can be achieved through relatively simple synthetic route.³³ An attractive feature of the pHP phototrigger is the formation of the rearranged *p*-hydroxyphenylacetic acid as the photoproduct from the chromophore. The skeletal rearrangement of the chromophore results in a blue shift in the absorption spectrum thereby making the photoproduct no longer competitive for the >300 nm incident radiation. Therefore the photorelease can be carried to higher conversions without loss in the reaction efficiency. One drawback of the pHP group is its weak absorptivity at wavelengths greater than 300 nm. This also can be overcome by introducing substituents or extending conjugation at the aryl ring of the pHP chromophore.³³

Although the pHP phototrigger has been a relatively recent addition to the arena of photoremovable protecting groups, it has been successfully applied in many biological studies.³⁶ These will be discussed in the second chapter of this thesis, “Novel Applications of the *p*-Hydroxyphenacyl Photoprotecting Group.”

Mechanistic Investigations of the Photo-Favorskii Rearrangement

In spite of extensive mechanistic work done by the Givens group^{36a,37,38,39,40} and others,^{41,42,43} elucidating the mechanism of the photorelease from the pHP phototrigger has remained a challenging quest. Although it is safe to state that major elements of the mechanism have been resolved by recent work by Givens, Wirz, *et al.*^{39,40} and by Phillips, *et al.*,^{42,43} a more complete understanding of the mechanism has yet to be established. The initial paper by Anderson and Reese³⁴ proposed the possibility of a mechanism resembling the ground-state Favorskii rearrangement⁴⁴ involving a putative spirodienedione intermediate to explain the skeletal rearrangement to the observed photoproduct. Thus, the term “Photo-Favorskii Rearrangement” came into being.

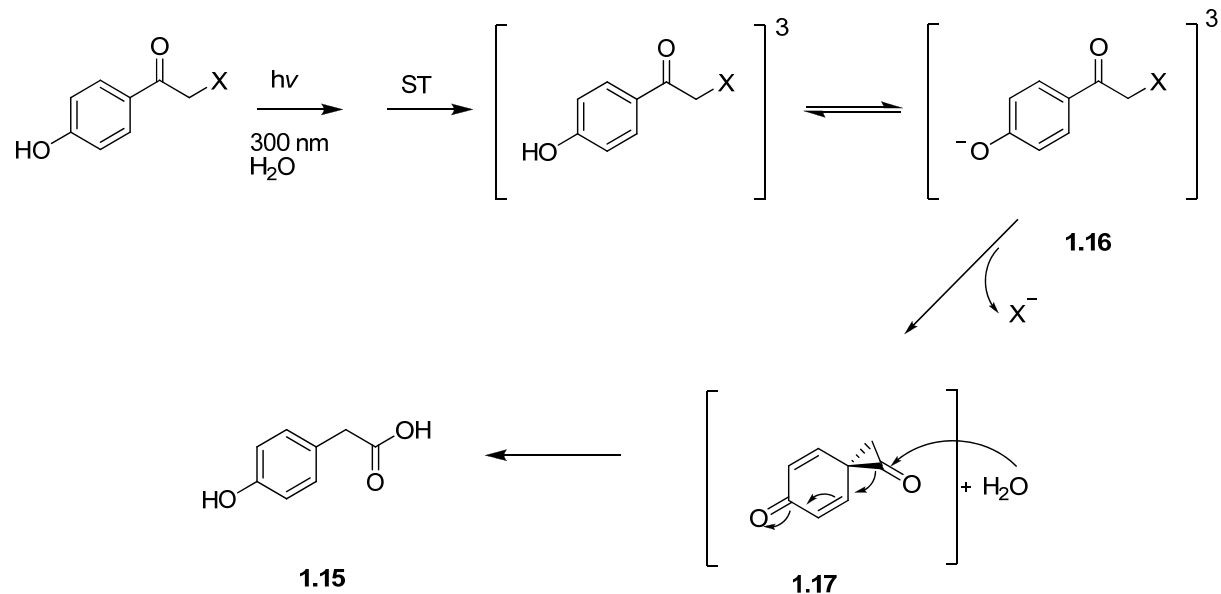
Three distinctive features of the pHP chromophore and its mechanistic features, when comparing it to other photoremovable protecting groups, are its ability to undergo a bathochromic shift at higher pH, the adiabatic photorelease sequence that takes place in the triplet manifold, and, in most cases, the singular nature of the formation of the photo-Favorskii intermediate as the exclusive route in aqueous media.³³

Several mechanistic features of the photo-Favorskii rearrangement were originally advanced by Givens, Wirz and coworkers.^{37,38} The authors demonstrated that the reaction takes place in the triplet manifold through a series of quenching experiments using the triplet quenchers potassium sorbate and sodium 2-naphthalenesulfonate.^{37,38} Initially proposed mechanisms³² involved direct heterolysis of the bond between the leaving group and the phenacyl chromophore to form the triplet hydroxyphenacyl cation, or homolytic cleavage of the same bond to a radical pair followed by electron transfer prior to the formation of the spiro dienedione **1.17**. The spirodienedione then undergoes hydrolysis to yield *p*-hydroxyphenylacetic acid. But

these mechanisms do not involve a role for the phenolic hydroxyl group nor do they require aqueous solvents for a photo-Favorskii rearrangement process.

Other mechanisms proposed by Givens *et al.*³⁸ include that illustrated in Scheme 1.2. Here, the initial absorption of light excites the chromophore to its singlet excited state, which then undergoes rapid intersystem crossing ($k_{ISC} = 2.7 \times 10^{11} \text{ s}^{-1}$) to the triplet state followed by adiabatic proton transfer to the solvent resulting in the triplet phenoxide anion (**1.16**). This deprotonation step was believed to be the rate determining step of the reaction. Departure of the leaving group will occur prior to the formation of the very short lived spirodienedione (**1.17**). As noted above, hydrolysis of **1.17** results in the rearranged *p*-hydroxyphenylacetic acid (**1.15**). However, the possibility of an essentially fully concerted loss of the proton and elimination of the leaving group with spirodienedione formation was not discounted at this point, but this has come to be viewed as less likely in the most recent evaluations of the data on the mechanism³⁹ and will be discussed later. Proof for the existence of the spirodienedione intermediate **1.17**, though essential for the skeletal rearrangement observed, has not been obtained and is still a goal of this research group.

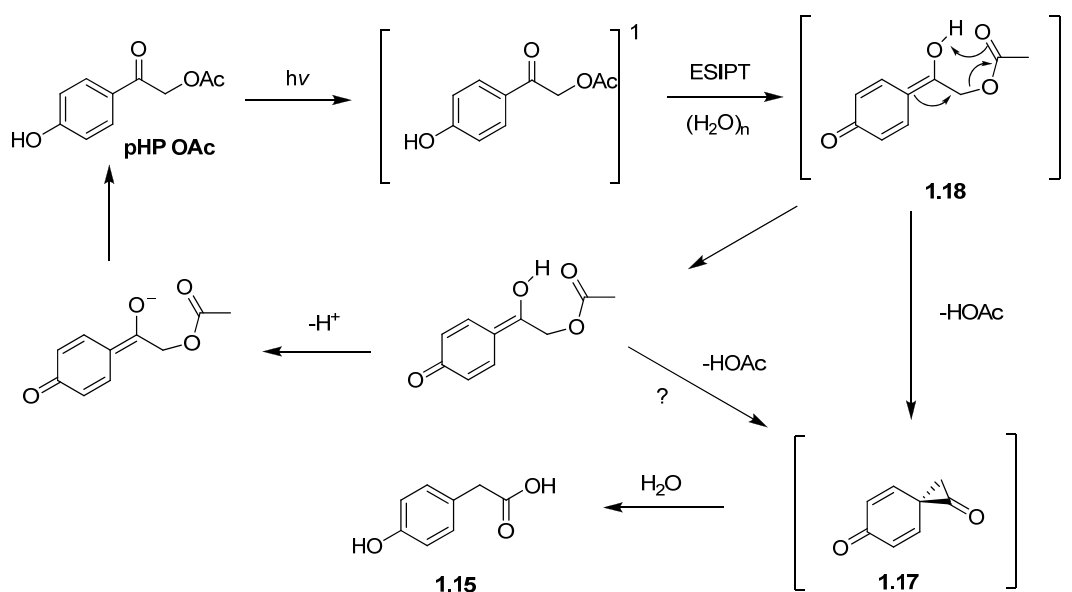
Scheme 1.2



Givens' identification of the triplet state as the reactive intermediate was questioned by Wan and coworkers.⁴¹ Based on their findings that the photochemistry of many hydroxy aromatic and phenol derivatives in aqueous solution is determined by a proton transfer from the hydroxyl group to the solvent or intramolecularly to a basic site on the excited molecule which occur in the singlet excited state,⁴⁵ they proposed a primary photochemical step of water-assisted excited state intramolecular proton transfer (ESIPT) from the hydroxyl group to the pHP carbonyl oxygen for the photo-Favorskii rearrangement. This proton transfer process generates a *p*-quinone methide intermediate (**1.18**). The excited or relaxed *p*-quinone methide (the authors equivocate on this) then undergoes further reaction releasing the caged derivative and produces the same strained spirodienedione intermediate (**1.17**) in its ground state proposed earlier. The spirodienedione subsequently hydrolyzes to the rearranged phenylacetic acid (**1.15**). The *p*-quinone methide intermediate can also undergo enol/enolate tautomerization that will simply regenerate the starting pHP acetate (pHP OAc, Scheme 1.3). The possibility of the excited pHP OAc undergoing a concerted deprotonation with the loss of the leaving group was not completely

discarded. This mechanism was supported by results of nanosecond laser flash photolysis (LFP).⁴¹ When pHP OAc was subjected to LFP in neat CH₃CN a strong absorption was observed at $\lambda_{\text{max}} \approx 380$ nm that was quenched by O₂. However, when the solvent was replaced with 1:1 H₂O/CH₃CN, a strong band at $\lambda_{\text{max}} \approx 330$ nm and a weak band at $\lambda_{\text{max}} \approx 380$ nm were observed. When purged with O₂ the 380 nm band completely disappeared while a fraction of the 330 nm remained, indicating that a part of the 330 nm band is not due to a triplet and, therefore, this part was wrongly assigned to a singlet state transient (see below).

Scheme 1.3

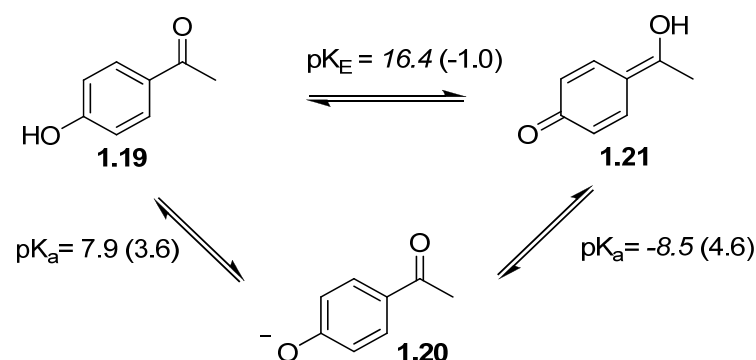


Evidence that the triplet state is the reactive state for pHP photorelease was supported by results obtained by Wirz *et al.*³⁷ in a study of *p*-hydroxyacetophenone (**1.19**) and *p*-methoxyacetophenone as model chromophores using LFP and density functional theory (DFT) calculations. LFP of *p*-methoxyacetophenone generated a strong absorption at 395 nm in 1:1 CH₃CN/H₂O and 385 nm in dry CH₃CN. These were quenched by triplet energy transfer to O₂ and also from energy transfer to added naphthalene as demonstrated by the production of

naphthalene triplet emission. Therefore, the emissive excited state for the *p*-methoxyacetophenone was assigned to the triplet state.

When the methoxy group was replaced by a hydroxyl group, the picture became more complicated because *p*-hydroxyacetophenone can deprotonate to its anion or conjugate base form, **1.20**, (ground state $pK_a = 7.9$), as well as tautomerize to the quinone methide enol **1.21**, ($pK_E = 16.4$) (Scheme 1.4). pK_a and pK_E values were obtained either by spectrophotometric titrations or DFT calculations using the thermodynamic cycle.³⁷

Scheme 1.4^a



^aValues for the lowest triplet state is given in brackets. Values calculated from DFT calculations are given in italics. See reference 37

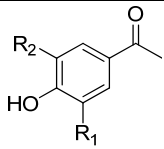
Upon photolysis of **1.19**, the triplet state is generated very rapidly ($k_{ISC} = 2.7 \times 10^{11}$, λ_{max} 395 nm in 50% CH_3CN/H_2O , λ_{max} 370 nm in CH_3CN) and is quenched by energy transfer to naphthalene. The triplet **1.19** can undergo the same proton transfer (ESIPT) and ionization to form the triplet enol and the triplet anion, respectively, as indicated for ground state acetophenone. The pK_a and pK_E values for the triplet states are given in parentheses in Scheme 1.4.

The absorption spectra of triplet **1.19** and the triplet anion are very similar, but the absorption maximum is shifted to 405 nm for the anion. The absorbance at 325 nm previously

assigned by Wan, *et al.*⁴¹ as the singlet state, was now assigned to the ground state anion (conjugate base) of *p*-hydroxyacetophenone. An interesting finding in this study was the increase in the acidity of the triplet *p*-hydroxyacetophenone ($pK_a = 3.6$) compared to the ground state ($pK_a = 7.9$). This increased acidity was also observed for several other pHP GABA derivatives.³³ The extent of the increase in acidity was found to be less with electron donating substituents compared with electron withdrawing groups (Table 1-2).

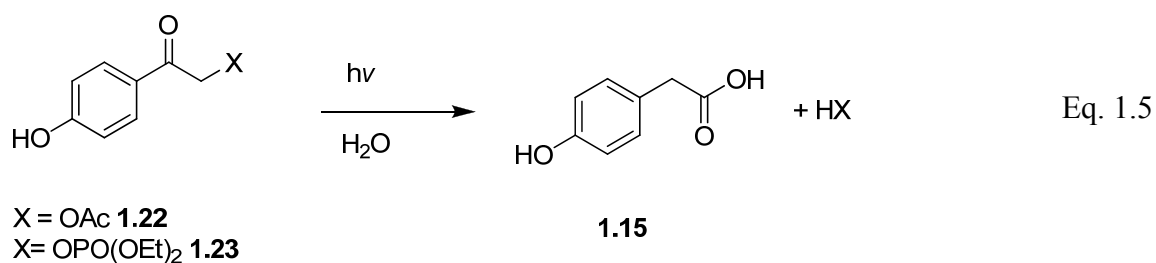
When pHP diethyl phosphate (pHP OPO(OEt)₂) was subjected to LFP in neat degassed CH₃CN, a transient absorption was observed at 395 nm.³⁷ Based on energy transfer to naphthalene, the transient was assigned to the triplet of pHP OPO(OEt)₂. Upon exposure to air or by the addition of piperylene to the medium, the decay rate of the triplet increased. This confirmed that the reactive excited state of the diethyl phosphate release from pHP OPO(OEt)₂ also occurred via the triplet state. Increasing water content in CH₃CN also resulted in a significant increase in the decay rate of triplet pHP OPO(OEt)₂.

Table 1-2. Ground State and Excited State pK_a s for Substituted pHP Derivatives³¹

Substituted pHP	R ₁	R ₂	pK_a	³ pK_a
	H	H	7.93	5.15
	OCH ₃	H	7.85	6.14
	OCH ₃	OCH ₃	7.78	6.16
	CONH ₂	H	6.15	3.75
	CO ₂ Me	H	7.66	4.28
	CO ₂ H	H	6.28	4.33

The mechanism of the photo-Favorskii rearrangement has also been independently investigated by Phillips and co-workers.^{42,43} Their work has focused on understanding three important elements of the reaction pathway; the multiplicity of the reactive species (triplet vs. singlet), the nature of the bond breaking process in the loss of the leaving group (heterolytic vs.

homolytic), and the importance and role of the solvent water.⁴³ To probe the multiplicity of the reaction, the photochemistry of pHP acetate (pHP OAc, **1.22**) and pHP diethyl phosphate (pHP OPO(OEt)₂, **1.23**) were studied employing Kerr-gated time-resolved fluorescence⁴⁶ (fs-KTRF) and Kerr-gated, time-resolved resonance Raman spectroscopy⁴⁷ (ps-KTR³) (Equation 1.5).⁴² fs-KTRF was used to study the spectral properties and the decay of the singlet state while ps-KTR³ was used to explore the generation and the molecular bonding changes occurring from the triplet state.



fs-KTRF studies with pHP OAc in neat CH₃CN showed two fluorescence emission bands, one at ~ 340 nm and the other at ~ 420 nm, suggesting two different electronic excited states (Figure 1-1). The two bands were assigned to two singlet excited states, the S₃ (340 nm, a π,π* state) and S₁ (420 nm, assigned an n,π* state), respectively.

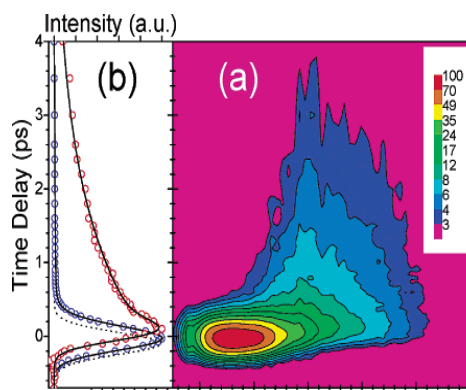


Figure 1-1. (a) Kerr gated time-resolved fluorescence contour of HPA (*p*-hydroxyphenacyl acetate) obtained with 267 nm excitation in MeCN. (b) Normalized fluorescence decay at 330 nm (circles in blue) and 440 nm (circles in red) for HPA in MeCN.⁴² Reproduced with permission from Journal of American Chemical Society.

KTRF measurements performed in 1:1 H₂O/CH₃CN and MeOH for both **1.22** and **1.23** showed a shift in fluorescence emission maximum compared to the spectra taken in neat CH₃CN, while spectra taken in THF resembled those taken in neat CH₃CN, indicating that there exists a solvent-solute H-bonding interaction affecting the excited singlet states. To explore the decay paths of these excited singlet states and to investigate the dynamics of the triplet formation, ps-KTRF³ spectra were taken for the two pHP derivatives in neat CH₃CN and 1:1 H₂O/CH₃CN (Figure 1-2). Bands at 1601, 1493, 1447, 1327, 770 and 755 cm⁻¹ are due to ring C-C stretching vibrations while those at 1161, 1097, and 927 cm⁻¹ are due to various ring C-H in-plane bending motions. The band due to the ring attached C=O stretching frequency in ground state pHP OAc is at 1656 cm⁻¹, but this is substantially down-shifted to the 1200-1300 cm⁻¹ region for the triplet state indicating that there is no localized C=O stretching in the triplet state.^{48,49} The early picosecond section of the spectra for both compounds in both solvents looked the same, while the lifetime of the triplet π,π^* state was substantially shorter in H₂O/CH₃CN solvent compared to neat CH₃CN. For pHP OPO(OEt)₂, the triplet lifetime in 1:1 H₂O/CH₃CN and neat CH₃CN were 420 ps and 150 ns, respectively. A kinetic comparison of the decay of the triplet state for both **1.22** and **1.23** is illustrated in Figure 1-3. This solvent and leaving group dependence of the triplet state are additional compelling evidence for the fact that the triplet state is the predominant reactive precursor for the photodeprotection reaction by the pHP photoprotecting group and thus eliminates the singlet mechanism.

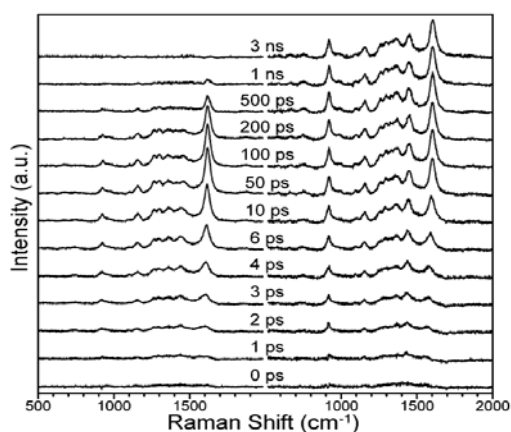


Figure 1-2. Picosecond Kerr gated time-resolved resonance Raman spectra of **1.23** obtained with 267 nm pump and 400 nm probe wavelengths in 50% H₂O/50% MeCN mixed solvent (left) and neat MeCN (right).⁴¹ Reproduced with permission from Journal of American Chemical Society.

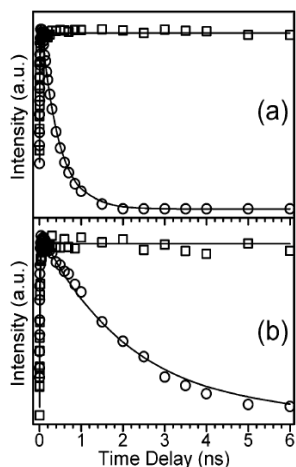


Figure 1-3. Temporal dependence of the triplet $\sim 1600\text{ cm}^{-1}$ band areas for **1.23** (a) and **1.22** (b) in 50% H₂O/50% MeCN mixed solvent (circles) and neat MeCN (squares) obtained in 400 nm probe ps-KTR3 spectra. Solid lines show an exponential fitting of the experimental data. Reproduced with permission from Journal of American Chemical Society.

Phillips and coworkers³³ further explored the mechanism of the photo-Favorskii rearrangement, specifically heterolytic vs. homolytic bond cleavage and the effect of the solvent, by femtosecond transient absorption (TA) experiments and picosecond time-resolved resonance Raman spectroscopy (ps-TR³).⁴³ Three pHP derivatives, pHP OAc (**1.22**), pHP OPO(OEt)₂ (**1.23**) and pHP diphenyl phosphate (pHP OPO(OPh)₂, (**1.24**) were subjected to TA experiments to investigate the mode of cleavage. The effect of the pK_a of the leaving group on the decay of the triplet state is expected to be substantially different for the two modes of cleavage under investigation. In 1:1 H₂O/CH₃CN the time constant for the triplet decays were found to be 150, 350 and 2130 ps for **1.24**, **1.23**, and **1.22**, respectively. The pK_a's of the leaving group anions, i.e., the pK_a's of the conjugate acids of the diphenyl phosphate anion, the diethyl phosphate

anion and the acetate anion, are 0.41, 1.39 and 4.76, respectively (Table 1-3). These pKa values are proportional to the free energies of the anions in aqueous media and a measure of the relative stabilities of the leaving groups for the caged species, if cleavage occurs through a heterolytic mode. The good correlation observed with the triplet decay rates and the pKa's of the anions strongly support a direct triplet heterolytic cleavage mechanism is operative in the loss of the leaving group from the pHP chromophore.

Table 1-3. Time Constants of the Triplet Decay Dynamics and the Rearrangement Reaction of pHP derivatives in H₂O/CH₃CN Mixed Solvent⁴²

H ₂ O%	Time constant of the triplet decay (t_1) ^a / ps							(t_2) ^b / ps	pKa
	75%	50%	40%	30%	25%	15%	10%		
1.24		150					830	600	0.4
1.23	290	350	530	800	1280	2400	9000	470	1.39
1.22		2130							4.76

^atime constant for triplet decay with an error of ± 20 ps. ^btime constant of the solvolytic rearrangement with an error of ± 40 ps.

To explore further the importance of water as the solvent in pHP photochemistry since previous studies had shown that the photo-Favorskii rearrangement occurred exclusively in aqueous or aqueous containing media,³⁷ the triplet decay dynamics of the pHP OPO(OEt)₂ and pHP OPO(OPh)₂ were investigated using TA spectroscopy in H₂O/CH₃CN solvent system with varying percentages of water (Table 1-3).⁴³ Confirming previous observations that the quantum yields of the photorelease increased with the amount of water present,³⁸ the TA spectra and triplet decay kinetics of **1.23** and **1.24** showed an increase in triplet decay rates with increasing water content. This was attributed to the solvation of the leaving group and the triplet excited state. The increase in the triplet decay rate becomes less sensitive to the water content as it reaches greater than 50%, approaching a constant release rate for the leaving group. Furthermore, a Stern-Volmer treatment of the triplet decay rate measurements with varying water content in

the solvent showed a quadratic dependence on water concentration. Thus the authors claimed that water plays an important role very early in the reaction mechanism which likely involves participation in the solvolytic rearrangement steps, thus making it an essential component in the photo-Favorskii rearrangement. Since water molecules can act as both hydrogen bond donors and a hydrogen bond acceptors, distinguishing the role that water plays in the reaction involved TA experiments using DMSO, a hydrogen bond acceptor (only), $\text{CF}_3\text{CH}_2\text{OH}$ (primarily a good hydrogen bond donor),⁵⁰ and 1:1 DMSO: $\text{CF}_3\text{CH}_2\text{OH}$, which provides both the H donor and acceptor. TA spectra in DMSO showed no change in the triplet decay rate and resembled those in neat CH_3CN while the TA spectra in $\text{CF}_3\text{CH}_2\text{OH}$ showed a small increase in the triplet decay rate compared with water. A considerable triplet decay rate increase was observed in 1:1 DMSO: $\text{CF}_3\text{CH}_2\text{OH}$ mixed solvent system, indicating that solvation at both acidic and basic sites of the pHP molecule are important. However, the extent of change in the triplet rate in 1:1 DMSO: $\text{CF}_3\text{CH}_2\text{OH}$ was smaller compared to that observed in the $\text{H}_2\text{O}/\text{CH}_3\text{CN}$ system (Figure 1-4). This can be explained by the stronger hydrogen bond donor and acceptor abilities and higher polarity of water compared with DMSO/ $\text{CF}_3\text{CH}_2\text{OH}$ mixed solvent systems.⁵¹

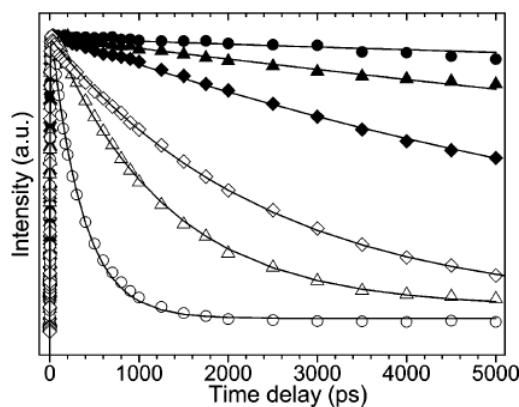


Figure 1-4. Triplet decay kinetics observed for **1.23** by transient absorption measurements in water/MeCN mixed solvent with water concentration of 0% (●), 10% (◆), 15% (◇), 25% (▲), and 50% (○). Data labeled by the filled triangles are obtained in a DMSO/CF₃CH₂OH (1:1 by volume) mixed solvent. Solid lines indicate dynamic fittings using a one exponential decay function to the experimental data points.⁴² Reproduced with permission from Journal of American Chemical Society.

Using ps-TR³, Phillips and coworkers were also able to observe the time-resolved formation of *p*-hydroxyphenylacetic acid for the first time in both photolysis of **1.23** and **1.24**. Unfortunately, even in this extensive study of the photo-Favorskii rearrangement, no evidence regarding the structural details of the intermediates leading to the carbon skeletal rearrangement could be gleaned. Nevertheless, the authors postulated that there is a transient intermediate (or intermediates) not observable in the 300-700 nm region that also shows no measurable absorption near 200 nm. Its occurrence is highly dependent on the water concentration. Inability to detect this intermediate can also be due to its low concentration at any given time. The previously proposed structure³⁸ of the spirodienedione intermediate may instead be a contact ion pair-solvation complex rather than the covalently bound intermediate suggested by other authors. The mechanism put forward by Phillips *et al.*⁴⁸ is illustrated in Scheme 1-5.

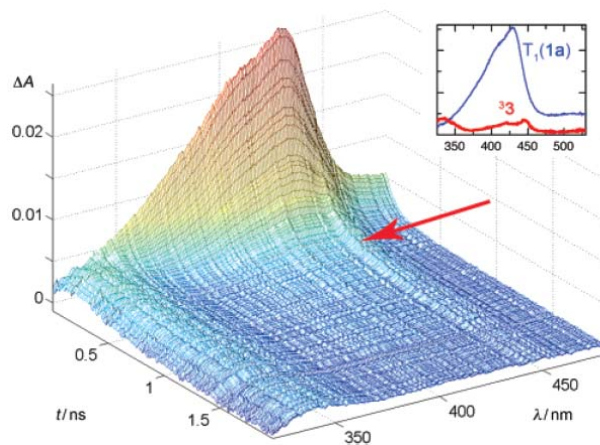


Figure 1-5. Pump-probe spectroscopy of **1.23** in 87% aqueous CH_3CN .³⁸ Reproduced with permission from Journal of American Chemical Society.

In the hope of detecting the spirodienedione intermediate, the authors followed the time dependent changes during photolysis of pHP diethyl phosphate via step-scan FTIR.³⁹ Although DFT calculations predict that the C=O stretching vibrations should appear around 1880 cm^{-1} (that of simple cyclopropanone is at 1813 cm^{-1}), no signal was observed in this region when **1.23** was irradiated at 266 nm. However, two new transient bands at 1450 cm^{-1} and 1300 cm^{-1} were observed and their decay resulted in the growth of a new band at 1647 cm^{-1} . The first two bands resembled those of triplet acetophenone and were assigned to the triplet state T_1 of **1.23**. Nanosecond laser flash photolysis of pHP diethyl phosphate (**1.23**) resulted in a transient absorption at $\lambda_{\text{max}} = 395\text{ nm}$ in aqueous CH_3CN that was also assigned to its T_1 . Its decay resulted in a broad absorption band at $\lambda_{\text{max}} = 276\text{ nm}$. The amount of this new byproduct of the reaction, identified as *p*-hydroxybenzyl alcohol (**1.27**) and the absorption band of the transient at 276 nm decreased with increasing water content. Therefore, the 276 nm transient was assigned to the precursor for *p*-hydroxybenzyl alcohol, which the authors suggested was *p*-quinone methide

(1.26). This assignment was supported by minor NMR signals observed in the photolysis of pHP diethyl phosphate in D₂O/CD₃CN at -25 °C.³⁹ The identification of the *p*-quinone methide intermediate can be considered to be indirect evidence for the intermediacy of the elusive spirodienedione since its formation as well as the Favorskii photoproduct (1.15 and 1.27) are logically explained as emanating from the same spirodienedione intermediate.

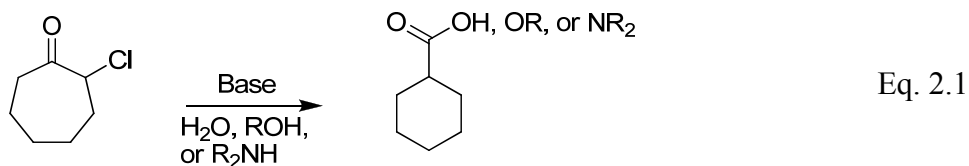
Further support of the Phillips' proposal of an aqueous solvated triplet precursor to heterolysis came from solvent kinetic isotope effect (SKIE) studies on the T₁ decay rate constants of pHP diethyl phosphate by Givens, Wirz, Schowen, and coworkers.³⁹ In an effort to probe the number of water molecules involved in the rate limiting transition state during the deprotection process, the "proton inventory" method,⁵² a powerful method for determining the number of protons transferred in the rate determining step though not very frequently applied in excited state reactions, was applied here. The overall SKIE was found to be $k_H/k_D = 2.17$ and the proton inventory plot was curved indicating that at least two water molecules were involved in the deprotection process as determined by the curve fit obtained from the Gross-Butler⁵³ modeling equation for the isotopic dependence on the rate of the disappearance of pHP diethyl phosphate.

Although the photorelease from a pHP photoprotected group occurs very cleanly for a photochemical process involving the photo-Favorskii rearrangement, the release process in aqueous media generally occurs with quantum yields less than unity. This implies that there are competing processes that do not result in the desired photorelease or decomposition of the starting pHP ester. This point was addressed, again by Givens and coworkers, in their 2009 article⁴⁰ regarding pump-probe photolysis of 3-OCF₃ pHP GABA. A transient that remained even after the decay of triplet was observed at $\lambda_{max} = 340$ nm which decayed with a rate constant

of $6.5 \times 10^6 \text{ s}^{-1}$. The lifetime and the amplitude of this transient were not affected by sorbate, ruling out the possibility of it being due to a triplet process. The finding that the lifetime of the transient was quenched by the addition of acid, however led to the conclusion that it was the ground state anion **1.20**, the conjugate base of the pHP ester. Based on all of these findings, the current mechanism advanced by Givens and coworkers,^{39,40} illustrated in Scheme 1.6, involves the following sequence: initial absorption of light results in the formation of the singlet excited state that undergoes fast ISC to the triplet state. The triplet T_1 can follow two divergent reaction pathways, i.e., (1) ionization to form the triplet anion that relaxes to the ground state conjugate base of the starting ester without any photorelease or (2) deprotonation with loss of the leaving group to form a triplet biradical. This biradical relaxes and closes to form the cyclopropanone of the yet to be detected spirodienedione intermediate (**1.17**). The intermediate either undergoes hydrolysis to form the *p*-hydroxyphenylacetic acid (**1.15**), the major photoproduct, or decarbonylation to form the quinone methide intermediate (**1.26**) that subsequently hydrolyzes to form *p*-hydroxybenzyl alcohol (**1.27**), the minor photoproduct.

2.0 A Comparison of the Ground State, Base-activated and Photoactivated Favorskii Rearrangement, a Mechanistic Study

Only a few structures are known to undergo the photo-Favorskii rearrangement. Among them, the pHP derivatives are the only ones that have been extensively studied. In contrast, an array of compounds is known to undergo the ground state Favorskii rearrangement through a base activated process. The formal Favorskii rearrangement is essentially a process that leads to the formation of carboxylic acids, esters or amides from α -halo ketones in the presence of the appropriate nucleophilic solvents like water, alcohols or amines, and was first reported by Favorskii in 1894 (Equation 2.1).⁵⁴ Since then, the Favorskii rearrangement has found many applications in synthetic chemistry.⁵⁵ It has been employed for the synthesis of functionalized cyclopentyl units,⁵⁶ steroids,⁵⁷ α,β unsaturated carboxylic acids,⁵⁸ and polycyclic caged structures.⁵⁹

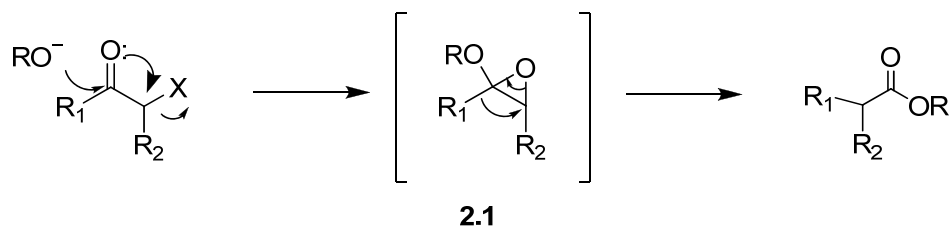


The Mechanism of Ground State Favorskii Rearrangement

The mechanism of the ground state Favorskii rearrangement has been studied extensively, and several mechanisms have been proposed by a number of different research groups. The earlier proposed mechanisms did not involve any symmetric intermediates and are named asymmetric mechanisms. Initially Favorskii⁶⁰ proposed a mechanism that involved attack of an alkoxide on the carbonyl carbon with concomitant removal of the halide resulting in an epoxyether (**2.1**). The rearrangement of the epoxyether resulted in the observed Favorskii product (Scheme 2.1). This mechanism was discarded when independently synthesized

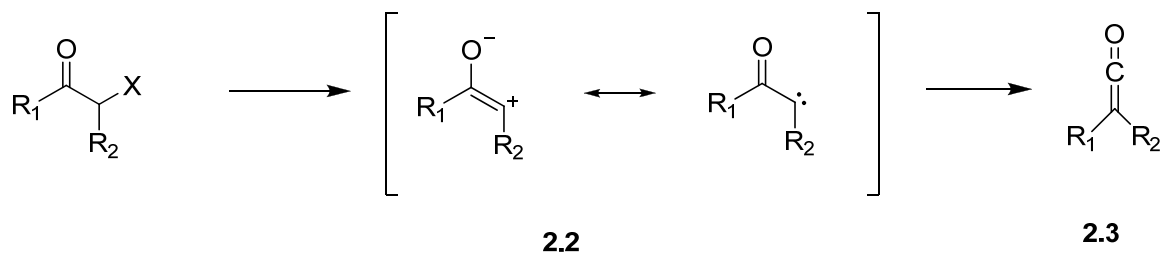
epoxyethers failed to undergo the rearrangement under a variety of conditions.⁶¹ However, the epoxyether intermediate is important in explaining the formation of byproducts.

Scheme 2.1



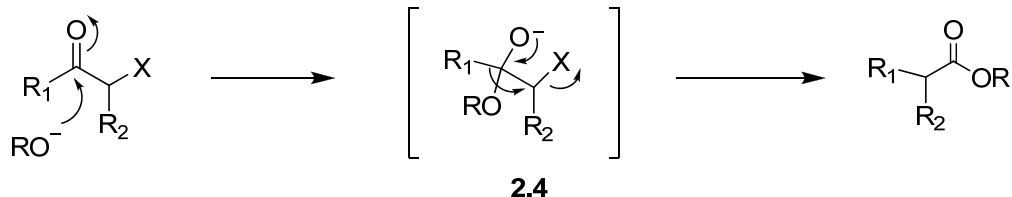
A second mechanism, proposed by Richard,⁶² predicted a ketene intermediate (**2.3**). The action of the base was represented as α -elimination of hydrogen halide to form an α -keto carbene **2.2**, which then rearranges to the ketene. The reaction of the ketene with the nucleophilic solvent results in product formation (Scheme 2.2). Direct formation of trialkyl acids and esters from a Favorskii reaction⁶³ are known and the ketene mechanism fails to explain these reaction products.

Scheme 2.2



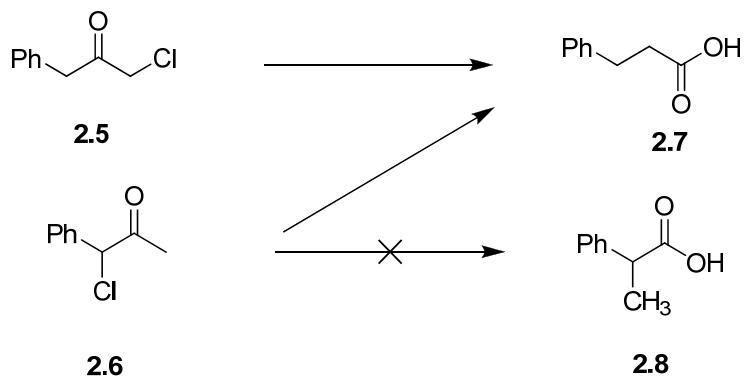
A third mechanism, termed a 'semibenzilic acid' rearrangement, due to its resemblance to the benzilic acid rearrangement,⁶⁴ was proposed by Tchoubar and Sackur in 1939.⁶⁵ The addition of the alkoxide to the carbonyl carbon results in intermediate **2.4**, which will undergo concerted removal of the halide ion with the 1,2 migration of the alkyl group producing the observed ester (Scheme 2.3).

Scheme 2.3



All three mechanisms discussed above fail in their prediction that the rearrangement product of an α -halo ketone will be different from that of the isomeric α' -halo ketone. They predict that chloro compounds **2.5** and **2.6** will give rise to rearranged products **2.7** and **2.8**, respectively. However, it was shown that both **2.5** and **2.6** result in same acid **2.7** (Scheme 2.4)⁶⁶ indicating that a convergence or an enforced symmetry of the two α -carbons must take place during the reactions. The only other possibility for the above three mechanisms to arrive at this result is by halogen migration prior to the rearrangement, which has not been observed.

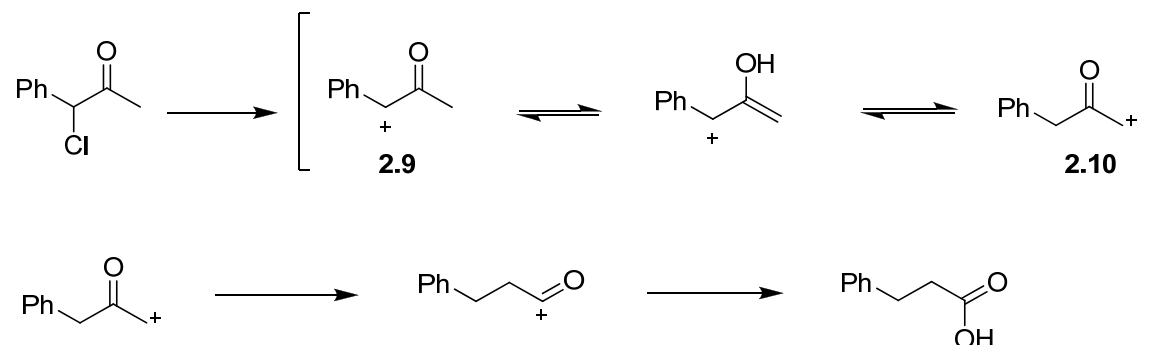
Scheme 2.4



McPhee and Klingsberg⁶⁶ then proposed a carbenium ion mechanism where the α -halo ketone initially undergoes dissociation to form the carbenium ion **2.9** that tautomerizes to form the carbenium ion **2.10** which subsequently rearranges to form the final acid. The main weakness of this mechanism is the inability to form carbenium ion **2.9** and the lack of any kinetic

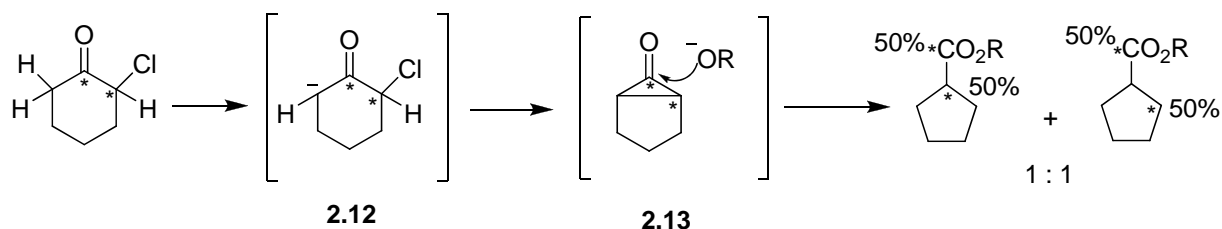
dependence on the base (Scheme 2.5). It should be noted that the Favorskii Rearrangement shows a 1st order dependence on base.

Scheme 2.5



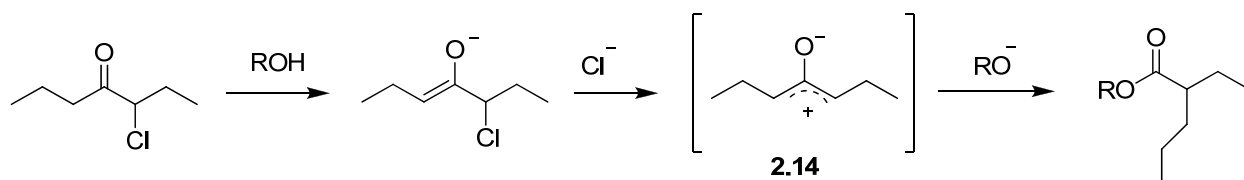
Following these reports, Loftfield⁶⁷ investigated the mechanism of the Favorskii rearrangement using C¹⁴ labeled 2-chlorocyclohexanone. When 1,2-(¹⁴C)-dilabeled-2-chlorocyclohexanone (the isotope equally distributed between the two adjacent carbon atoms) was reacted with sodium isoamyloxide in isoamyl alcohol, the product isoamyl cyclopentanecarboxylate had a labeled-carbon distribution of 50% of the ¹⁴C on the carbonyl carbon, 25% on the ring α -carbon and 25% on the ring β -carbon. The recovered chloroketone had the same distribution as the starting ketone. This finding necessitated a mechanism that symmetrizes the α and α' carbons at some point in the reaction sequence. Consequently, Loftfield proposed a mechanism going through a cyclopropanone intermediate that equates the two α -carbons (Scheme 2.6). This step is accomplished by first removing a proton from α' -carbon to form the enolate anion **2.12**. Concerted removal of the halide by nucleophilic S_N2 attack by the α' -carbanion results in cyclopropanone **2.13** that subsequently undergoes attack by the solvent to form the final rearranged product. Loftfield also reported that the reaction was first order with respect to both the haloketone and the base.

Scheme 2.6



Dewar⁶⁸ proposed a modification to the Loftfield mechanism based on his computational work which showed that an S_N2 type displacement of the halogen by the enolate **2.11** is unlikely due to unfavorable orbital overlap. He favored a dipolar oxyallyl zwitterion **2.14**, first suggested by Aston,⁶⁹ as the intermediate leading to the Favorskii product (Scheme 2.7). The zwitterion intermediate becomes important in explaining the formation of α -methoxyketones, a common byproduct in the Favorskii rearrangement.

Scheme 2.7

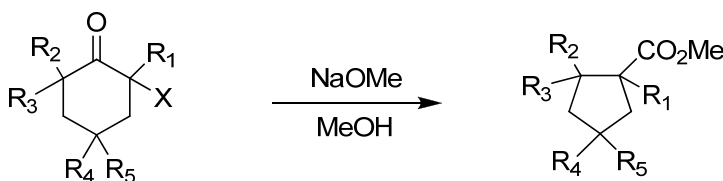


The most extensive and informative work on elucidating the mechanism of the Favorskii rearrangement was done by Bordwell and coworkers in a series of 11 papers over the period from 1967- 1973. Bordwell's work consisted of exploring different aspects of the Favorskii rearrangement and a very concise, abbreviated description of his work is given below.

Initial investigations by Bordwell *et al.*⁷⁰ dealt with identifying whether the formation of the cyclopropanone or dipolar intermediate was concerted by a 1,3 elimination or stepwise by halogen extrusion from the enolate form. The Loftfield⁶⁷ mechanism identifies the hydrogen

(the halogen containing and hydrogen containing carbons will be named as α and α' carbons, respectively, throughout this description) abstraction to form the enolate as the rate determining step (RDS). This was probed using leaving group effects (Cl vs. Br), kinetic isotope effects, and deuterium labeling studies on 4,4-disubstituted halocyclohexanones (Scheme 2.8). The results are illustrated in Table 2-1.

Scheme 2.8



2.15 $R_1, R_2, R_3 = H, R_4, R_5 = Ph, X = Br$

2.16 $R_1, R_2, R_3 = H, R_4, R_5 = Ph, X = Cl$

2.17 $R_1, R_2, R_3 = D, R_4, R_5 = Ph, X = Br$

2.18 $R_1, R_2, R_3 = D, R_4, R_5 = Ph, X = Cl$

Table 2-1. Rates of Halide Ion Release from α -Halocyclohexanones and Hydrogen Exchange During Reaction of Deuterated Cyclohexanones with NaOMe/MeOH at 0 °C.⁷⁰

α -Halo ketone	Rate Constant (k)/ $M^{-1}S^{-1} \cdot 10^4$	k_H/k_D	k_{Br}/k_{Cl}	Deuterons per molecule in halo ketone	Deuterons per molecule ($t_{1/2}$)	Deuterons per molecule (pdt)
2.15	71					
2.17	17	4.1		2.8 ^a (2.28) ^b	1.5 ^a (1.68) ^b	0.7 ^a (0.78) ^b
2.16	0.61		116			
2.18	0.58	1.05		2.0 ^a (1.80) ^b	0 ^a (0.03) ^b	0 ^a (0.05) ^b

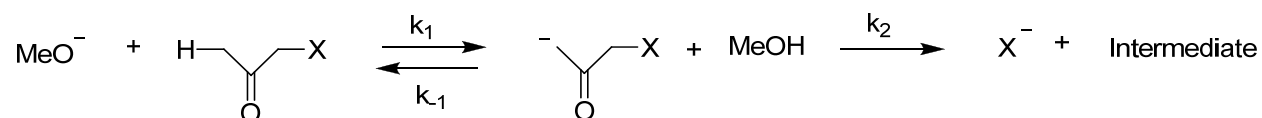
^afrom NMR analysis ^bfrom mass spectrometric analysis

Previous work had shown that chloride was a better candidate for Favorskii rearrangement than bromide,⁷¹ but 4,4-diphenyl-2-bromocyclohexanone (**2.15**) underwent the Favorskii reaction more efficiently and cleanly than the chloride derivative. This unusual observation of an element effect can be explained in terms of a combination of configurational and conformational interactions. The trans configuration is required for epoxyether formation for one of the reactions that competes with the Favorskii rearrangement. From this isomer (**2.15**), the conformation for the competing process demands that both the bromide and the phenyl group

be in axial positions. The unfavorable steric interaction between the phenyl and bromo groups makes this conformation less favorable rendering the Favorskii reaction the dominant pathway for 4,4-diphenyl-2-bromocyclohexanone.

From kinetic studies, the relatively large element effect of the leaving group ($k_{\text{Br}}/k_{\text{Cl}} = 116$) and the lack of a primary kinetic isotope effect (PKIE) for the chloro compound **2.16** suggests that the carbanion formation for this derivative is reversible. The PKIE for the bromo isomer **2.17** is relatively small for a primary isotope effect and indicates partial deuterium loss by exchange is occurring before the halide release. This is supported by a hydrogen/deuterium exchange study. For **2.18** ($X = \text{Cl}$), complete exchange at both α - and α' - positions is achieved in one half life, whereas for **2.17** ($X = \text{Br}$) the exchange is evident but not complete. This complete exchange for the chloro derivative and partial exchange for bromo derivative was further supported by isotope distribution studies performed with NaOMe in MeOD for 4-methyl-4-phenyl-2-chlorocyclohexanone and 4-methyl-4-phenyl-2-bromocyclohexanone.

The rate constant observed (k_{obsd}) for the reaction can be written as shown in equation 2.2 employing a steady state approximation for carbanion formation.



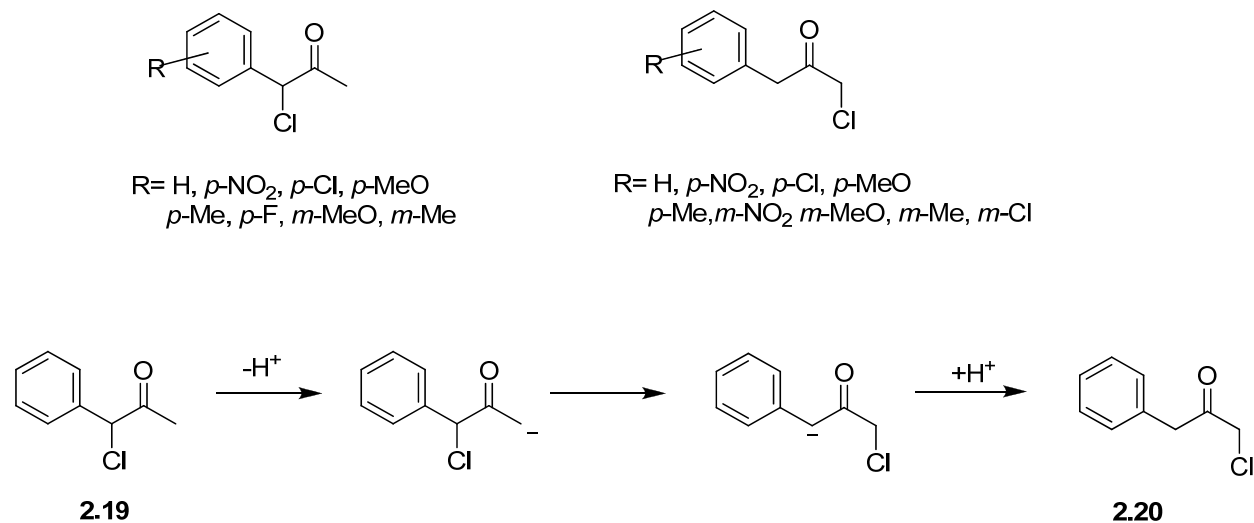
$$k_{\text{obsd}} = k_1 k_2 / (k_{-1} [\text{MeOH}] + k_2) \quad \text{Eq. 2.2}$$

For the chloro isomer **2.16**, k_{-1} is much larger than k_2 , thus k_{obsd} simplifies to $k_{\text{obsd}} = k_1 k_2 / (k_{-1} [\text{MeOH}]) = K k_2$, where K is the equilibrium constant for carbanion formation. However, for the bromide **2.15**, assuming 25% exchange at the α' position, loss of halide (k_2) is greater than k_{-1} , making k_1 limiting for k_{obsd} . Therefore, for the bromocyclohexanone **2.15**, the Loftfield postulate that α' -hydrogen abstraction is rate limiting holds but not for the chlorocyclohexanone

2.16, for which the loss of the halide becomes rate limiting. In any event, it is evident that the loss of the halide occurs from the enolate form and not from a concerted 1,3 elimination process as suggested by others.⁷²

The next investigation by Bordwell and coworkers^{73,74} was based on two acyclic isomers, ArCHClCOCH_3 and $\text{ArCH}_2\text{COCH}_2\text{Cl}$, and their meta and para substituted analogs. The study was designed to investigate two major facets of the reaction mechanism; the effect of electronic and structural variations and the possibility of halide migration prior to the rearrangement (Scheme 2.9). Halide migration was proposed as a possible route to the observed Favorskii products from the asymmetric mechanisms discussed earlier.⁷¹

Scheme 2.9



A deuterium exchange study done on the 1-chloro-1-phenylpropan-2-one (**2.19**) showed extensive exchange at the α' position in accordance with the previous study⁷⁰ suggesting a fast, reversible deprotonation followed by halide loss in the RDS. Therefore, meta and para substituents on the aryl ring of **2.19** should give evidence for the formation of either the cyclopropanone⁶⁷ intermediate or the dipolar zwitterion intermediate.^{68,69} The rates of chloride

release for the substituted ketones are shown in Table 2-2. The data clearly show that electron donating groups accelerate the reaction while electron withdrawing groups hinder it. It is interesting to note that the *p*-NO₂ derivative yielded no Favorskii product under these conditions. The Hammett plot generated by plotting log k_{cor} (from Table 2-2) vs. σ^+ , gave a ρ value of -2.37. σ^+ Values were used as an attempt to generate a Hammett plot with σ values failed, indicating that the substituents stabilize the positive charge developing in the transition state by direct resonance. Both the negative ρ value and the correlation with the σ^+ values are supportive of a rate determining transition state with carbenium ion character.

Table 2-2. Rates of Chloride Ion Release in the Reactions of *meta* and *para* Substituted Derivatives of **2.19** with Excess NaOMe in MeOH at 0 °C⁷²

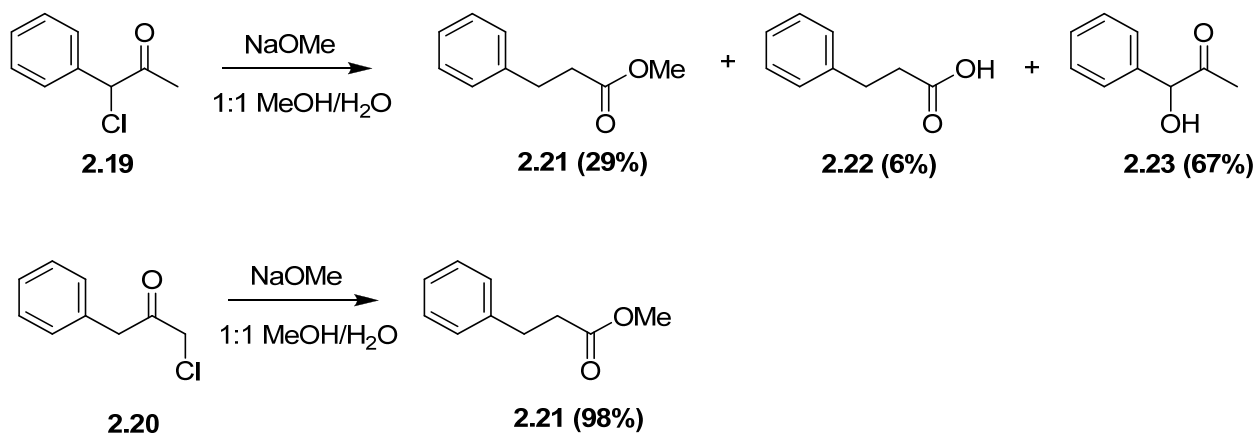
R	$k_{\text{obsd}} / 10^3$	$k_{\text{Favorskii}} / 10^{3a}$	$k_{\text{cor}} / 10^3 b$
H	3.09	0.40	0.40
<i>p</i> -NO ₂	5.09		
<i>p</i> -Cl	6.21	0.31	0.26
<i>p</i> -MeO	39.4 ^c	26.8	36.3
<i>m</i> -MeO	2.72	0.33	0.29
<i>p</i> -Me	6.00	1.50	1.79
<i>m</i> -Me	3.23	0.45	0.49
<i>p</i> -F	7.5	0.83	0.77

^a corrected for only the Favorskii ester formation, ^b corrected for changes in the equilibrium constant, ^c only 31% hydrogen exchange at the α' position

The prominent byproduct from these reactions is a hydroxy ketal, arising from the epoxy ether intermediate.⁶⁷ The effects of temperature, methoxide ion concentration and the ionic strength on the Favorskii reaction were also explored for the chloroketone **2.19**. The yield of the Favorskii ester increases at higher temperatures. In 2.0 M NaOMe the Favorskii ester yield increased from 21% to 61% when the temperature was raised from 0 °C to 65 °C. Parallel to this, the yield of the hydroxy ketal byproduct decreases with increasing temperature. Similarly, the

increase of methoxide concentration and addition of LiClO₄ also resulted in the increase of Favorskii product.⁷³ The chloroketone **2.20** behaved in a similar manner when tested at higher temperatures, alkoxide concentrations and ionic strengths. The effects of the substituents were also similar to **2.19**, i.e. electron donating groups made the Favorskii reaction more favorable while electron withdrawing groups had the opposite effect. The noticeable difference between these two chloropropanones was their difference in product distribution under identical conditions: ketone **2.19** in 0.05 m NaOMe (1:1 MeOH:H₂O) gave the Favorskii ester **2.21**, Favorskii acid **2.22** and the byproduct α -hydroxy ketone **2.23** in 29% , 6%, and 67% yield respectively. The 1-chloro isomer **2.20** under the same conditions resulted in the formation of the Favorskii ester **2.21** in 98% yield and no byproducts were observed (Scheme 2.10). However, the formation of the α -hydroxyl ketone byproduct was observed for *m*-Cl and *m*-NO₂ derivatives of **2.20**.

Scheme 2.10



The complete lack of byproduct formation from **2.20** and the difference in product distribution between **2.19** and **2.20** essentially excludes the possibility of halogen migration prior to the rearrangement. Substituent effects on the **2.20** system gave a Hammett correlation with a

ρ value of -2.93 ($\log k_{\text{obsd}}$ vs. σ^+). If a concerted 1,3-elimination were operative for the generation of the cyclopropanone intermediate, the Hammett correlation should have given a positive ρ value by analogy with the 1,2-elimination of $\text{ArCH}_2\text{CH}_2\text{Cl}$ where the ρ values range from +2.07 to +3.77.⁷⁵ This and the extensive deuterium exchange at the α' position disfavor a concerted mechanism. The large ρ value observed for **2.20** also excludes the possibility of carbene formation as the loss of halide from the carbanion $[\text{ArCH}_2\text{COCHCl}]^-$ should be relatively insensitive to substituent effects. The authors account for the observed ρ value by breaking it down to a combination of two steps in the reaction, the initial carbanion formation and the subsequent chloride loss from the carbanion. The carbanion generation should give rise to a positive ρ value. The observed negative value indicates that there is substantial positive charge development at the carbon atom bonded to the chloride leaving group during the departure of the chloride which, therefore, is the rate determining transition state leading to either the zwitterionic or cyclopropanone intermediates as illustrated as in Figure 2-1. This is also supported by the greater substituent effects observed for **2.19** compared to **2.20**. The Favorskii reaction is more favorable in 0.1 M LiClO_4 and in the presence of water which is also indicative of an ionic or highly polar rate determining transition state.

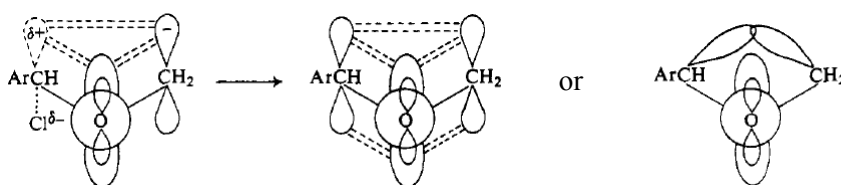
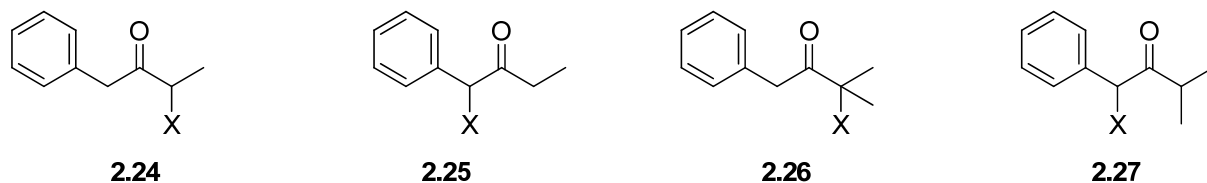


Figure 2-1. Possible transition states for the formation of the zwitterion or cyclopropanone intermediates.⁷⁴ Reproduced with permission from Journal of American Chemical Society.

Due to the polar character of the transition state, methyl substitution on the chloride bearing carbon (α carbon) should greatly enhance the ionization process making the Favorskii

reaction more favorable. This hypothesis was tested by Bordwell and coworkers employing four di- and monomethyl substituted halo ketone systems (Scheme 2.11).^{76,77}

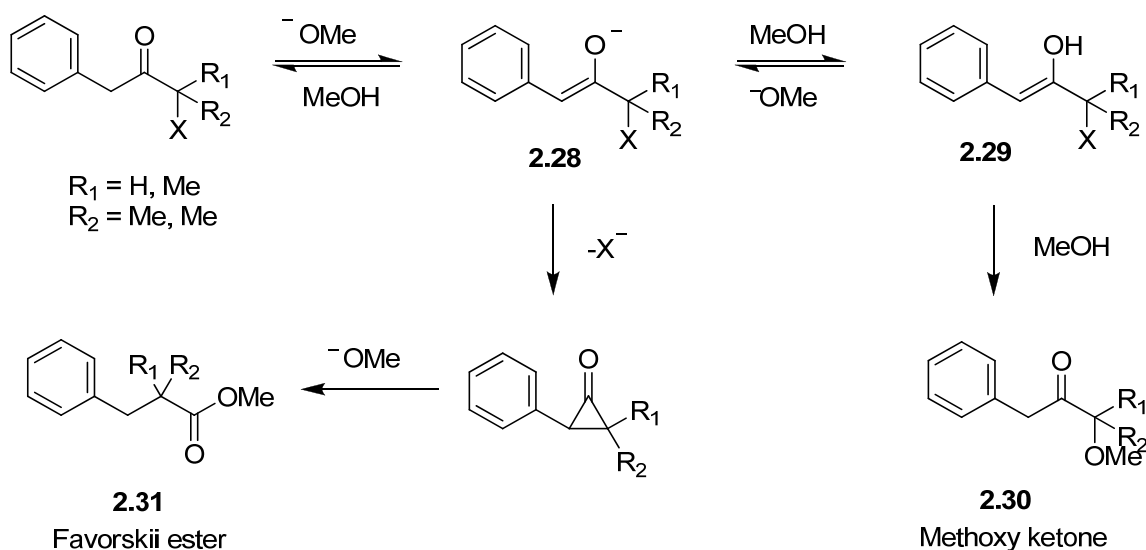
Scheme 2.11



As previously mentioned, 1-chloro-2-phenylpropan-2-one (**2.20**) undergoes exclusively Favorskii rearrangement in 0.05 M NaOMe in MeOH at 0 °C.⁷⁴ In contrast, when an α hydrogen is replaced with a methyl group (i.e., **2.24**) the major product observed is the α -methoxy ketone.⁷⁶ The formation of the Favorskii ester was observed at higher concentrations of methoxide. This observation was accompanied by a smaller extent of deuterium exchange, a smaller element effect ($k_{\text{Br}}/k_{\text{Cl}}$) and a positive, though smaller magnitude Hammett ρ value of + 0.95. These indicate that the rate determining step (RDS) for **2.24** is proton abstraction by the methoxide ion to form the enolate as opposed to the halide loss as is the case for **2.20**. On the other hand, replacing an α' -hydrogen of 1-chloro-1-phenylpropan-2-one (**2.19**) with a methyl group results in the formation of the Favorskii ester and methoxy ketone (byproduct) while the parent chloro compound **2.19** gave mostly α -hydroxy ketone (formed by degradation of α -methoxyoxarines) with very low yields of the Favorskii ester (13%).⁷⁴ When the tertiary halo ketone **2.26** was exposed to Favorskii conditions (0.05 M NaOMe in MeOH), α methoxy ketone (97%) along with a small amount of the Favorskii ester (3%) were observed. When 1.0 M NaOMe was employed, the percentage of the Favorskii product increased to 35% at the expense of the α -methoxy ketone. A similar observation was recorded for the secondary halo ketone **2.27**. When

2.27 (X=Br) was subjected to 1.0 M NaOMe, the major product was the α -hydroxy ketone (65%) with smaller amounts of α -methoxy ketone (15%) and Favorskii ester (15%). Kinetic studies done on **2.27** revealed a $k_{\text{Br}}/k_{\text{Cl}}$ ratio of 1.5. These observations were important in understanding the mechanism of the Favorskii rearrangement as they revealed the importance of enol-enolate equilibrium. The decrease in Favorskii products in methyl substituted 1-halo systems (**2.20**, **2.24**, **2.26**) is attributed to preferable formation of the enol form at low ethoxide concentration (Scheme 2.12). The enol will undergo solvolysis by methanol to form the α -methoxy ketone while the enolate will undergo Favorskii rearrangement. As the ratio of enolate/enol (**2.28/2.29**) will be directly proportional to the concentration of the methoxide, this mechanism suggests that the ratio of the two products, Favorskii ester to α -methoxy ketone (**2.31** to **2.30**), will increase linearly with methoxide concentration. This was empirically demonstrated by the authors for the 1-chloro ketone **2.24**.⁷⁶ A plot of methoxide concentration vs. **2.29/2.28** was linear with a correlation coefficient of 0.994. The mechanism of α -methoxy ketone formation was explored by Bordwell *et al.* in a separate study.⁷⁸

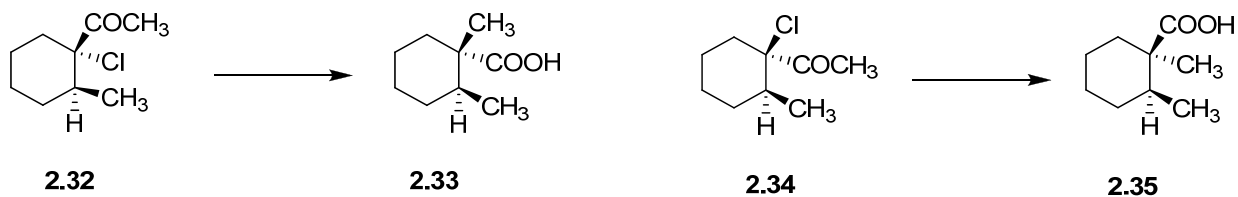
Scheme 2.12



All in all, Bordwell and coworkers' extensive study of the mechanism of the Favorskii rearrangement employed only two basic systems, ArCHXCOCH_3 and $\text{ArCH}_2\text{COCH}_2\text{X}$. After an all encompassing study on these two models, it was evident that these systems undergo Favorskii rearrangements by two mechanistic paths. When unsubstituted chloroketones were used, the desired path is the reversible formation of a carbanion (enolate) followed by rate determining halide extrusion. However with α -methyl substituents, halide loss is greatly accelerated, making the proton removal rate limiting. This was further established using α -halodiphenyl and α -halotriphenylpropanones.⁷⁹

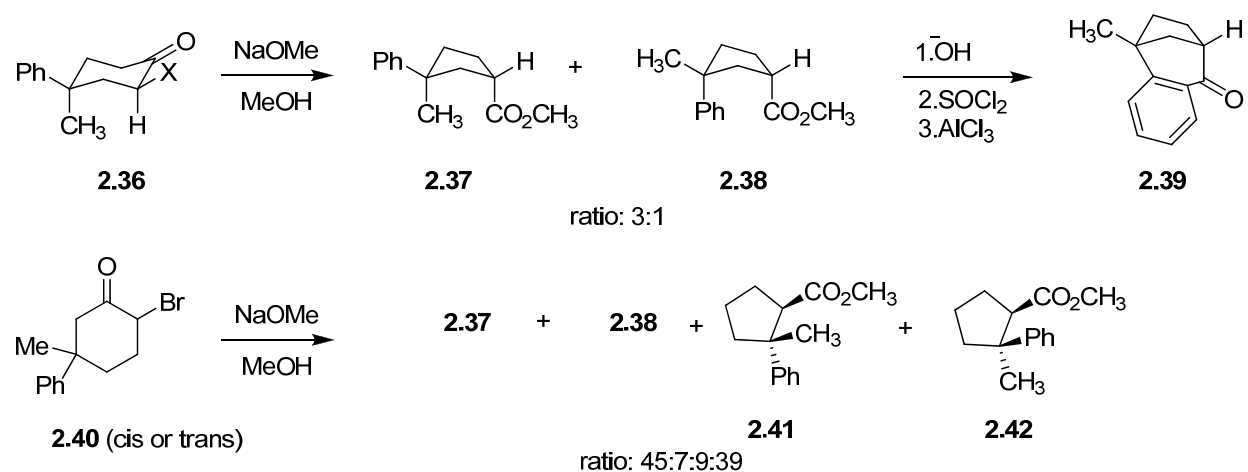
Stereospecific implications of the Favorskii rearrangement have also been explored by Bordwell and co-workers.⁸⁰ The stereochemistry of the Favorskii product is important in distinguishing between a concerted formation of the cyclopropanone intermediate and the intermediacy of a zwitterionic species. If the cyclopropanone is formed by an $\text{S}_{\text{N}}2$ displacement of the halide from the enolate as Loftfield⁶⁷ suggested, the reaction should proceed with inversion at the α -carbon (the halogen containing carbon). But if the reaction proceeds via the zwitterionic intermediate as suggested by Dewar,⁶⁸ racemization at the α -carbon should be observed. Prior work done by Stork *et al.*,⁸¹ which supported the Loftfield postulate, showed that 1-chloro-1-acetyl-2-methylcyclohexane **2.32** rearranged to form the acid **2.33** while the epimeric haloketone **2.34** gave the Favorskii acid **2.35** (Scheme 2.13).

Scheme 2.13



Bordwell's⁸⁰ investigation of stereochemistry of the Favorskii rearrangement was based on two cyclohexanones **2.36** and **2.40**. When **2.36** was subjected to 0.2 M NaOMe/MeOH, two esters, **2.37** and **2.38**, were formed in a ratio of 3:1. When the esters were further converted to their acid chlorides and reacted with aluminum chloride the cis ester **2.38** cyclized to form the bicyclic ketone **2.39**. Bicyclic ketone formation is impossible for the trans isomer **2.37** (Scheme 2.14). When 2-bromo-5-methyl-5-phenylcyclohexanone (**2.40**, cis or trans) was subjected to the same conditions the same esters, **2.37** and **2.38**, and two new esters, **2.41** and **2.42**, were observed in 45:7:9:39 yields, respectively.

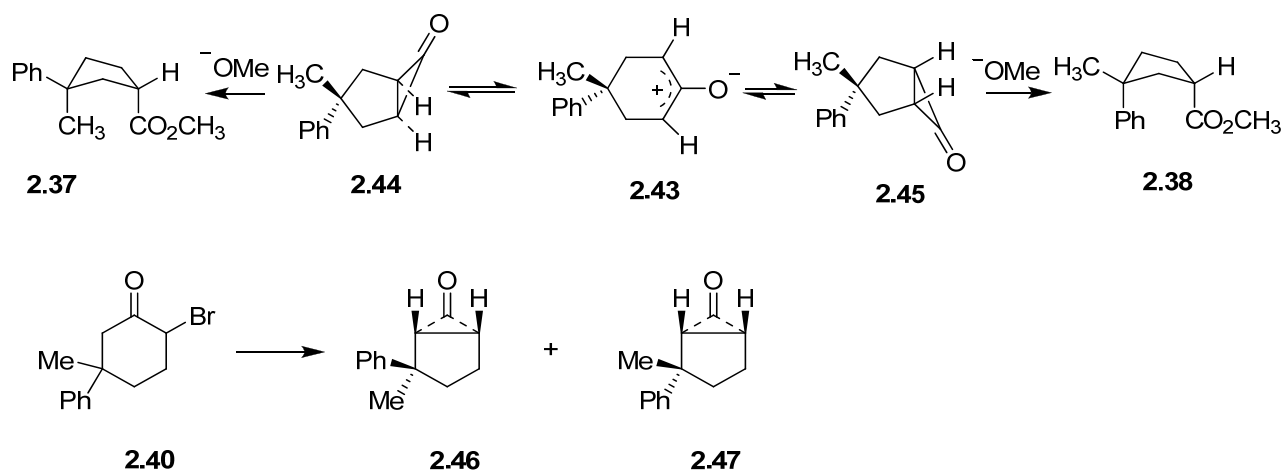
Scheme 2.14



For **2.36**, if the Lofthield mechanism were operative, inversion of configuration should result when the halogen is equatorial and retention when the halogen is axial. The major product observed, **2.37**, is formed with retention of configuration. In the case of **2.40**, an S_N2 displacement should result in ester **2.38**, but the major product observed is the same ester obtained from **2.36**, i.e. ester **2.37**. The product distribution for **2.36** is explained in terms of a dipolar ion (**2.43**) that can close in a disrotatory manner to give the cyclopropanone **2.44** or **2.45** (Scheme 2.14). The observation that the ratio of product changes with methoxide concentration

is a further indication that there may be more than one intermediate. The authors explain the formation of four esters from **2.40** by two different cyclopropanone intermediates (**2.46** and **2.47**) that can each ring open to give the two products (Scheme 2.15).

Scheme 2.15



After this extensive study on the mechanism of the Favorskii rearrangement, the most probable pathway portrayed from the results of Bordwell, *et al.* would be described as below. The initial α' -hydrogen abstraction by alkoxide results in the enolate ion that will undergo loss of the halide to generate a dipolar intermediate. The RDS of the reaction can be either the enolate formation or the halide loss depending on the molecule in question. The dipolar ion intermediate can then undergo ring closure to form the cyclopropanone intermediate that will further react with alkoxide to generate the Favorskii products. The enolate ion is in equilibrium with the enol form, which is especially favored at low alkoxide concentrations, and leads to the formation of the byproducts. Although this mechanism is acceptable for most cases, more work is necessary to understand the stereochemical outcomes of the rearrangement.

Several computational studies have been performed on the Favorskii rearrangement. The work reported by Schadd *et al.*⁸² employing *ab initio* calculations (Ditch-

field, Hehre, and Pople's 4-13G Gaussian basis set⁸³) for 1-halo-2-propanone systems showed that the cyclopropanone is 49 kcal/mol more stable than the dipolar zwitterion and identifies a zwitterions like transition state leading to the cyclopropanone. Andres *et al.*^{84,85} used extensive computational calculations, using Hartree-Fock level theory with 6-31G* and 6+31G* basis sets and electron corrections at the MP2/6-31G* level DFT calculations⁸⁶ to distinguish between the semibenzilic acid and cyclopropanone mechanisms. Their initial investigation⁸⁴ included the development of the potential energy surface (PES) for the Favorskii rearrangement of α -chlorocyclobutanone for both mechanisms in vacuo and with solvent molecules present. In the semibenzilic acid mechanism, the initial step was nucleophilic attack on the carbonyl carbon by the hydroxyl group followed by the ring contraction with the loss of the halide. Thus, the semibenzilic acid is a two step mechanism with the last step being rate limiting. This was further supported by data obtained from quantum mechanical and molecular mechanics studies on α -chlorocyclobutanone and α -chlorocyclohexanone.⁷⁶ The stationary points and the PES for the semibenzilic acid mechanism for α -chlorocyclobutanone are illustrated in Figure 2-2. In the cyclopropanone mechanism, the initial step is the removal of an α' -hydrogen by hydroxide. The subsequent loss of halide by the attack of the carbanion thus formed gives rise to the bicyclic intermediate that is hydrolyzed to the Favorskii product. The last step of the reaction was shown to be rate limiting. The stationary points and the PES for the cyclopropanone mechanism for α -chlorocyclobutanone are illustrated in Figure 2-3. Another step was added to this reaction mechanism by the authors in their 2001 publication.⁸⁵ After the formation of the bicyclic intermediate, the bond between the carbonyl carbon and the α' carbon breaks to generate an acylium ion. The final product results from the general base catalyzed hydration of the acylium ion.

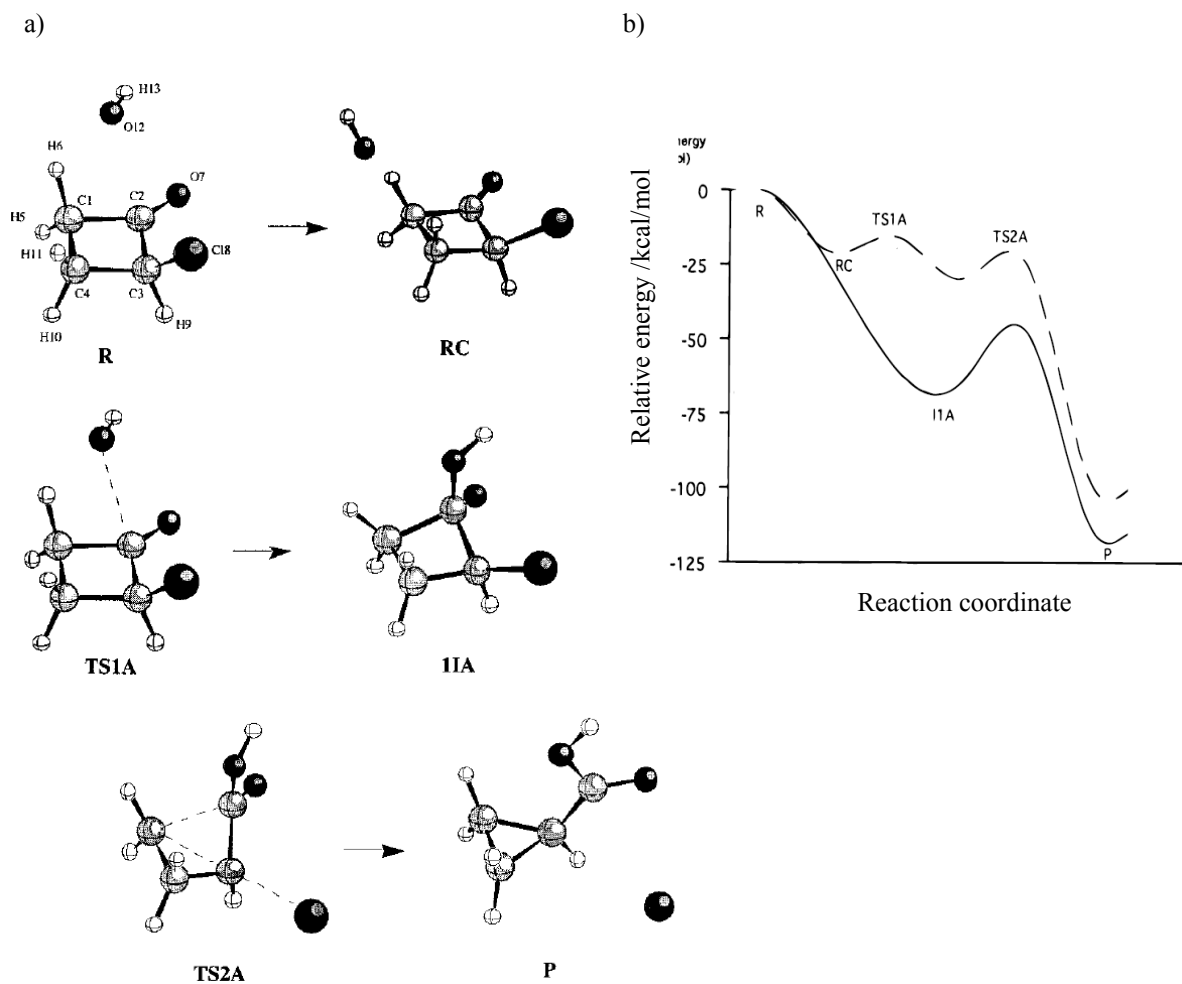


Figure 2-2. (a) Representation of stationary points for semibenzoic acid mechanism (b) Schematic potential energy diagram with relative energies of stationary points for semibenzoic acid mechanism. Continuous lines *in vacuo* and broken lines in aqueous media.⁸⁴ Reproduced with permission from Journal of the American Chemical Society.

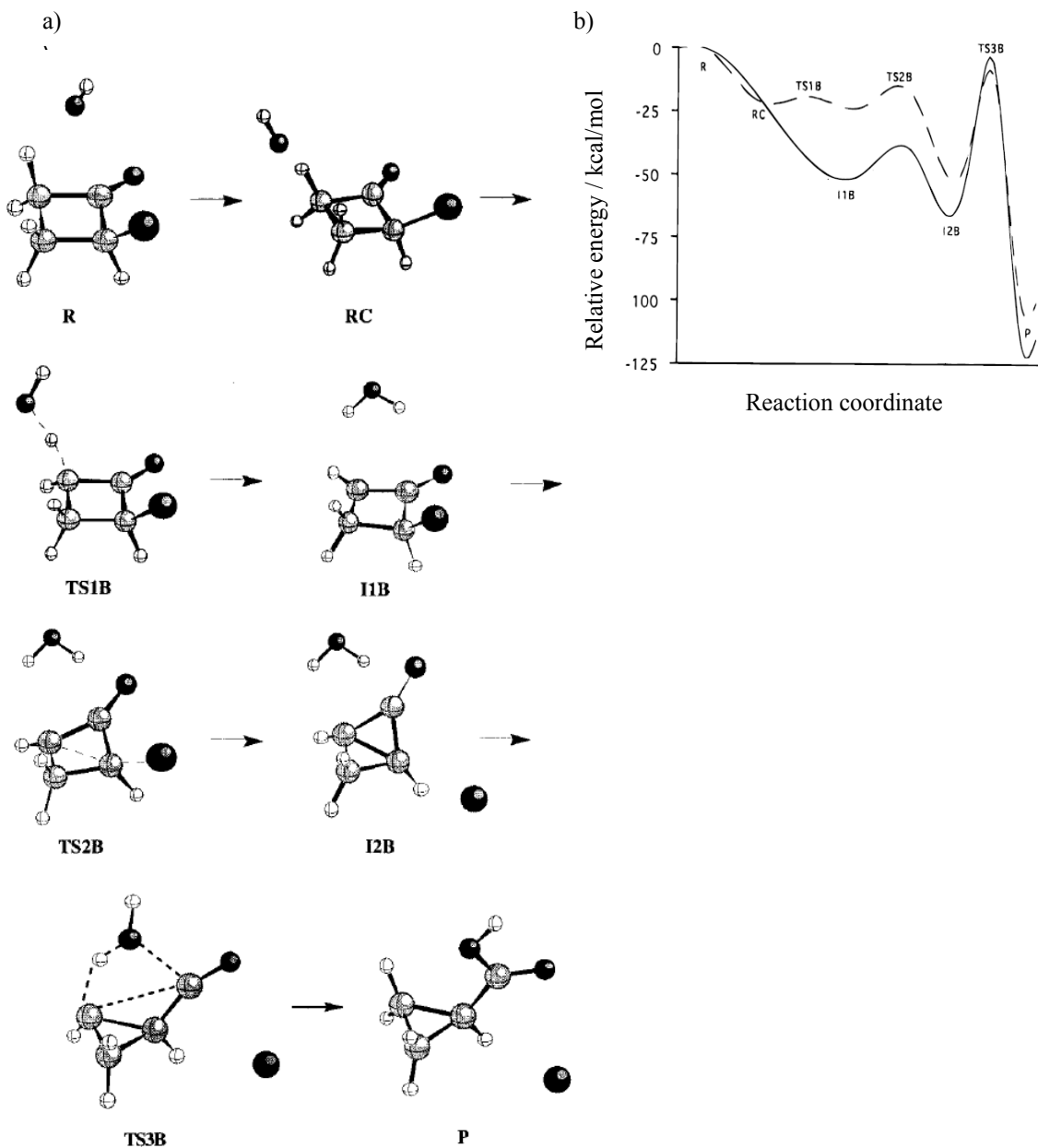


Figure 2-3. (a) Representation of stationary points for cyclopropanone mechanism (b) Schematic potential energy diagram with relative energies of stationary points for cyclopropanone mechanism. Continuous lines *in vacuo* and broken lines in aqueous media.⁸⁴ Reproduced with permission from Journal of the American Chemical Society.

According to this theoretical investigation, the semibenzilic acid mechanism ($E_a \sim 17.6$ kcal/mol where E_a is activation energy for the RDS) was clearly favored over the cyclopropanone mechanism in gas phase studies ($E_a \sim 42.6$ kcal/mol). When solvent effects were considered, solvent-solute interactions were shown to reduce the energy barrier for the cyclopropanone mechanism more than the semibenzilic acid mechanism. The semibenzilic acid mechanism still remained more favorable. However the authors state that the solvent effects are strong enough to control which mechanism a molecule will follow under given conditions. The theoretical investigation⁸¹ based on both α -chlorocyclobutanone and α -chlorocyclohexanone revealed that the semibenzilic acid mechanism is preferred for the strained α -chlorocyclobutanone while the cyclopropanone mechanism is the more favorable path for α -chlorocyclohexanone.

Sorensen and coworkers⁸⁷ conducted a theoretical study to investigate the formation of the cyclopropanone intermediate including the stereochemical outcome. Their initial investigation of the simple chloroketone, 1-chloropropan-2-one, furnished an interesting observation. The route to the cyclopropanone formation from the ground state enolate showed two different transition states (TS) leading to two different cyclopropanone structures. These transition states, when relaxed to the ground state enolates, gave two enolates with different dihedral angles, one with a dihedral angle less than 90° and the other with a dihedral angle close to 180° . This was found to be true for several other acyclic haloketones and it was generalized that when the dihedral angle is 60 - 80° for the ground state enolate, the cyclopropanone is formed with inversion of configuration at the carbon containing the halogen while those enolates with dihedral angles of $\sim 180^\circ$ resulted in cyclopropanones with retention of configuration (Figure 2-4)

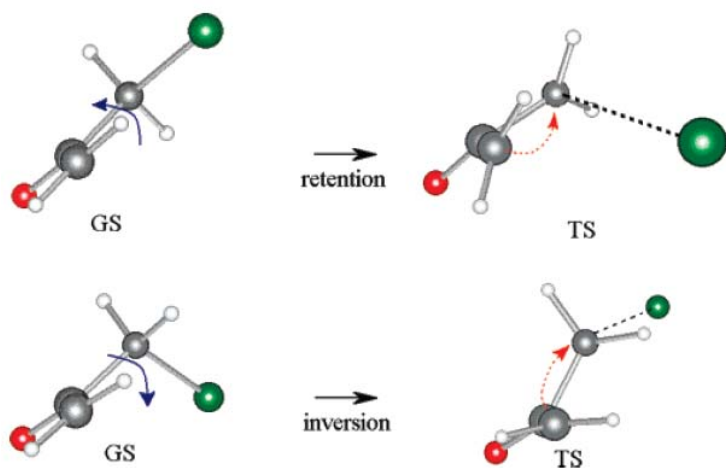


Figure 2-4. The inversion and retention transition state structures for the enolate of **2.36**.⁸⁷ Reproduced with permission from Journal of Organic Chemistry.

When 1-(1-chlorocyclohexyl)ethanone was subjected to the same investigation, both retention and inversion TS's were involved when chloride was in the axial position while only retention TS's were observed for the equatorial isomer. For 2-chlorocyclohexanone, two ground state enolates were predicted, both having the ability to undergo cyclopropanone formation with retention or inversion of configuration. The TS's for both isomers were shown to be sterically less hindered since they take a chair-like conformation compared to the half chair of the ground state enolates.

The authors claim that the inversion of configuration occurs from a concerted S_N2 type displacement of the halogen. This claim was supported by the plot of C-Cl bond distance as a function of cyclopropanone ring closure for the chloroenolate (red line in Figure 2.5). Retention of configuration takes place mostly in an asynchronous manner (blue line in Figure 2-5). The new carbon-carbon bond between the α,α' -carbons is only about 30% formed at the transition state. For all compounds investigated in this study, the inversion route was more favorable and any possibility of forming an oxyallyl intermediate in the inversion path was discarded. However, solvation-simulation calculation studies applying a polarizable continuum mode⁸⁸

indicated that the retention transition state was favorable in the presence of solvent-solute interactions.

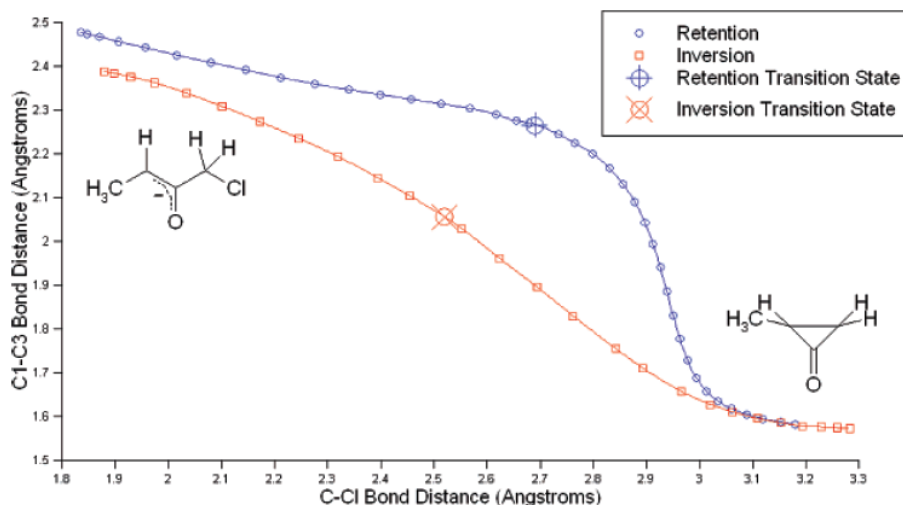


Figure 2-5. Cyclopropanone ring formation as a function of C-Cl bond distance.⁸⁷ Reproduced with permission from Journal of Organic Chemistry.

Yamabe and coworkers⁸⁹ performed an investigation of the cyclopropanone formation with explicit consideration of hydrogen bond formation using DFT calculations (B3LYP method⁹⁰). The study was based on α -chlorocyclopropanone in NaOMe/MeOH and their calculations showed that the ring opening of the cyclopropanone intermediate is much more favorable when more than one methanol molecule is included (Figure 2-6). The decrease in activation energy is such that the cyclopropanone pathway becomes energetically more favorable than the semibenzilic acid (39.52 kcal/mol) route under these considerations. However, the addition of the methoxide to the carbonyl carbon in the first step of the semibenzilic mechanism requires so little energy (2.77 kcal/mol), it is possible that the resulting tetrahedral intermediate coexists with the starting chlorocyclohexanone.

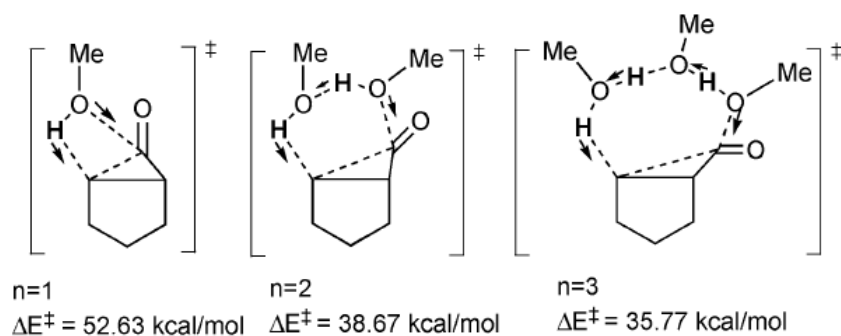
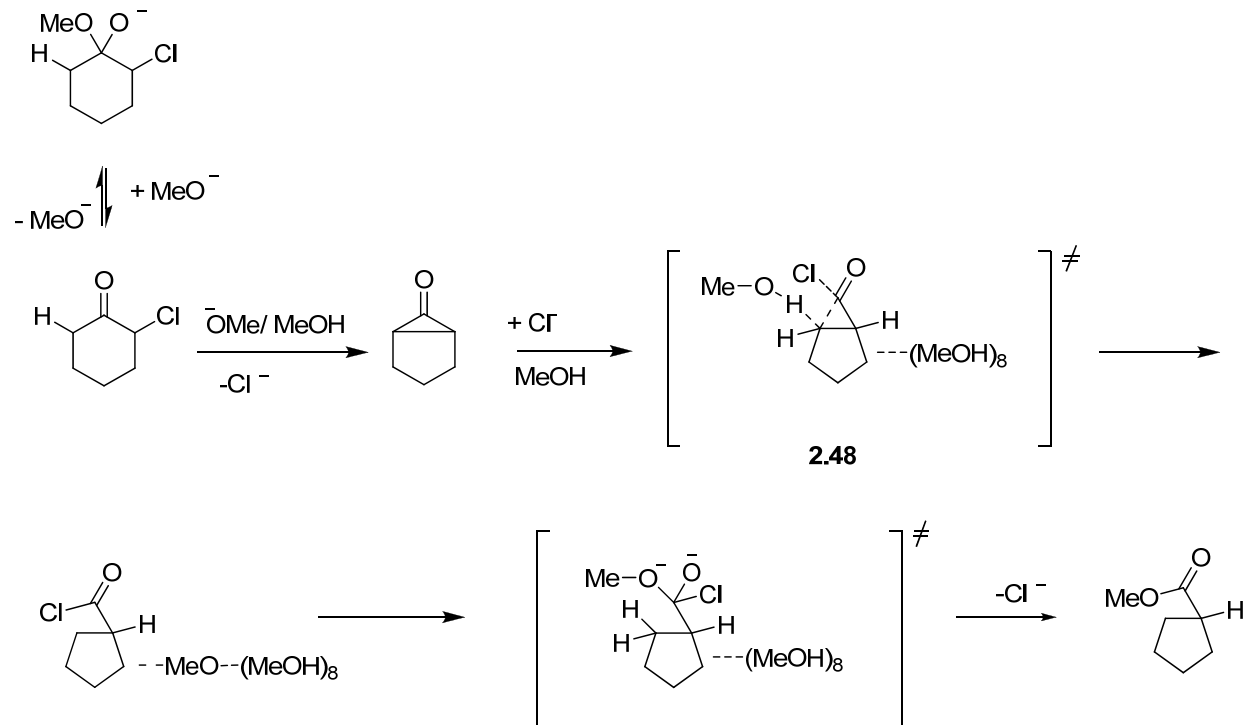


Figure 2-6. Concerted proton relays in MeOH addition to the cyclopropanone transition state⁸⁹
 Reproduced with permission from Organic and Biomolecular Chemistry.

The authors also claim that the cyclopropanone intermediate is surrounded by a tight MeOH cluster and the energy required for methoxide to approach the intermediate is high. They propose that the released chloride ion, which will be in close proximity, can act as the nucleophile and induce the ring opening of the cyclopropanone to form an acyl chloride intermediate (**2.48**) with the assistance of 9 methanol molecules. The acyl chloride intermediate then will undergo subsequent attack by methoxide to yield the Favorskii product. This new mechanism for the Favorskii rearrangement is illustrated in Scheme 2.16.

59Scheme 2.16



Despite these extensive studies, it is clear that the mechanism of both the photo-activated and base-activated Favorskii rearrangement is yet to be fully understood.

1.1 Statement of the Problem

The *p*-hydroxyphenacyl (pHP) moiety has acquired a reputation as an efficient photoremovable protecting group (PPG) over the last decade, and attracted the interest of researchers in many areas of chemistry. One shortcoming of the pHP group is its relatively narrow useful range of absorbing wavelengths, especially at wavelengths > 300 nm. A logical approach is to extend the absorption spectrum by introducing auxochromes, i.e., substituents that will extend the range. Givens *et al.*^{38,40,91} have screened the effects of substituents on the photochemistry of the pHP chromophore with an array of attached auxochromes that contain both electron donating and electron withdrawing examples. The results have shown that electron donating groups generally shift the absorbance to longer wavelengths but this has led to lower quantum yields. Electron withdrawing groups increase the quantum yields, they unfortunately, have not significantly extended the absorption range.

The mechanism of the photorelease has been extensively studied but is not yet fully understood. Structure-activity relationships that can be obtained by studying the effects of these same substituents would further contribute immensely to a more complete understanding of the mechanism. The cyano group is a strong electron withdrawing group due to its more electronegative nitrogen. Its enhanced π - accepting capability also contributes to the electron withdrawing ability. Furthermore, the CN group has a smaller size than most substituents; it is incapable of forming strong H-bonds. Thus, its function as an electron withdrawing group alone has made the cyano substituent a desirable addition to our previous set of substituent studies. The objective of the research project is to fine tune the properties of the pHP chromophore in hopes of making it a more striking, more useful PPG for photorelease applications and to explore the

effects of the cyano group on the mechanistic parameters affecting the photo-Favorskii rearrangement.

2.1 Statement of the problem

The ground state, base-activated Favorskii rearrangement has been known since 1984⁵⁴ and has found many applications in organic synthesis. The mechanism of the reaction was vigorously pursued by Bordwell *et al.*,^{70,73,74} whereas the photochemical counterpart, the photo-Favorskii rearrangement, has received less scrutiny and has been limited to investigating only a narrow range of structural entities, most notably the *p*-hydroxyphenacyl (pHP) group. The pHP entity possesses the functional apparatus necessary for delivering the required elements for rearrangement, namely a potential for a zwitterions intermediate and a putative cyclopropanone intermediate, upon treatment with base.

The possibility that these caged pHP derivatives might undergo a ground state, base-activated Favorskii rearrangement is an intriguing one. If pHP derivatives did undergo the well established ground state Favorskii rearrangement, the potential exists that other known Favorskii substrates by analogy might undergo a similar reaction in the excited state, and thereby expand the number of examples of the heretofore elusive photo-Favorskii rearrangement. Literature precedence for Favorskii rearrangement of molecules similar in structure to the pHP chromophore is rare. Therefore exploring the behavior of pHP derivatives with varying leaving groups, under traditional Favorskii conditions would be instructive.

The applicability of using photoremovable protecting groups in any given study will depend on a variety of features including wavelength, solubility, stability, and rate of photorelease. Among these, good to excellent stability of the caged compound under the conditions used in the investigation is essential. Therefore, a study of the stability of a variety of pHP derivatives with different leaving groups under both basic and acidic conditions would be a resourceful study and provide useful information for future applications of the pHP group.

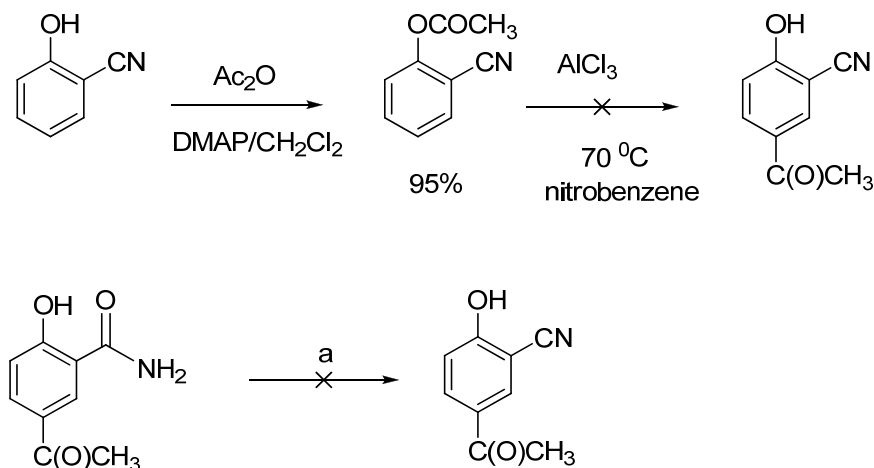
Results

1.2 Effect of Cyano Substituent on the Photophysical and Photochemical Properties of the *p*-Hydroxyphenacyl (pHP) Photoremovable Protecting Group

Synthesis of cyano substituted pHP GABA derivatives

Synthesis of cyano substituted pHP derivatives was challenging. Normal approaches such as the Fries rearrangement⁹² and dehydration of amides^{93,94,95} under various conditions did not work or gave very poor yields (Scheme 1.7).

Scheme 1.7

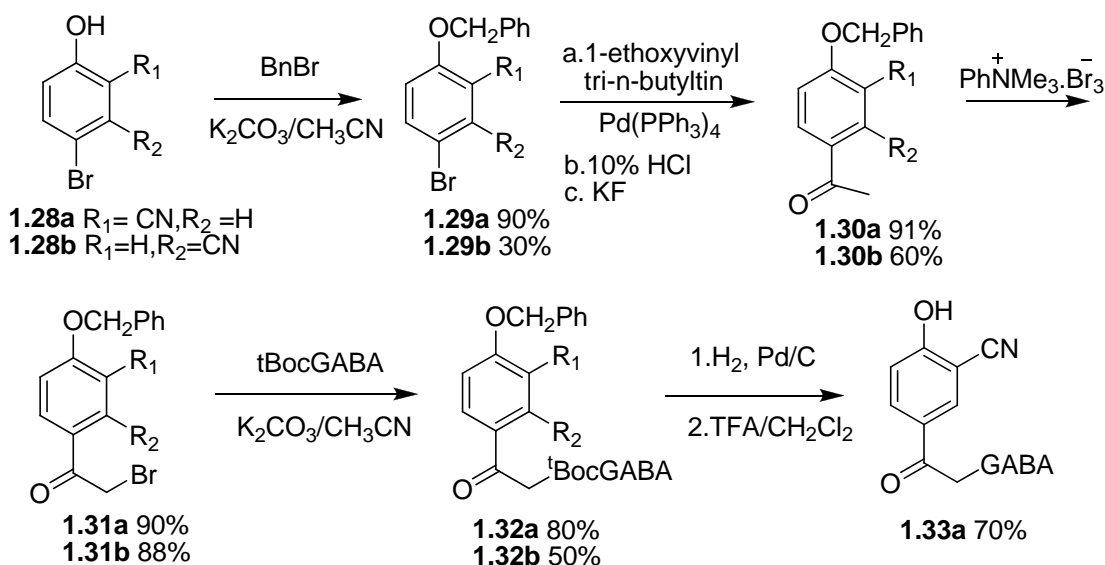


a: attempted conditions :- (CF₃CO)₂O/Py² / CCl₃CH₂OCOCI/CH₂Cl₂³ / P₂O₅⁴/POCl₃⁴

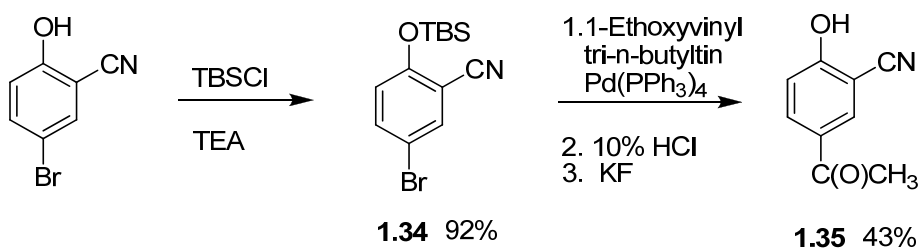
Ultimately, the target compounds were synthesized using the Stille reaction (Scheme 1.8). Commercially available 5-bromo-2-hydroxybenzonitrile was benzyl protected using benzyl bromide, followed by the Stille reaction using 1-ethoxyvinyl(N-butyl)₃Sn in the presence of Pd(PPh₃)₄. Subsequent hydrolysis of the resulting enol ether gave **1.30a** in 91% yield. KF was employed to remove excess tin. α -Bromination was achieved using phenyltrimethylammonium tribromide followed by S_N2 attachment of Boc protected GABA to give **1.32a**. Sequential

removal of the benzyl and Boc protecting groups with H₂ Pd/C and 50% TFA/CH₂Cl₂, respectively, gave rise to the target compound **1.33a** (3-CNpHP GABA) as a TFA salt (Scheme 1.8). Simultaneous removal of the two protecting groups could be achieved using 100% TFA but resulted in lower yields and long reaction times. The reaction sequence could also be carried out using silyl protection, but resulted in lower yields (Scheme 1.9).

Scheme 1.8



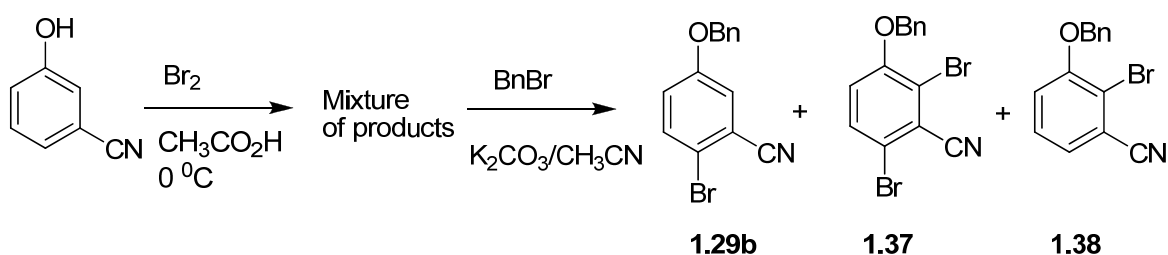
Scheme 1.9



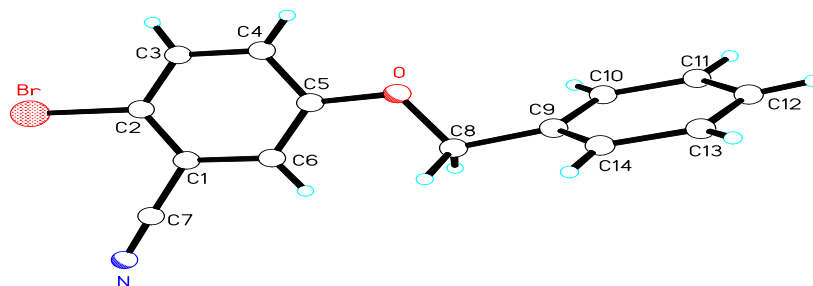
Synthesis 2-cyano pHP GABA could also be achieved by the same sequence. However, since the corresponding 2-bromo-5-hydroxybenzonitrile was not commercially available, it was synthesized by brominating 3-hydroxybenzonitrile (Scheme 1.10).⁹⁶ The resulting mixture of products was difficult to separate, but after benzylation separation was achieved using column chromatography and recrystallization. From the two major products formed, the desired 2-bromo-

5-(phenylmethoxy)benzonitrile (**1.29b**) was obtained as light yellow needle-like crystals with a melting point of 98⁰C. The other bromination product, 2,6-dibromo-5-(phenylmethoxy) benzonitrile (**1.37**), was a white crystalline material with a melting point of 144 ⁰C. Crystal structures of the two compounds that were isolated were obtained to confirm the assignments of the regioisomeric structures **1.29b** and **1.37** (Figure 1-6). However, 2-bromo-3-(phenylmethoxy) benzonitrile (**1.38**) was observed in trace amounts and was not isolated.

Scheme 1.10



a)



b)

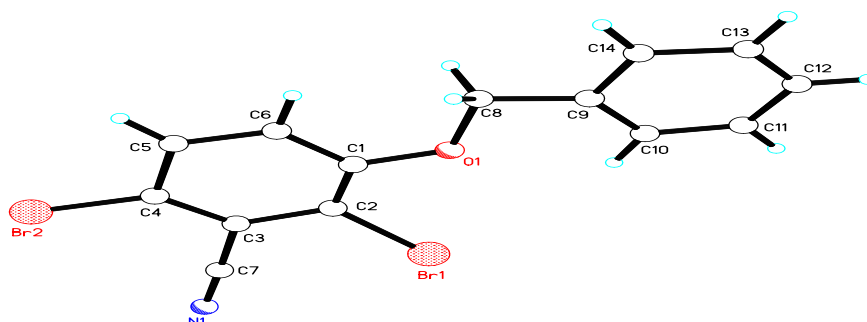
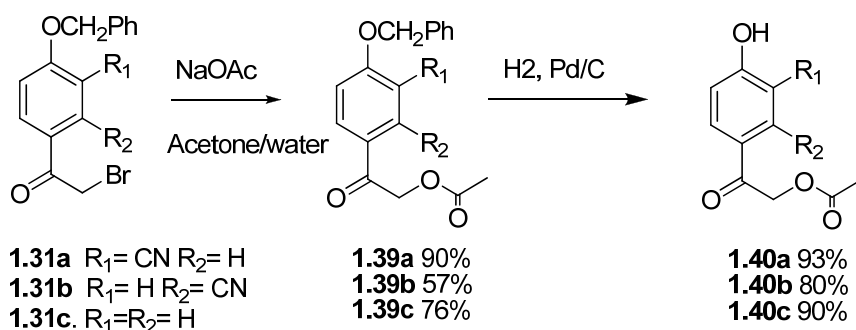


Figure 1-6. a) Crystal structure of 2-bromo-5-(phenylmethoxy) benzonitrile(**1.29b**), b) 2,6-dibromo-5-(phenylmethoxy) benzonitrile (**1.37**).

Synthesis of cyano substituted pHP OAc derivatives:

Synthesis of cyano-pHP acetates followed the same procedure as the GABA counterparts. Reaction of the bromo compounds (**1.31a** and **1.31b**) with sodium acetate in acetone/water followed by debenzoylation using H₂/Pd/C yielded the desired compounds. Unsubstituted pHP OAc was also synthesized for comparison purposes (Scheme 1. 11). The photochemistry of pHP OAc had been previously reported by Wan and co-workers.⁴⁵

Scheme 1.11



pKa Determination of 5-Acetyl-2-hydroxybenzonitrile (**1.35**).

The *pKa* of 5-acetyl-2-hydroxybenzonitrile (**1.35**) was determined by pH titration. A 0.025 M solution of **1.35** was titrated with standardized NaOH. The pH was measured at 0.2 ml increments. A plot of pH vs. volume of NaOH is illustrated in Figure 1-7. Using the equality of the *pKa* at the pH half-equivalent point, the *pKa* was determined to be 5.2.

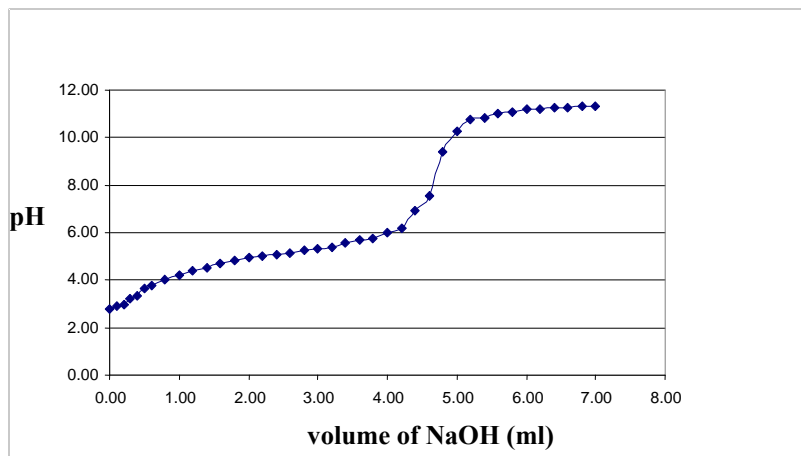


Figure 1-7. Titration curve of 5-acetyl-2-hydroxybenzoxonitrile (**1.8**) against 0.0461 M NaOH.

UV-vis spectroscopic studies of 3-cyano pHP GABA (**1.33a**)

The UV-vis spectra of 3-cyano pHP GABA (**1.33a**) were studied in water over a range of pH conditions (Table 1.4). In water at pH 5.00 and higher the only form present is the phenolate, the conjugate base of **1.6a**. At pH 3.7 both the phenolate and the phenol form are observed (Figure 1.8). This is in accord with the pK_a value derived by titration. The UV spectra remained unchanged for 48 hrs, demonstrating that the caged GABA was stable at pH 3.7.

Table 1-4. UV Data of 3-cyano pHP GABA in Water and Varying pH Levels

Conditions	λ_{max} /nm	$\epsilon/M^{-1}cm^{-1}$
Water	322	1200
pH 9.05	321	2800
pH 7.05 ^a	322	2900
pH 5.00 ^a	321	2200
pH 3.70 ^a	273	2100

^a ammonium acetate buffer

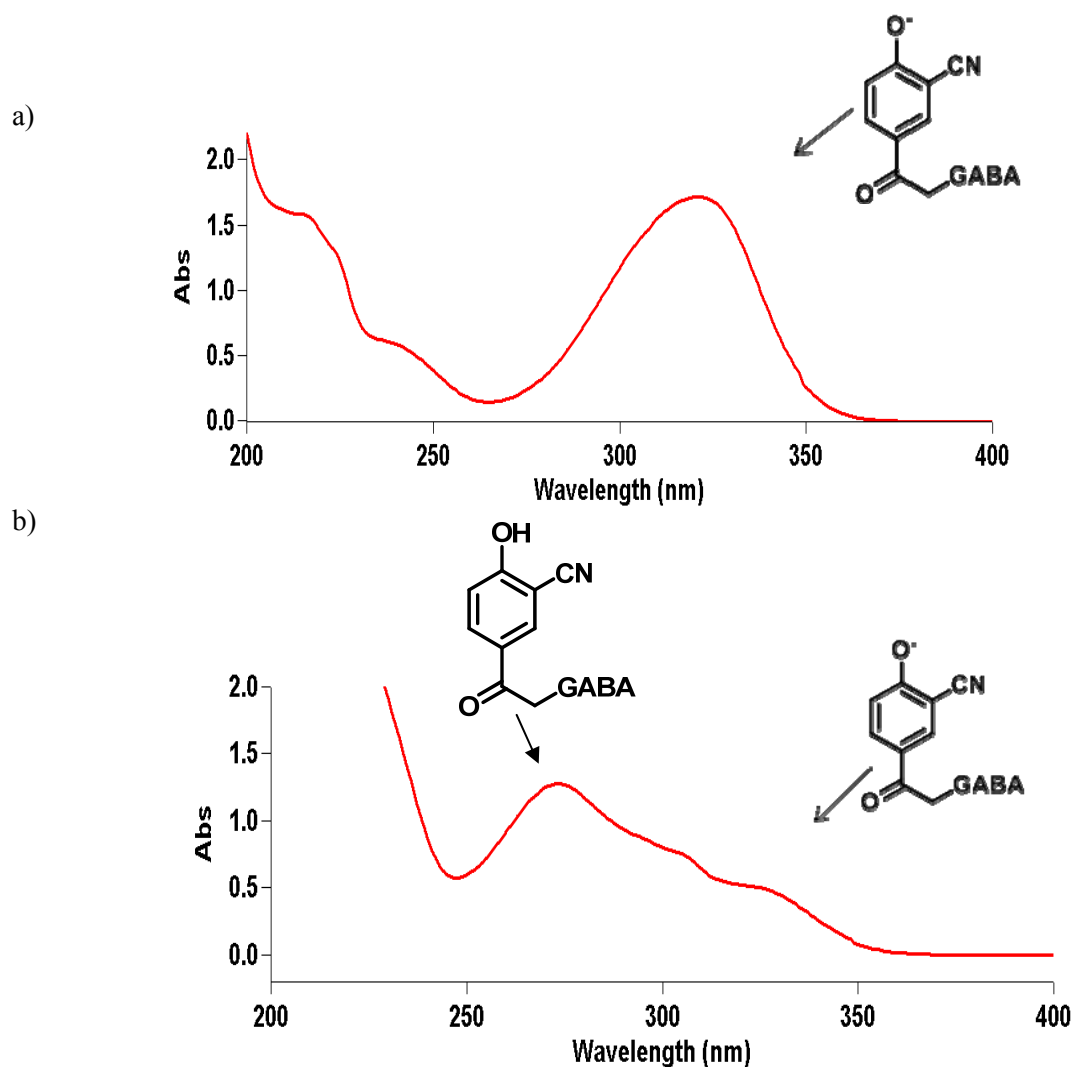
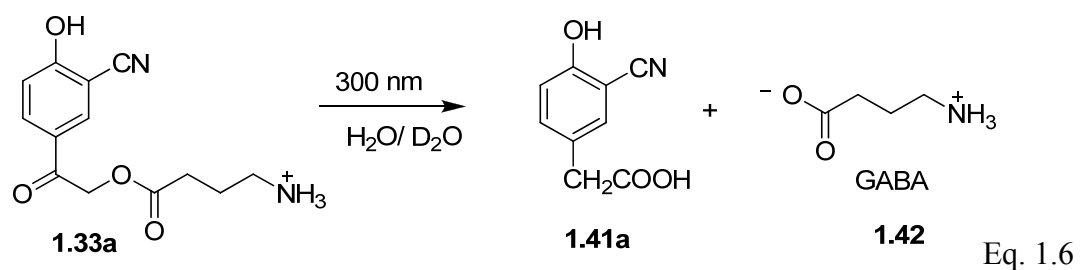


Figure 1-8. UV-Vis Spectrum of 3-cyano pHP GABA (**1.33a**) in ammonium acetate buffer a) pH 7.05 (concn. 4.33×10^{-4}), b) pH 3.70 (concn. 6.02×10^{-4}).

Photochemical Explorations of 3-cyano pHP GABA

Quantum Yield Studies:



Photochemistry of **1.33a** was explored using both ^1H NMR and LC/MS/MS analyses. The NMR experiments were performed in a Pyrex NMR tube. A 10 mg sample of **1.33a** was dissolved in D_2O and photolyzed in a Rayonet photoreactor with two 3000 Å lamps. ^1H NMR spectra were obtained at 10 min intervals. Clean release of GABA and the formation of 3-cyanophenylacetic acid were observed (Equation 1.6). ^1H NMR spectra at time zero and 60 minutes are illustrated in Figure 1-9. At 60 minutes the photolysis was about 50 % complete and two new peaks were visible. The peak observed at 3.51 ppm is assigned to the methylene group of 3-cyano-4-hydroxyphenylacetic acid (**1.41a**), while the peak at 2.46 ppm is for the methylene group of free GABA.

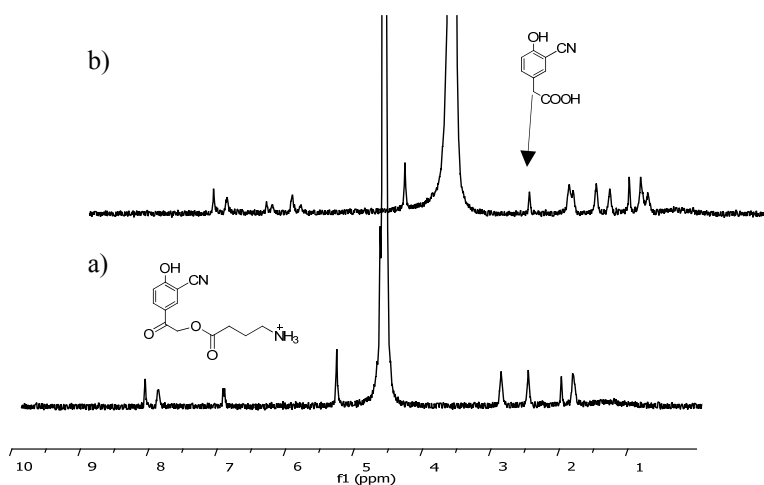


Figure 1-9. ^1H NMR spectra of the photolysis of **1.33a** in D_2O at a) time = 0, b) time = 60 min.

The quantum yield studies were performed using the same setup for the photoreactor as NMR studies. Aliquots were removed at 30 s intervals and starting material disappearance and product appearance were quantified using LC/MS/MS analysis with caffeine as the internal standard. Quantum yield studies were performed in aqueous buffer at pH 5.01, 7.05 and 9.05 (Table 1-5).

Table 1-5. Quantum Yield Studies of 3-cyano pHP GABA (**1.33a**) at various pH's.

Condition	Φ_{Dis}^a	Φ_{GABA}^b	Φ_{pHPAA}^c
Water ^g	0.42 ± 0.02	0.35 ± 0.03	0.39 ± 0.02
pH 7.05 ^{g,e}	0.33 ± 0.01	0.28 ± 0.02	0.28 ± 0.03
pH 5.01 ^{d,e}	0.21 ± 0.01	0.13 ± 0.01	0.19 ± 0.01
pH 9.05 ^{d,e}	0.19 ± 0.02	-	-
Water ^f	0.08 ± 0.01	0.07 ± 0.02	0.05 ± 0.02

^a Φ for disappearance of **1.33a**. ^b Φ for the appearance of GABA. ^c Φ for the appearance for phenylacetic acid. Appearance of the acid was quantified by using 4-hydroxy-3-trifluoromethylphenylacetic acid as a model. ^d at 3000 Å ^e Ammonium acetate buffer. ^f at 3500 Å.

Stern-Volmer Quenching Studies.

To determine the multiplicity and to calculate the rate constants for release of GABA from **1.33a**, Stern-Volmer quenching studies were performed using potassium sorbate as the quencher. Five solutions of **1.6a** with varying concentrations of the quencher were prepared and the quantum yields for the disappearance of **1.33a** for each solution were measured via Ultra Performance Liquid Chromatography (UPLC) analysis. The UPLC technique is very similar to HPLC, but uses columns with smaller particle size (sub 2 μm), making it possible to increase flow rates without the loss of resolution.⁹⁷ The resulting Stern-Volmer plot of the quenching data (Table 1.6) is illustrated in Figure 1-10.

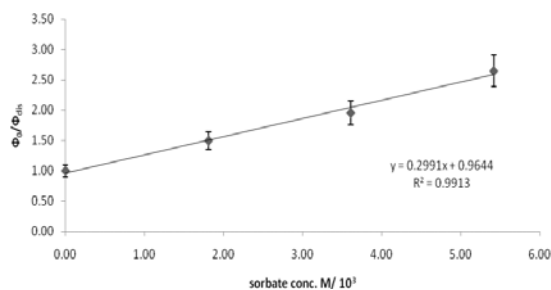


Figure 1-10. The Stern-Volmer plot of sorbate quenching of the photoreaction of 3-cyano pHP GABA (**1.33a**) at 3000 Å in water.

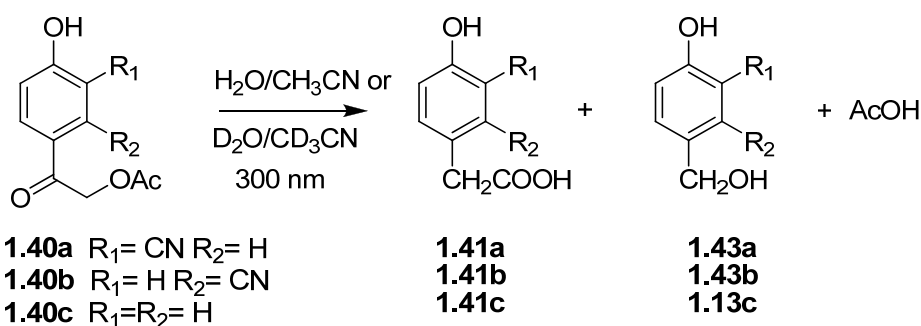
Table 1-6. Stern-Volmer Quenching Data of **1.33a**

Sorbate Conc. (M) / 10 ³	Φ_{Dis}	Φ_0 / Φ_{Dis}
0.00	0.45 ± 0.02	1.00
1.81	0.37 ± 0.03	1.49
3.61	0.23 ± 0.01	1.95
5.42	0.17 ± 0.02	2.65

$\Phi_0 = \Phi$ in the absence of quencher. The straight line with slope = 299.1 and intercept = 0.9644 results from a linear fit to the respective data.

The slope of the best-fit linear regression line gives the Stern-Volmer constant (K_{sv}) of 299.1. From the relationship, $K_{sv} = \tau^3 \times k_{diff}$, where τ^3 is the lifetime of the triplet excited state and k_{diff} is estimated to be the rate of diffusion in water (i.e., $7.40 \times 10^9 M^{-1}s^{-1}$)⁹⁸ τ^3 was found to be 4.05×10^{-8} s or 40.5 ns. Thus, the rate constant for the reaction (k) is calculated to be $1.11 \times 10^7 s^{-1}$ from the relationship $k = \Phi / \tau^3$

Photochemistry of 3-cyano pHP OAc (1.40a) and 2-cyano pHP OAc (1.40b)



Eq. 1.7

Photolysis of **1.40b** was performed in an NMR tube with 20% D_2O/CD_3CN using the same photoreactor setup described under photolysis studies of **1.33a**. 1H NMR spectra were obtained at 60 min intervals. Release of acetate and formation of two photoproducts, 2-cyano-4-hydroxyphenylacetic acid (75%, 3.72 ppm (CH_2) in 1H NMR) and 2-cyano-4-hydroxybenzyl alcohol (25%, 4.59 ppm (CH_2) in 1H NMR), were observed (Equation 1.7, Figure 1-11).

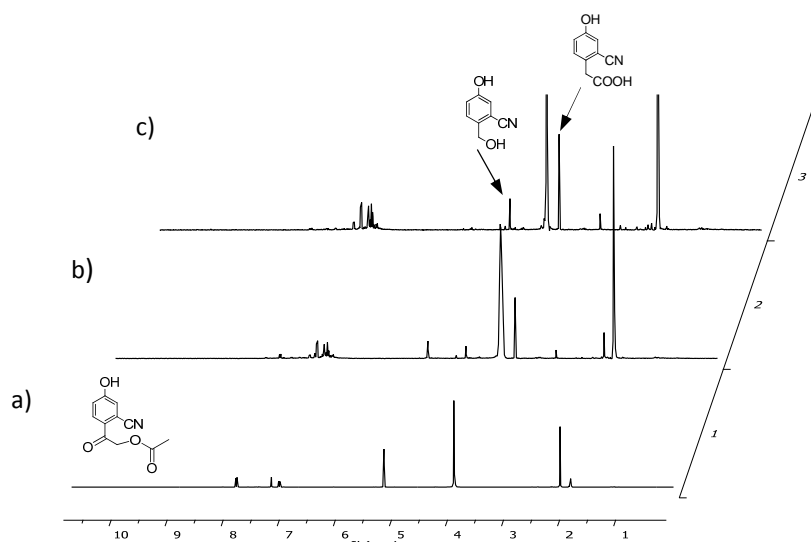


Figure 1-11. ^1H NMR spectra of photolysis of **1.40b** in 20% $\text{D}_2\text{O}/\text{CD}_3\text{CN}$ at a) $t = 0$ h, b) $t = 4$ h, c) $t = 8$ h.

Quantum yield studies of **1.40a**, **1.40b**, and **1.40c** were performed in 20% water/acetonitrile and 20% water/dimethyl sulfoxide. In a typical experiment 10 mg of compound was dissolved in 4 ml of solvent and photolysis in a 5ml quartz tube using a Rayonet Photoreactor equipped with two 3000 Å lamps and a Merry-go-round apparatus. Samples were not degassed prior to photolysis. The progress of the reaction was followed via UPLC analysis. The data are tabulated in Table 1-7.

Table 1-7. Quantum Yields for the Disappearance of Cyano Substituted pHP Acetates in 20% $\text{H}_2\text{O}/\text{CH}_3\text{CN}$ and 20% $\text{H}_2\text{O}/\text{DMSO}$ at 3000 Å

pHP Derivative	Φ_{Dis} in 20% $\text{H}_2\text{O}/\text{CH}_3\text{CN}$	Φ_{Dis} in 20% $\text{H}_2\text{O}/\text{DMSO}$
1.13a	0.17 ± 0.03	0.12 ± 0.02
1.13b	0.08 ± 0.02	0.06 ± 0.02
1.13c	0.30 ± 0.02	0.29 ± 0.01

Ionic Strength Studies of 3-cyano pHP GABA and pHP OAc

The effect of ionic strength of the solvent on photolysis was explored using LiClO_4 and NaClO_4 . Photolysis of **1.33a** and **1.40c** were performed with increasing concentrations of LiClO_4 or NaClO_4 . Photolysis of **1.40c** was carried out in 37% $\text{H}_2\text{O}:\text{MeOH}$ due to difficult solubility in

water. The quantum yield for disappearance of **1.33a** and **1.40c** decreased with increasing concentrations of both salts. The plots for **1.33a** in both LiClO₄ and NaClO₄ are illustrated in Figure 1-12. The quantum yield values for all three compounds are given in Table 1-8.

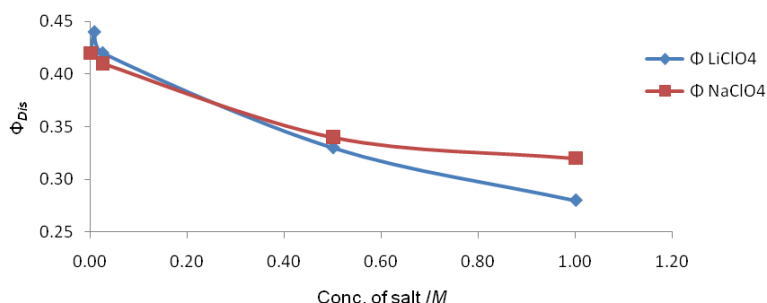


Figure 1-12. Plot of Φ_{dis} vs. concentration of salt for 3- cyano pHP GABA.

Table 1-8. Φ_{Dis} of 2-cyano pHP GABA (**1.33a**) and pHP OAc (**1.40c**) as a Function of Concentration of LiClO₄ or NaClO₄

Conc. of the salt/M	Φ_{Dis} of 1.6a in LiClO ₄	Φ_{Dis} of 1.6a in NaClO ₄	Φ_{Dis} of 1.13c in LiClO ₄ ^a
0.000	0.42	0.42	0.56 ^a
0.008	0.44	nd	nd
0.025	0.42	0.41	0.53
0.500	0.33	0.34	0.43
1.00	0.28	0.32	0.42

^a in 37% H₂O:MeOH

2.2 Comparison of the base-activated and excited state Favorskii rearrangements.

The possibility of pHP derivatives undergoing ground state, base-activated Favorskii rearrangements⁵⁴ was tested with a series of leaving groups which included bromide, carboxylate, phosphate, phenolate and sulphonate (Figure 2-7). The syntheses of these compounds are reported elsewhere.^{99,100,101} The test for base-catalyzed, ground state Favorskii rearrangement was carried out with excess 0.05 M NaOMe at 0 °C and room temperature and at reflux. As the reaction progressed, the appearance of several possible products, each

independently synthesized or commercially available, was monitored by the relative retention times in UPLC (Figure 2-8). Spiking experiments with the authentic samples were also performed to confirm the products in each experiment via UPLC. Product isolation and spiking in NMR samples were also performed on some pHP derivatives for product confirmation.

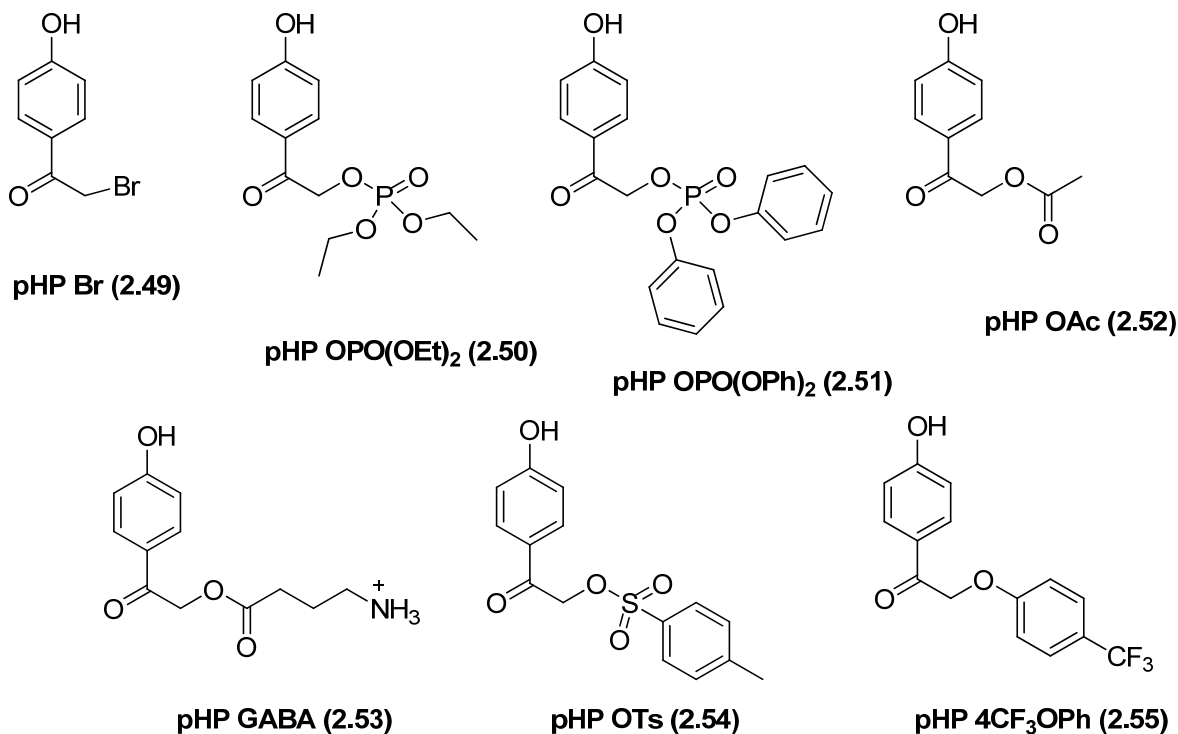


Figure 2-7. pHP derivatives tested for possible base activated Favorskii rearrangements.

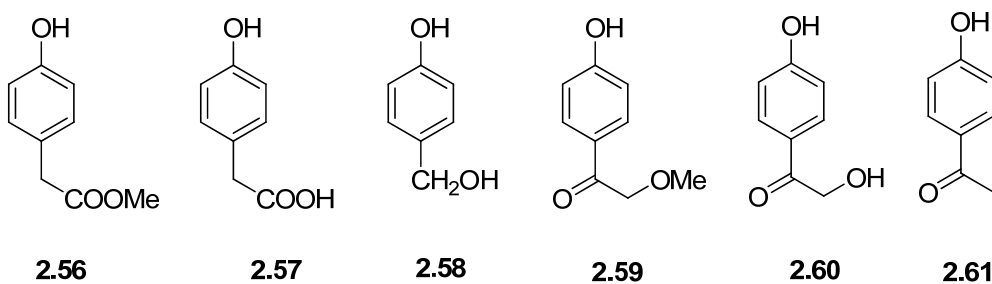


Figure 2-8. Potential base-catalyzed Favorskii and hydrolysis products from the pHP derivatives in Figure 2-7.

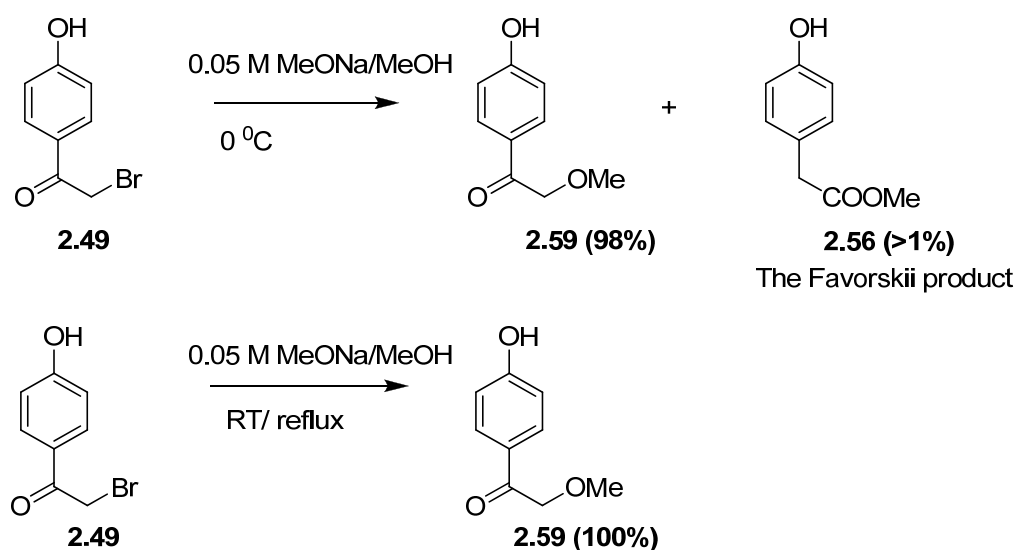
Among products investigated, methyl *p*-hydroxyphenylacetate (**2.56**), *p*-hydroxyphenyl acetic acid (**2.57**), and *p*-hydroxybenzyl alcohol (**2.58**) are the possible Favorskii products. In contrast, *p*-hydroxyphenacyl alcohol (**2.60**) results from the hydrolysis at the carboxylate or the phosphate ester function. *p*-Hydroxyphenacyl alcohol (**2.60**) and *p*-hydroxyphenacyl methyl ether (**2.59**) can also be formed by an S_N2 displacement of all the leaving groups investigated.

Methyl *p*-hydroxyphenylacetate (**2.56**) was synthesized under Fischer esterification¹⁰² conditions by refluxing *p*-hydroxyphenylacetic acid (**2.57**) in acidic methanol in 50% yield. *p*-Hydroxyphenacyl methyl ether (**2.59**) was synthesized by stirring *p*HP Br in methanol in the presence of K₂CO₃.

Test for base activated Favorskii rearrangement of the selected *p*HP derivatives

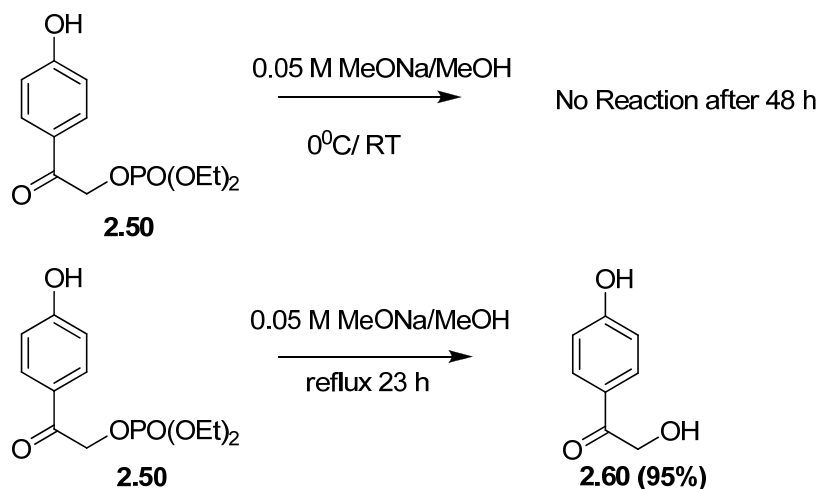
***p*HP Br (**2.49**):** Both at room temperature and at reflux the only product observed was the displacement product **2.59**. At 0 °C the major product was still **2.59** but a trace amount (less than 1%) of methyl *p*-hydroxyphenylacetate (**2.56**), the Favorskii product, was observed (Scheme 2.17).

Scheme 2.17



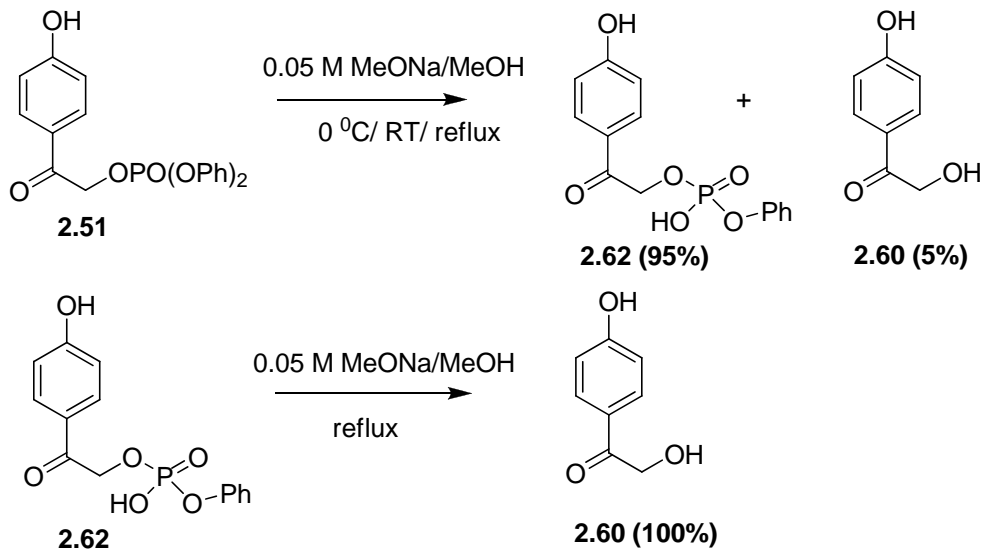
pHP OPO(OEt)₂ (2.50): No reaction was observed at 0 °C or at room temperature over a 48 h period. At reflux (65 °C), hydrolysis of the phosphate gave **2.60** in 95% yield (Scheme 2.18). The reaction was complete in 23 h.

Scheme 2.18

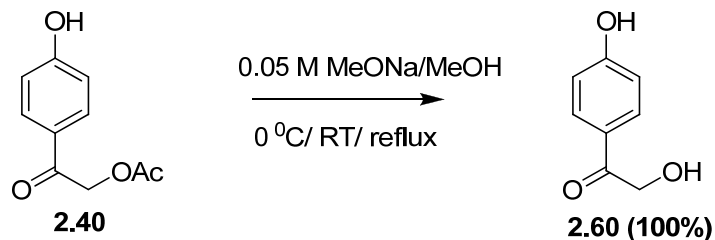


pHP OPO(OPh)₂ (2.51): At reflux and at room temperature, pHP diphenyl phosphate underwent rapid hydrolysis at the phosphate group to give the monophenyl product **2.62**. The α -hydroxyl pHP **2.60** was also observed in small amounts (5%). The reaction was relatively slow at 0 °C. Upon continuous reflux at 65 °C, **2.62** underwent further hydrolysis to give **2.60** at 100% yield (Scheme 1.19).

Scheme 2.19



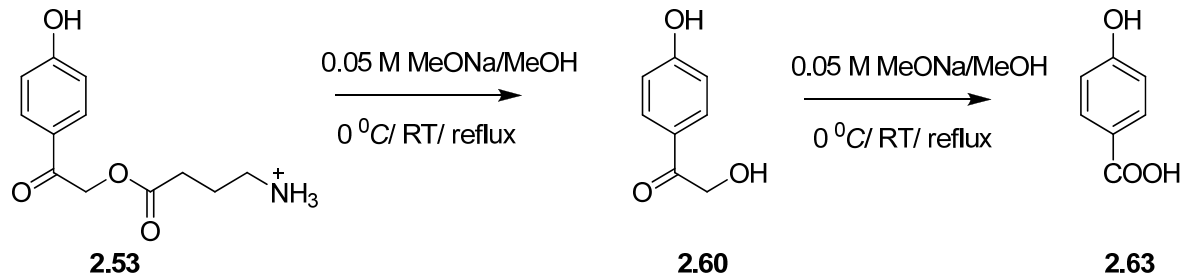
pHP OAc (2.52): At reflux, room temperature, and at 0 °C, pHP OAc hydrolyzed rapidly by the attack at the carboxylate carbon to give **2.60** as the only product (Equation 2.3).



Eq. 2.3

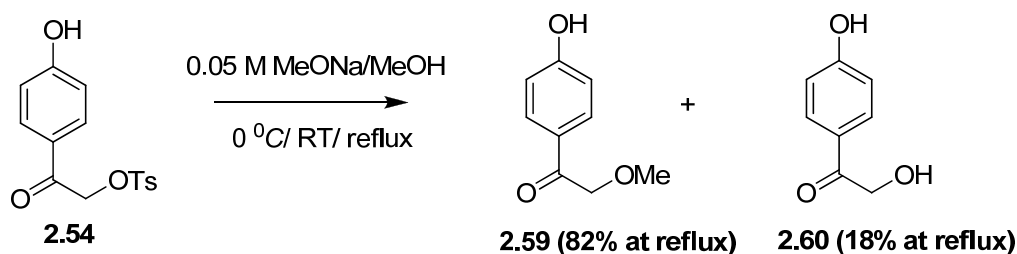
pHP GABA (2.53): pHP GABA was extremely reactive under these conditions. It underwent rapid hydrolysis to produce **2.60** even at 0 °C. Interestingly, upon further reaction **2.60** oxidized to *p*-hydroxybenzoic acid (Scheme 2.20).

Scheme 2.20



To test the role of oxygen in the oxidation reaction, pHP GABA (**2.53**) and **2.60** were reacted in 0.05 M MeONa/MeOH and either exposed to air or under argon. *p*-Hydroxybenzoic acid was formed from both compounds when treated with base in the presence of air, but formation of *p*-hydroxybenzoic was not observed for either **2.53** or **2.60** under argon.

pHP OTs (2.54): At all three temperatures, pHP OTs gave primarily the S_N2 type displacement product **2.59**. During reflux, the hydrolysis product **2.60** was obtained in 18% yield. At room temperature and at 0 °C **2.60** was observed in 8% and 6% yields, respectively (Equation 2.4).



Eq. 2.4

pHP 4-CF₃OPh (2.55) No reaction was observed for reactions for 48 h at all three temperatures.

Rate constant determinations Rate constants for the pHP derivatives were determined under pseudo first-order reaction conditions as illustrated with pHP OPO(OEt)₂ as an example. The pseudo-first order rate expression for the hydrolysis of pHP OPO(OEt)₂ can be written as,

$$\text{Rate} = - \frac{d[\text{pHP OPO(OEt)}_2]}{dt} = k_{obs} \times [\text{pHP OPO(OEt)}_2] \quad \text{Eq. 2.5}$$

where k_{obs} is the pseudo first-order rate constant for the disappearance of pHP OPO(OEt)₂. Upon integration, the expression for the first order dependence on pHP concentration becomes,

$$\ln [\text{pHP OPO(OEt)}_2]_t = -k_{obs}t + \ln [\text{pHP OPO(OEt)}_2]_0 \quad \text{Eq. 2.6}$$

A plot of the log of the concentration ($\ln [\text{pHP OPO(OEt)}_2]$) vs. time was linear giving the k_{obs} values from the slopes (Figure 2-9). The kinetic runs were performed for solutions at reflux unless otherwise stated. The disappearance of pHP derivatives was followed by UPLC. The results are tabulated in Table 2-3.

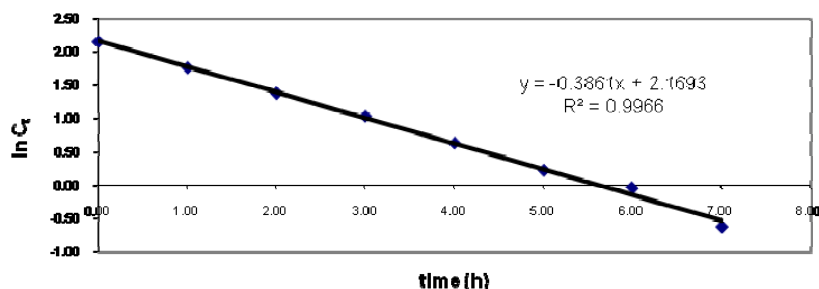


Figure 2-9. A plot of $\ln[\text{pHP OPO(OEt)}_2]$ vs. time for pHP OPO(OEt)₂. Data points were obtained in 0.05 M NaOMe/MeOH at 65°C and fitted with linear least squares method,¹⁰³ that gave a slope of 0.33861 that corresponds to a rate constant of $0.107 \times 10^{-3} \text{ s}^{-1}$

Table 2-3. Rate Constants for the Disappearance of pHP Derivatives in 0.05 M NaOMe/MeOH

pHP Derivative	Rateconstant ($k_{obs}/10^{-3} s^{-1}$)	Conditions	Products formed
pHP Br	2.26 ± 0.15	at reflux	2.59
pHP OAc	2.04 ± 0.05	at 0 ^o C	2.60
pHP OTs	1.40 ± 0.04	at reflux	2.59, 2.60
pHP OPO(OEt) ₂	0.103 ± 0.004	at reflux	2.60

Stability Study: Acidic Conditions

The stabilities of the pHP derivatives were tested in 0.1 M HClO₄ acid in 10% H₂O/MeOH for 24 h. Under these highly acidic conditions, the pHP bromide (**2.49**), diethyl phosphate (**2.50**), phenolate (**2.55**), and tosylate (**2.54**) were very stable for 24 h, whereas, pHP OAc was completely hydrolyzed to give the alcohol **2.60** within 6 h. In 24 h pHP OPO(OPh)₂ and pHP GABA were hydrolyzed to the extent of 15% and 50%, respectively. The results are tabulated in Table 2-4.

Table 2-4. Stability of pHP derivatives in 0.1m HClO₄ acid

pHP derivative	Stable for 24 h	Hydrolyzed to form 2.60	% Hydrolyzed
pHP Br	√		
pHP 4-CF ₃ OPh	√		
pHP OTs	√		
pHP OPO(OEt) ₂	√		
pHP OPO(OPh) ₂	×	×	15 % in 24 h
pHP GABA	×	×	50% in 24 h
pHP OAc	×	×	100 % in 6 h

√ = Stable to the conditions, × = Unstable, hydrolysis occurs

Discussion

1.3 Effect of Cyano substituent on the Photophysical and Photochemical Properties of the *p*-Hydroxyphenacyl (pHP) Photoremovable Protecting Group

Synthetic Strategies

The synthesis of 3-cyano pHP GABA (**1.33a**), 3-cyano pHP OAc (**1.40a**), and 2-cyano pHP OAc (**1.40b**) all followed the same general protocol (Scheme 1.8 *Results*). For 3-cyano derivatives the synthesis began with benzyl protection of commercially available 5-bromo-2-hydroxybenzotrile. But the corresponding bromo derivative for the 2-cyano compound was not commercially available and was synthesized by bromination of 3-hydroxybenzotrile with Br₂/CH₃COOH at 0 °C (Scheme 1.10 *Results*). In contrast to the literature procedures, careful temperature control was necessary to obtain monobrominated product,⁹⁶ and even at 0 °C both mono and dibrominated compounds were obtained in a ratio of 1:2. Since separation of the mixture was difficult at this point, the separation of the two regioisomers was performed after benzylating the mixture using benzyl bromide/K₂CO₃. The separation of the benzyl protected bromobenzotriles was accomplished by column chromatography followed by recrystallization. Two crystalline bromobenzotriles **1.29b** and **1.37** were obtained in 30% and 64% yields, respectively. The crystal structures of each benzyl protected bromobenzotrile were determined and are depicted in Figure 1-6 in the *Results* section.

Stille acylation of the benzyl protected bromobenzotriles **1.29a** and **1.29b**, developed for the synthesis of fluoro substituted pHP derivatives by Stensrud,^{91,104} furnished the corresponding acetophenones after hydrolysis of the corresponding enol ethers. The hydrolysis of the 3-cyano derivative was achieved in 10% HCl in 2 h, but the 2-cyano derivative required

24 h of stirring in 60% HCl to achieve complete hydrolysis. Hydrolysis of the enol ether of the 2-cyano derivative required the protonation of an electron deficient carbon that might lead to the observed difficulty in hydrolysis (See Figure 1-13).

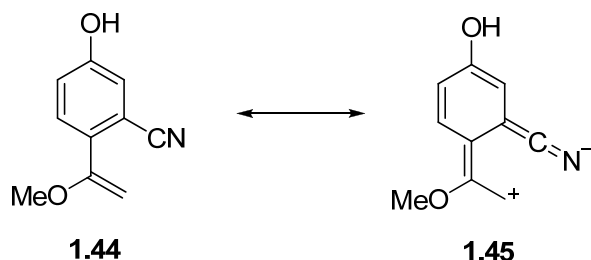


Figure 1-13. Resonance structures of enol ether **1.44** produced from the Stille reaction of 2-bromo-5-(phenylmethoxy) benzonitrile (**1.29b**)

The removal of excess tin reagents and byproducts at the end of the reaction was difficult. Initial attempts to purify the product using column chromatography and employing a variety of solvents failed. The impurities were finally removed by saturating the reaction mixture with KF. The tributyltin fluoride forms a white precipitate that could easily be filtered from the supernatant containing the cyanoacetophenone. The overall yield of the reaction was lower for the 2-cyanoacetophenone than the 3-cyano derivative.

α -Bromination of the cyanoacetophenones **1.30a** and **1.30b** was achieved using phenyltrimethylammonium tribromide. The reaction gave high yields of the monobrominated compound with only trace amounts of the dibrominated species. During the reaction the color of the mixture changed from bright red/orange to colorless, marking the completion of the reaction. However, when unprotected phenols were used the reaction resulted in a mixture of unidentified compounds and a lower yield of the desired derivatives. Caging of t Boc protected GABA and acetate was achieved using a facile S_N2 displacement of the α -bromoketone in good yield (70-90%). For benzyl protected 3-cyano pHP t Boc GABA (**1.32a**), the benzyl and t Boc protecting groups were sequentially removed using hydrogenolysis (H_2/Pd) followed by treatment with

50% TFA/CH₂Cl₂. Both protecting groups could be removed in one pot by prolonged exposure to 100 % dry TFA, but the yields were poor. Therefore, the two step procedure was employed. For the 2-cyano pHP derivative (**1.32b**), the removal of the benzyl protecting group was uneventful, but attempts to remove the 'Boc protecting group resulted in decomposition of the compound. Overall, the yields were comparatively better for the combined reaction sequence for the 3-cyano pHP analog than for the 2-cyano pHP derivative.

The effect of cyano substitution on the pKa and UV-vis spectra of pHP GABA

The pKa of 5-acetyl-2-hydroxybenzotrile (**1.35**) was determined to be 5.2, a value that is within the same range of pKa's of several known difluoro and trifluoromethyl substituted pHP acetophenones.^{91,104} The increase in acidity is expected due to the electron withdrawing nature of the cyano group. This was clearly demonstrated by the pH profile of the UV-vis spectra of 3-cyano pHP GABA (**1.33a**). At high pH (~8.5) the absorption maximum was 322 nm, corresponding to the phenolate ion (conjugate base). When the pH was lowered below 5, another absorption peak due to the phenolic form appeared at 273 nm. Interestingly even at pH 3.7, where only the phenolic form is present, a small absorption peak possibly due the conjugate base was observed (Figure 1-8, *Results*). The amount of the conjugate base present at this pH is estimated to be about 9%. These data suggest that in water at pH 7.05, one of the conditions under which the quantum yield studies and quenching studies were performed, the prominent form of the pHP derivative photolyzed was as its conjugate base.

Photochemical studies of 3-cyano pHP GABA (**1.33a**).

3-Cyano pHP GABA behaved in accordance with other pHP GABA derivatives. Based on NMR data, the only photoproduct observed during photolysis in D₂O was the rearranged 4-hydroxy-3-cyanophenylacetic acid (**1.41a**). Stern-Volmer quenching studies performed on **1.33a** with potassium sorbate (0-6 mM) as a triplet quencher showed a considerable drop in quantum efficiencies with increasing sorbate concentration (see Table 1-6 and Figure 1-10 in *Results*). This behavior was consistent with the previously reported Stern-Volmer quenching of other substituted pHP derivatives,^{40,91,104} and provides good empirical evidence that the reactive excited state is the triplet, in accord with the other substituted pHP derivatives. The slope (K_{SV}) of the Stern-Volmer quenching correlation gave a rate constant of $1.11 \times 10^7 \text{ s}^{-1}$ based on a value of $7.4 \times 10^9 \text{ M}^{-1} \text{ s}^{-1}$ for the release of GABA from **1.33a**. This value is also within the range of the reported values for other, similar pHP derivatives.

A high quantum yield of 0.42 was measured for photolysis of **1.33a** in water. This is among the highest quantum yields for a pHP GABA derivative, e.g., the quantum efficiency for the parent pHP GABA is reported to be 0.20.³³ A decrease in quantum efficiency to 0.32 was observed when a pH 7.05 buffer was used as the medium. Surprisingly, the quantum yield decreased even further when the pH was lowered to 5.01. A decrease in quantum yield was also observed when the pH was raised to 9.05. Here, similar pH profiles were observed for the fluoro pHP GABA reactions by Stenstrud,^{91,104} e.g., for trifluoromethyl and mono and difluoro substituted pHP GABA derivatives. Precedence for similar dependence of quantum efficiencies on the pH can also be found in studies reported by Wan and coworkers⁴⁵ for caged pHP acetates as shown in Figure 1-14.

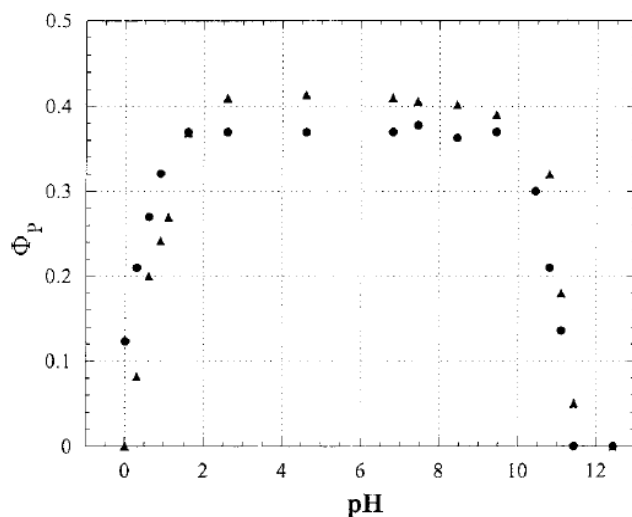
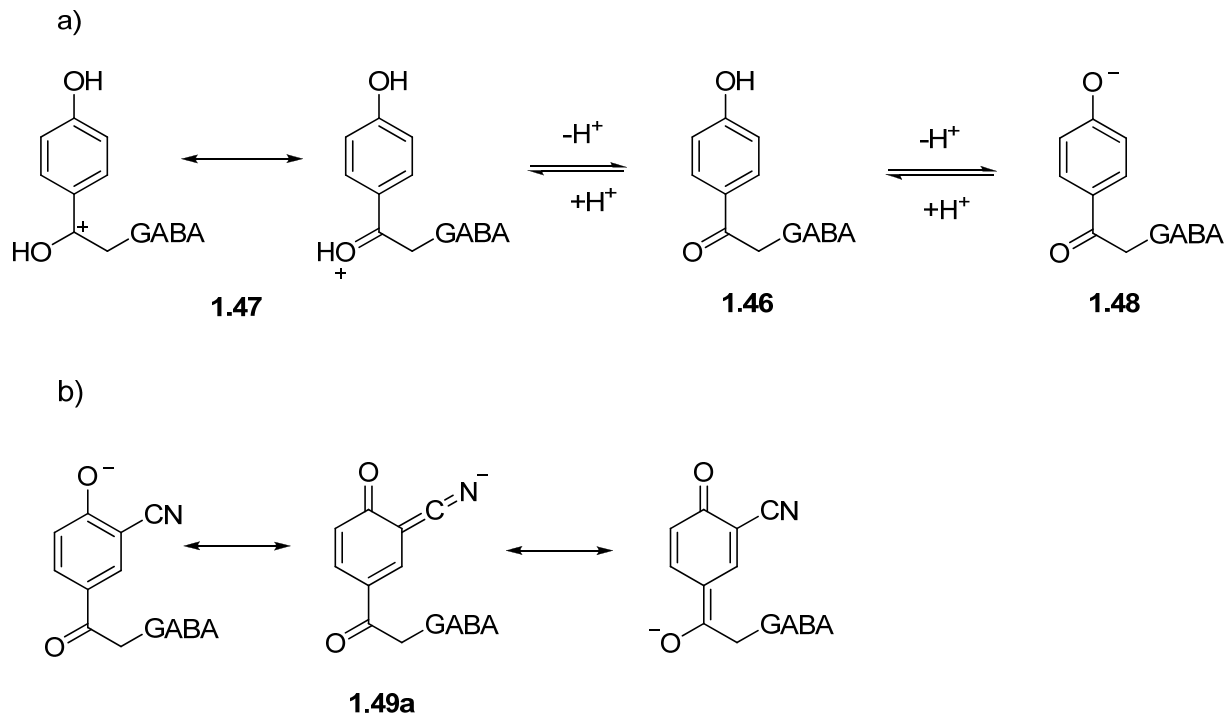


Figure 1-14. A plot of Φ of phenylacetic acid appearance (Φ_p) at different pH conditions for pHP OAc (triangles) and 3,5-di-*t*-butyl pHP OAc (circles) in 1:1 $\text{H}_2\text{O}/\text{CH}_3\text{CN}$. Reproduced with permission from American Chemical Society

The change in quantum efficiency with pH can be best understood by considering the state of protonation of the pHP derivative as a function of pH (Scheme 1.12a). At low pH the carbonyl group attached to the phenyl ring will be protonated (**1.47**), as shown by the resonance structures, that will hinder the photochemistry of the chromophore,⁴⁵ as in the protonated form the absorption of the chromophore will be blue shifted. At high pH the prominent form is the conjugate base (**1.48**). Recent work by Givens and Wirz *et al.*,⁴⁰ has shown that the conjugate base is inefficient in forming product. Once excited the conjugate base simply relaxes and then reprotonates to give the starting pHP ester. The unreactivity of the conjugate base, can be rationalized in terms of resonance, which arises from the disruption of the n,π^* contribution from the carbonyl group. Thus the ideal pH for pHP photorelease will lie in the pH range where the carbonyl group and the phenolic hydrogen are still intact, a “neutral region” for the pHP chromophore.

Scheme 1.12

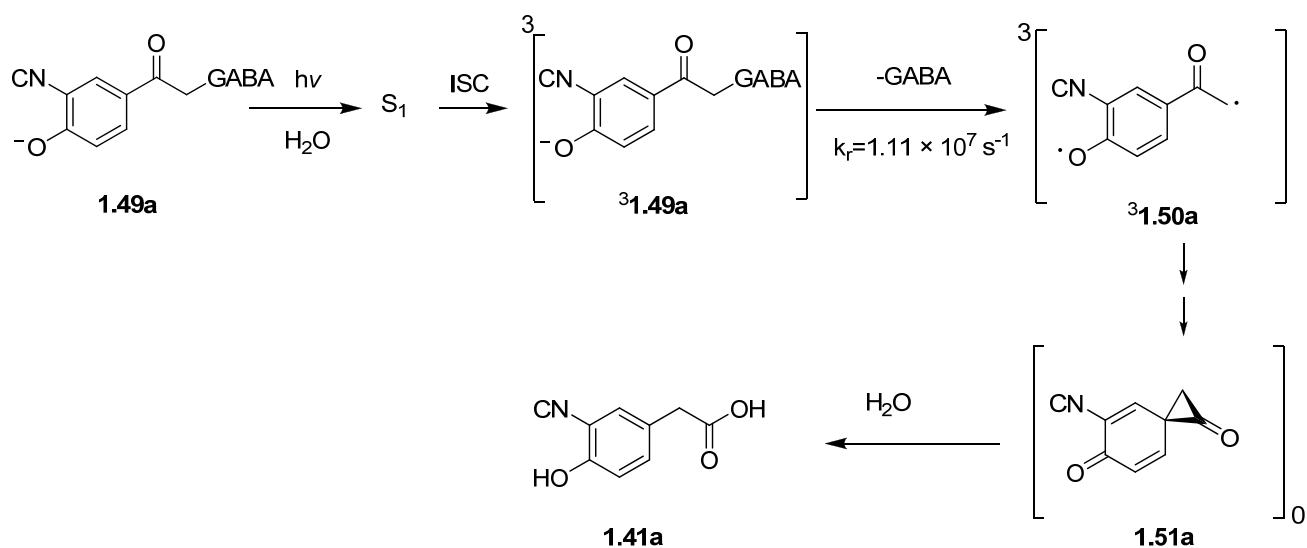


However, for 3-cyano pHP GABA the measured pK_a of 5.2 suggests that in water, where it showed the highest quantum yield, the prominent form present would be the conjugate base. This is in contradiction to other pHP derivatives. However, in the presence of the cyano group another resonance structure can be drawn where the anion electron density is distributed to the cyano group making the conjugate base more stable, and as shown in Scheme 1.12b. In this resonance structure the carbonyl group intact to participate in photorelease and an observed higher quantum efficiency.

Under these conditions a revised mechanism for the photo Favorskii rearrangement of 3-cyano pHP GABA can be envisioned beginning with the conjugate base of cyano pHP GABA as the excited substrate. The mechanism, which is outlined in Scheme 1.13, begins with the initial absorption of light by the conjugate base **1.49a**, raising the molecule to its singlet state (¹**1.49a** = S₁). The singlet ester intersystem crosses (ISC) to form the triplet conjugate base ³**1.49a**. The

release of GABA will result in the formation of the triplet biradical **1.50a** that relaxes to the singlet biradical and then cyclize to form the spirodienedione intermediate **1.51a**. Loss of GABA occurs with a rate constant of $1.11 \times 10^7 \text{ s}^{-1}$ and is the RDS of the reaction. Formation of the neutral biradical **1.50a** from the negatively charged conjugate base ³**1.49a** can be thought of as the driving force of the reaction. The spirodienedione **1.51a** will further react to form the phenylacetic acid **1.41a**, the only other product beside GABA observed in the photolysis of **1.33a**.

Scheme 1.13



Photochemical studies of 3-cyano pHP OAc (**1.40a**) and 2-cyano pHP OAc (**1.40b**)

Photochemical studies on pHP OAc derivatives required the use of 20% $\text{H}_2\text{O}/\text{CH}_3\text{CN}$ due to low solubility of the compound in water. Previous work by Wan⁴⁵ and by Phillips^{42,43} reported the use of similar solvent systems with the parent pHP acetate and were chosen here in order to provide comparison among these studies. Photolysis resulted in the formation of two

photoproducts, 4-hydroxyphenylacetic acid **1.41** (75%), and a much lesser amount of 4-hydroxybenzyl alcohol **1.43** (25%), in accord with the recent reports by Givens *et al.*^{39,40} The greater yield of the 4-hydroxybenzyl alcohol in this study compared with the absence of hydroxybenzyl formation in the photolysis of the 3-cyano pHP GABA is suggestive of a solvent dependence as one factor in the formation of the benzyl alcohol products. The photolysis studies for 3-cyano pHP GABA was performed in 100% water whereas a 20% H₂O in CH₃CN mixture has been employed for acetate derivatives. Another factor may be the nature of the leaving group. It is worthy of note that the TR IR and TR UV-vis studies that provided evidence of a quinone methide intermediate (**1.26** in Scheme 1.6 in *Introduction*) as reported by Givens and Wirz *et al.*³⁹ were performed in CH₃CN with only 2% H₂O.

The quantum yield for disappearance of the parent pHP OAc (**1.40c**) is 0.30 in 20% H₂O/CH₃CN. By comparison, the value reported by Wan and coworkers in 1:1 H₂O/CH₃CN was 0.41.⁴⁵ The difference can be attributed to the amount of water present which has been well documented for its dependence of photorelease quantum yields for the diethyl phosphate release.^{40,45} The quantum efficiencies for 3-cyano and 2-cyano pHP OAc, **1.40a**, and **1.40b**, in 20% H₂O/CH₃CN are 0.17 and 0.08, respectively. These values are substantially lower than those reported for the parent compound. Quantum efficiencies for studies done in 20% H₂O/DMSO are still farther reduced but follow the same trend. However, as discussed above, the Φ of the 3-cyano pHP GABA in 100% water is significantly higher than the unsubstituted pHP, indicating a strong dependence on amount of H₂O in the solvent. The UV-vis spectrum of 3-cyano pHP OAc (**1.40a**) in 20% H₂O/CH₃CN has two absorption bands, one at $\lambda_{\text{max}} = 319$ nm and the other at $\lambda_{\text{max}} = 270$ nm, corresponding to the conjugate base and the phenol form, respectively. The spectrum of 2-cyano pHP OAc (**1.40b**) has three bands at $\lambda_{\text{max}} = 348, 305$ and

270 nm, whereas only conjugate base is observed in 100% water for 3-cyano pHP GABA (**1.33a**). In contrast to previously reported pHP derivatives, it appears that the conjugate base of this cyano substituted pHP derivative gives rise to high quantum yields due to reasons discussed above.

The change in Φ can also be attributed to the difference in the leaving group (GABA vs. acetate). Cope¹⁰⁰ examined several different leaving groups, such as mesylate, tosylate, formate and benzoate, and determined that there was a correlation between the quantum efficiency and the pKa of the conjugate acid of the leaving group that took the form of a Bronsted linear free energy relationship (LFER) (Figure 1-15). The equation for the Bronsted plot is given as,

$$\log(k) = \beta_{LG}(\text{pK}_a) + \log(C) \quad \text{Eq. 1.8}$$

Where k is the rate constant of the reaction and β_{LG} is a measure of the sensitivity of the reaction to the acidity of the leaving group.¹⁰⁵ k can be obtained from the quantum yield by the relationship,⁹⁸

$$k = \Phi / \tau^3 \quad \text{Eq. 1.9}$$

Therefore, a plot of $\log (\Phi / \tau^3)$ vs pKa of the leaving group will give rise to a Bronsted plot with a slope corresponding to β_{LG} . The plot obtained by Cope¹⁰⁰ revealed a β_{LG} value of -0.238, indicating that rate of the reaction decreases with increase of the pKa of the conjugate acid of leaving group. The magnitude of 0.238 reveals that the photorelease reaction is less sensitive to the leaving group ability in comparison to the reference reaction, deprotonation of water. The pKa's of GABA and acetate are 4.00 and 4.75, respectively; thus, the observed difference in Φ of 3-cyano pHP GABA and 3-cyano pHP OAc might be partially attributed to the difference in pKa's of the conjugate acid of the leaving groups.

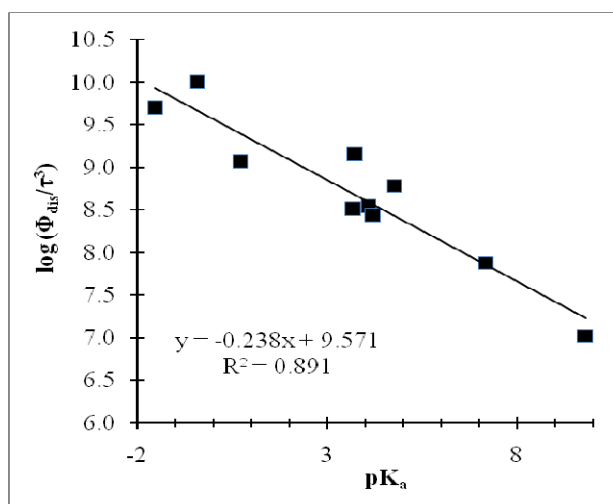
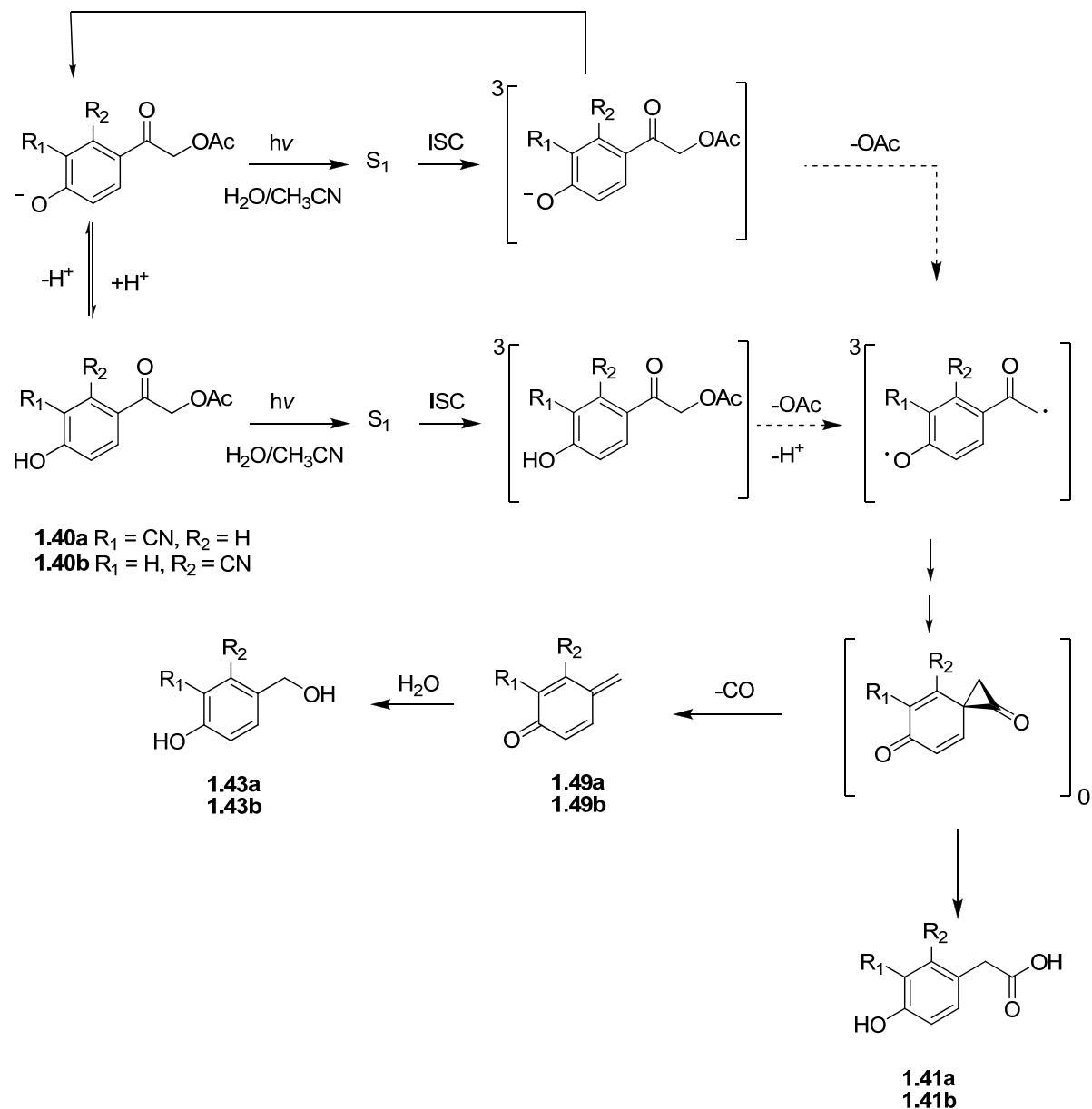


Figure 1-15. Brønsted Linear Free Energy Relationship. LFER between $\log(\Phi_{\text{dis}}/\tau^3)$ and the pK_a values of the acids released during photolysis of pHP esters in aqueous acetonitrile. Reproduced with permission from E. Cope

The mechanism of the photo-Favorskii rearrangement for 3-cyano pHP OAc and 2-cyano pHP OAc differ from that of 3-cyano pHP GABA, due to the presence of both the phenol form and the conjugate base under photolysis conditions (see above). Therefore, the path for acetate release from the cyano substituted pHP chromophore, illustrated in Scheme 1.14, follows a partitioning of the neutral and the conjugate base forms as both can lead to acetate release. The quinone methide intermediate (**1.49**), the precursor to the minor photoproduct, 4-hydroxybenzyl alcohol, is formed by the decarbonylation of the spirodiendione intermediate. Further reaction of the quinone methide (**1.49**) results in the formation of 4-hydroxybenzyl alcohol derivatives.

Scheme 1.14

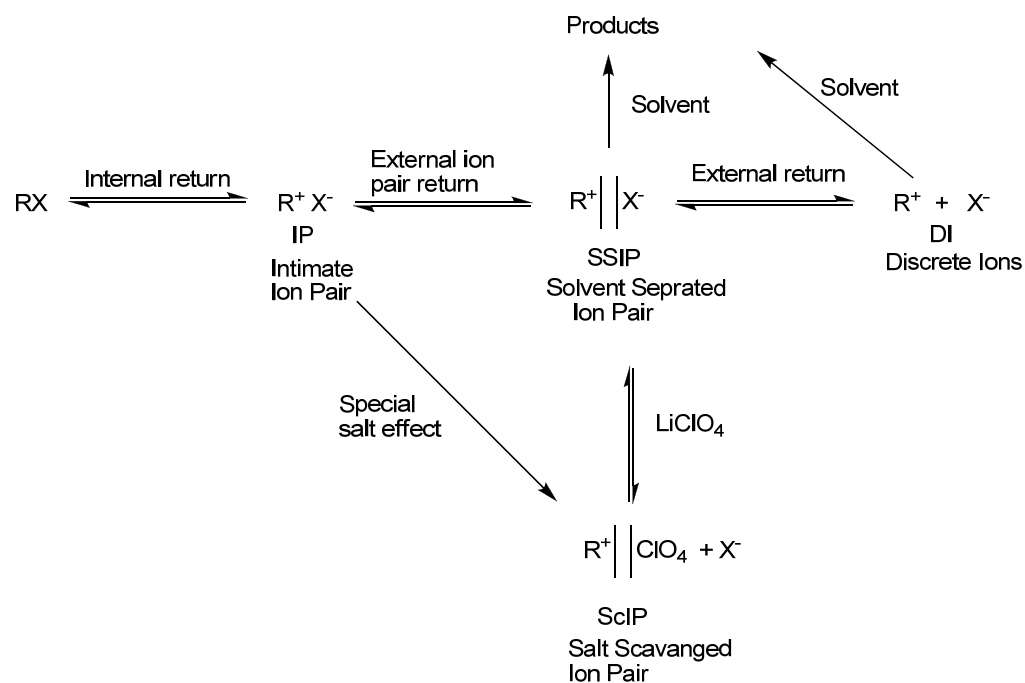


Ionic strength effects

In the 1960's, Winstein^{106,107,108,109} proposed that the rate of a solvolysis reaction could be increased by addition of salts. This phenomenon, commonly known as a "salt effect", is attributed to the intervention of ions into the solvent cage surrounding the initially formed ion pair during solvolysis. The Winstein ion-pair mechanism is illustrated in Scheme 1.15. The

initial ion pairs formed by the heterolysis of the R-X bond are described as “intimate” or “tight” ion pairs (IP). IPs can proceed on to solvent separated ion pairs (SSIP’s) or may revert to the starting covalent substrate in a process termed ion pair return.

Scheme 1.15



SSIP may proceed on to products or it, too, can return to R-X. The SSIP also may further partition directly to the formation of discrete ions (DI) that will subsequently generate the same products. When a salt is added to the medium, the increase in ionic strength tends to make ion pair separation more favorable forming salt scavenged ion pairs (ScIP). This phenomenon stabilizes the ions, which decreases the possibility of ion pair return, and thereby increases the apparent rate of the product formation (and thus the rate of reaction). When LiClO₄ is used as the salt, Li⁺ can assist in the dissociation of SSIP’s by coordinating with the leaving group and forming a salt scavenged ion pairs (ScIP). Generally, added salts cannot intercept the intimate

ion pair and aid in their dissociation. However, LiClO₄ is an exception and has been shown to insert between IP's, forming ScIP. This phenomenon has become known as a "special salt effect".

An increase in the quantum yield of photorelease of 3-cyano pHP GABA (**1.6a**) may be anticipated in the presence of an added salt, given that an ion-radical pair is postulated upon release of the leaving group in the currently accepted mechanism of the photo-Favorskii rearrangement. An increase in the ionic strength of the solution will stabilize the ionic components and thereby reduce the potential driving force for ion pair return. However, in the case of **1.33a**, Φ_{diss} decreased from 0.42 to 0.28 with the increase from 0 to 1.0 M LiClO₄ and from 0.42 to 0.32 for NaClO₄ was observed. The Φ_{diss} at low concentrations of salt (from 0 to 0.025 M) remains essentially constant within experimental error (Table 1-8 and Figure 1-12 in *Results*). These results contrast with Stensrud's¹⁰⁴ findings on several fluoro substituted pHP GABA's (e.g., 2-fluoro pHP GABA, pKa = 7.2) and for pHP GABA itself (pKa = 8.0) that showed an increase in quantum yields with increasing salt concentration. However, for 2,5-difluoro pHP GABA and 2,3-difluoro pHP GABA, with pKa's of 5.6 and 5.9, respectively, the variation of Φ_{diss} with added salt concentration was more complicated. For compounds with lower pKa's, including the 3-cyano pHP chromophore (pKa = 5.2), the dominant form present at neutral pH in water would be the conjugate base under the conditions applied for this study. Because the conjugate base is a polar, ionic species, it will be more highly solvated prior to the photolysis and could be thought of as trapped in an already structured solvent cage. Upon photolysis, ion-radical pair formation is now within a confined, closely proximate solvent-salt cage. With increasing salt concentration the solvent sphere around the conjugate base will be strengthened and the separation of the developing anion from the conjugate base will be more

difficult, resulting in recombination which appears as a decrease in the quantum yield. Attempts to carry out photolysis in low pH buffered salt solutions failed since **1.33a** was not soluble in the combined salt/buffer combinations.

To investigate the ionic strength effect on pHP OAc **1.40c**, quantum yield studies were carried out in 37% H₂O/MeOH due to solubility constraints. The water fraction was replaced by aqueous solutions containing different concentrations of LiClO₄. As in the case of **1.33a**, Φ_{diss} decreased with increasing salt concentrations (Table 1-8 in *Results*). Note that Φ_{diss} in 37% H₂O/MeOH is 0.56, much higher than the 0.31 value measured in 20% H₂O/ CH₃CN suggesting a methanol assisted photorelease for the pHP OAc.

Future directions: 3-cyano pHP GABA (**1.33a**) has shown quantum efficiencies superior to many other pHP derivatives. This is in conflict with previous results as pHP derivatives with lower pK_a values similar to **1.33a** have shown lower quantum efficiencies.^{91,104} Time resolved resonance Raman and laser flash photolysis studies on this pHP derivative will be useful in understanding the mechanism of photorelease. Synthesis and study of the 2-cyano pHP GABA will also be valuable since it will give information about the effect of the cyano group in ortho vs. meta positions. Rates of acetate release from the two cyano derivatives will also give important mechanistic information that will help understand the large difference in quantum efficiencies of 3-cyano pHP GABA and 3-cyano pHP OAc. It is clear that ionic strength of the medium affects the efficiency of photorelease, but the origin of this observation is not clear. More studies are necessary to fully comprehend the salt effect.

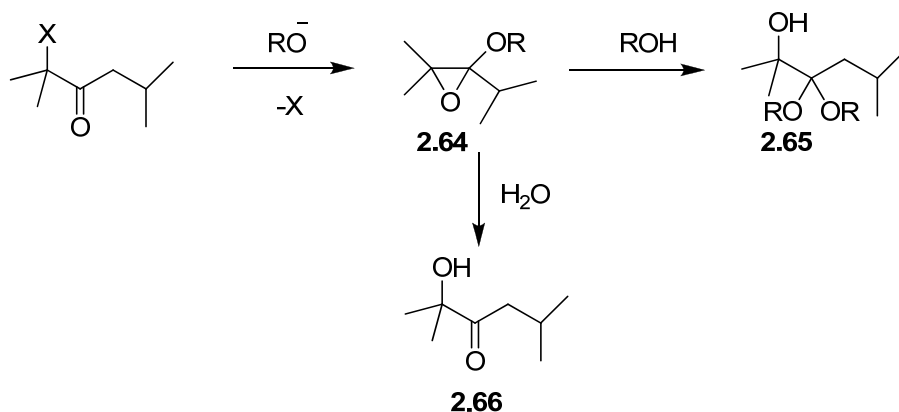
1.4 Conclusions: Cyano pHP esters were designed and synthesized to explore structure activity relationships and to fine tune the physical and photochemical properties of the pHP chromophore. Addition of the cyano substituent, an electron withdrawing group, substantially reduced the pKa of the phenolic proton. When the leaving group was GABA, a significant increase in the quantum efficiency of photorelease was observed compared to parent pHP. Under the experimental conditions the major species present is the conjugate base. Work done by Givens and Wirz⁴⁰ suggests that photorelease from the conjugate base is inefficient. Therefore, the observed high Φ for 3-cyano pHP GABA is unique. However the photoproducts observed are in accord with other pHP derivatives indicating that mechanism of photorelease involves a photo Favorskii rearrangement. Stern-Volmer quenching studies using potassium sorbate revealed that the reactive species is the triplet and gave a rate constant of $1.1 \times 10^7 \text{ s}^{-1}$ for photorelease. Best Φ 's were observed when photolysis was performed in water or pH 7.05 buffer. Φ decreased with both the increase and decrease of pH. Φ also decreased with increase ionic strength of the medium. In contrast to 3-cyano pHP GABA, cyano substituted pHP acetates showed lower Φ than parent pHP.

2.3 Comparison of the base-activated and excited state Favorskii rearrangements.

Background: Common byproducts of the Favorskii rearrangement.

The most widely observed byproducts of the base activated Favorskii rearrangement are epoxy ethers, α -hydroxy ketals, α -hydroxy ketones and α -alkoxy ketones.^{71,78} Unsaturated ketones and acids from secondary reaction products are less frequently observed.^{110,111} The major course of many side reactions is generally believed to be nucleophilic addition of the alkoxide to the carbonyl group (Scheme 2.21). Subsequent loss of halide results in the formation of labile epoxy ether (**2.64**) that can give rise either to α -hydroxy ketals (**2.65**) or α -hydroxy ketones (**2.66**). α -Hydroxy ketones are also formed by direct S_N2 type displacement of halide in the presence of hydroxides.

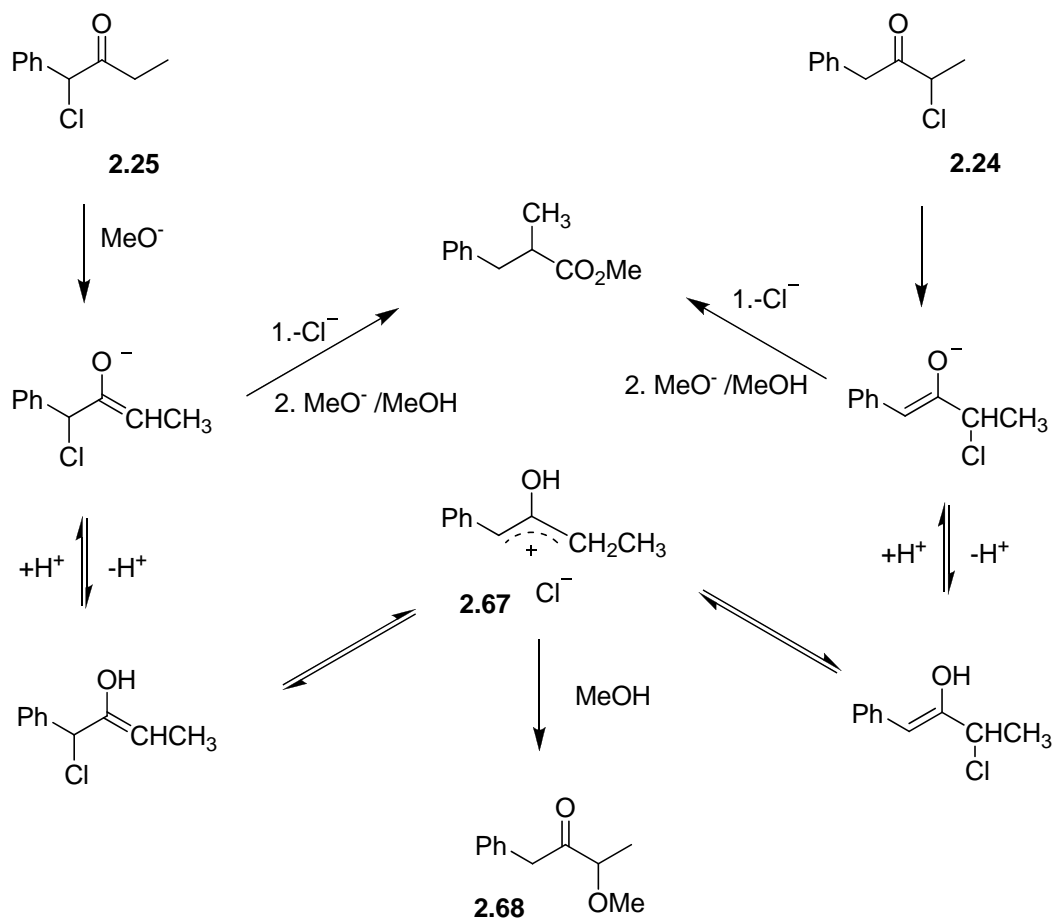
Scheme 2.21



The mechanism of formation of α -alkoxy ketones has been pursued by several groups and several mechanisms have been proposed. S_N2 ,¹¹² S_N2' ,¹¹³ cleavage of an allene oxide,¹¹⁴ rearrangement of the epoxy ether,^{1090,111} reaction of the dipolar ion,¹¹⁵ reaction of the cyclopropanone,¹¹⁶ and alcoholysis of enol allylic intermediates⁷⁸ have been reported. Bordwell and coworkers⁷⁸ found that the two isomeric chloro ketones **2.24** and **2.25** gave rise to the same α -methoxy ketone **2.68** when exposed to 0.05 M NaOMe in MeOH (Scheme 2.22). Therefore the

authors favor a mechanism involving the enol-allylic chloride intermediate **2.67**, which can generate the same byproduct from both chloro isomers **2.24** and **2.25**.

Scheme 2.22

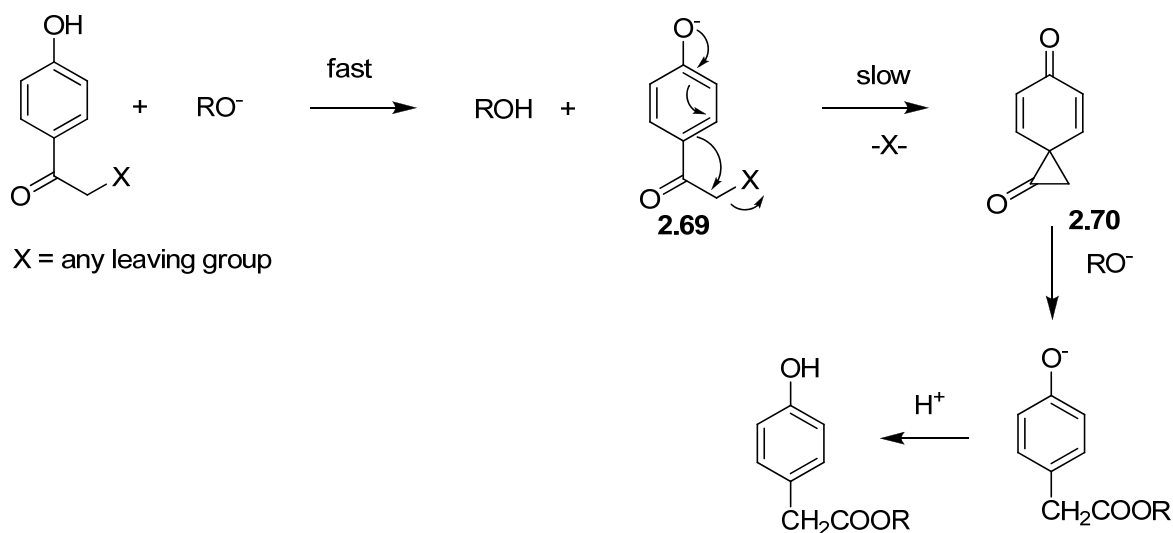


Extending the base activated Favorskii rearrangement to the pHP derivatives:

In principle, the mechanism of the base activated Favorskii rearrangement can be applied to pHP derivatives as depicted in Scheme 2.23. Initial loss of the proton will result in the formation of the conjugate base (**2.69**) that will further react to form the dienedione intermediate **2.70**. The formation of **2.70** can occur either by the concerted loss of the leaving group (shown in Scheme 2.23) or via a zwitterionic intermediate (not shown). Subsequent attack by a nucleophile, e.g., hydroxide or alkoxide, on **2.70** will result in the formation of the rearranged Favorskii

product. For base activated Favorskii rearrangements, the rate determining step (RDS) is either the removal of an α' -hydrogen or the loss of the halide depending on the system under investigation (see *Introduction*). However, for the pHP derivatives the loss of the phenolic hydrogen to form the conjugate base is fast, rendering the removal of the leaving group the most probable RDS of this hypothetical reaction.

Scheme 2.23

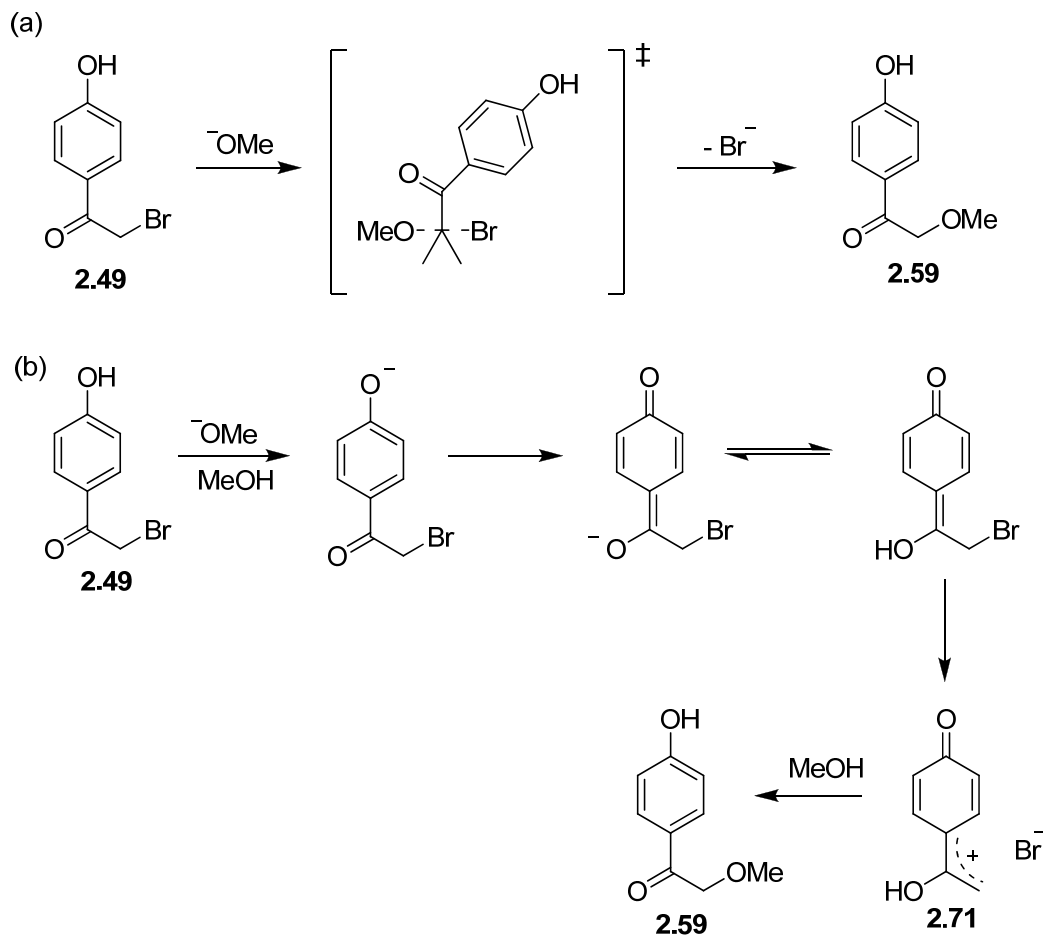


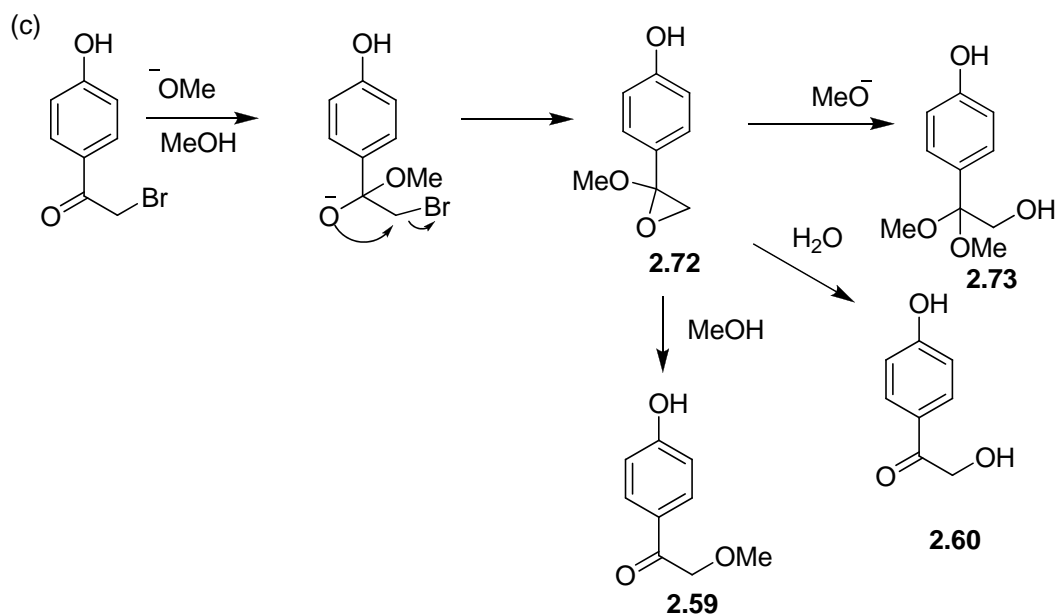
Interestingly, the only pHP derivative that showed even a trace amount of the Favorskii rearrangement product was pHP Br. Less than 1% of methyl *p*-hydroxyphenylacetate (**2.56**) was formed at 0 °C. The major product at 0 °C and the only product observed at RT and reflux was *p*-hydroxyphenacyl methyl ether (**2.59**).

The mechanism for formation of the ether can be easily explained by direct S_N2 displacement of the bromide by methoxide (Scheme 2.24 (a)). A mechanism can also be imagined that involves the proton tautomeric methylene quinone. Loss of bromide yields the cation intermediate (**2.71**) through this sequence similar to a mechanism proposed by Bordwell⁷⁹ (Scheme 2.24(b)). Yet another route for *p*-hydroxyphenacyl methyl ether would be the

hydrolysis of the epoxy ether **2.72** formed by direct attack on the carbonyl carbon by methoxide (Scheme 2.24(c)). However the signature byproduct of this reaction, α -hydroxy ketals (**2.73**), was not observed in the reaction of pHP Br or any other pHP derivative subjected to this study. Therefore pathways involving epoxy ethers are highly unlikely for pHP derivatives.

Scheme 2.24





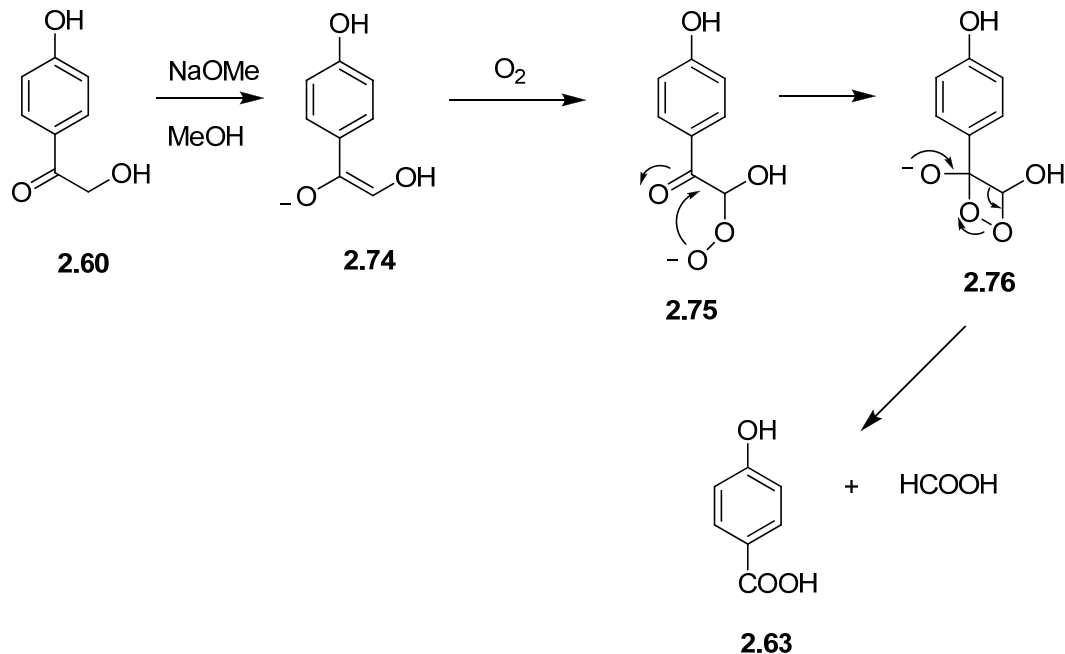
*p*HP OPO(OEt)₂ was surprisingly stable under Favorskii conditions. The compound reacted to give *p*-hydroxyphenacyl alcohol (**2.60**) only at refluxing MeOH temperatures. Formation of *p*-hydroxyphenacyl alcohol is best explained via hydrolysis of the phosphate group. An entirely different reactivity to that of *p*HP OPO(OEt)₂ was observed for *p*HP OPO(OPh)₂, which was extremely reactive. The major product, the monophenyl compound **2.62** (95%), arises from the hydrolysis at the phosphate group accompanied by loss of a phenolate ion, the better leaving group in this phosphate ester. The minor product, *p*-hydroxyphenacyl alcohol (**2.60**, 5%), occurs from the loss of the *p*HP component or possibly another route like those discussed above. The monophenyl compound **2.62** further reacts to give *p*-hydroxyphenacyl alcohol.

*p*HP OAc reacts rapidly to give *p*-hydroxyphenacyl alcohol (**2.60**). Therefore the determination of the rate constants had to be carried out at 0 °C, where the reaction was relatively slow. Formation of *p*-hydroxyphenacyl alcohol can be explained by the hydrolysis of the acetate ester through nucleophilic attack at the ester carbonyl carbon. **2.60** can also be made by direct displacement process of the acetate by hydroxide ion. However absence of *p*-hydroxyphenacyl

methyl ether (**2.59**), the product of direct displacement by methoxide, favors hydrolysis pathway. pHP GABA was even more reactive than pHP OAc. It was rapidly converted to *p*-hydroxyphenacyl alcohol as the only product and the reaction was too fast to measure rate constants even at 0 °C with our conditions for this study. The formation of **2.60** is due to the hydrolysis of the GABA ester through nucleophilic attack at the carboxylate carbon by the reasoning outlined above. Further reaction of *p*-hydroxyphenacyl alcohol (**2.60**) under the basic hydrolysis conditions used for these reactions gave rise to *p*-hydroxybenzoic acid (**2.63**). A similar transformation of cyclohexanecarboxylic acid from chloromethyl cyclohexyl ketone in the presence of NaOMe/ MeOH had been reported by Loftfield and Schaad.¹¹⁰ Formation of the acid was greatly diminished in the absence of water and the authors assign the formation of the acid to hydrolytic cleavage of the α -hydroxy ketone, formed by the hydrolysis of the epoxy ether, to generate the acid and formaldehyde.

However, lack of *p*-hydroxybenzoic acid formation when the reaction was carried out under argon suggests participation by oxygen. Literature precedence for oxygen mediated oxidation of ketones with acidic α -hydrogens in the presence of base is available.¹¹⁷ However, mechanistic information on the reaction path way is limited and is believed to involve oxidation of the enolate form of the ketone. A plausible mechanism for the reaction is given in Scheme 2.25. Reaction between the enolate **2.74** and molecular oxygen will generate peroxy anion **2.75** that will attack the carbonyl carbon to form the cyclic peroxide **2.76**. This collapses to give the observed *p*-hydroxybenzoic acid.

Scheme 2.25



Under Favorskii conditions pHP OTs primarily gave *p*-hydroxyphenacyl methyl ether (2.59) at all temperatures. The amount of the minor product, *p*-hydroxyphenacyl alcohol (2.60), was dependent on the temperature. The amount of *p*-hydroxyphenacyl alcohol increased from 6% to 8% to 18% when the temperature was changed from 0 °C then RT and finally to reflux. The formation of *p*-hydroxyphenacyl methyl ether (2.59) can be credited to an S_N2 displacement of the tosyl group by methoxide since tosylate is a good leaving group, one of the best among the series examined. However, the formation of *p*-hydroxyphenacyl alcohol cannot be attributed to the hydrolysis of the sulfonates as was suggested for the carboxylate and possibly the phosphate derivatives since sulphonates are much less susceptible to hydrolysis at the sulfur atom. Therefore the formation of *p*-hydroxyphenacyl alcohol is best rationalized as the product of an S_N2 displacement by water.

In the presence of 0.05 M NaOMe/MeOH, pHP 4-CF₃PhO was stable at all temperatures studied, i.e. 0 °C, RT, and at reflux,. The greater stability of pHP 4-CF₃PhO may be due to the

poor leaving group ability of the phenolate ion compared to the other leaving groups investigated here. It is interesting to note that pHP 4-CF₃PhO did undergo photorelease with formation of 4-hydroxyphenylacetic acid and *p*-trifluoromethylphenol with a quantum efficiency of 0.09.¹⁰¹

In contrast to the conventional belief, most pHP derivatives proved to be quite stable to the strongly acidic conditions examined in this study (0.1 M HClO₄). The least stable, pHP OAc, hydrolyzed completely to form *p*-hydroxyphenacyl alcohol (**2.60**) in 6 h. pHP GABA hydrolyzed to give the same alcohol **2.60** in yields up to 50% within 24 h while pHP OPO(OPh)₂ hydrolyzed only to the extent of 15% in 24 h. The other pHP derivatives tested were stable under acidic conditions for at least 24 h. When comparing the reactivity of pHP esters in both acidic or basic media, the results of the control experiments for base activated Favorskii rearrangements at RT and the lack of reactivity in 0.1M HClO₄, one must conclude that pHP derivatives, in general, are quite stable for studies in biological media. Furthermore, it is readily apparent that they are generally more stable in acidic conditions than in basic conditions.

Future directions: In this study, only a single set of basic conditions, 0.05 M NaOMe/MeOH, was explored for the base activated Favorskii rearrangements. It is known that the extent of Favorskii product formation depends on the concentration of base, type of base, temperature and solvent.⁷³⁻⁸⁰ It would be very useful to investigate the behavior of pHP derivatives further, especially under more optimal Favorskii reaction conditions. For example, it was generally found that chloride would be a better leaving group candidate for Favorskii rearrangement than bromide.⁷³ As the only pHP derivative that shows even trace amounts of Favorskii product in this study was the pHP Br, it would be important to explore the behavior of pHP Cl under strong basic conditions toward its Favorskii rearrangement propensity.

2.4 Conclusions: Based on the results from the test for base activated Favorskii rearrangement, it is clear that the pHP derivatives examined in this study, with the minor exception of pHP Br, do not undergo the Favorskii rearrangement under conditions investigated. When the caged compound has a carboxylate or a phosphate ester linkage, hydrolysis at the carboxylate carbon or possibly at the phosphorus dominates. When the leaving group is bromide or tosylate S_N2 displacement becomes dominant. The 4-trifluoromethylphenoxide leaving group is extremely stable to displacement under both acid and basic conditions. Stability studies further show that pHP derivatives are quite stable under acid conditions and less so under base conditions, which, in turn, are generally only slowly degraded at room temperature. Among the derivatives studied, the carboxylates are the least stable group under both acid and base conditions.

Experimental

General Methods. Melting points were conducted with open ended capillary tubes using a non-calibrated melting point apparatus. Products of all reactions were assessed for purity using the following instrumental techniques: ^1H , and ^{13}C , were obtained using Bruker 400 HZ instrument unless otherwise stated. Exact masses were obtained using a triple quadrupole electro spray ionization mass spectrometer. UV/vis data were obtained using 1.5 mL quartz cuvettes on a Cary 100 spectrophotometer (Varian, Inc., Palo Alto, CA). IR data were obtained with pressed potassium bromide (KBr) pellets. Product separation was achieved by flash chromatography using silica gel and gradient hexanes/ethyl acetate as eluting solvents unless otherwise stated.

Photolysis studies were performed in a Rayonet RPR-100 photoreactor equipped with two 15 W, 3000 Å lamps and a merry-go-round apparatus. Quantum yield studies and product identification was achieved through UPLC or LC/MS/MS, triple quadrupole electrospray ionization mass spectrometer, analysis equipped with a UV-Vis dual wavelength detector set at 250 and 280 nm. The reservoirs used were as follows: A) 99% water, 1% acetonitrile, and 0.06% formic acid; B) 99% acetonitrile, 1% water, and 0.08% formic acid. The compounds were separated on a reverse-phase (C18, 5 μm mesh), 50 mm length column. Three injections of 5 μl-100 μl were made with an automated sampler for each sample. The mobile phase gradient was optimized for compound separation and the flow rate was set at 200 μl/min. During data analysis, smoothing functions were used for peak area determinations of the chromatographic peaks. Calibration curves were constructed for all compounds and photoproducts for quantification purposes.

Synthesis

5-bromo-2-(phenylmethoxy)benzonitrile (1.29a). The general method of Freché, *et al.*¹¹⁸ was followed. 5-bromo-2-hydroxybenzonitrile (1 g, 5.05 mmol), benzyl bromide (0.533 ml, 4.54 mmol), and K₂CO₃ (1.75 g, 12.62 mmol) were stirred in CH₃CN (25 ml) at room temperature for 16 h. The resulting solution was evaporated to dryness, dissolved in water and extracted with ethyl acetate. The ethyl acetate layer was dried with anhydrous MgSO₄ and the solvent evaporated in vacuo. The white solid obtained was used without further purification (1.27 g, 87%): mp 80-81 °C, IR (KBr): 3068, 3035, 2229, 1591, 1487, 1454, 1287, 1132, 1132, 1018, 813, 742, 696 cm⁻¹. ¹H NMR (400 MHz, CD₃CN): δ 5.22 (s, 2H); 7.14 (d, 1H); 7.45 (m, 5H); 7.73 (dd, 1H); 7.81 (d, 1H). ¹³C NMR (100 MHz, CD₃CN): δ 71.9, 104.5, 112.5, 115.9, 116.2, 128.7, 129.4, 129.7, 136.7, 136.8, 138.4, 160.6. HRMS calculated for C₁₄H₁₀BrNO = 286.9946, observed = 286.9937.

5-acetyl-2-(phenylmethoxy)benzonitrile (1.30a). The general method of Kosugi, *et al.*¹¹⁹ was followed. A solution of 1.29a (2.4 g, 8.72 mmol), tetrakis (triphenylphosphene), Pd (0.53 g, 0.44 mmol), and 1-ethoxyvinyl tri-N-butyltin (2.88 ml, 9.60 mmol) in dry toluene (15 ml) was stirred at 100 °C under argon for 24 h. Special care was taken to keep the reaction mixture under dry conditions. The resulting black solution was stirred for 3 h with 10 % HCl, filtered through Celite to remove Pd. The organic layer was stirred for 8 h with saturated aqueous KF to remove tin, separated and purified by column chromatography (5:1 hexane: ethyl acetate) to obtain 5-acetyl-2-(phenylmethoxy)benzonitrile (0.91 g, 90 %): mp, 120-123 °C. IR (KBr): 3068, 3033, 2229, 1681, 1602, 1500, 1419, 1355, 1275, 1137, 977, 817, 750, 630 cm⁻¹. ¹H NMR (400 MHz, CD₃CN): δ 2.53 (s, 3H), 5.31 (s, 2H), 7.26 (d, 1H), 7.44 (m, 5H), 8.17 (dd, 1H), 8.26 (d, 1H). ¹³C NMR (100 MHz, CD₃CN): δ (ppm) 25.4, 70.8, 101.5, 112.6, 115.3, 127.5, 128.2, 128.4, 130.2,

134.2, 134.5, 1335.3, 163.0, 194.9. HRMS calculated for $C_{16}H_{13}NO_2 = 252.1024$, observed = 252.1022.

5-(2-bromoacetyl)-2-(phenylmethoxy)benzonitrile (1.31a). The general method of Holman, *et al.*¹²⁰ was followed. 5-acetyl-2-(phenylmethoxy)-benzonitrile (1.30a) (1.00 g, 3.97 mmol) and phenyltrimethylammonium tribromide (1.707 g, 4.37 mmol) in 3:1 CH_2Cl_2 : MeOH (20 ml) was stirred at room temperature for 16 h. The solvent was evaporated *in vacuo* and to the resulting oil was added 20 ml H_2O/CH_2Cl_2 and the CH_2Cl_2 layer extracted and washed with water five times, dried with anhydrous $MgSO_4$, and the solvent evaporated. The resulting solid was purified by column chromatography (1:1 hexane:ethyl acetate) to obtain 1.195 g of 5-(2-bromoacetyl)-2-(phenylmethoxy)benzonitrile (91%): mp 94-96 °C; IR ($CDCl_3$): 688, 833, 1037, 1247, 1280, 1600, 1735, 2115, 2258, 3091. 1H NMR (400 MHz CD_3CN): δ (ppm) 4.63 (s, 2H), 5.35 (s, 2H) 7.16(d, 1H), 7.46 (m, 5H), 8.25(dd, 1H), 8.32(d, 1H). ^{13}C NMR (100 MHz, CD_3CN): δ (ppm) 32.3, 71.3, 102.3, 113.3, 115.3, 117.4, 127.3, 127.9, 128.6, 128.8, 135.1, 135.5, 135.5, 163.9, 188.9. HRMS calculated for $C_{16}H_{13}BrNO_2 = 330.0130$; observed = 332.0134.

2-(4-(benzyloxy)-3-cyanophenyl)-2-oxoethyl 4-(tert-butoxycarbonylamino)butanoate (1.32a)) The general method of Hiyama, *et al.*¹²¹ was applied. 5-(2-Bromoacetyl)-2-(phenylmethoxy)-benzonitrile (1.31a) (0.356 g, 1.07 mmol), 4-(*tert*-butoxycarbonylamino)butanoic acid (t Boc GABA, 0.263 g, 1.30 mmol), and K_2CO_3 (0.37g, 2.70 mmol) in CH_3CN (20 ml) was stirred at room temperature for 24 h. The solvent was evaporated, the resulting residue dissolved in water, and the water layer extracted with ethyl acetate three times. The compound was further purified by column chromatography (3:1 ethyl acetate: hexane) to yield the desired product, 2-(4-(benzyloxy)-3-cyanophenyl)-2-oxoethyl 4-(tert-butoxycarbonylamino)butanoate (**1.32a**) as white solid (0.395 g, 81%): mp 119-120 °C. IR ($CHCl_3$): 3456, 2252, 1743, 1706, 1600, 1502,

1271, 1166 cm^{-1} ; ^1H NMR (400 MHz CD_3CN): δ (ppm) 1.39 (s, 6H), 1.78 (t, 2H), 2.20 (m, 2H), 3.10 (t, 2H), 5.31 (s, 4H), 7.29 (d, 1H), 7.40 (m, 5H), 8.17 (dd, 1H), 8.25 (d, 1H); ^{13}C NMR (100 MHz, CD_3CN): δ (ppm) 24.5, 25.5, 27.3, 30.3, 9.0, 65.6, 70.8, 70.9, 77.7, 101.9, 112.6, 112.9, 115.0, 117.0, 127.0, 127.5, 128.2, 133.9, 134.2, 135.1, 155.6, 163.6, 172.2, 189.9. The HRMS was calculated for $\text{C}_{25}\text{H}_{25}\text{N}_2\text{O}_7 + \text{H} = 453.2026$; observed = 453.2021

4-(2-(3-cyano-4-hydroxyphenyl)-2-oxoethoxy)-4-oxobutan-1-aminium-2,2,2-trifluoroacetate (3-cyano pHP GABA, 1.33a) Pd/C (34 mg, 10% by weight) was added to a solution of **1.32a** (340 mg, 3.07 mmol) in ethyl acetate and H_2 bubbled into the solution. The reaction was followed by TLC and was complete after 4 h to yield 2-(3-cyano-4-hydroxyphenyl)-2-oxoethyl 4-(tert-butoxycarbonyl amino)butanoate as a white solid. This was further reacted with 10 ml of 50% TFA/ CH_2Cl_2 for 15 min at room temperature. Solvent was removed *in vacuo* and ethyl acetate (10 ml) and water (10 ml) added to the residue and water layer extracted, frozen and lyophilized to remove water to yield 4-(2-(3-cyano-4-hydroxyphenyl)-2-oxoethoxy)-4-oxobutan-1-aminium-2,2,2-trifluoroacetate (**1.33a**) in 70% yield as a white solid (140 mg): mp 147-149 $^\circ\text{C}$ IR (KBr) 3388, 2358, 2343, 2237, 1677 (broad), 1610, 1438, 1205, 1137, 842, 802, 723. ^1H NMR (400 MHz D_2O): δ (ppm) 1.94 (t, 2H), 2.59 (m, 2H), 3.08 (t, 2H), 5.39 (s, 2H), 7.05 (d, 1H), 8.01 (dd, 1H), 8.18 (d, 1H). ^{13}C NMR (100 MHz, D_2O): δ (ppm) 22.0, 29.4, 38.5, 66.6, 99.2, 112.8, 115.1, 117.4, 119.7, 134.9, 162.8, 172.4, 192.3. The HRMS was calculated for $\text{C}_{13}\text{H}_{15}\text{N}_2\text{O}_4 = 263.1032$, observed = 263.1023.

The same result could be achieved by stirring **1.32a** (100 mg, 0.22 mmol) for 10 days in dry TFA. Following the same procedure described above 4-(2-(3-cyano-4-hydroxyphenyl)-2-oxoethoxy)-4-oxobutan-1-aminium-2,2,2-trifluoroacetate was obtained as a waxy oil (30mg, 50%).

2-bromo-5-(phenylmethoxy)benzotrile (1.29b) The general method of Boykin *et al.*⁹⁶ was utilized. 3-Hydroxybenzotrile (1.00 g, 8.39 mmol) was dissolved in acetic acid (9.6 ml) and cooled to 0 °C. Bromine (1.33 ml, 8.39 mmol) was added drop-wise to the solution and stirred for 2 h. The reaction was quenched by adding sodium thiosulfate and the mixture was extracted with ethyl acetate. The ethyl acetate was removed *in vacuo* resulting in a white solid (0.82 g) which contained a mixture of products. The phenolic OH was benzyl protected by reacting with benzyl bromide (0.5 ml) in the presence of K₂CO₃ (1.43 g). From the mixture, 2-bromo-5-(phenylmethoxy) benzotrile (**1.29b**) was isolated using column chromatography (ethyl acetate/hexane) as a light yellow crystalline solid (0.72 g, 30 %): mp 98-99 °C. IR (KBr) 2231, 1591, 1473, 1319, 1244, 1130, 1004, 835, 756. ¹H NMR (400 MHz (CD₃)₂CO): δ (ppm) 5.12 (s, 1H), 7.30 (dd, 1H), 7.43 (m, 6H), 7.72 (d, 1H). ¹³C NMR (100 MHz, (CD₃)₂CO): 70.4, 114.8, 115.9, 116.6, 120.2, 122.1, 127.7, 128.1, 12.5, 134.1, 136.2, 158.2. The ESMS was calculated for C₁₄H₁₀BrNO = 286.9946, observed = 287.9897.

2-acetyl-5-(phenylmethoxy)benzotrile (1.30b) The same procedure as used for **1.30a** was followed yielding 2-acetyl-5-(phenylmethoxy)benzotrile: (0.20 g, 60 %): mp 111 - 113 °C. ¹H NMR (400 MHz (CD₃)₂CO): δ 2.62 (s, 3H), 5.34 (s, 2H), 7.37 (m, 4H), 7.43 (m, 3H), 8.14 (d, 1H), ¹³C NMR (100 MHz, (CD₃)₂CO): δ (ppm) 25.5, 70.8, 112.4, 113.1, 117.5, 127.5, 127.7, 128.1, 128.2, 132.1, 134.3, 136.0, 161.5, 194.9. The HRMS was calculated for C₁₆H₁₃NO₂ = 252.1024, observed = 252.1033.

2-(2-bromoacetyl) -5-(phenylmethoxy)benzotrile (1.31b). The same procedure as used for **1.31a** was followed to generate 2-(2-bromoacetyl) -5-(phenylmethoxy) benzotrile (0.531 g, 88%). Compound was not pure. Therefore coupling of ^tBocGABA was carried out without

further purification. ^1H NMR (400 MHz CD_3CN): δ (ppm) 4.64 (s, 1H), 5.21 (s, 2H), 7.40 (m, 7H), 7.47 (d, 1H).

2-(4-(benzyloxy)-2-cyanophenyl)-2-oxoethyl 4-(tert-butoxycarbonylamino)butanoate (1.32)

b) The same procedure used in synthesis of **1.32a** was employed to obtain 2-(4-(benzyloxy)-2-cyanophenyl)-2-oxoethyl 4-(tert-butoxycarbonylamino)butanoate as a light yellow solid (0.113 g, 50%): mp 120-121 $^\circ\text{C}$. IR (KBr): 3456, 2252, 1743, 1706, 1600, 1502, 1271, 1166 ^1H NMR (400 MHz CD_3CN): δ (ppm) 1.75 (s, 9H), 1.79 (t, 2H), 2.46 (m, 2H), 3.10 (t, 2H), 5.22 (s, 2H), 5.29 (s, 2H), 7.42 (m, 7H), 7.98 (d, 1H), ^{13}C NMR (100 MHz, CD_3CN): δ (ppm) 24.7, 27.3, 30.3, 39.0, 65.8, 70.3, 77.8, 112.3, 118.0, 122.2, 127.6, 128.1, 128.4, 128.4, 131.6, 135.5, 155.6, 161.7, 172.2, 160.1. HRMS calculated for $\text{C}_{25}\text{H}_{25}\text{N}_2\text{O}_7 + \text{H} = 453.2026$, observed = 453.2021

5-bromo-2-(tert-butyldimethylsilyloxy)benzonitrile (1.34) The general method of Palomo *et al.*¹²² was followed. A solution of 5-bromo-2-hydroxy benzonitrile (1 g, 5.05 mmol), *tert*-butyldimethylsilylchloride (TBS, 0.84 g, 5.55 mmol), triethylamine (0.78 ml, 5.55 mmol) and DBU (0.07 ml, 0.5 mmol) in methylene chloride was stirred at room temperature for 16 h under argon. The completion of the reaction was confirmed by TLC. The resulting solution was stirred with 10% HCl, washed with water and solvent evaporated *in vacuo*. The resulting oil was purified by column chromatography (1:1 hexane: ethyl acetate) to obtain a white solid (1.45 g, 92%). ^1H NMR (400 MHz, CDCl_3): 0.89 (s, 6 H), 1.20 (s, 9H), 6.83 (d, 1H, $J = 8.77$ Hz), 7.58 (dd, 1H, $J = 8.78, 2.25$ Hz), 7.64 (d, 1H, 2.15 Hz).

5-acetyl-2-hydroxybenzonitrile (1.35) The same procedure as used for **1.30a** was followed to yield 5-acetyl-2-hydroxybenzonitrile as a white solid (1.4 g, 43%): mp 183-185 $^\circ\text{C}$. IR (KBr) 3282, 2233, 1674, 1602, 1413, 1382, 1236, 968, 829, 574 units. ^1H NMR (400 MHz CD_3CN): δ (ppm) 2.51 (s, 1H), 7.07 (d, 1H), 8.04 (dd, 1H), 8.20 (d, 1H), 8.98 (s, 1H); ^{13}C NMR (100

MHz, CD₃CN): δ 25.4, 99.5, 115.3, 115.7, 129.7, 134.1, 134.3, 162.4, 194.9. HRMS calculated for C₉H₇NO₂ = 161.0477, observed = 161.0482. UV (water) λ_{max} = 315, ϵ = 32300

2-(acetyloxy)-1-[3-cyano-4-(phenylmethoxy)phenyl] ethanone (1.39b) A solution of NaOAc (175 mg, 2.13 mmol) and **1.31b** (470 mg, 1.42 mmol) in acetone was stirred overnight. The resulting solution was evaporated to dryness, 15 ml of water was added and the mixture was extracted with ethyl acetate (3 \times 15 ml). The ethyl acetate layer was dried with anhydrous MgSO₄. The solvent removed and the resulting solid was further purified by column chromatography (1:1 hexane: ethyl acetate) to give 2-(acetyloxy)-1-[3-cyano-4-(phenylmethoxy)phenyl] ethanone (**1.39b**) as a white solid (250 mg, 57%): mp 122-124 °C. IR (KBr) 2225, 1735, 1701, 1595, 1321, 1222, 1078, 989, 761 units. ¹H NMR (400 MHz (CD₃Cl): δ (ppm) 2.20 (s,3H),5.17 (s, 2H),5.27 (s, 2H), 7.21 (m, 1H),7.37(m,6h),7.87(d,1H) . ¹³C NMR (100 MHz, (CD₃CN) : 19.3, 65.8, 70.3, 112.2, 118.0118.2, 122.2, 127.4, 127.6, 128.1, 128.3, 128.4, 128.4, 131.5, 135.5, 161.7, 169.9, 190.0.HRMS calculated for M+Na C₁₈H₁₅NO₄Na = 332.0899 , observed = 332.0901.

2-(acetyloxy)-1-[2-cyano-4-(phenylmethoxy)phenyl] ethanone (1.39a) The same procedure as used for **1.39b** was followed to yield 2-(acetyloxy)-1-[2-cyano-4-(phenylmethoxy)phenyl] ethanone as a white solid (90%): mp 92-94 °C. IR (KBr) 2231, 1741, 1691, 1604, 1377, 1284, 1224, 1085, 823,738. ¹H NMR (400 MHz (CD₃Cl): δ (ppm) 2.22 (s, 3H),5.24 (s, 2H), 5.30 (s, 2H), 7.08 (d, 2H), 8.05(m, 5H), 8.16(d, 2H) . ¹³C NMR (100 MHz, (CD₃Cl): 20.6, 65.6, 71.2, 113.2, 115.1, 127.0, 127.4, 128.7, 128.9, 134.1, 134.2, 134.6, 163.8, 170.4, 189.3. HRMS calculated for M+Na C₁₇H₁₆NO₄Na = 332.0899, observed = 332.0916.

2-(acetyloxy)-1-(4-phenylmethoxy)phenyl ethanone (1.39c) The same procedure as used for **1.12b** was followed to obtain 2-(acetyloxy)-1-(4-phenylmethoxy)phenyl ethanone as a white

solid (76%): mp 109-110 °C. ¹H NMR (400 MHz (CD₃Cl): δ (ppm) 2.23 (s,3H),5.14 (s, 2H), 5.30 (s, 2H), 7.02 (d, 2H), 7.39(m,5h), 7.91(d,2H) . ¹³C NMR (100 MHz, (CD₃Cl) : 20.63, 65.76, 70.20, 114.89, 127.39 127.47, 128.32, 128.73, 130.07, 135.94, 161.17, 170.51, 190.57. HRMS calculated for M+Na C₁₇H₁₆NO₄Na = 307.0946, observed = 307.0923.

2-(acetyloxy)-1-(2-cyano-4-hydroxyphenyl) ethanone (1.40b) Pd/C (14 mg, 10% by weight) was added to a solution of **1.39b** (140 mg, 0.42 mmol) in ethyl acetate and H₂ gas bubbled to it. The reaction was followed from TLC and was complete after 4 h .Compound was further purified by column chromatography (1:1 hexane/ ethyl acetate) (79 mg, 80%): mp 158-160 °C. IR (KBr) 3203, 2227, 1741, 1672, 1604, 1560, 1321, 1220, 1122, 1074, 896, 837, 740. ¹H NMR (400 MHz (CD₃)₂CO): δ (ppm) 2.13 (s, 3H), 5.37 (s, 2H), 7.23 (m, 1H), 7.25 (s, 1H), 8.10(d, 1H). ¹³C NMR (100 MHz, (CD₃)₂CO): 19.5, 65.9, 113.0, 117.2, 118.1, 122.5, 128.0, 132.1, 161.5, 169.6, 189.6, HRMS calculated for M+Na C₁₁H₉NO₄Na = 242.0429, observed = 242.0417. UV (water/acetonitrile) λ_{max} = 348 (ε = 625), λ_{max} = 305 (ε = 2440), λ_{max} = 275 (ε = 2830)

2-(acetyloxy)-1-(3-cyano-4-hydroxyphenyl) ethanone (1.40a) The same procedure as used for **1.40b** was followed to obtain the desired compound, 2-(acetyloxy)-1-(3-cyano-4-hydroxyphenyl) ethanone in 90% yield. mp 185-186 °C. IR (KBr) 3150, 2237, 1739, 1666, 1585, 1508, 1421, 1379, 1240, 1124, 1083, 941, 835. ¹H NMR (400 MHz (CD₃)₂CO): δ (ppm) 2.14 (s, 3H), 5.42 (s, 2H), 7.19 (d, 1H) 8.12 (dd, 1H), 8.29 (d, 1H). ¹³C NMR (100 MHz, (CD₃)₂CO):19.5, 65.8, 100.0, 115.3, 116.8, 129.9, 133.8, 134.0, 163.1, 169.6, 189.7. HRMS calculated for M+Na C₁₁H₈NO₄ = 218.0453, observed = 218.0443. UV (20% water/acetonitrile) λ_{max} = 319 (ε = 9240), λ_{max} = 270 (ε = 6620)

2-(acetyloxy)-1-(4-hydroxyphenyl) ethanone (1.40c) The same procedure as used for **1.40b** was followed to obtain the desired compound, 2-(acetyloxy)-1-(4-hydroxyphenyl) ethanone (93%): mp 130-131 °C ¹H NMR (400 MHz (CDCl₃): δ (ppm) 2.23 (s, 3H), 5.29 (s, 2H), 5.54 (s, 1H) 6.88 (d, 2H), 7.86 (d, 2H). ¹³C NMR (100 MHz, CDCl₃): 20.6, 65.8, 115.7, 127.4, 130.4, 160.5, 170.7, 190.5. HRMS calculated for M+Na C₁₀H₁₀O₄Na = 217.0477, observed = 217.0445. UV (20% water/acetonitrile) λ_{max} = 279 (ε = 18300)

***pKa* Determination.**

5-Acetyl-2-hydroxybenzoxonitrile (**1.35**) (41 mg) was dissolved in 10 ml of water and titrated using 0.0461 M NaOH . The NaOH solution was standardized using potassium hydrogen phthalate prior to use. The pH was measured at every 0.2 ml increments of NaOH. The *pKa* was determined using a plot of pH vs. volume of NaOH.

$$pK_a = \text{pH (at half equivalence point)}$$

Exploratory Photochemistry

Quantum yield studies of 3-cyano pHP GABA (1.33a) A solution of 12.89 mg of **1.33a** and 1.53 mg of caffeine (internal standard) dissolved in 4 ml of water or buffer solution was photolyzed using two 3000 Å lamps in a Rayonet RPR-100 photoreactor fitted with merry-go-round apparatus. 100 µl were removed every 60 seconds, diluted to 10 ml with water and the solution analyzed using LC/MS/MS or UPLC. The quantum yield data are given in Table1-9.

Stern-Volmer quenching studies In a general experiment about 30 mg of 3-cyano pHP GABA (**1.33a**) and 2.5 mg of caffeine were dissolved in 5 ml of water. 1 ml of this solution was added to four flasks labeled A, B, C, and D. 10 mg of potassium sorbate was dissolved in 10 ml of water and 0, 1, 2, or 3 ml of this solution was added to the series of flasks. Water was added to

make a total volume of 4 ml in each flask. Each of these solutions was photolyzed using two 3000 Å lamps in a Rayonet photoreactor described above. Quantum yields for each solution were determined using the same procedure described under quantum yield studies. The slope of the plot of Φ_0 (Φ in the absence of the quencher)/ Φ (Φ at different concentrations of the quencher) vs. concentration of quencher gave the Stern-Volmer constant K_{sv} (Table 1-6, Figure 1-10).

Quantum yield studies of 3-cyano pHP OAc (1.40a), 2-cyano pHP OAc (1.40b) and pHP OAc (1.40c) In a general experiment about 10.00 mg of pHP acetate derivative and 2.00 mg of caffeine (internal standard) was dissolved in 4 ml of 20% H₂O : CH₃CN or 20% H₂O/DMSO and photolyzed using two 3000 Å lamps in a Rayonet RPR-100 photoreactor fitted with merry-go-round apparatus. 100 µl were removed every 60 seconds, diluted to 10 ml with the same solvent system and the solution analyzed using LC/MS/MS or UPLC. The quantum yield data are given in table 1-4 results section.

Ionic strength studies on 3-cyano-pHP GABA (1.33a) and pHP OAc (1.40c) Quantum yield of 3-cyano pHP GABA was determined according to the same procedure described above, replacing water with 0.008, 0.025, 0.5, and 1.0 M LiClO₄ in water. Same was repeated with NaClO₄. (Table 1-5). For pHP OAc quantum yield studies were performed in 37% LiClO₄ : MeOH with increasing concentration of LiClO₄ (0.025, 0.5 and 1.0 M). The graphs and tables corresponding to these data are illustrated in figure 1-6 and table 1-5 in results section.

Construction of calibration curves In a general method, 5 mg of the desired compound was dissolved in 5 ml of the solvent used for the photolysis. 50, 100, 150, 200, 250 µl of this solution was added to five 5 ml volumetric flasks. A separate solution was made by dissolving 3mg of caffeine, internal standard, in 5 ml of the same solvent and 50 µl was added to the above mentioned five volumetric flasks and diluted up to the mark with the same solvent. The resulting

solutions were analyzed by LC/MS/MS or UPLC analysis. The calibration curve was constructed (by plotting peak area of the compound) / (peak area of caffeine vs. mmol of the compound)

X-ray crystal structure for pHP Derivatives The X-ray crystallographer would like to thank the National Science Foundation (grant CHE-0079282) and the University of Kansas for funds to purchase the x-ray instrument and computers.

2-bromo-5-(phenylmethoxy)benzotrile (1.29b) Colorless plate-shaped crystals of $C_{14}H_{10}BrNO$ are, at 100(2) K, monoclinic, space group $C2/c - C_{2h}^6$ (No. 15)¹²³ with $a = 18.640(3) \text{ \AA}$, $b = 5.689(1) \text{ \AA}$, $c = 23.071(3) \text{ \AA}$, $\beta = 98.676(3)^\circ$, $V = 2418.5(6) \text{ \AA}^3$ and $Z = 8$ molecules $\{d_{\text{calcd}} = 1.583 \text{ g/cm}^3$; $\mu_a(\text{MoK}\alpha) = 3.380 \text{ mm}^{-1}\}$. A full hemisphere of diffracted intensities (1850 10-second frames with a ω scan width of 0.30°) was measured for a single-domain specimen using graphite-monochromated $\text{MoK}\alpha$ radiation ($\lambda = 0.71073 \text{ \AA}$) on a Bruker SMART APEX CCD Single Crystal Diffraction System.¹²⁴ X-rays were provided by a fine-focus sealed x-ray tube operated at 50kV and 30mA. Lattice constants were determined with the Bruker SAINT software package using peak centers for 4707 reflections. A total of 13586 integrated reflection intensities having $2\theta(\text{MoK}\alpha) < 61.11^\circ$ were produced using the Bruker program SAINT¹²⁵; 3679 of these were unique and gave $R_{\text{int}} = 0.043$ with a coverage which was 99.6% complete. The data were corrected empirically for variable absorption effects using equivalent reflections; the relative transmission factors ranged from 0.542 to 1.000. The Bruker software package SHELXTL was used to solve the structure using “direct methods” techniques. All stages of weighted full-matrix least-squares refinement were conducted using F_o^2 data with the SHELXTL Version 6.10 software package.¹²⁶

The final structural model incorporated anisotropic thermal parameters for all nonhydrogen atoms and isotropic thermal parameters for all hydrogen atoms. All hydrogen

atoms were located in a difference Fourier and included in the structural model as independent isotropic atoms whose parameters were allowed to vary in least-squares refinement cycles. A total of 194 parameters were refined using no restraints, 3679 data and weights of $w = 1 / [\sigma^2(F^2) + (0.0436 P)^2 + 2.5902 P]$, where $P = [F_o^2 + 2F_c^2] / 3$. Final agreement factors at convergence are: $R_1(\text{unweighted, based on } F) = 0.037$ for 2940 independent absorption-corrected “observed” reflections having $2\theta(\text{MoK}\alpha) < 61.11^\circ$ and $I > 2\sigma(I)$; $R_1(\text{unweighted, based on } F) = 0.051$ and $wR_2(\text{weighted, based on } F^2) = 0.091$ for all 3679 independent absorption-corrected reflections having $2\theta(\text{MoK}\alpha) < 61.11^\circ$. The largest shift/s.u. was 0.002 in the final refinement cycle. The final difference map had maxima and minima of 0.68 and $-0.67 \text{ e}^-/\text{\AA}^3$, respectively.

2,6-dibromo-5-(phenylmethoxy) benzonitrile (1.37). Colorless plate-shaped crystals of $\text{C}_{14}\text{H}_9\text{Br}_2\text{NO}$ are, at 100(2) K, monoclinic, space group $P2_1 - C_2^2$ (No. 4)¹²³ with $\mathbf{a} = 4.795(1) \text{ \AA}$, $\mathbf{b} = 33.168(8) \text{ \AA}$, $\mathbf{c} = 8.128(2) \text{ \AA}$, $\beta = 91.387(4)^\circ$, $V = 1292.2(5) \text{ \AA}^3$ and $Z = 4$ molecules $\{d_{\text{calcd}} = 1.887 \text{ g/cm}^3; \mu_a(\text{MoK}\alpha) = 6.259 \text{ mm}^{-1}\}$. This primitive monoclinic unit cell corresponds metrically to a C-centered orthorhombic cell with $\mathbf{a} = 9.336(2) \text{ \AA}$, $\mathbf{b} = 16.692(4) \text{ \AA}$ and $33.168(8) \text{ \AA}$. The crystals were invariably twinned. A small principally single-domain specimen was therefore cut from one of the twinned bundles. A full hemisphere of diffracted intensities (1850 10-second frames with a ω scan width of 0.30°) was measured for this specimen using graphite-monochromated MoK α radiation ($\lambda = 0.71073 \text{ \AA}$) on a Bruker SMART APEX CCD Single Crystal Diffraction System.¹²⁴ X-rays were provided by a fine-focus sealed x-ray tube operated at 50kV and 30mA. Lattice constants were determined with the Bruker SAINT software package using peak centers for 6372 reflections. A total of 14628 integrated reflection intensities having $2\theta(\text{MoK}\alpha) < 61.25^\circ$ were produced using the Bruker program SAINT¹²⁵; 7446 of these were

unique and gave $R_{\text{int}} = 0.123$ with a coverage which was 97.0% complete. The data were corrected empirically for variable absorption effects using equivalent reflections; the relative transmission factors ranged from 0.407 to 1.000. The Bruker software package SHELXTL was used to solve the structure using “direct methods” techniques. All stages of weighted full-matrix least-squares refinement were conducted using F_o^2 data with the SHELXTL Version 6.10 software package.¹²⁶

Refinement of anisotropic thermal parameters for all nonhydrogen atoms resulted in non-positive-definite thermal parameters for a high percentage of the oxygen, nitrogen and carbon atoms. This was presumably the result of pseudo-symmetry described below and/or twinning which could not be taken into account. All O, N and C atoms were therefore assigned variable isotropic thermal parameters. All hydrogen atoms were included in the structural model as idealized atoms (assuming sp^2 - or sp^3 -hybridization of the carbon atoms and C-H bond lengths of 0.95 – 0.99 Å) “riding” on their carbon atoms. The isotropic thermal parameters of all hydrogen atoms were fixed at values 1.2 times the equivalent isotropic thermal parameter of the carbon atom to which they are covalently bonded.

As mentioned above, the primitive monoclinic unit cell corresponds metrically to a C-centered orthorhombic cell. The two crystallographically-independent $C_{14}H_9Br_2NO$ molecules in the primitive monoclinic cell are also related by a noncrystallographic inversion center, and they pack in a manner that mimics space group $P2_1/n$ [an alternate setting of $P2_1/c - C_{2h}^5$ (No. 14)]. In fact, the structure refines reasonably well in $P2_1/n$ with anisotropic Br atoms and isotropic O, N, C and H atoms; this refinement converges to: R_1 (unweighted, based on F) = 0.120 for the independent absorption-corrected “observed” reflections having $2\theta(\text{MoK}\alpha) < 61.25^\circ$ and $I > 2\sigma(I)$.

The final structural model utilized space group $P2_1$ with racemic twinning and incorporated anisotropic thermal parameters for all bromine atoms and isotropic thermal parameters for all other nonhydrogen and hydrogen atoms. The two racemic domains had nearly identical volumes (51% and 49% of the total). A total of 166 parameters were refined using 1 restraint, 7446 data and weights of $w = 1 / [\sigma^2(F^2) + (0.1071 P)^2 + 11.8458 P]$, where $P = [F_o^2 + 2F_c^2] / 3$. Final agreement factors at convergence are: R_1 (unweighted, based on F) = 0.088 for 5735 independent absorption-corrected “observed” reflections having $2\theta(\text{MoK}\alpha) < 61.25^\circ$ and $I > 2\sigma(I)$; R_1 (unweighted, based on F) = 0.110 and wR_2 (weighted, based on F^2) = 0.233 for all 7446 independent absorption-corrected reflections having $2\theta(\text{MoK}\alpha) < 61.25^\circ$. The largest shift/s.u. was 0.001 in the final refinement cycle. The top 14 peaks in the final difference map ($3.68 - 1.49 \text{ e}^-/\text{\AA}^3$) were within 0.94 Å of a Br atom.

Methyl *p*-hydroxyphenylacetate (2.56) This is a known compound.¹²⁷ ^1H NMR (400 MHz CD_3CN): δ 3.52 (s, 2H), 3.62 (s, 3H), 6.76 d, 2H), 7.08 (d, 2H), 7.20 (s, 1H), ^{13}C NMR (100 MHz, CD_3CN): δ (ppm) 39.1, 51.0, 114.8, 114.9, 117.5, 25.3, 130.1, 155.6, 172.1.

1-(4-hydroxyphenyl)-2-methoxyethanone (2.59) This is a known compound.¹²⁸ ^1H NMR (400 MHz CD_3CN): δ 3.39 (s, 3H), 4.64 (s, 2H), 6.89 (d, 2H), 7.84 (d, 2H). ^{13}C NMR (100 MHz, CD_3CN): δ (ppm) 58.0, 74.3, 114.9, 127.1, 129.9, 161.4, 194.5.

Test for base activated Favorskii rearrangement

The test for base activated Favorskii rearrangement was performed according to the method reported by Bordwell and co-workers.^{73,74} In a general procedure, at room temperature (23°C), about 70 μmol pHP derivative was dissolved in 1 ml of methanol and added to 7 ml of 0.05 M NaOMe in MeOH (350 μmol , ~ 5 equivalent). The reaction vessel was stirred continuously and

reaction progress monitored using UPLC by periodically taking 100 μl samples and diluting with 1 ml of MeOH. Spiking the samples with known derivatives of the potential products was performed in order to identify the products. The same procedure was also followed at 0 $^{\circ}\text{C}$ and at reflux (65 $^{\circ}\text{C}$).

Rate constant determinations

The kinetic experiments were performed as described under the test for base activated Favorskii rearrangement at reflux. The concentration of pHP derivative as the reaction progressed (generally 0.5 h intervals) was determined by UPLC analysis. Caffeine was added as the standard to the UPLC vials prior to the analysis. A plot of \ln [pHP derivative] vs. time (h) was linear with rate constant as the slope. The data for pHP derivatives are given in Tables 2-4- 1-7, and the graph for pHP OPO(OEt)₂ is illustrated in Figure 2.9 (*Results*).

Table 2-5. Concentration of pHP OPO(OEt)₂ in 0.05M NaOMe/MeOH at Reflux at Different Time Intervals

Time/ h	C_t / mM	$\ln C_t$
0.00	8.67	2.16
1.00	5.87	1.77
2.00	3.98	1.38
3.00	2.83	1.04
4.00	1.88	0.63
5.00	1.25	0.23
6.00	0.96	-0.04
7.00	0.53	-0.63

C_t = concentration of pHP OPO(OEt)₂

Table 2-6. Concentration of pHP OAc in 0.05M NaOMe/MeOH at Reflux at Different Time Intervals

Time/ h	C_t / mM	$\ln C_t$
0.00	8.58	2.15
4.00	5.38	1.68
8.00	2.88	1.06
12.00	1.95	0.67
16.00	1.23	0.21

C_t = concentration of pHP OAc

Table 2-7. Concentration of pHP Br in 0.05M NaOMe/MeOH at Reflux at Different Time Intervals

Time/h	C _t / mM	ln C _t
0.00	9.30	2.23
4.00	5.72	1.74
8.00	3.25	1.18
12.00	1.82	0.60
16.00	0.97	0.02
20.00	0.53	0.63

C_t = concentration of pHP Br

Table 2-8. Concentration of pHP OTs in 0.05M NaOMe/MeOH at Reflux at Different Time Intervals

Time/h	C _t / mM	ln C _t
0.00	8.70	2.16
4.00	5.63	1.73
8.00	3.94	1.37
12.00	2.84	1.04
16.00	2.21	0.80
20.00	1.63	0.50

C_t = concentration of pHP OTs

Stability study of pHP derivatives in acid

In a general experiment, 20 mg of the pHP derivative was dissolved in 0.1 M HClO₄ as a 10% water-methanol solution. The reaction mixtures was stirred at room temperature and monitored via UPLC for 24 h according to the process described in the rate constant determinations. The results are given in Table 2-4 *Results* section.

References

- ¹ Ellis-Davis, G. C. R.; Kaplan, J. H.; Barsotti, R. J. *Biophys. J.* 1996, 70-1006-1016.
- ² Kaplan, J. H.; Forbush, B. III; Hoffman, J. F. *Biochemistry* **1978**, *17*, 1929-1935.
- ³ Barltrop, J. A.; Schofield, P. *Tetrahedron Letts.* **1962**, 697-699.
- ⁴ Lee, H.; Larson, D. R.; Lawrence, D. S. *Chem. Bio.* **2009**, *4*, 409-427.
- ⁵ Mayer, G.; Heckel, A. *Angew. Chem. Int. Ed.* **2006**, *45*, 4900-4921
- ⁶ *Methods in Enzymology*; Marriott, G., Eds.; Academic Press, San Diego, 291, 1998.
- ⁷ (a) Morrison, H. *Bioorganic Photochemistry*, Wiley, New York, 2, 1993. (b) Adams, S. R.; Tsien, R. *Y. Annu. Rev. Physiol.* **1993**, *55*, 755-784.
- ⁸ Barth, A.; Kreuz, W.; Mantele, W. *FEBS Lett.* **1990**, *277*, 147-150.
- ⁹ Dorm, G.; Prestwich, G. D. *Trends Biotechnol.* **2000**, *18*, 64-77.
- ¹⁰ Callaway, E. M. Yuste, R. *Curr. Opin. Neurobiol.* **2002**, *12*, 587-592.
- ¹¹ Shao L.; Dudek. F. E. *J. Neurophysiol.* **2005**, *93*, 3007-3011.
- ¹² Lopez-Aguado, L.; Ibarz, J. M.; Varona, P.; Herreras, O. *J. Neurophysiol.* **2002**, *85*, 2809-2820.
- ¹³ Sheehan, J. C.; Umezawa, K. *J. Org. Chem.* **1973**, *38*, 3771-3774.
- ¹⁴ Lester, H. A.; Nerbonne, J. M. *Ann. Rev. Biophys. Bioeng.* **1982**, *11*, 151-175.
- ¹⁵ (a) Sheehan, J. C.; Wilson, R. M. *J. Am. Chem. Soc.* **1964**, *86*, 5277-5281. (b) Givens, R.S.; Matuszewski, B. *J. Am. Chem. Soc.* **1984**, *106*, 6860-6861.
- ¹⁶ (a) Zimmerman, H. E. J. *Phys. Chem. A* **1998**, *102*, 5616-5621. (b) DeCosta, D.P.; Pincock, J.A. *J. Am. Chem. Soc.* **1993**, *115*, 2180-2190.
- ¹⁷ (a) Epstein, W.W.; Garrossian, M. *J. Chem. Soc. Chem. Comm.*, **1987**, 532-533. (b) Givens, R. S.; Athey, P.S.; Matuszewski, B.; Kueper, L. W.; Xue, J.; Fisher, T. *J. Am. Chem. Soc.* **1993**, *115*, 6001-6012.
- ¹⁸ Barltop, J.A.; Plant, P. J.; Schofield, P. *J. Chem. Soc. Chem. Comm.*, **1966**, 822-823.
- ¹⁹ Engels, J.; Schlaeger, E. J. *J. Med. Chem.* **1977**, *20*, 907-911.
- ²⁰ (a) Gurney, A. M.; Lester, H. A. *Physiol. Rev.* **1987**, *67*, 583-617. (b) Amit, B.; Ben-Efraim, D. A.; Patchornik, A.; *J. Am. Chem. Soc.* **1976**, *98*, 843-844. (c) Pass, S.; Amit, B.; Patchornik, A. *J. Am. Chem. Soc.* **1981**, *103*, 7674-7675.
- ²¹ Barth, A.; Corrie, J. E. T.; Gardwell, M. J.; Marda, Y.; Mantele, W.; Meier, T.; Trentham, D. R. *J. Am. Chem. Soc.* **1997**, *119*, 4149-4159.
- ²² Shigeri, Y.; Tatsu, T.; Yumoto, N. *Pharmacol. Ther.* **2001**, *91*, 85-92.
- ²³ Brubaker, M. J.; Dyer, D. H.; Stoddard, B.; Koshland, D. E. *Biochemistry* **1996**, *35*, 2854-2864.
- ²⁴ Scott, R. H.; Pollock, J.; Ayer, A.; Thatcher, N. M.; Zehavi, U. *Methods Enzymol.* **2000**, *312*, 387-400.
- ²⁵ Corrie, J. E. T.; Barth, A.; Munasingee, V. R. N.; Trentham, D. R.; Hutter, M.C. *J. Am. Chem. Soc.* **2003**, *125*, 8546-8554.
- ²⁶ Chen, J.; Prestwich, G.D. *Tetrahedron Lett.* **1962**, *38*, 969-972.
- ²⁷ Ellis-Davies, G. C. R.; *Methods Enzymol.* **2003**, *360*, 226-238.
- ²⁸ Margerum, J. D.; Petrusis, C. T. *J. Am. Chem. Soc.* **1969**, *91*, 2467-2472.
- ²⁹ Corrie, J. E. T.; Trentham, D. R. In *Bioorganic Photochemistry* Morrison, H. Ed., Wiley, New York, Vol. 2, 1993; 243-305.
- ³⁰ Walker, J. W.; Reid, G. P.; McCary, J. A.; Trentham, D. R. *J. Am. Chem. Soc.* **1988**, *110*, 7170-7177.
- ³¹ Il'ichev, Y. V.; Wirz, J. *J. Phys. Chem. A* **2000**, *104*, 7856-7870.
- ³² Park, C.H.; Givens, R. S. *J. Am. Chem. Soc.* **1997**, *119*, 2453-2463.
- ³³ Givens, R. S.; Yousef, A. L. In *Dynamic Studies in Biology* Goeldner, M.; Givens, R. S. Eds.; Wiley-Vch, Weinheim, 2005; 55-75.
- ³⁴ Anderson, J.C.; Reese, C. B. *Tetrahedron Lett.* **1962**, *1*, 1-4.
- ³⁵ Givens, R. S.; Park, C. H. *Tetrahedron Lett.* **1996**, *35*, 6259-6266.
- ³⁶ (a) Givens, R.S.; Jung, A.; Park, C. H.; Weber, J.; Bartlett, W. *J. Am. Chem. Soc.* **1997**, *119*, 8369-8370. (b) Sul, J. y.; Orosz, D.; Givens, R. S.; Haydon, P. G. *Neuron Glia Biology* **2004**, *1*, 3-11. (c) Geibel, S.; Barth, A.; Amslinger, S.; Jung, A. H.; Burzic, C.; Clarke, R. J.; Givens R. S.; Fendler, K. *Biophys. J.* **2000**, *79*, 1346-1357. (d) Dixon, J. E.; Zhang, Z. Y. *Adv. Enzymil. Relat. Areas Mol. Biol.* **1994**, *68*, 1-36.
- ³⁷ Conrad, P. G. II, Givens, R. S.; Hellrung, B.; Rajesh, C. S.; Ramseier, M.; Wirz, J. *J. Am. Chem. Soc.* **2000**, *122*,

- 9346-9347.
- ³⁸ Conrad, P. G. II; Givens, R. S.; Weber, F.W.; Kandler, K. *Org. Lett.* **2000**, *2*, 1545-1547.
- ³⁹ Givens, R. S.; Heger, D.; Hellrung, B.; Kamdzhilov, Y.; Mac, M.; Conrad, P. G., II; Cope, E.; Lee, J. I.; Mata-Segreda, J. F.; Schowen, R. L.; Wirz, J. *J. Am. Chem. Soc.* **2008**, *130*, 3307-3309.
- ⁴⁰ Stensrud, K.; Kandler, K.; Noh, J.; Wirz, J.; Heger, D.; Givens, R.S. *J. Org. Chem.* **2009**, *74*, 5219-5227.
- ⁴¹ Zhang, K.; Corrie, J. E. T.; Munasinghe, R. N.; Wan, P. *J. Am. Chem. Soc.* **1999**, *121*, 5625-5632.
- ⁴² Ma, C.; Kwok, W. M.; Chan, W. S.; Zuo, P.; Kan, J. T. W.; Toy, P. K.; Phillips, D. L. *J. Am. Chem. Soc.* **2005**, *127*, 1463-1472.
- ⁴³ Ma, C.; Kwok, W. M.; Chan, W. S.; Du, Y.; Kan, J. T. W.; Toy, P. K.; Phillips, D. L. *J. Am. Chem. Soc.* **2006**, *128*, 2558-2570.
- ⁴⁴ Favorskii, A. *J. Russ. Phys. Chem. Soc.* **1894**, *26*, 559.
- ⁴⁵ Fischer, M.; Wan, P. *J. Am. Chem. Soc.* **1998**, *120*, 2680-2682.
- ⁴⁶ Arzhantev, S.; Maroncelli, M. *Appl. Spectrosc.* **2005**, *59*, 206-221.
- ⁴⁷ Science and Technology Facilities Council home page www.clf.rl.ac.uk/Facilities/LSF/USL/Techniques/Kerr/Kerr.htm (accessed Aug 19 2009)
- ⁴⁸ Ma, C.; Kwok, W. M.; Chan, W.; Zue, P.; Phillips, D. L. *J. phys. Chem. B* **2004**, *108*, 9264-9276.
- ⁴⁹ Ma, C.; Kwok, W. M.; Chan, W.; Zue, P.; Phillips, D. L. *J. phys. Chem. B* **2004**, *108*, 9264-9276.
- ⁵⁰ Reichardt, C.; *Solvent and Solvent Effects in Organic Chemistry*; VCH Verlagsgesellschaft mbH, D-6940, Weinheim, 1988.
- ⁵¹ Huck, L.A.; Wan, P. *Org. Lett.* **2004**, *6*, 1797-1799.
- ⁵² Alvarez, F.J.; Schowen, R.L. In *Isotopes in Organic Chemistry*; Buncl, E., Lee, C.C., Eds, 1987; vol.7 pp 1-59.
- ⁵³ Chang, T. K.; Chiang, Y.; Guo, H. X.; Kresge, A. J.; Mathew, L.; Powell, M. F.; Wells, J. A. *J. Am. Chem. Soc.* **1996**, *118*, 8802-8807.
- ⁵⁴ Favorskii, A. *J. Russ. Phys. Chem. Soc.* **1894**, *26*, 559.
- ⁵⁵ Guijarro, D.; Yus, M. *Curr. Org. Chem.* **2005**, *9*, 1713-1735.
- ⁵⁶ a) Silva, L. F. *Tetrahedron* **2002**, *58*, 9137-9161 (b) Lee, E.; Yoon, C. H. *Chem. Commun.* **1994**, 479-481.
- ⁵⁷ Auclair, J. P.; Gramain, J. C. *J. Chem. Soc., Perkin Trans. 1* **1988**, 23-9.
- ⁵⁸ (a) Lonkin, A. S.; Marshall, W. J.; Fish, B. M. *Org. Lett.* **2008**, *10*, 2303-2305 (b) Chatterjee, A. K.; Choi, T. L.; Sanders, D. P.; Grubbs, R. H. *J. Am. Chem. Soc.* **2003**, *125*, 11360-11370. (c) Hatsuda, M.; Kurodo, T.; Seki, T. *Synth. Commun.* **2003**, *31*, 427-434 (d) Stio, S.; Nakagawa, S.; Koizumi, T.; Hirayama, K.; Yamamoto, Y. *J. Org. Chem.* **1999**, *64*, 3975-3978.
- ⁵⁹ (a) Eaton, P. E.; Chakraborty, U. R. *J. Am. Chem. Soc.* **1978**, *100*, 3634. (b) Mehta, G.; Padma, S. *Tetrahedron* **1991**, *47*, 7783. (c) Mehta, G.; Padma, S. *Tetrahedron* **1991**, *47*, 7807. (d) Forman, M.A.; Dailey, W. P. *J. Org. Chem.* **1993**, *58*, 1501. (e) Mehta, G.; Reddy, S. H. K.; Padma, S. *Tetrahedron* **1991**, *47*, 7821. (f) Boyer, L. E.; Brazzillo, J.; Forman, M. A. *J. Org. Chem.* **1996**, *61*, 7611-7613.
- ⁶⁰ Favorskii, J. *Prakt. Chem.* **1913**, *88*, 641.
- ⁶¹ Stevens, C. L.; Malik, W.; Pratt, R. *J. Am. Chem. Soc.* **1950**, *72*, 4758-3950.
- ⁶² Richard, G. *Compt. Rend.* **1933**, *197*, 1432-1434.
- ⁶³ Horner, L.; Gross A. *Ann.* **1951**, *573*, 17-30.
- ⁶⁴ Robinson, J.; Flynn, E. T.; McMahan, T. L.; Simpson, S. L.; Trisler, J. C.; Conn. K. B. *J. Org. Chem.* **1991**, *56*, 6709- 6712.
- ⁶⁵ Tchoubar, B.; Sackur, O. *Compt. Rend.* **1939**, *208*, 1020-1022.
- ⁶⁶ McPhee, Klingsberg, E. *J. Am. Chem. Soc.* **1944**, *66*, 1132-1136.
- ⁶⁷ (a) Lofffield, R. B. *J. Am. Chem. Soc.* **1950**, *72*, 632-633 (b) Lofffield, R. B. *J. Am. Chem. Soc.* **1951**, *73*, 4707-4714.
- ⁶⁸ Burr, J. G.; Dewar, M. J. S. *J. Chem. Soc.* **1954**, 1201-1203.
- ⁶⁹ Aston, J. G.; Newkirk, J. D. *J. Am. Chem. Soc.* **1951**, *73*, 3900-3902.
- ⁷⁰ Bordwell, F. G.; Frame, R. R.; Scamehorn, R. G.; Strong, J. G.; Meyerson, S. *J. Am. Chem. Soc.* **1967**, *89*, 6704-6711
- ⁷¹ Kende, A. S. In *Organic Reactions*, Cope, A. C., Eds.; Krieger: New York, 1975; Vol. 11, pp 261-316
- ⁷² Fort, A. W. *J. Am. Chem. Soc.* **1962**, *84*, 2620-2625.
- ⁷³ Bordwell, F. G.; Scamehorn, R. G. **1968**, *90*, 6751-6758.
- ⁷⁴ Bordwell, F. G.; Scamehorn, R. G.; Springer, R. W. *J. Am. Chem. Soc.* **1969**, *91*, 2087-2093

- ⁷⁵ Bunnett, A. *Chem. Int. Ed.* **1962**, *1*, 225.
- ⁷⁶ Bordwell, F. G.; Carlson, M. W.; Knipe, A. C. *J. Am. Chem. Soc.* **1969**, *91*, 3949-3950.
- ⁷⁷ Bordwell, F. G.; Almy, J. *J. Org. Chem.* **1973**, *38*, 575-579.
- ⁷⁸ Bordwell, F. G.; Carlson, M. W. *J. Am. Chem. Soc.* **1970**, *92*, 3377-3385.
- ⁷⁹ Bordwell, F. G.; Scamehorn, R. G. *J. Am. Chem. Soc.* **1971**, *93*, 3410-3415.
- ⁸⁰ Bordwell, F. G.; Strong, J. G. *J. Org. Chem.* **1973**, *38*, 579-585.
- ⁸¹ Stork, G.; Borowitz, I. *J. Am. Chem. Soc.* **1960**, *82*, 4307-4315.
- ⁸² Schadd, L. J.; Hess, B. H. *J. Org. Chem.* **1981**, *38*, 1909-1911.
- ⁸³ Ditchfield, R.; Hehre, W. J.; Pople, J. A. *J. Chem. Phys.* **1970**, *52*, 5001-5007.
- ⁸⁴ Moliner, V.; Castillo, R.; Safont, V. S.; Oliva, M.; Bohn, S.; Andres, J. *J. Am. Chem. Soc.* **1997**, *119*, 1941-1947.
- ⁸⁵ Castillo, R.; Andres, J.; Moliner, V. *J. Phys. Chem. B* **2005**, *105*, 2453-2460.
- ⁸⁶ Moller, C.; Plesset, M. S. *Phys. Rev.* **1934**, *46*, 618.
- ⁸⁷ Hamblin, G. D.; Jimenez, R. P.; Sorensen, T. S. *J. Org. Chem.* **2007**, *72*, 8033-8045.
- ⁸⁸ Cossi, M.; Rega, N.; Scalmani, G.; Barone, V. *J. Comput. Chem.* **2003**, *24*, 669-681.
- ⁸⁹ Tsuchida, N.; Yamazaki, S.; Yamabe, S. *Org. Biomol. Chem.* **2008**, *6*, 3109-3117.
- ⁹⁰ Lee, C.; Yang, W.; Parr, R. G. *Phys. Rev. B* **1998**, *37*, 785.
- ⁹¹ Stensrud, K. F.; Heger, D.; Sebej, P.; Wirz, J.; Givens, R. S. *Photochem. Photobiol. Sci.* **2008**, *7*, 614-624.
- ⁹² Wagner, P.; Sakamoto, M. *J. Am. Chem. Soc.* **1989**, *111*, 8723-8725.
- ⁹³ Campagna, F.; Caritti, A.; Casini, G. *Tetrahedron Lett.* **1977**, *21*, 1813-1816.
- ⁹⁴ Bose, D. S.; Kumar, K. K. *Synth. Commun.* **2000**, *30*, 3047-3052.
- ⁹⁵ Mowry, D. T. *Chem. Rev.* **1948**, *42*, 189-283.
- ⁹⁶ Ismail, M. A.; Anbazhagan, M.; Stephens, C. E.; Boykin, D. W. *Synth. Commun.* **2004**, *34*, 751-758.
- ⁹⁷ You, Y.; Uboh, C.E.; Soma, L.R.; Guan, F. Li.; X. Ruby, J.A.; Liu, Y.; Chen, J. *Rapid Commun. Mass Spectrom.* **2009**, *23*, 2035-2044.
- ⁹⁸ Turro, N. J. In *Modern Molecular Photochemistry*, University Science Books, California, 1991.
- ⁹⁹ Senadheera, S. University of Kansas, KS. Unpublished data, 2008
- ¹⁰⁰ Cope, Elizabeth. Dissertation 2008, Chemistry Department, University of Kansas
- ¹⁰¹ Chicheng Ma. University of Kansas, KS. Unpublished data, 2007
- ¹⁰² Fischer, E.; Speier, A. *Ber. Dtsch. Chem. Ges.* **1895**, *28*, 3252.
- ¹⁰³ Tbshirani, R. J. Royal. Statist. Soc. B. 1996, *58*, 267-288.
- ¹⁰⁴ Stensrud, K. F. Ph D Dissertation 2008, Chemistry Department, University of Kansas.
- ¹⁰⁵ Anslyn, E.V.; Gougherty, D. A. In *Modern Physical Organic Chemistry*, University Science Books, California, 2006 pp 464-465.
- ¹⁰⁶ Winstein, S.; Klinedinst, P. E.; Robinson, G. C. *J. Am. Chem. Soc.* **1961**, *83*, 885-895.
- ¹⁰⁷ Winstein, S.; Robinson, G. C. *J. Am. Chem. Soc.* **1958**, *80*, 169-181.
- ¹⁰⁸ Winstein, S.; Klinedinst, P. E.; Clippinger, E. *J. Am. Chem. Soc.* **1961**, *83*, 1986-4989.
- ¹⁰⁹ Winstein, S.; Masaru, H.; Smith, S. G. *Tetrahedron Lett.* **1960**, *22*, 12-19
- ¹¹⁰ Loftfield R. B.; Schaad, L. *J. Am. Chem. Soc.* **1954**, *76*, 35.
- ¹¹¹ Smith, B. B.; Nace, H. R. *J. Am. Chem. Soc.* **1954**, *76*, 6119-6122.
- ¹¹² (a) Aston, J. G.; Clark, J. T.; Burgess, K. A.; Grennburg, R. G. *J. Am. Chem. Soc.* **1942**, *64*, 300-302 (b) Kopp-Mayer, M.; Troefouel. M. J. *Compt. Rend.* **1955**, *240*, 1115-96. Cox, J. S. G. *J. Chem. Soc.* **1960**, 4508-4511.
- ¹¹³ Cox, J. S. G. *J. Chem. Soc.* **1960**, 4508-4511
- ¹¹⁴ (a) House, H. O.; Frank, G. A. *J. Org. Chem.* **1965**, *30*, 2948-. (b) Cookson, R. C.; Nye, M. J. *J. Chem. Soc.* **1965**, 2009-2018.(c)Turro, N. J.; Gagosian, R. B.; Rappe, C.; Knutson, L. *Chem. Commun.* **1969**, 270-1.
- ¹¹⁵ (a) House, H. O.; Thompson, H. W.; . *J. Org. Chem.* **1963**, *28*, 164-168 (b) Turro, N. J.; Smith, W. B.; Gonzalez, C. *J. Am. Chem. Soc.* **1965**, *87*, 3258-3559.
- ¹¹⁶ Smith, W. B.; Gonzalez, C. *Tetrahedron* **1966**, 5751-5755.
- ¹¹⁷ (a)Wallace, T. J.; Pobiner, H.; Schriesheim, A. *J. Org. Chem.* **1965**, *30*, 3768-3771. (b) Kertesz, D. J.; Marx, M. *J. Org. Chem.* **1986**, *51* 2315-2328. (c) Moryasu, M.; Maki, T. Japanese Patent 92-9484 19920122, 1993 (b) Zabjek, A.; Petric, A. *Tetrahedron Lett.* 1999, *40*, 6077-6078.
- ¹¹⁸ Hawker, C.J.; Lee, R.; Freché, J.M. *J. Am. Chem. Soc.*, **1991**, *113*, 4583-4588.
- ¹¹⁹ Kosugi, M.; Sumiya, T.; Obara, Y.; Suzuki, M.; Sano, H.; Migita, T. *Bull. Chem. Soc. Jpn.* **1987**, *60*, 767-768

-
- ¹²⁰ Vasquez-Martines, Y.; Ohri, R.V.; Kenyon, V.; Holman, T.; Sepulveda-Boza, S. *Bioorg. Med. Chem.* **2007**, *23*, 7408-7425.
- ¹²¹ Hiyama, T.; Fujita, M. *J. Org. Chem.* **1988**, *53*, 5405-5414.
- ¹²² Aizapurua, J.; Palomo, C. *Tetrahedron Lett.* **1985**, *26*, 475-478.
- ¹²³ International Tables for Crystallography, Vol A, 4th ed., Kluwer: Boston (1996)
- ¹²⁴ Data Collection: SMART Software Reference Manual (1998). Bruker-AXS, 5465 E. Cheryl Parkway, Madison, WI 53711-5373 USA.
- ¹²⁵ Data Reduction: SAINT Software Reference Manual (1998). Bruker-AXS, 6300 Enterprise Dr., Madison, WI 53719-1173, USA.
- ¹²⁶ Sheldrick S. M. (2000). SHELXTL Version 6.10 Reference Manual. Bruker-AXS, 5465 E. Cheryl Parkway, Madison, WI 53711-5373 USA
- ¹²⁷ Laura, D.; Miguel, A.; Rodriguez-Medina, M. *J. Organomet. Chem.* **2005**, *690*, 261-268.
- ¹²⁸ Shetty, U.; Nelson, W. *J. Med. Chem.* **1988**, *31*, 55-59.

Chapter 2: Novel Applications of the *p*-Hydroxyphenacyl Photoremovable Protecting Group

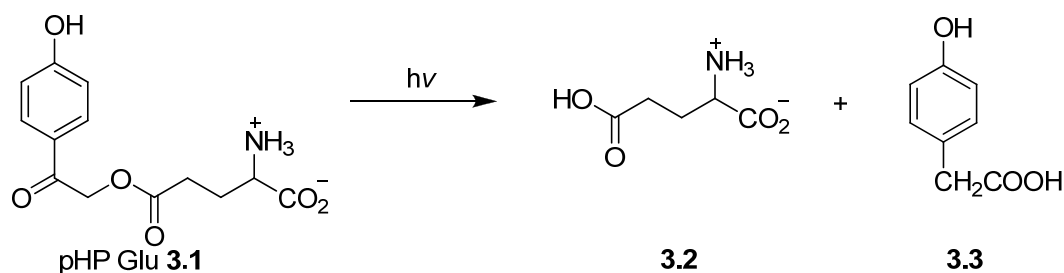
3.0 Instant Fluorescence from Release of Quencher-Fluorescent Dye Bifunctional

Phototriggers: Photorelease Reactions, Synthesis, and Proof of Concept

Introduction

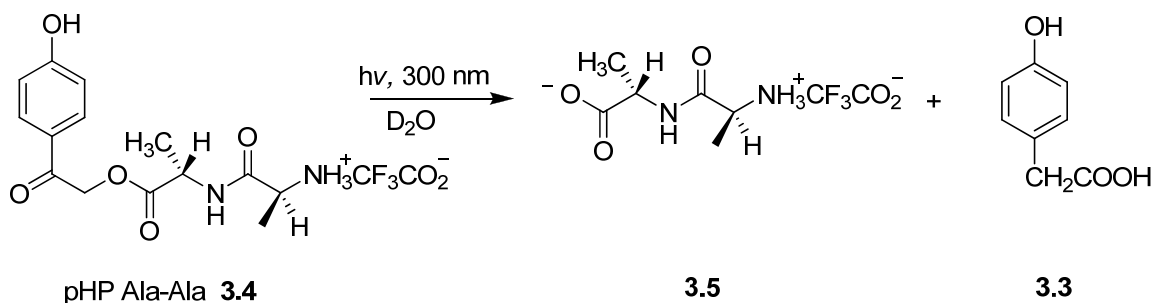
p-Hydroxyphenacyl (pHP) is a new and promising addition to the family of photoremovable protecting groups (PPG). The mechanistic endeavors pertaining to the pHP moiety were discussed in *Chapter one*. The following two Chapters will focus on novel applications of the pHP photochemistry. Several advantageous properties of the pHP chromophore, like formation of photoproducts that do not compete for light, relative ease of synthesis, and fast release (10^7 - 10^8 s⁻¹) of the caged species in a primary photochemical step, make pHP a good candidate for studying biological processes.¹

The pHP group has been successfully employed for the release of neurotransmitters. Givens *et al.*² reported the release of L-glutamate and GABA in buffer solutions with quantum efficiencies (Φ) of 0.35 and 0.21 respectively (Equation 3.1 for pHP glutamate). Glutamate is an excitatory (agonist) neurotransmitter whereas GABA is an inhibitor (antagonist) that are found in mammalian nervous systems and are commonly used in studies of neurotransmission,³ brain neuronal mapping,⁴ and neuronal stimulation.⁵ pHP Glu (**3.1**) was used by Kandler *et al.*⁶ to probe postsynaptic long-term depression (LTD) in CA1 hippocampal pyramidal cells, cells believed to play an important role in learning and memory. pHP Glu was infused into CA1 hippocampal pyramidal cells and irradiated with time-resolved pulsed UV lamp. Rapid glutamatergic currents that were suppressed by glutamate receptor antagonists were observed upon photolysis indicating that localized release of glutamate from pHP Glu led to LTD of glutamate receptors.



Eq. 3.1

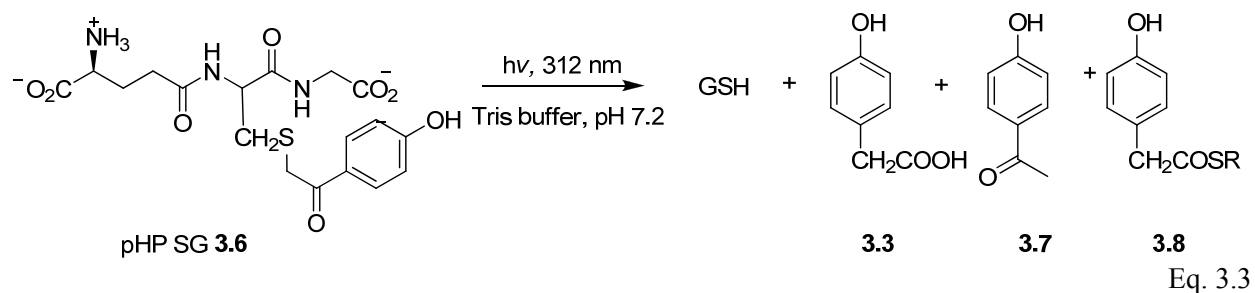
The pHP group has also been used for the release of peptides. Givens and coworkers⁷ demonstrated that optically active dipeptide Ala-Ala can be released from pHP protected Ala-Ala with complete retention of optical activity (Equation 3.2). The authors' report a Φ of 0.27 for the disappearance of pHP Ala-Ala in D_2O , and the reaction could be continued until conversion to product was complete. In another example, Haydon *et al.*⁸ probed the nature of the connectivity between signaling astrocytes in hippocampal preparations using the pHP caged oligopeptide bradykinin.



Eq. 3.2

Release of the thiol bearing peptide glutathione from the pHP group was reported by Goeldner *et al.*⁹ in 2002. The photorelease of glutathione in Tris buffer was accompanied by the formation of three photoproducts, 4-hydroxyphenylacetic acid (3.3), 4-hydroxyacetophenone (3.7) and the thioester 3.8 (Equation 3.3). The thioester 3.8 was proposed to be formed by the

attack of the released glutathione on the spirodienedione intermediate (Scheme 1.6 Introduction Chapter 1)



Release of nucleotides from pHP chromophore was first reported by Givens *et al.*¹⁰ in 1996 in their pioneering paper on pHP photoremovable protecting groups. They reported the synthesis and release of pHP ATP (Equation 1.4, *Introduction Chapter 1*). An application of pHP ATP release was demonstrated by Fendler *et al.*¹¹ to derive the kinetics of ATP action when other phototriggers failed. The authors used pHP ATP to investigate the Na⁺, K⁺-ATPase assisted Na⁺ and K⁺ ion migration through cell membranes. When lipid membranes with added fragments of pig kidney with Na⁺, K⁺-ATPase and pHP ATP were exposed to laser pulses (XeCl excimer laser at 308 nm) the discharge of ATP activated the Na⁺-K⁺-ATPase resulting in a change in transient current.¹¹ The release of ATP was measured by time-resolved Fourier transform infrared spectra (TR-FTIR) of the ATP absorption band disappearance and appearance of bands for inorganic phosphate, H₂PO₄⁻¹. Similarly release of pHP GTP (pHP caged guanosine triphosphate) was used to study the mechanism of GTP hydrolysis by the protein Ras.¹²

Oligopeptides and larger proteins, including enzymes, have also been caged by the pHP chromophore and in one case it has been successfully demonstrated to act like a photoswitch. When a photolabile group is attached to the active site of an enzyme, it temporarily inhibits the activity at that site of the enzyme. The activity can be revived by exposure to light. Thus PPG groups can be used as on/off switches for enzymes.¹ In 1999, Pei and coworkers¹³ introduced

pHP caged protein tyrosin phosphatase (PTP) as a new class of covalent PTP inhibitors whose inhibition activity can be reversed by light. PTPs are enzymes that catalyse the hydrolysis of phosphotyrosine to tyrosine and inorganic phosphate. The mechanism of tyrosine regulation by PTPs is not clearly understood.¹⁴

Bayley and co-workers¹⁵ extended the pHP photochemistry to protein cell signaling. They caged the active site C, (Figure 3.1) of protein kinase A (PKA) via an activating phosphate. PKA is a cAMP dependent cell signaling protein. PKA contains a regulatory subunit and a catalytic (C) subunit. The two lobes of C subunit are illustrated in Figure 3.1. In this study, Thr-197 of unphosphorylated C subunit was thiophosphorylated and alkylated with pHP bromide to obtain the caged enzyme pHP P_sT¹⁹⁷C_α. Upon photolysis in buffer solution the free enzyme was released with a Φ of 0.21.

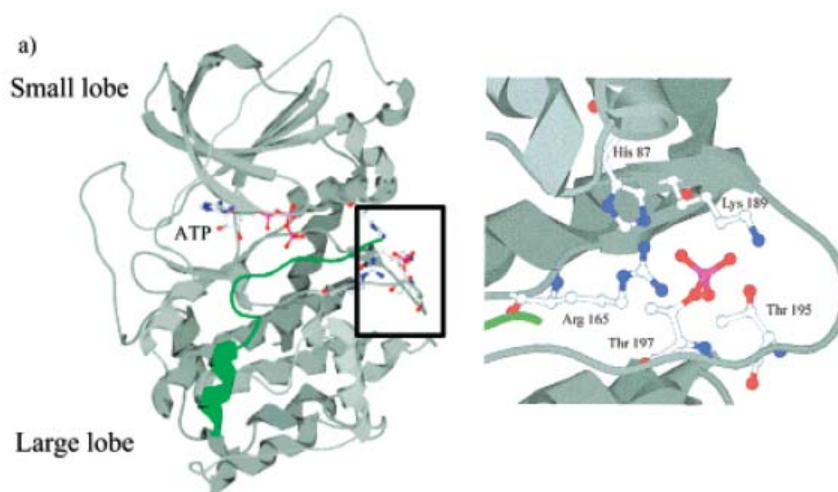


Figure 3-1. Structure of subunit C of PKA. The key residues are illustrated in expanded view. Reproduced with permission from the ACS

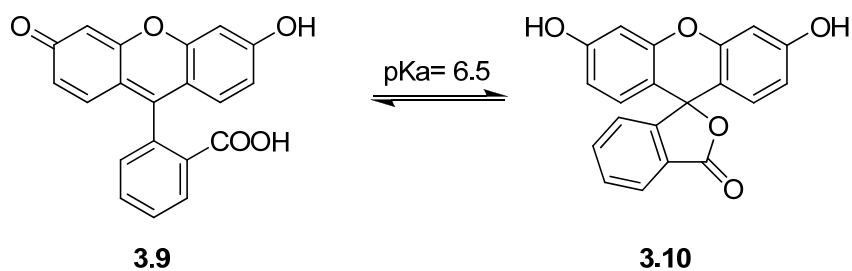
Further expanding the scope of pHP photochemistry, a proof of concept investigation is proposed to design and construct pHP based phototriggers that can function as caged fluorophore probes that become fluorescent upon release.

Caged fluorophore probes

Fluorescence spectroscopy is one of the most powerful tools used to investigate dynamics in molecular biology. The classical approach using fluorescent probes was to study regeneration of fluorescence in dark areas generated by photobleaching, on a fluorescent surface.¹⁶ However, this approach has several inherent disadvantages. Oxygen used for photobleaching tends to oxidize components of the cell and probing for fluorescent areas on a highly fluorescent surface is cumbersome and results in a poor signal-to-noise ratio. To overcome these drawbacks, fluorescent probes that remain dormant until the system is temporally and spatially aligned are highly sought after. Light activated fluorescent probes based on caged compounds are appropriate to meet these requirements and would be termed caged fluorophores.¹⁷ Caged fluorophores are designed such that the fluorophore is made non-fluorescent or has a shifted fluorescence at a different wavelength when caged with a PPG. The fluorescence is regenerated or returned to the nascent or original wavelength when exposed to light.¹⁸ This approach is very attractive because it provides the researcher both spatial and temporal control of the developing fluorescence. Moreover, since the caged fluorescent probes ideally are non-fluorescent, the surface will exhibit a high signal-to-noise ratio when compared with the released fluorescent probe.

Requirements for an effective fluorescent probe as discussed by Mitchison^{18,19} are, “biostability, rapid and efficient photoactivation, good brightness, photostability of the uncaged fluorochrom, practicable synthesis, and friendly protein chemistry”.¹⁹ All research pertaining to

caged fluorescent probes thus far has been based on applications of *o*-nitrobenzyl (ONB) as the photoremovable protecting group. The first caged fluorescent probe synthesized by Mitchison^{19,20} was based on fluorescein. Fluorescein, known since the 19th century²⁰, is highly fluorescent. It is biologically benign and thus has been widely employed as a fluorescent tag in both *in vivo* and *in vitro* biological studies.²¹ Some advantageous properties of fluorescein are its high fluorescence quantum efficiency (~ 0.9), high molar absorptivity near 490 nm, and high water solubility under physiological conditions.^{22,23} However, there are several disadvantages associated with the fluorescein group. It is highly susceptible to photobleaching²⁴ and it possesses a relatively broad fluorescence emission spectrum.²⁵ It also displays pH sensitive fluorescence. Fluorescein can exist in two forms, the carboxylic acid and the lactone form (Equation 3.4). The carboxylic acid form (**3.9**) is highly fluorescent emitting at 521 nm while the lactone form (**3.10**) is non-fluorescent. The prominent form present in non aqueous solvents or under acidic conditions (pH < 6.5) is the lactone form, making fluorescein unsuitable for fluorescence studies under these conditions.



Eq. 3.4

Mitchison *et al.*^{19,20} caged fluorescein derivatives using two ONB groups attached to the phenolic positions locking fluorescein in its non fluorescent lactone form. Synthesis of the caged fluorescein was achieved by the reaction between 1-(bromomethyl)-2-nitrobenzene and

fluorescein in the presence of Ag₂O in 6:1 benzene THF in 25% yield. Structures of caged fluorescent probes used in Mitchisons studies are illustrated in Figure 3-2. When the caged fluorophores are exposed to UV radiation at 365 nm the free fluorescein in its fluorescent carboxylic acid form was released (Equation 3.5) and the fluorescence yield was increased by 300 fold.

The mechanism of photorelease from ONB group was discussed in *Chapter one*.

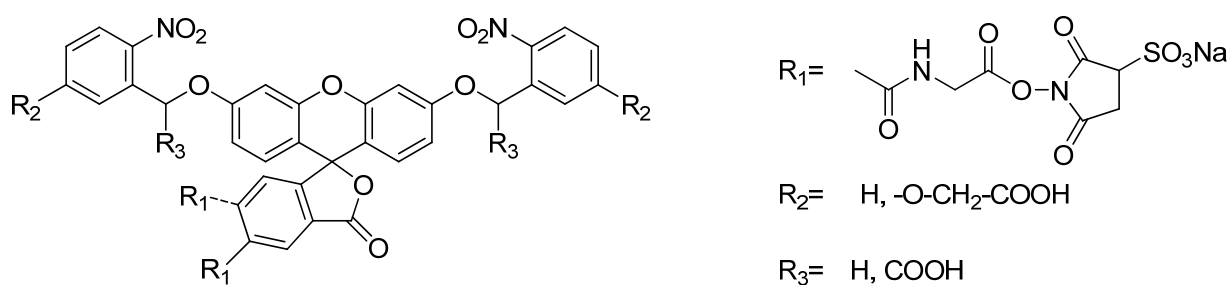
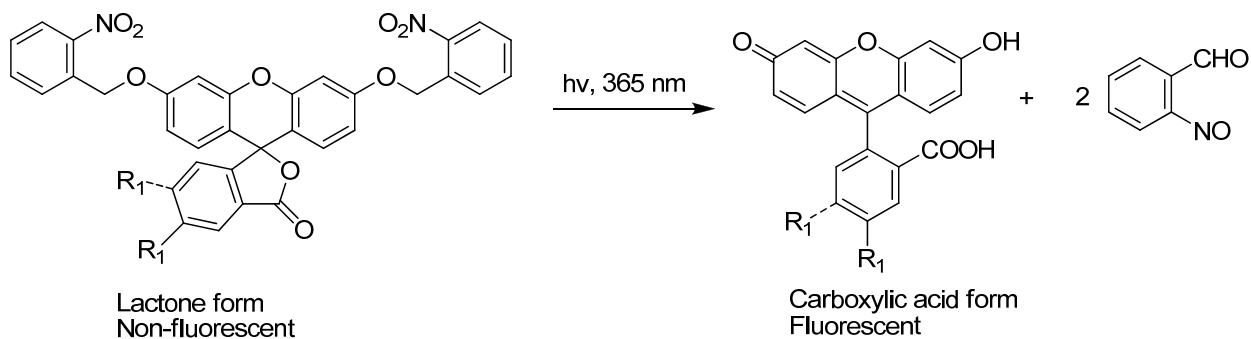
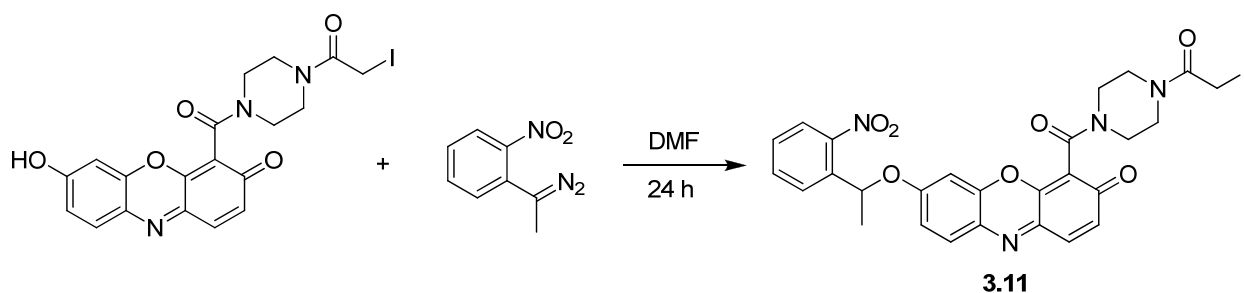


Figure 3-2. Caged fluoresceins.¹⁸



Eq. 3.5

Mitchison *et al.*¹⁹ attached the caged fluoresceins to tubulin and injected the complex into mitotic tissue culture cells to study the polewards flux of kinetochore microtubules.¹ Although these caged fluorescent probes performed well for tubulin labeling, they failed when the authors attempted to use this approach for actin labeling. This was mainly due to the hydrophobic nature of the caged fluorophores and that proteins other than tubulin aggregated when labeled with the caged fluorescein. To overcome this drawback Mitchison and Theriot²⁶ caged resorufin confining the fluorophore in a non-ionizable form (**3.11**) that resulted in a blue shift in absorbance rendering the assembly nonfluorescent (Equation 3.6).



Eq. 3.6

Both fluorescein and resorufin undergo rapid photobleaching once exposed to light, limiting their applicability in cell imaging.¹⁸ Photobleaching causes difficulty in repeated imaging of a cell over time and releases species that form reactive oxygen which is cytotoxic.²⁷ To overcome this problem, rhodamine, a fluorophore less susceptible to photobleaching, was caged in a manner similar to fluorescein derivatives.^{18,28} Caged rhodamine fluorochromes proved to be more photostable than fluorescein and resorufin analogs. However, syntheses of

¹ Kinetochores are proteins that assemble on centromeric DNA. They attach chromosomes to spindle microtubules (kinetochore microtubules) to assist segregation to daughter cells during cell division. (Desai, D. *Cell Biol.*, **2000**, *10*, 508-509),

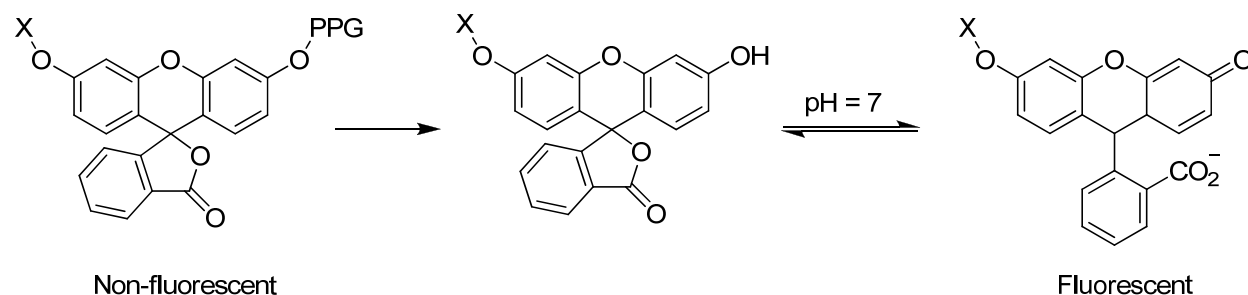
rhodamine probes were difficult. Table 3-1 summarizes features of fluorophores explored by Mitichison *et al.*

Table 3-1. Practical Considerations for Different Fluorophores. Reproduced with permission from Academic press.

Caged fluorophore	$\lambda_{EX}/\lambda_{EM}$	Photostability	Biostability	Φ of uncaging	Ease of synthesis
Fluorescein	485-495/495-520	Poor	Good	Good	Medium
Rhodamine	540-550/560-580	Good	Good	Poor	Difficult
Resorufin	580-590/590-610	Poor	Poor	Good	Easy

One common disadvantage of the fluorescein and rhodamine caged fluorophores is the need to use two PPGs to lock the fluorophore in a non-fluorescent configuration. This, in turn, required prolonged exposure to UV radiation to release the two groups of the bis caged fluorophore to attain the full, high intensity fluorescence.

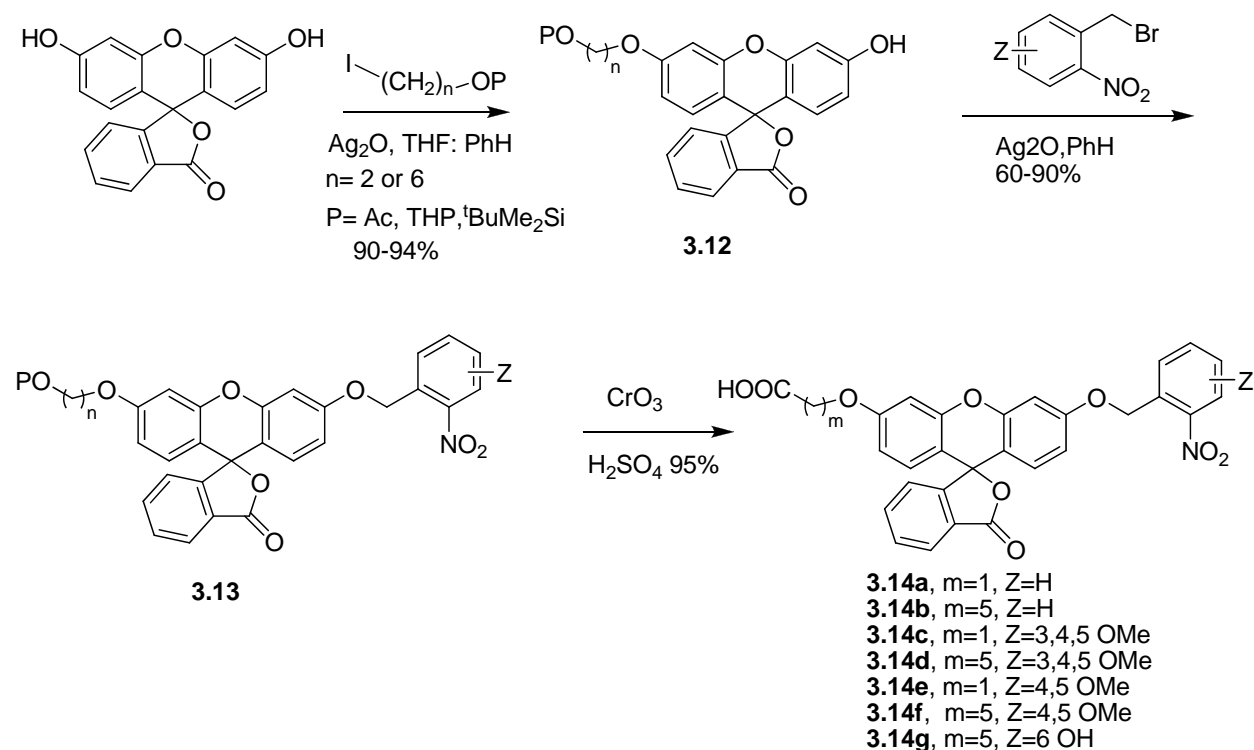
In 1988, Kraft and coworkers²⁹ suggested the use of only one PPG to cage fluorescein and another photoinactive group on the remaining phenolic oxygen to lock both phenolic groups thus holding the fluorophore in the non fluorescent lactone configuration (Equation 3.7).



Eq. 3.7

Several monoether fluorescein derivatives, based on the unsubstituted fluorescein and 5-aminofluorescein structures, were synthesized and their photochemistry explored. Synthesis of monoether fluorescein derivatives were more complicated than Mitchison's approach but gave good yields. Unsubstituted fluorescein derivatives were converted to the desired monoalkyl ethers by initially alkylating the phenolic oxygen with an alkyl iodide in the presence of Ag_2O to give the monoalkylated derivatives (**3.12**) followed by another Ag_2O mediated alkylation with appropriate *o*-nitrobenzyl bromide to generate caged fluorescein derivatives (**3.13**). Further removal of the hydroxyl protecting group and Jones oxidation of the resulting free alcohol to the acid, produced the final caged fluorophores **3.14a-g** (Scheme 3.1). Conversion of the alcohol to the acid was carried out in order to obtain a more aqueous soluble final product.

Scheme 3.1



Synthesis of 5-aminofluorescein derivatives followed the same path. However, another step was introduced between the first and second alkylations to protect the amine group by acetylation. The structures of the 5-aminofluorescein-based caged fluorophores are illustrated in Figure 3-3.

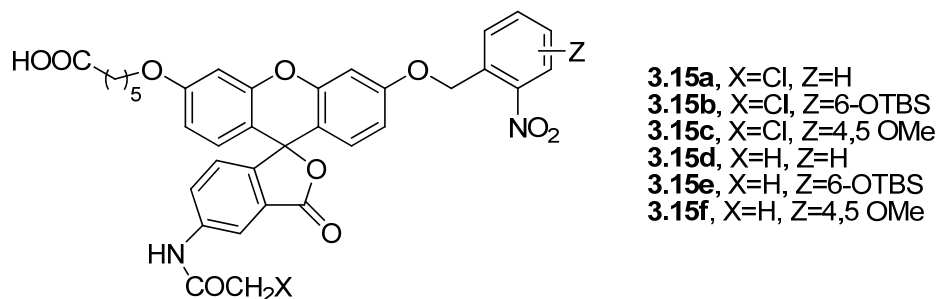


Figure 3-3. 5-aminofluorescein based caged fluorophores.²⁸

From the caged fluorescent probes investigated here, the highest quantum yield of fluorescence (Φ_F) of 0.26 was observed for caged 5-aminofluorescein derivative **3.15a**, which is consistent with the Φ_F obtained with ONB caged alcohols.³⁰ **3.15a** has a relative fluorescence yield of 0.121 which was also among the highest. All the other caged fluorophores showed low Φ_F ranging from 0.008-0.07.

In 2004, Li and co-workers²⁸ reported the use of the coumarin fluorophore in caged fluorescent probes.²⁸ The coumarin derivative of choice was 6-chloro-7-hydroxycoumarin-3-carboxamide (**3.16**) due to its high Φ_F (0.93), good absorption at about 400 nm and pH independent fluorescence.³¹ Coumarin **3.16** was caged with three ONB groups (Equation 3.8) and the photochemical properties were explored (Table 3-2). All caged coumarins were essentially non-fluorescent prior to photolysis and a prominent fluorescent enhancement was observed upon photolysis at 365 nm. The 4,5-dimethoxy analog **3.17c** showed an almost 800 fold increase in fluorescence when photolyzed which was substantially higher than that reported for caged fluorescein.¹⁸ The quantum yield of uncaging was highest for 1-(2-nitrophenyl)ethyl

analog **3.17a** (0.33),. However, all of the other caged coumarin derivatives showed low quantum yields of uncaging (Table 3-2).

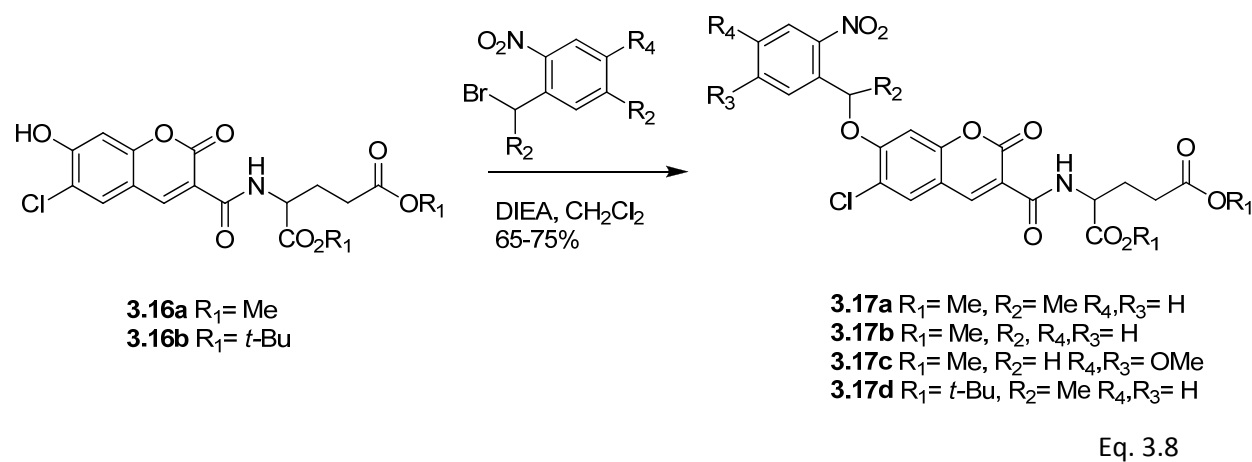


Table 3-2. Fluorescent and Photochemical Properties of Caged Coumarins.²⁸

Caged coumarin	Φ_{F2}^a	$\Phi_{F1}^b / \Phi_{F2}^c$	Φ_u^d	$\epsilon^e / M^{-1} cm^{-1}$	Uncaging cross section (δ_u)
3.17a	0.0025	372	0.33	20,000	6600
3.17b	0.0048	194	0.04	14,000	560
3.17c	0.0012	775	0.0036	26,000	94

^a Fluorescence quantum yields of caged coumarins. ^b Fluorescence quantum yield of **3.16a** = 0.93. ^c fluorescence enhancement after photoreleasing. ^d Quantum yield of uncaging at 365 nm. ^e extinction coefficient

Coumarin is a well studied PPG in its own right,³² and the product investigations in this study employing HPLC led the authors to conclude that only basic ONB chemistry is occurring here. However, due to the high uncaging cross section observed for **3.17a**, Li *et al.*²⁸ propose that the “coumarin moiety serves as an antenna to enhance the light harvesting capability of the molecule and to boost the photolytic efficiency of the ONB group”.²⁸ 4-methylcoumarines (6-bromo-7-hydroxycoumarin-4-ylmethyl) have also been developed as PPGs for two photon excitation.³³ Two photon excitation is a highly sought after property as the infrared radiation sources provide deeper penetration into tissue, reduced photodamage, and can be focused on very minute excitation volumes.³⁴ ONB groups are generally not good candidates for two-photon

excitation.³⁵ But the two-photon uncaging action cross section (δ_u), a measure of the sensitivity of a PPG to two photon excitation,³⁵ for **3.17a** and its derivative without the 6-chloro group were found to be 0.37 and 0.68 GM, respectively, at 740 nm compared with a value of 0.01-0.03 GM in ONB derivatives providing a potential model for further extending the study of caged coumarins as two photon activateable cages.

To test the applicability of the new caged fluorescent probes, the authors²⁸ successfully incorporated the acetoxymethyl derivative **3.18** of the caged coumarin fluorophore **3.17a** into HeLa cells. The cells showed no fluorescence before photolysis but became highly fluorescent when photolyzed. An image of the HeLa cells prior to and after exposure to 365 nm irradiation is illustrated in Figure 3-4. However, fluorescence of **3.18** was not stable when loaded into human fibroblasts. To overcome this drawback, Li and coworkers²⁸ incorporated cis-1,4-diaminocyclohexane into the coumarin fluorophore via amide linkages **3.19** in hope that sterics introduced by the cyclohexane moiety would result in good stability, which proved to be accurate.

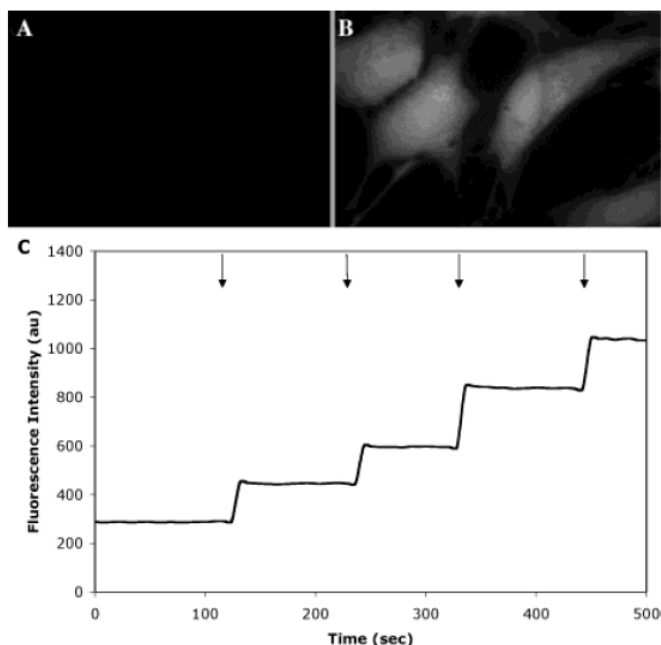


Figure 3-4. Fluorescence imaging of HeLa cells loaded with a caged and cell permeable coumarin **318**. During the imaging, cells were briefly illuminated with UV light (330-380 nm), indicated by the arrows in part C. The first two arrows denote 0.1 s UV exposures, and the last two arrows represent 0.2 s UV. (A and B) Fluorescent images of cells before and after UV uncaging, respectively. (C) Average fluorescence intensity of cells in the field of view over the course of four episodes of UV photolysis. Reproduced with permission from Journal of American Chemical Society.

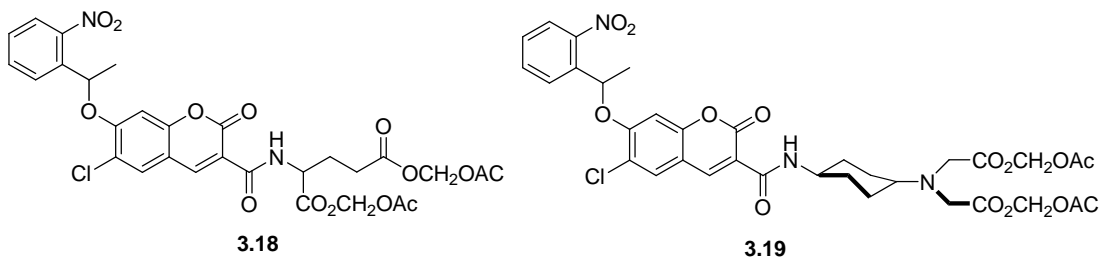


Figure 3-5 Structures of caged coumarins employed in HeLa cell and human fibroblast studies

Li and coworkers adopted a slightly different approach to caged fluorescent probes in their latest publication.³⁶ In general, the PPG is attached to the fluorophore and the fluorophore is, in turn, attached to the biomolecule (macromolecule) of interest (Figure 3-6a). In this setup

the fluorescent moiety will be attached to the macromolecule after photolysis. Li *et al.*³⁷ changed the design such that the PPG is now attached to both the fluorophore and the macromolecule (Figure 3-6b). A caged chromophore of this novel design **3.20**, was obtained from a 12 step synthesis and showed almost no fluorescence prior to photolysis and attained a 260 fold increase in fluorescence once it was completely photoreleased using 365 nm radiation. Chromophore **3.20** was employed by the authors to investigate *in vivo* dye transfer via gap junction channels in embryos of *Caenorhabditis elegans*.³⁷

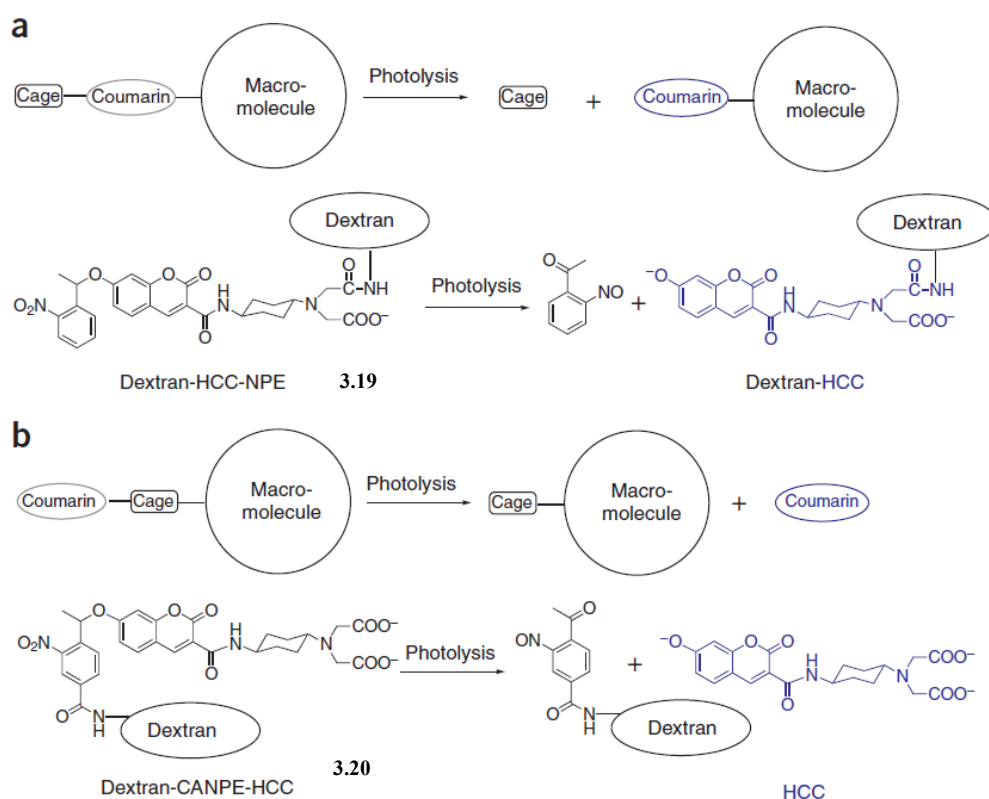


Figure 3-6. Bioconjugates of caged probes. (a) Schematic showing photolysis of conventional bioconjugates. (b) Schematic diagram showing photolysis of novel bioconjugates. Examples for each type of bioconjugates used in this study and their photolyzed products are also shown (bottom). Reproduced with permission from Nature Methods.

A completely different approach than that adopted by Mitchison,^{18,19,20} for caging fluorescent probes based on fluorescein was developed by Nagano *et al.*³⁸ Although fluorescein and its derivatives are the most extensively employed of the fluorophores used in fluorescent labeling, the mechanism that governs the Φ_F is not fully understood. Nagano and coworkers proposed that Φ_F is determined by a photoinduced electron transfer (PET)^{39,40} between the benzene moiety (donor) of fluorescein and the xanthene moiety (Figure 3-7a).⁴¹

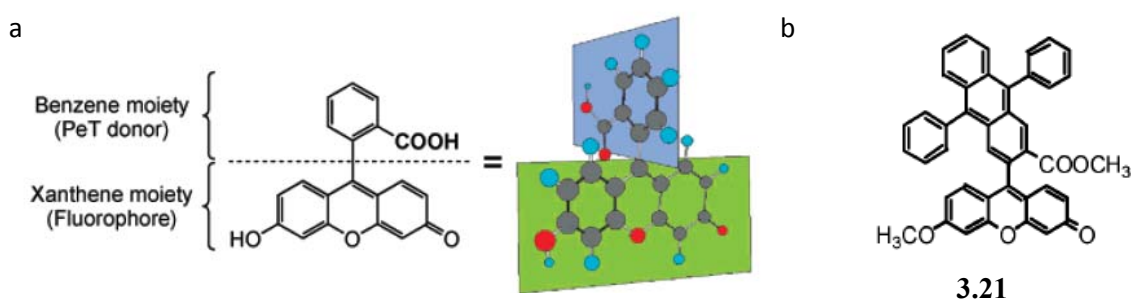


Figure 3-7. (a) Fluorescein structure divided into two parts, the benzene moiety and the fluorophore.⁴² (b) structure of fluorescein derivative 3.21.⁴³ Reproduced with permission from the Journal of American Chemical Society.

PET between the donor and the fluorophore leads to quenching of the fluorescence. This was supported by the observation of radical cations of diphenylanthracene-2-carboxylic acid and the xanthene radical anion in flash photolysis and EPR studies of fluorescein derivative **3.21**,⁴² and was further strengthened by the observation that Φ_F decreased in fluorescein derivatives when electron donating groups were placed on the benzene moiety.⁴² Their investigation also led to the finding that the carboxylic acid in the benzene moiety is not required for fluorescence, and simply functions as a barrier for achieving a planar conformation. This led to the design of a new series of fluorescein derivatives, by substituting the carboxylic acid function with a methyl

group, which the authors named TokyoGreen (Figure 3-8). One attractive feature of TokyoGreen dyes is the pH independence of the fluorescence.⁴²

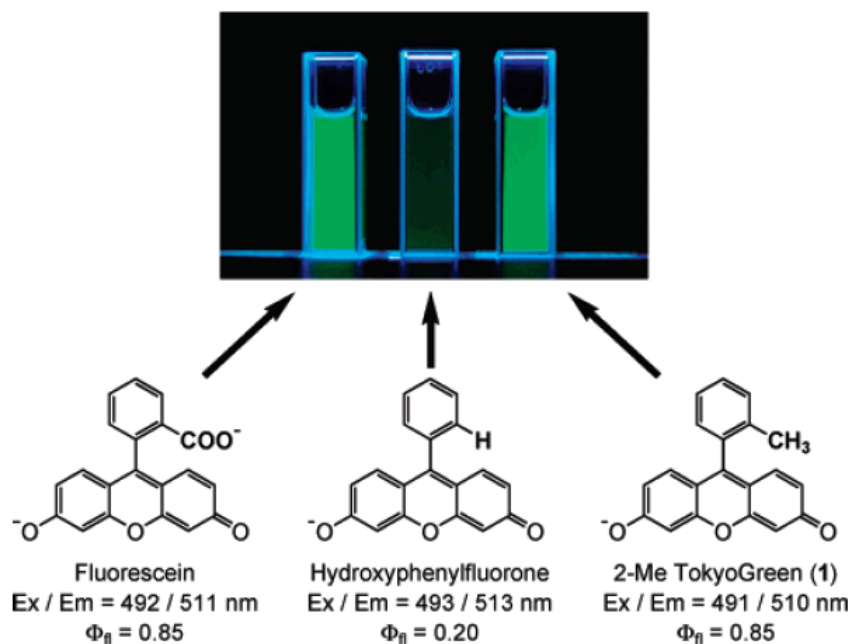
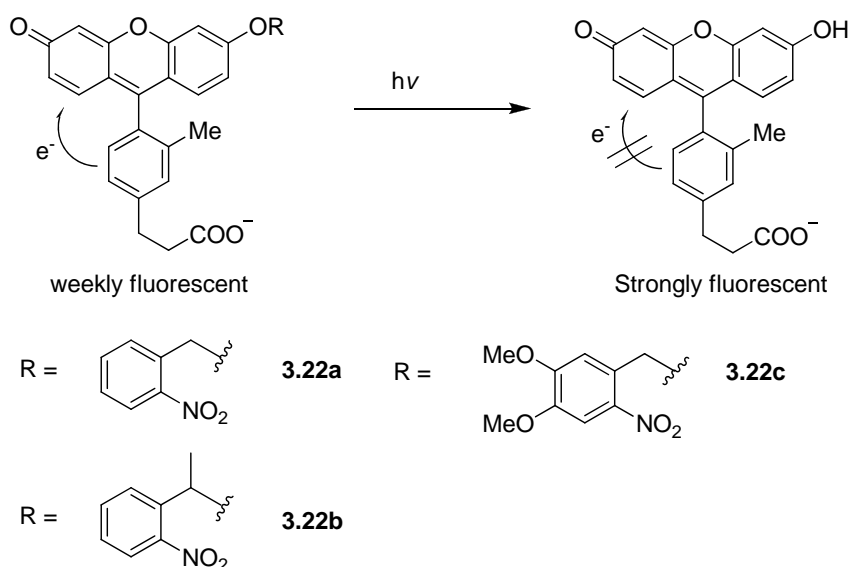


Figure 3-8. Photos of the fluorescence of fluorescein (left), 6-hydroxy-9-phenylfluorone (middle), and new fluorescein-based molecule (2-Me Tokyo Green, right).⁴² Reproduced with permission from Journal of American Chemical Society.

Based on these findings, Nagano and coworkers³⁹ designed a new set of caged fluorescent probes employing the TokyoGreen fluorophore. The probes were developed such that there was favorable electron transfer between the benzene moiety and xanthene moiety when caged by ONB derivatives. When exposed to light, free dye would be released in which electron transfer was no longer favorable, resulting in fluorescence (Equation 3.9). The synthesis of caged TokyoGreen was achieved in a five-steps starting from 4-bromo-3-methylphenol.



Eq. 3.9

The Φ_F of the three ONB caged TokyoGreen fluorophores **3.22a**, **3.22b** and **3.22c**, were 0.001, 0.001 and 0.002 respectively. Therefore the caged fluorophores were very weakly fluorescent prior to photolysis. When exposed to light (350 nm in pH 7.4 phosphate buffer) a maximum increase in fluorescence was observed for 1-(2-nitrophenyl)ethyl derivative **3.22b** followed by 4,5-dimethoxy derivative **3.22c** and unsubstituted ONB **3.22a**. Fluorescence increases in all three TokyoGreen fluorophores were higher than that observed for bis ONB caged fluorescein. However, uncaging Φ for **3.22b** was reported to be 0.03 compared to 0.13 of bis ONB caged fluorescein. To explore the applicability of the novel caged fluorophores in biological systems, Nagano and coworkers labeled HeLa cells with acetoxymethyl derivative of **3.22b** and, upon irradiation with UV light (330-385 nm), the labeled cells became brightly fluorescent. In an identical experiment where HeLa cells were labeled with biscaged fluorescein, no fluorescence was observed within the time frame investigated, highlighting the superiority of the novel fluorophores.

Research that has been reported thus far on caged fluorescent probes has shown that they have good potential for probing dynamics within a cell. However, only a few actual applications

of caged fluorescent probes have surfaced so far.¹⁸ This is mainly due to the lack of availability of caged fluorescent probes that satisfy all the criteria needed for compatibility in biological environments. Therefore, caged fluorescent probes are an arena with an unlimited potential for development.

Statement of the problem

Probes based on fluorescent dyes are widely used to explore dynamics within biological systems. Two recently developed popular applications of fluorescent probes are molecular beacons (an oligonucleotide (ON) that contains a fluorophore and a quencher at the two ends of the strand),⁴³ and hybridization probes (two ONs, one labeled with a donor fluorophore and the other with an acceptor fluorophore, a FRET pair).⁴⁴ Molecular beacons are non-fluorescent when in the hairpin conformation⁴³ but achieve fluorescence when hybridized with a target. In hybridization probes, a shift in fluorescence from donor to acceptor will be observed when hybridized to a target.

Probes based on photoprotected fluorophores, termed caged fluorophore probes, are a very new addition to fluorescent probes. Caged fluorophore probes have the advantages of controlled reactivation of fluorescence that is achieved through the researcher's choice of time and location of the activation event.¹⁷ Since their discovery in the 1980s, only a handful of caged fluorophore probes have been developed. The only PPG explored has been the *o*-nitrobenzyl group and the fluorescent dyes have been limited to fluoresceins,^{17,18} rhodamines¹⁹ and more recently coumarins.²⁸

The *p*-hydroxyphenacyl (pHP) photoremovable protecting group, being a new and more effective PPG that has shown great promise because of its very fast photorelease of the pHP protected group (10^7 - 10^8 s⁻¹),¹ has a release rate advantage for exploring very rapid, i. e., the fastest, of the biological phenomena. Furthermore, the pHP group and its products are not cytotoxic⁴⁵ in contrast to *o*-nitrobenzyl PPG. Therefore, the design, synthesis, and photochemical

development of a caged fluorophore probe based on the pHP chromophore are especially attractive.

The general approach to caged fluorophore probes based on fluorescein dyes has been to trap fluorescein in its closed, lactone (non-fluorescent) form by the PPG group.^{17,18} However, commonly used fluorescent probes such as molecular beacons and hybridization probes, are based on a fluorophore-quencher pairs. Paralleling those approaches, a new type of three component caged fluorophore probe can be envisioned where the fluorophore (F) and the quencher (Q) are both attached to the pHP moiety. The three component molecule will not fluoresce as the quencher will be fixed in close proximity to the fluorescent dye. Exposure to light that causes the departure of either the fluorophore or the quencher from the proximate partner freeing the fluorophore from the quencher, stimulated fluorescence emission will be regained. As implied above, these probes can be constructed either by attaching the fluorophore or the quencher as the leaving group and the other as a substituent on the pHP nucleus.

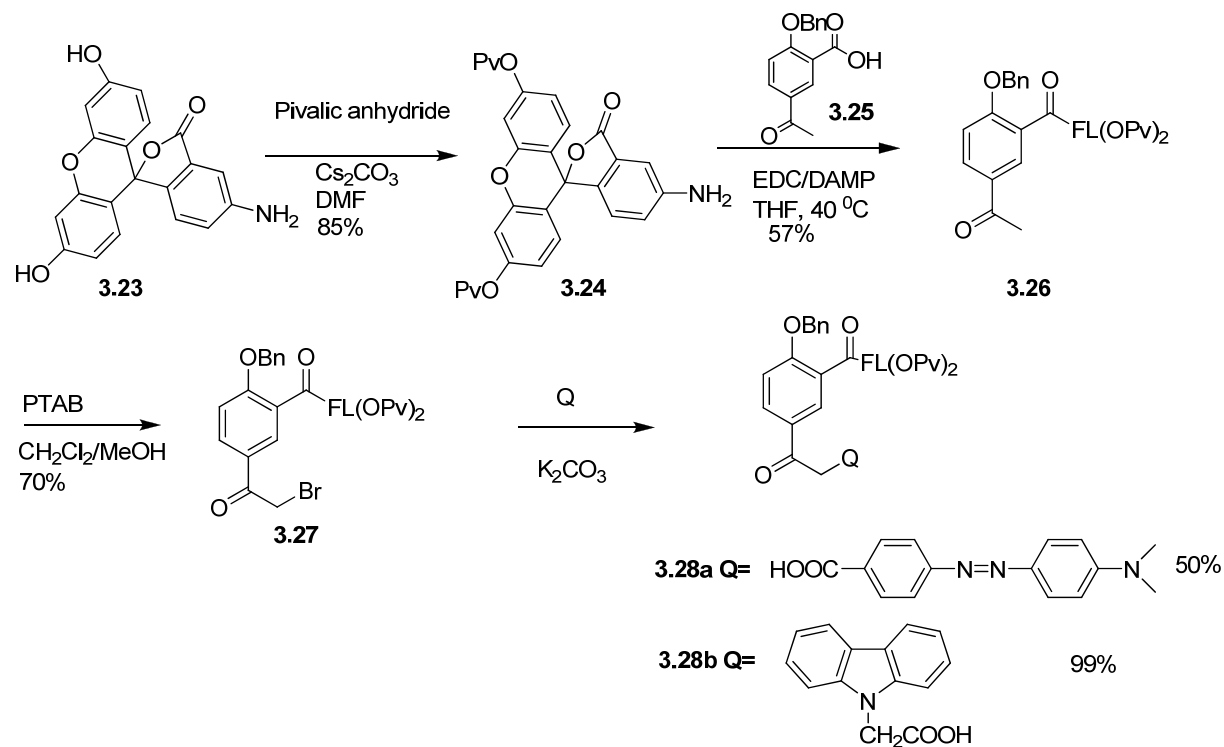
Results

Synthetic strategies

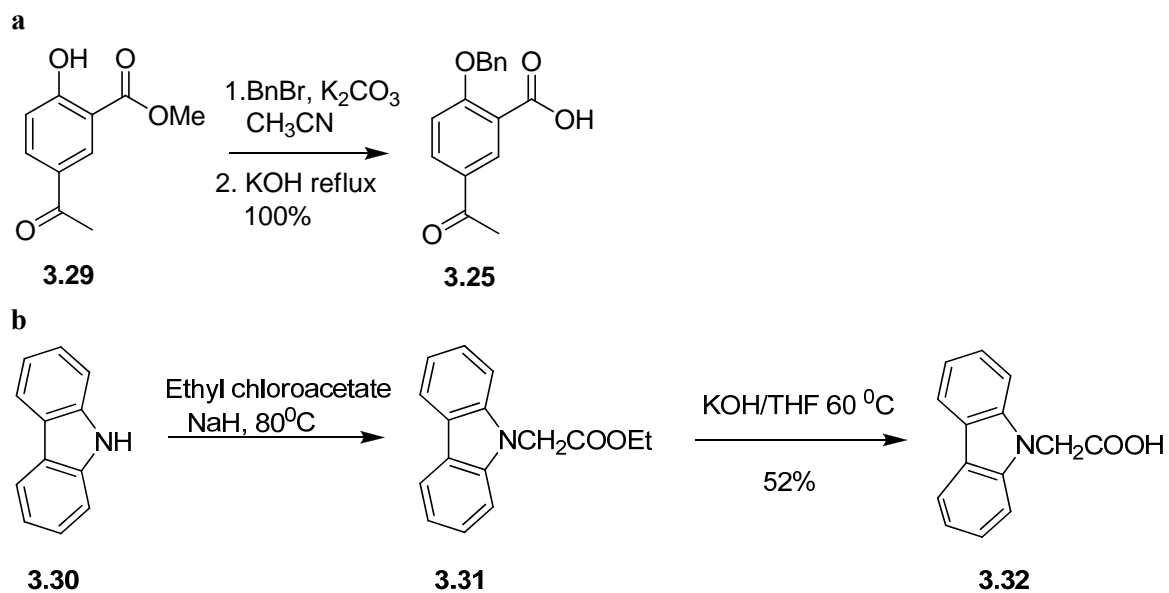
Synthesis of fluorescent dye pHP quencher ensembles (FlpHPQ).

Synthesis of quencher-fluorescent dye phototrigger assembly where the fluorophore is a pHP substituent and the quencher is the leaving group were constructed by the synthetic route shown in Scheme 3.2. The fluorophore selected for this approach was 5-aminofluorescein (**3.23**) whereas carbazole and 4-[2-[4-(dimethylamino)phenyl]diazenyl] benzoic acid (DABCYL) were explored as quenchers. DABCYL is a quencher widely used in fluorescent probes⁴³ and the use of carbazole as a quencher for fluorescein has been reported by Hong *et al.*⁴⁶ Synthesis of the FlpHPQ construct began with the readily available 5-acetylsalicylic acid. The acid functionality of 5-acetylsalicylic acid was used to attach the fluorophore as a substituent on the pHP nucleus. EDC coupling between the benzyl protected 5-acetylsalicylic acid (**3.25**) and bispivalate protected 5-aminofluorescein (**3.24**) provided fluorescein substituted pHP **3.26** in 57% yield. Reaction of 5-aminofluorescein (**3.23**) and pivalic anhydride in the presence of Cs₂CO₃ gave bispivalate protected 5-aminofluorescein **3.24** in 85% yield, while benzyl protection of methyl 5-acetylsalicylate (**3.29**) followed by subsequent hydrolysis generated **3.25** in 100% yield (Scheme 3.3a). S_N2 displacement of α -bromo species **3.27** with either DABCYL or carbazole-9-acetic acid (**3.32**) produced the desired connectivity of the fluorophore and the quencher to the pHP core. Carbazole-9-acetic acid (**3.32**) was synthesized by the base activated hydrolysis of methyl 2-(9H-carbazol-9-yl)acetate (**3.31**) generated by the reaction between carbazole (**3.30**) and ethyl chloroacetate in the presence of NaH (Scheme 3.3b).

Scheme 3.2



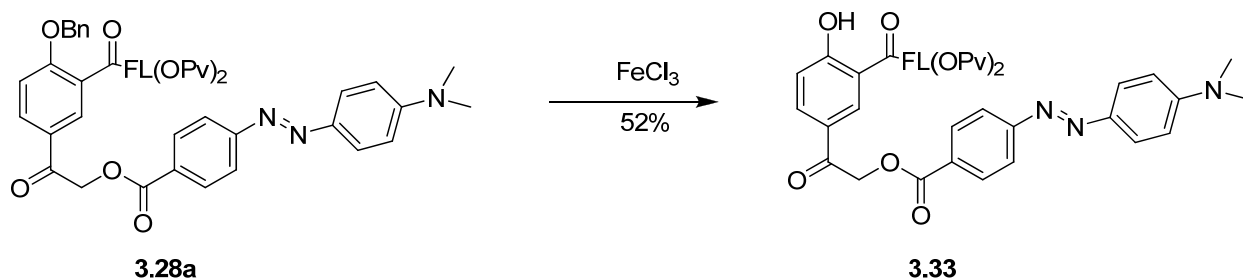
Scheme 3.3



Attempts to remove benzyl protection of caged DABCYL derivative **3.28a** under hydrogenolysis conditions ($\text{H}_2/\text{Pd/C}$) resulted in the breakdown of the azo linkage. However, use of ferric chloride provided the desired product **3.33** in 52% yield (Scheme 3.4). The

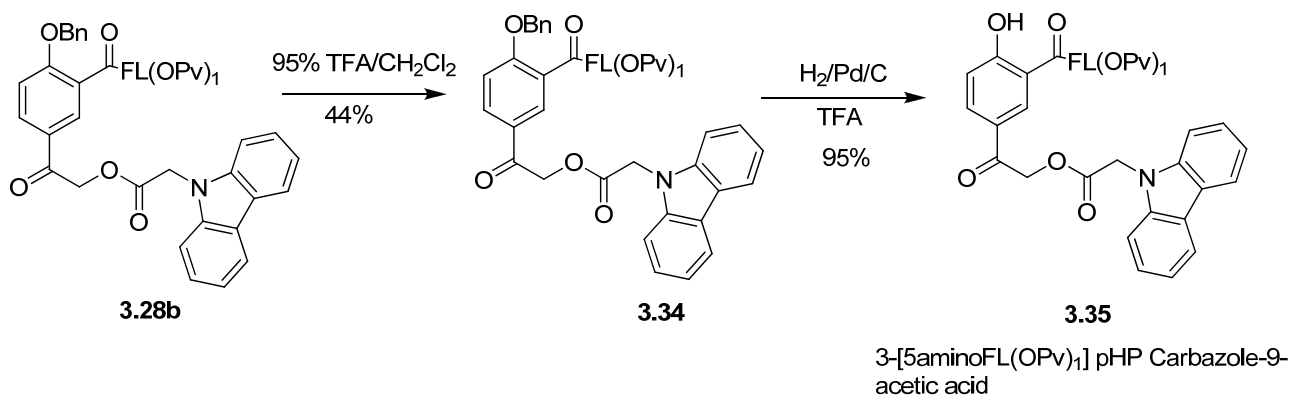
photochemical reactions of **3.33** provided unfavorable results that will be discussed later, and further attempts to remove the pivalic groups were abandoned.

Scheme 3.4



Removal of the pivalate groups in caged carbazole derivative **3.28b** presented some difficulties. Exposure to base, the standard removal method for pivalate groups,⁴⁷ resulted in hydrolysis of both the amide and ester linkages. Stirring in 95% TFA/CH₂Cl₂ at room temperature for 2 h gave rise to **3.34** containing one pivalate group. Attempts to further remove the other pivalic acid group failed as the molecule decomposed with prolonged exposure to TFA. The removal of the benzyl protecting group via hydrogenolysis produced the final desired compound 3-[5-aminofluorescein] (OPv)₁ pHP carbazole-9-acetic acid (**3.35**) in 95% yield.

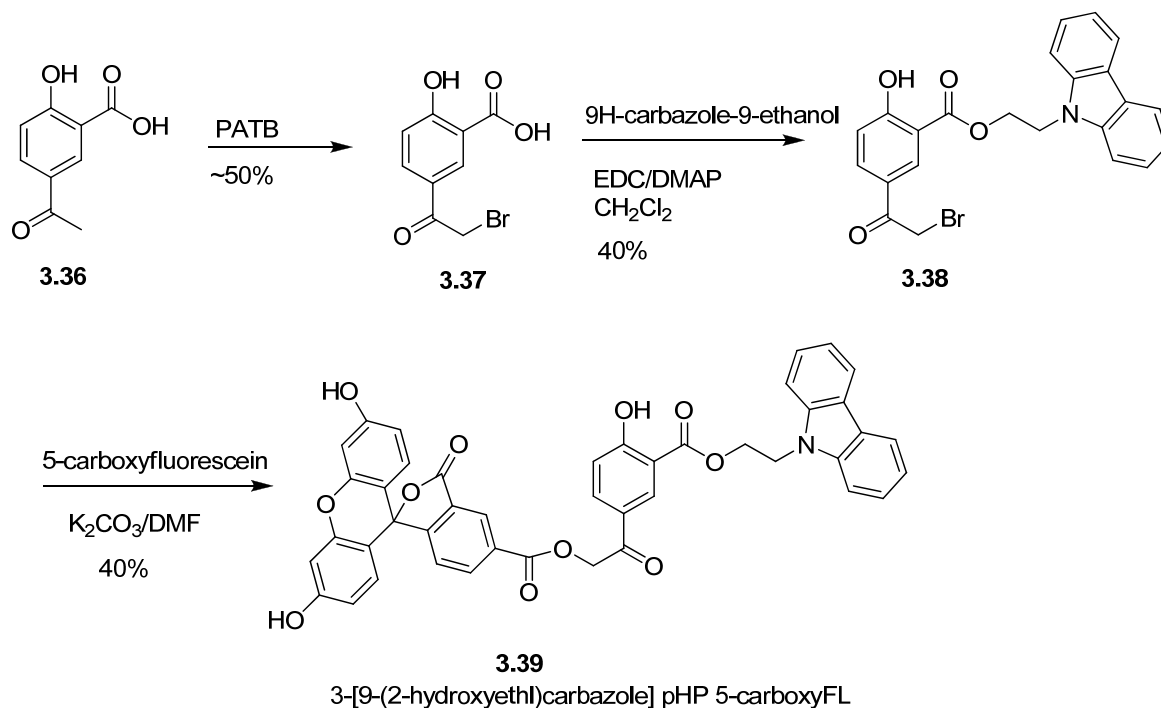
Scheme 3.5



Synthesis of quencher pHP Fluorescent dye ensembles (QpHPFI)

Synthesis of this ensemble, where the fluorophore is the leaving group and the quencher is the pHP substituent, was also based on the 5-acetylsalicylic acid (**3.36**) framework. The synthetic route is outlined in Scheme 3.6. Initial bromination of 5-acetylsalicylic acid with phenyltrimethyl ammonium tribromide (PTAB) resulted in the α -bromo derivative **3.37**. EDC coupling reaction between **3.37** and 9H-carbazole-9-ethanol gave rise to **3.38**. Subsequent S_N2 displacement of bromide on **3.38** by 5-carboxyfluorescein furnished the designed connectivities to the pHP moiety in 40% yield.

Scheme 3.6

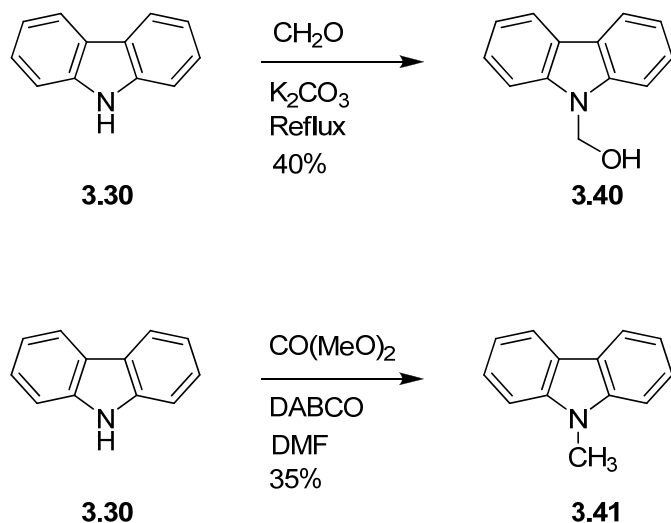


Synthesis of potential photoproducts of 9H-carbazole-9-acetic acid (**3.32**)

9H-Carbazole-9-methanol (**3.40**) was synthesized by in 40% yield the reaction of carbazole (**3.30**) and formaldehyde in refluxing methanol in the presence of K_2CO_3 . Likewise, 9-methyl-

9H-carbazole (**3.41**) was obtained by the reaction between carbazole (**3.30**) and dimethyl carbonate in the presence of 1,4 diazabicyclooctane (DABCO, 40%) (Scheme 3.7).

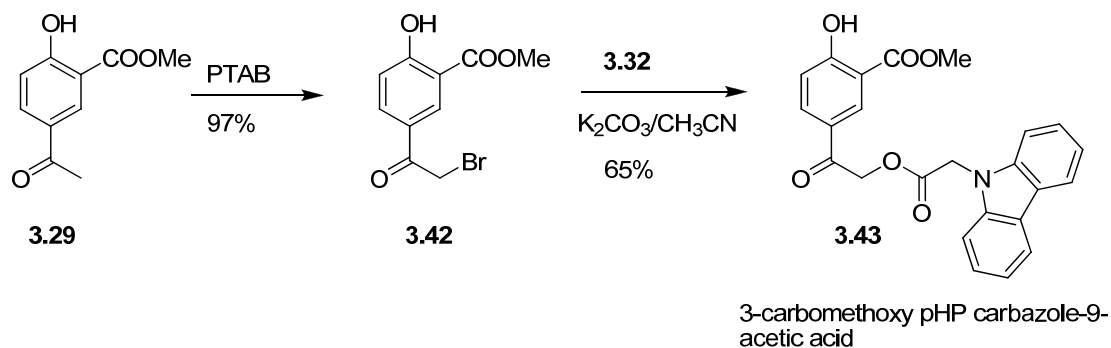
Scheme 3.7



Synthesis of other pHP derivatives pertaining to this study

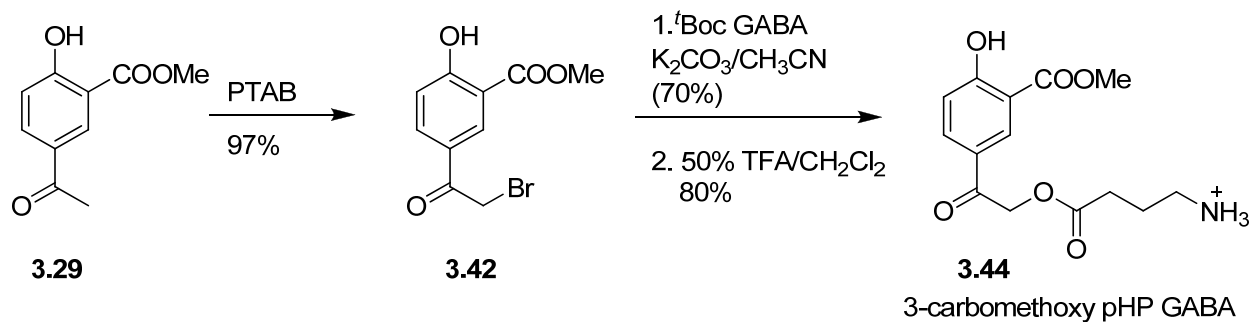
3-Carbomethoxy pHP Carbazole-9-acetic acid (**3.43**) and 3-carbomethoxy pHP GABA (**3.44**) were synthesized to explore the effects of the fluorescein and carbazole moiety on the photochemistry of the pHP chromophore (Scheme 3.8 and 3.9). The α -bromo derivative of methyl 5-acetylsalicylate (**3.42**) was obtained by the reaction with PTAB and subsequent $\text{S}_{\text{N}}2$ displacement of the bromide with carbazole-9-acetic acid gave rise to **3.43** in 65% yield (Scheme 3.8).

Scheme 3.8



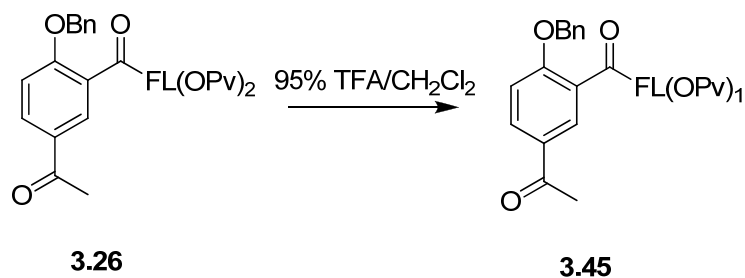
Synthesis of **3.44** also followed the same route of an $\text{S}_{\text{N}}2$ displacement reaction between bromo ketone **3.42** and ^tBocGABA, followed by removal of the ^tBoc protecting group by TFA to yield 3-carbomethoxy pHP GABA (**3.44**) (Scheme 3.9). The synthesis and photochemistry of **3.44** has been previously reported by Givens *et al.*¹

Scheme 3.9



3-[5-AminoFL(OPv)₁]-4-phenylmethoxyacetophenone (**3.45**) was synthesized to use as a standard for studies involving **3.35**. Removal of one pivalate group of **3.26** by 95% TFA/CH₂Cl₂ produced **3.45** in 50% yield (Scheme 3.10).

Scheme 3.10



UV-vis studies of 3-[5-aminoFL(OPv)₁] pHP Carbazole-9-acetic acid (3.35), 5-amino fluorescein (3.23) and carbazole-9-acetic acid (3.32)

UV-vis spectra of all the components in the pHP ensemble **3.35** were explored in water/methanol with the pH of the water fraction adjusted to 5.0, 7.54, and 9.0. UV-vis spectra of carbazole-9-acetic acid (**3.32**) were insensitive to pH variations (Figure 3-9b) whereas the UV-vis spectra of 5-aminofluorescein (**3.23**) displayed the typical pH dependent behavior for fluorescein-based dyes. When the pH was 9, the absorption bands were indicative of the xanthene form of fluorescein. When the pH was reduced to 5, a blue shift of the absorption bands was observed, marking the presence of the lactone form (Figure 3-9c). The equilibration of the lactone and xanthene forms of fluorescein were discussed in the *Introduction* (Scheme 3.5). The UV-vis spectra of pHP derivative **3.35**, which contains both a fluorophore and a quencher attached to it, showed the same pH dependence as free fluorescein (Figure 3-9a). UV-vis data for all three compounds are given in Table 3-3.

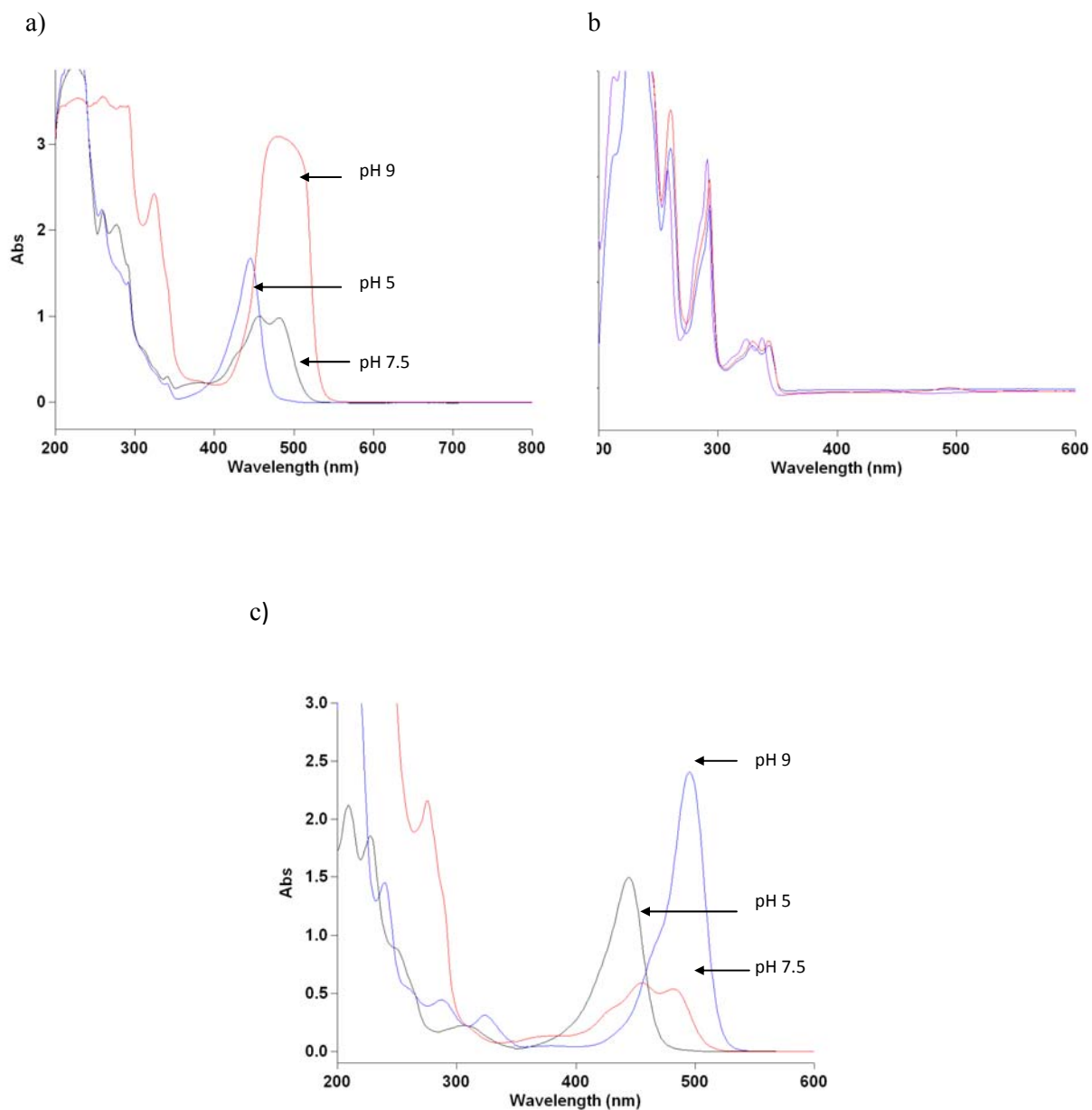


Figure 3-9. UV-vis spectra of the three components of pHP ensemble at different pHs (a) 3-[5aminoFL(OPv)₁]pHP Carbazole-9-acetic acid (**3.35**) with overlay spectra at pH's of 5, 7.5, and 9, (b) carbazole-9-acetic acid (**3.32**) with overlay spectra at pH 5, 7.5, and 9.5, and (c) 5-aminofluorescein (**3.23**) with overlay spectra at pH's of 5, 7.5, and 9.

Table 3-3. UV-vis data of 3-[5-aminoFL(OPv)₁]pHP Carbazole-9-acetic acid (**3.35**), 5-aminofluorescein(**3.23**) and carbazole-9-acetic acid (**3.32**) in 16% aqueous/MeOH

Compound	$\lambda_{\max}^a(\epsilon^b)$ at pH 5	$\lambda_{\max}(\epsilon)$ at pH 7.5	$\lambda_{\max}(\epsilon)$ at pH 9
3.35	445 (11000), 291 (9600), 258 (15700)	481 (6300), 456 (7100), 341 (2200), 277 (14400), 259 (15200)	492 (21600), 324 (14200), 291 (23900), 260 (24700)
3.32	336 (1620), 326 (1600), 291 (7400)	343 (1400), 329 (1400), 292 (5900)	342(1500), 329(1500)
3.23	442 (17600)	481 (8055), 453 (7200)	488 (24300)

^aextinction coefficient ^maximum absorbance in nm ^bextinction coefficient (M⁻¹cm⁻¹)

Exploratory Photochemistry of 3-[5-aminoFL(OPv)₂]pHP DABCYL (**3.33**)

Photolysis of **3.33** was attempted with 10% D₂O/DMSO in a Pyrex NMR tube. A 10 mg sample of **3.33** in 10% D₂O/DMSO was photolyzed in a Rayonet photoreactor with 2 x 3000 Å lamps in a merry-go-round apparatus. However, photorelease of DABCYL was not observed even on prolonged exposure to light (72 h). Therefore further studies with DABCYL quencher were not conducted.

Exploratory Photochemistry of 3-[5-aminoFL(OPv)₁]pHP Carbazole-9-acetic acid (**3.35**)

Photochemistry of **3.35** was explored using both ¹H NMR and UPLC analysis. The NMR experiments were performed in a Pyrex NMR tube. A 10 mg sample of **3.35** was dissolved in 20% D₂O/CD₃CN and photolyzed in a Rayonet photoreactor with 2 x 3000 Å lamps and a merry-go-round apparatus. ¹H NMR spectra were obtained at 10 min intervals. Initial spectra revealed the release of carbazole-9-acetic acid (**3.32**) with a signature peak at 5.05 ppm. However, another peak at 5.77 ppm also appeared which tended to grow with longer irradiation times while the peak at 5.05 ppm decreased (Figure 3-10). This observation led us to suspect that released carbazole-9-acetic acid (**3.32**) undergoes further reaction. The photoproducts of the pHP

chromophore showed no indication of the formation of the anticipated rearrangement product, the phenylacetic acid, which should produce a peak near 3.6 ppm. However, a peak at 4.66 ppm was observed arising from α -hydroxy compound **3.46** (Figure 3-10c). The mechanism of photoproduct formation from the pHP phototrigger was discussed in *Chapter 1*.

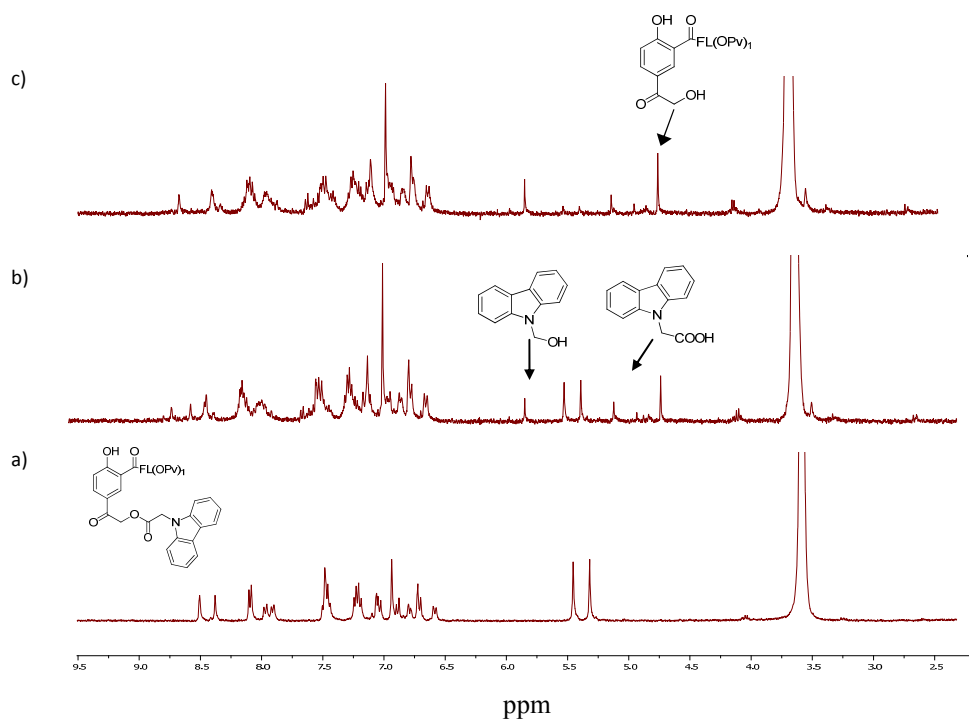
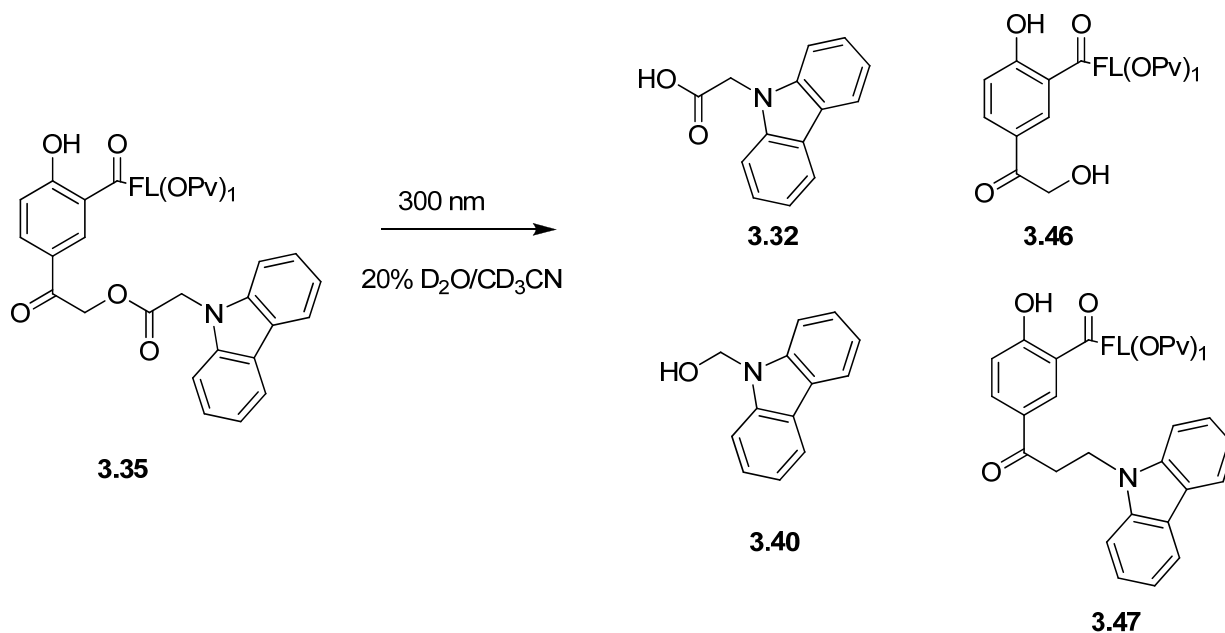


Figure 3-10. ^1H NMR spectra of the photolysis **3.35** in 20% $\text{D}_2\text{O}/\text{CD}_3\text{CN}$ at a) time = 0, b) time = 55 min, (c) 1h 25 min. (see text for explanation and description of the selected peaks)

The peak at 5.77 was assigned to 9H-carbazole-9-methanol (**3.40**) which was independently synthesized by the route shown in Scheme 3.7 and its formation during photolysis was confirmed by spiking the samples during photolysis experiments followed by both ^1H NMR and by UPLC. When the photolysis mixture was subjected to analysis by LS/MS/MS, a new peak with m/z 773.3 was observed which was assigned to structure **3.47**. Close examination of the ^1H NMR spectra also showed triplets at 3.03 ppm and 4.02 ppm which also were assigned to

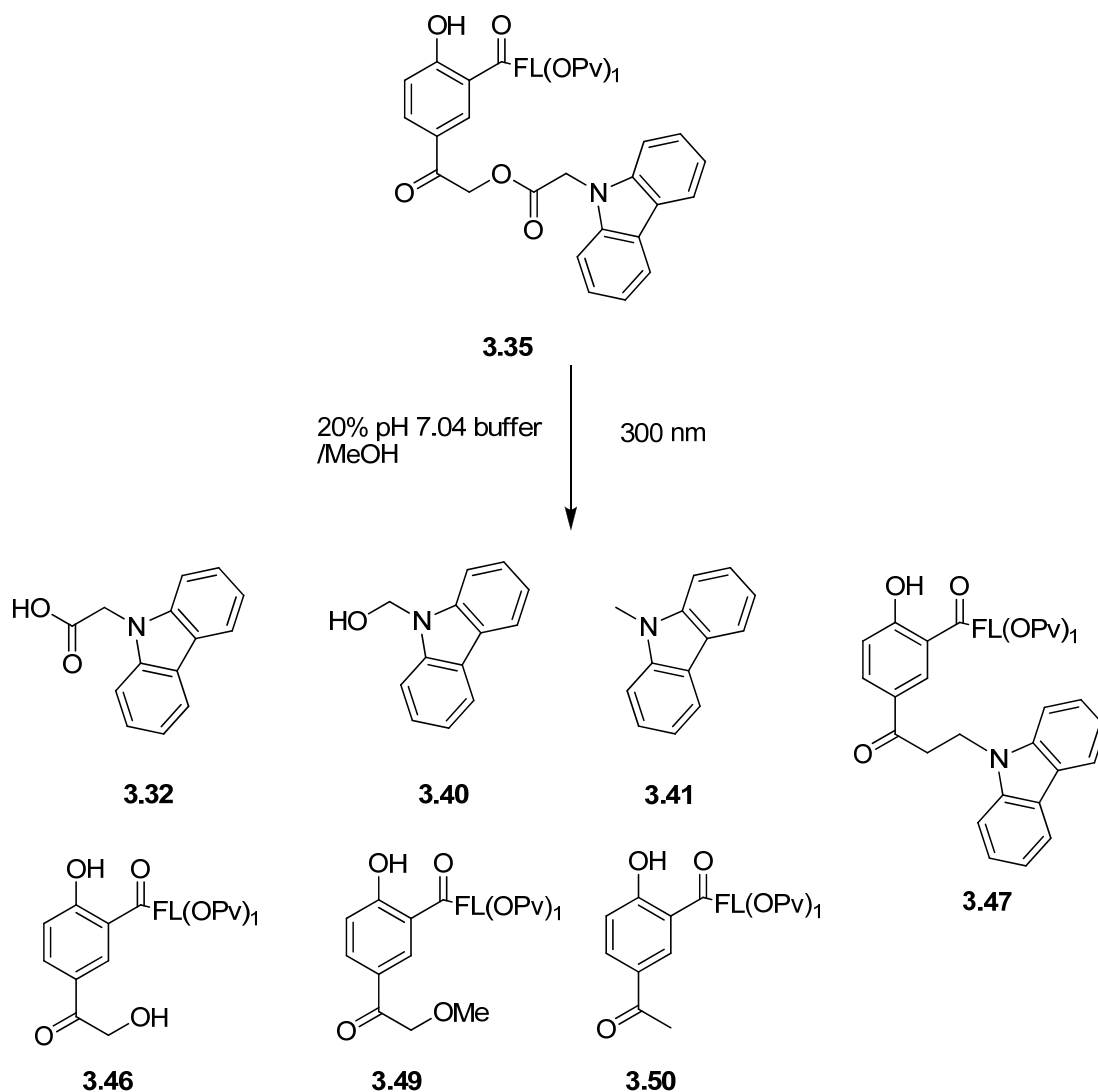
methylene H's in **3.47**. The smaller peaks observed at 4.7-4.9 were not identified. All of the products identified in the photolysis of **3.35** in 20% D₂O/CD₃CN are illustrated in Scheme 3.11

Scheme 3.11



When photolysis was performed in a 1:1 mixture of pH 7.52 Tris buffer:MeOH, methylated forms of both **3.46** and **3.40** and the acetophenone **3.50** were also observed by LC/MS/MS, in addition to all the products shown in Scheme 3.11. UPLC studies done with the same solvent system showed another product which was assigned to 9-methyl-9H-carbazole **3.48**, which was independently synthesized according to the route shown in Scheme 3.7. Spiking experiments of the type discussed earlier were performed with UPLC studies to confirm its formation. All of the products formed by photolysis conducted in 1:1 pH 7.52 Tris buffer:MeOH are shown in Scheme 3.12. Close examination of the LC/MS/MS data obtained from photolysis studies in 20% D₂O/CD₃CN also revealed the presence of trace amounts of **3.48** and **3.50**.

Scheme 3.12

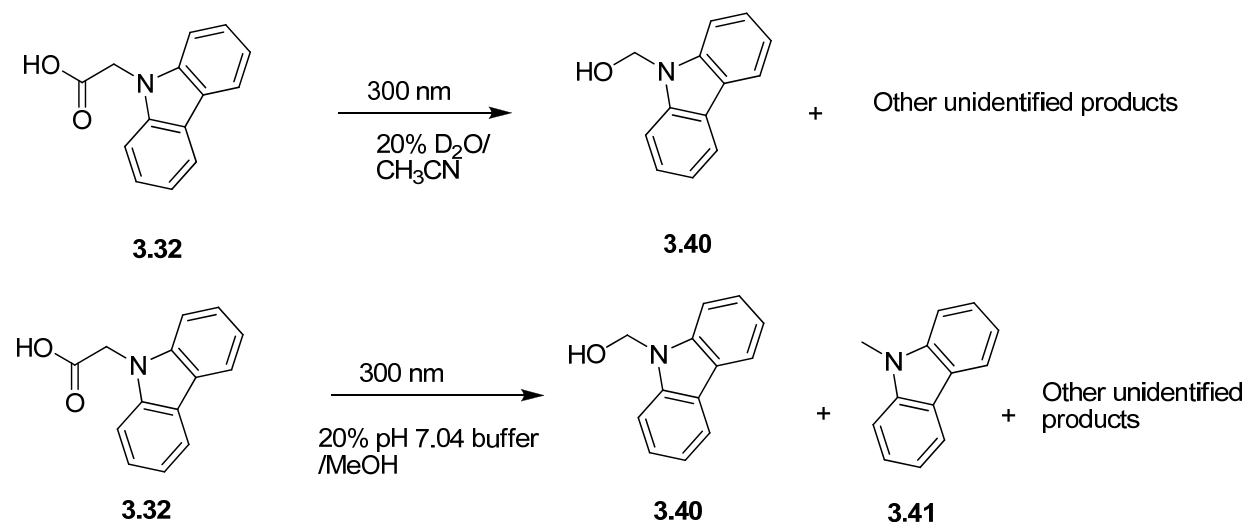


Photochemical investigation of carbazole-9H-acetic acid (3.32)

To investigate whether some products observed in the photolysis of **3.35** arise from secondary photochemistry, carbazole-9-acetic acid (**3.32**) was independently subjected to the photolysis conditions in 20% D₂O/CD₃CN using a similar photoreactor set up equipped with 16 x 3000 Å lamps. H¹ NMR spectra were recorded every hour and the reaction was monitored for 30 h (Figure 3-11). The photochemistry of **3.32** was comparatively less efficient than that of **3.35**

as complete conversion could not be achieved even after exposure to irradiation for 30 h while **3.35** reached complete conversion with in 2 h. But the formation of the 9-hydroxymethyl carbazole (**3.40**) that has an H^1 NMR signal at 5.77 ppm was clearly observed. Other unidentified peaks at 4.68 and 4.78 ppm were also observed. Photolysis was also conducted in 20% pH 7.52 Tris buffer/MeOH in the same photoreactor setup and reaction progress followed via UPLC analysis. The results show prominent formation of 9-methylcarbazole (**3.41**), 9-hydroxymethylcarbazole (**3.40**) and some other minor photoproducts (Scheme 3.13).

Scheme 3.13



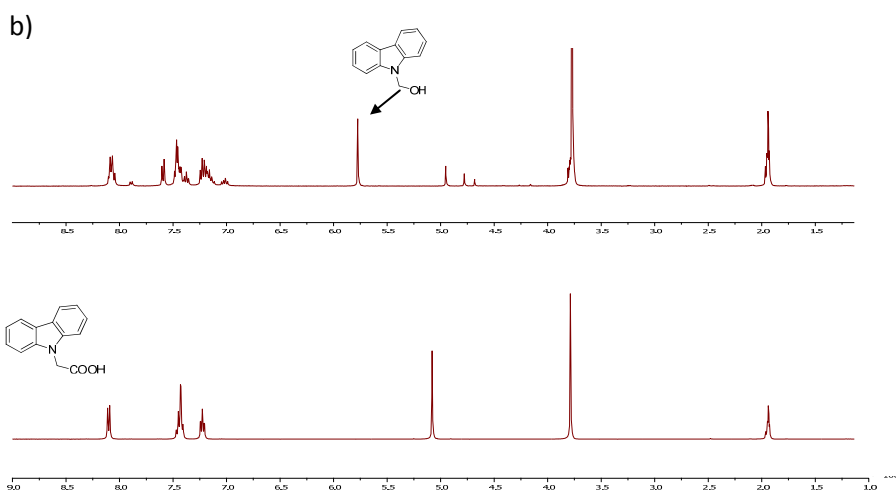


Figure 3-11. ^1H NMR spectra of carbazole-9H-acetic acid (**3.32**) in 20% $\text{D}_2\text{O}/\text{CD}_3\text{CN}$ at a) time = 0, b) time = 30 h. see text for explanation

Photochemical investigation of 3-carbomethoxy pHP Carbazole-9-acetic acid (**3.43**)

Photochemistry of **3.43** was explored using ^1H NMR to study the effect, if any, on the photochemical behavior of the pHP chromophore with an attached fluorescein moiety. Photolysis was conducted in a Rayonet photoreactor with 16 x 3000 Å lamps in 20% $\text{D}_2\text{O}/\text{CH}_3\text{CN}$ as the solvent. The photolysis products were similar to those observed for **3.35**. However, the formation of the coupling product **3.51** was more pronounced.

Quantum yield (Φ) studies

Quantum yield studies of 5-aminoFL(OPv)₁ pHP carbazole-9-acetic acid (**3.35**) were conducted using the same photolysis reactor setup with 16 x 3000 Å. Samples for photolysis were prepared by dissolving 10.0 mg of **3.35** in 16% pH 7.5 Tris buffer/MeOH. Aliquots were removed at 1 minute intervals and starting material disappearance was quantified using UPLC analysis with caffeine as the internal standard. To investigate the effect of the presence of the 5-aminofluorescein and carbazole-9-acetic acid, both light absorbing chromophores, on the

efficiency of photorelease by the pHP group, the quantum yields of 3-carbomethoxy pHP GABA (**3.44**) and 3-carbomethoxy pHP carbazole-9-acetic acid (**3.43**) were also determined. Quantum yield studies of **3.44** and **3.43** were conducted with 2 x 3000 Å bulbs instead of the 16 used for **3.35**. The quantum yield (Φ) of 3-carbomethoxy pHP GABA (**3.44**) was significantly higher than that of both **3.35** and **3.43**, the reported Φ for 3-carbomethoxy pHP GABA (**3.44**), of 0.31 in pH 7 buffer (Givens *et al.*).¹ Comparing 3-carbomethoxy pHP carbazole-9-acetic acid (**3.43**) and 5-aminoFL(OPv)₁ pHP carbazole-9-acetic acid (**3.35**) revealed that the quantum yield of the former was four times higher than that of **3.35**. The quantum yield data are shown in Table 3-4.

Table 3-4. Quantum Yields for the Disappearance of **3.35**, **3.43** and **3.44**. in 16% pH 7.50 Tris Buffer/MeOH

pHP derivative	Φ_{Dis} at 3000 Å	Φ_{Dis} at 3500 Å
3-[5aminoFL(OPv) ₁] pHP Carbazole-9-acetic acid (3.35)	0.021 ± 0.001	0.015 ± 0.001
3-carbomethoxy pHP Carbazole-9-acetic acid (3.43)	0.07 ± 0.01	nd ¹
3-carbomethoxy pHP GABA (3.44)	0.35 ± 0.02	nd

¹nd = not determined

Quenching studies

To establish the ability of the selected quenchers (carbazole-9-acetic acid and DABCYL) to quench the fluorescence of 5-aminofluorescein, solutions of 5-aminofluorescein were prepared by dissolving 10 mg of the fluorophore in MeOH (2.88 mM), the quencher was added and the fluorescence spectra recorded. The fluorescence of 5-aminofluorescein was completely quenched when the DABCYL concentration reached 7.2 mM. However, addition of 0.288 M carbazole-9-acetic acid was necessary to observe significant quenching. This concentration effect

may be due to a difference in the mechanisms of quenching by these two acceptors. This will be addressed further in the *Discussion* section.

Combined photorelease and fluorescence studies of 3-[5-aminoFL(OPv)₁] pHP Carbazole-9-acetic acid (3.35)

In an ideal situation, the 3-[5-aminoFL(OPv)₁] pHP carbazole-9-acetic acid (**3.35**) assembly should be nonfluorescent and should achieve fluorescence only when released after exposure to photocleavable energies of light of the protecting group. However, **3.35** itself showed slight fluorescence emission when excited at 487 nm. When compared to the fluorescence of **3.45**, the standard, about 7 fold decrease in fluorescence was observed for **3.35**. To investigate whether the expected increase in fluorescence occurs, the photolysis of **3.35** was monitored by both fluorescence and UPLC analyses. In a typical experiment, 10 mg of **3.35** was dissolved in 5 ml of 25% pH 7.50 Tris buffer/ MeOH and photolyzed in the same photoreactor setup described above. At 10 min intervals, 200 µl aliquots were removed, diluted to 5 ml in volumetric flasks, and the fluorescence spectra recorded. Samples were also analyzed by UPLC to follow the progress of the reaction. The photolysis was complete in 1 h. The fluorescence spectra observed at different time intervals are illustrated in Figure 3-12 (a). A photographic representation can be seen in Figure 3-12 (b). The expected increase in the fluorescence was observed upon photolysis but the fluorescence intensity reached only about 50% of the maximum fluorescence compared with a standard.

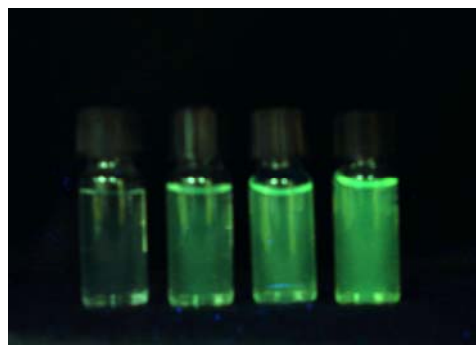
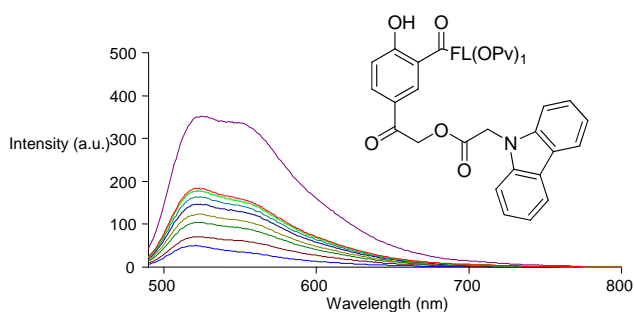


Figure 3-12. (a) Fluorescence spectra recorded at time intervals 0, 5, 10, 15, 20, 30, 40, 50, 60 min during photolysis of **3.35**. Fluorescence of **3.45**, the standard, is shown in purple. The concentration was 9.72×10^{-5} M for all samples ($\lambda_{\text{exi}} = 480$ nm, $\lambda_{\text{emi}} = 522$). (b) A photograph illustrating the increase of fluorescence with time during photolysis of **3.35**. $t = 0, 10, 20,$ and 50 min from left to right.

Exploratory photochemistry of 3-[9-(2-hydroxyethyl)carbazole] pHP 5-carboxyFL (**3.39**).

In a typical experiment 10 mg of **3.39** was dissolved in 5 ml 20% pH 7.10 Tris buffer/MeOH and photolyzed in a 10 ml quartz tube using a Rayonet Photoreactor equipped with 16 x 3000 Å lamps and a Merry-go-round apparatus. The progress of the reaction was followed by UPLC. The quantum yield for disappearance (Φ_{dis}) of **3.39** was determined to be 0.04 ± 0.01 , slightly higher than that of **3.35** (Table 3-4).

Combined photorelease and fluorescence studies of 3-[9-(2-hydroxyethyl)carbazole] pHP 5-carboxyFL (**3.39**)

These photolysis experiments were performed in a manner similar to those for **3.35**. The samples were removed at 2 min intervals and 5-carboxyfluorescein was used as the standard. The extent of quenching by carbazole in **3.39** was greater. A ~20 fold decrease of fluorescence was observed when compared with 5-carboxyfluorescein. Figure 3.13 illustrates the increase of fluorescence with time during photolysis of **3.39**. The pattern was similar to that observed for **3.35** (Figure 3-12(a)). However, the maximum fluorescence reached was about 30% of the standard.

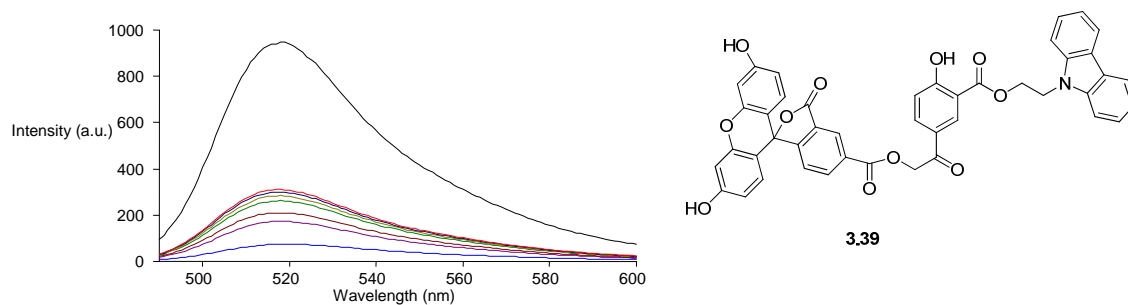


Figure 3-13. Fluorescence spectra recorded at time intervals 0, 2, 4, 8, 10, 12, 14 min during photolysis of **3.39**. The fluorescence of 5-carboxyfluorescein, the standard, is shown in black. Concentration was 8.01×10^{-7} M for all samples. The λ_{exi} was 480 nm and λ_{emi} was 518 nm.

Computational studies

In order to computationally evaluate the relative energies of linear versus π -stacked conformations, the structures were analyzed in SYBYL⁴⁸ in conformations that were manually constructed to approximate the more stable conformations of the combination fluorophore-pHP- quencher ensemble. The individual conformational structures were then subjected to molecular mechanics minimization (allowing unlimited optimization steps) with SYBYL according to default optimization algorithms and convergence threshold criteria. Forces and energies were quantified via the Tripos molecular force field,⁴⁹ Gasteiger-Marsili electrostatics⁵⁰ and a nonbonding interaction threshold of 15.0 Å. For geometric characterization of the molecules, aryl ring centroids were defined as the position within the ring plane approximately equidistant to all ring carbons, and distances between centroids were obtained from SYBYL's geometry measurement utilities.

The energies of two different π -stacked conformations of 3-[5aminofluorescein] pHP carbazole-9-acetic acid (**3.35**) were explored (1) when the pivalic group is positioned over the

carbazole ring (Figure 3-14a) and (2) when the pivalic group is away from the carbazole ring (Figure 3-14b).

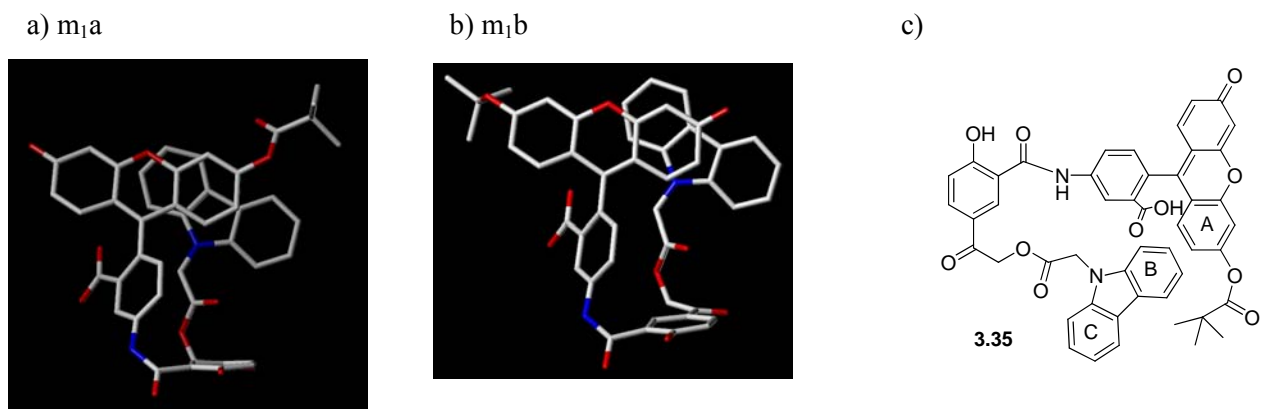
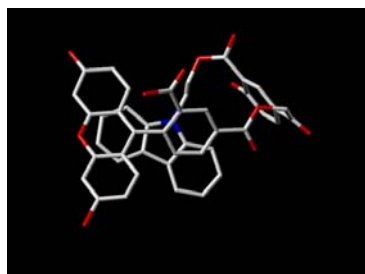


Figure 3-14. Possible π -stacked conformations of **3.35**. a) π -Stacked confirmation with pivalate group towards the carbazole rings. b) π -Stacked confirmation with pivalate group away from the carbazole rings. C) Ring assignment of **3.35**

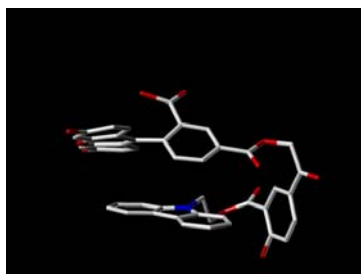
In the m_1a conformer the distance between the A-B rings was 3.90 Å and between the A-C rings was 3.76 Å. The energy of the molecule was found to be 22.63 kcal/mol. The assignment of the rings is illustrated in Figure 3-14c. For the m_1b conformer where the pivalate group is away from the carbazole ring, the A-B ring distance was 5.34 Å, while the A-C rings were 8.37 Å apart. The energy of this conformer was 23.09 kcal/mol. Modeling studies were also performed for the derivative where both pivalate groups were absent. In the π -stacking orientation the distance between the A-B rings and the A-C rings were 3.41 and 4.28 Å, respectively, indicating that the pivalate groups keep the quencher and the fluorophore apart. The energy of the conformer was 25.92 kcal/mol.

For 3-[9-(2-hydroxyethyl)carbazole] pHP 5-carboxyFL (**3.39**), the lowest energy conformer was found to be the π -stacked structure m_2a with an energy of 15.5 kcal/mol. The extended, narrower structure was substantially higher in energy (28.00 kcal/mol; Figure 3-15).

a) m_2a



b) m_2b



C)

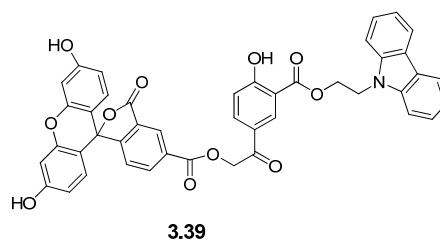


Figure 3-15. a) π -stacked and b) extended conformations of **3.39**. (c) Structure of **3.39**

Discussion

Design of the quencher-fluorescent dye bifunctional phototriggers utilizing a pHP core (FQ pHP) employed two different approaches. In one ensemble, the fluorophore is to be attached as a substituent on the pHP nucleus and the quencher connected as the leaving group (Figure 3-16(a)). In the second, the two components changed positions on the pHP moiety (Figure 3-16(b)). Widely used fluorescein derivatives were chosen as the fluorophores while carbazole derivatives and DABCYL were employed as the quenchers in these designs.

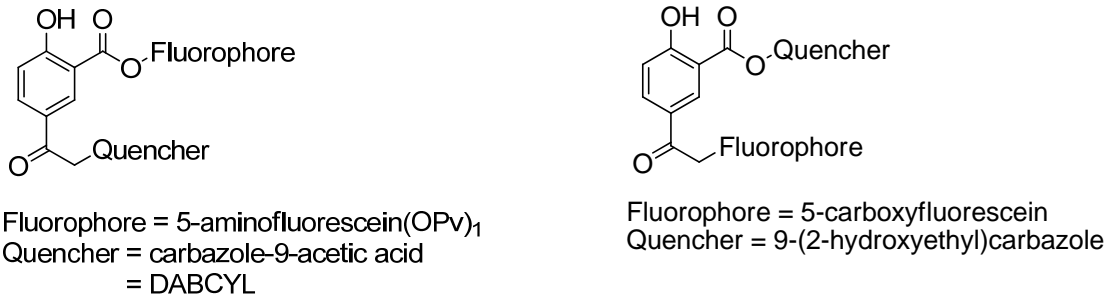


Figure 3-16. Structures of novel pHP-based fluorophore quencher ensembles.

DABCYL is a quencher widely employed to quench green fluorescent protein.⁴³ The use of carbazole as the quencher was inspired by the work of Hong *et al.*⁴⁶ who developed a molecular tripod based on fluorescein and carbazole to study streptavidin binding. The quenching mechanisms of carbazole and DABCYL, the quenchers used in this study, are different. A brief discussion of mechanisms of quenching follows.

Quenching mechanisms

Molecular probes, such as FRET-based and beacon probes, are based on fluorescence quenching. The probes generally involve the interaction of two dyes, an absorbing fluorophore

and a quencher or acceptor fluorophore. The fluorescence of the absorbing fluorophore is quenched when in close proximity to the quencher fluorophore.⁵¹ Quenching mechanisms can be broadly divided into two types, dynamic and static quenching.⁵² In dynamic quenching, the quenching occurs by excited state processes. Förster⁵³ and Dexter⁵⁴ mechanisms fall under this category. Static quenching occurs through dimer or exciplex formation.

The Dexter mechanism: The Dexter mechanism is also known as an exchange or coulombic energy transfer process, which occurs at short range by a collision controlled quenching process that is essentially an electron exchange.⁵¹ A schematic diagram of Dexter energy transfer is illustrated in Figure 3-17. Spin is conserved during the Dexter process. The efficiency of Dexter quenching is dependent on the spatial overlap of donor and acceptor molecular orbitals and the efficacy of quenching decreases exponentially with R where R is the donor-acceptor separation.⁵¹ Therefore, bimolecular collision of the donor and acceptor in solution is required or the fluorophore and the quencher need to be held in a rigid system at a distance of 5-10 Å in order to observe quenching. The Dexter mechanism is generally operative in Molecular Beacons.⁴³

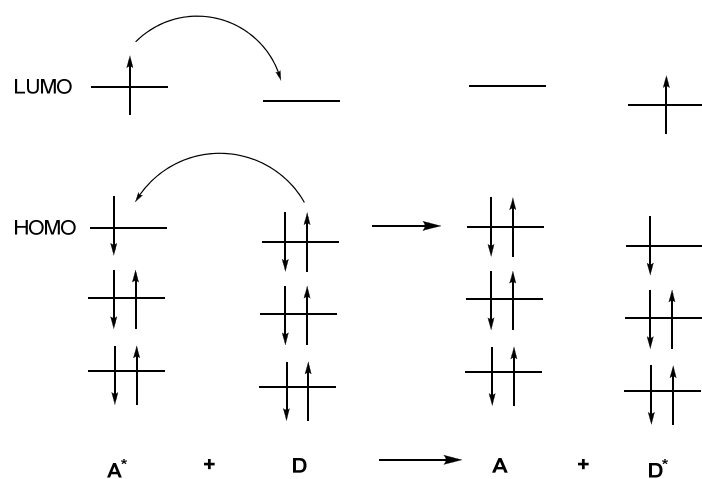


Figure 3-17. A schematic representation of electron movement in Dexter mechanism.

The Förster mechanism. The Förster mechanism is the most commonly observed phenomenon with binary probes⁵⁵ and is referred to as Förster Resonance Energy Transfer (FRET). Generally two dyes like fluorescein and rhodamine that emit at different wavelengths are employed as the acceptor and the donor. For FRET to occur spectral overlap between the donor emission and acceptor absorption is essential (Figure-18). When FRET is operative, the fluorescence of the acceptor will be observed when the donor is excited. Recently non-fluorescent dyes such as DABCYL, also known as dark quenchers, have been used as acceptors that show no fluorescence when FRET is operative as the quencher will simply undergo nonradiative decay.⁵⁵ FRET occurs from dipole-dipole interactions between the donor and the acceptor, is also dependent on the distance between the two dyes, and can be operative up to 100 Å. The efficiency of FRET is proportional to $1/R^6$. FRET also depends on the orientation of the dipoles. Maximum quenching is observed when the two dipoles are aligned parallel to each other. A highly schematic representation of the Förster mechanism is illustrated in Figure 3-19 simply to show the difference between the Dexter and the Förster mechanism

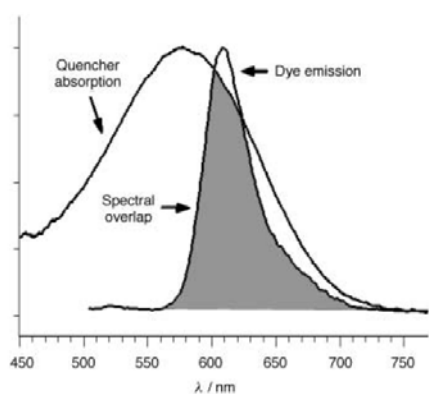


Figure 3-18. Acceptor emission and quencher absorption with large spectral overlap. Reproduced with permission from European Journal of Chemistry.

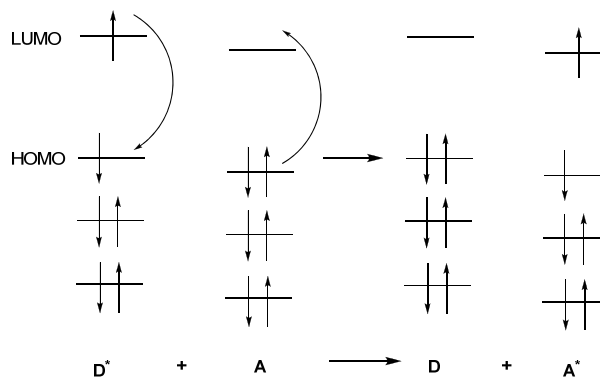


Figure 3-19. A schematic representation of Förster mechanism.

Static quenching. Intramolecular formation of ground state dimers, with unique spectral properties, between the fluorophore and the quencher gives rise to static quenching.⁵¹ The reason for the dimer formation is generally attributed to an hydrophobic effect. Quenching of fluorescein fluorescence by carbazoles used in this study is attributed to ground state dimer formation. However, the actual mechanism of static quenching is not fully understood.⁴⁴ When homodimers are formed, complete quenching of fluorescence is observed when the transition dipoles are completely cancelled. However, in heterodimers only a reduction of fluorescence can be expected. Fluorescence quenching can also occur from exciplex formation. (An exciplex is an excited state complex which is formed after the donor is excited) For exciplex formation to be operative in molecular probes, close proximity of the donor and acceptor is necessary and a long-lived excited state must be a property of the donor.⁵⁶

A synthetic approach to novel pHP based fluorophore quencher ensembles. Synthesis of the [FQ pHP] ensembles started with 5-acetylsalicylic acid as the base unit of the design. 5-Acetylsalicylic acid is attractive since it provides two handles that can be manipulated separately and is a relatively inexpensive, commercially available starting material. Initial steps of the synthesis of FlpHPQ ensembles **3.33** and **3.35** were the EDC coupling reaction between bispivalate protected 5-aminofluorescein and benzyl protected 5-acetylsalicylic acid (Scheme 3.2 *Results*). Attempts to carry out the subsequent synthetic steps without the benzyl protection of the phenolic OH led to polymer formation. α -Bromination of fluorescein substituted acetophenone **3.26** was achieved using phenyltrimethylammonium tribromide in good yield (70%) with only trace amounts of the dibromo byproduct. Caging of DABCYL and carbazole-9-acetic acid was achieved using a facile S_N2 displacement of the α -bromoketone.

Removal of the pivalate protecting groups from the 5-amnoffluorescein moiety was difficult. The standard method for pivalate deprotection is employing base hydrolysis.⁴⁷ Attempts made using strong basic conditions such as NaOH, LiOH, basic alumina and milder environments like K₂CO₃ or CsCO₃ in different solvents systems including MeOH/H₂O, THF/H₂O, DMF, CH₃CN resulted in the hydrolysis of the amide linkage. The compound was stable to NaHCO₃. Finally one pivalate group was removed under acid conditions (90% TFA/CH₂Cl₂). Attempts to remove the second pivalate group under same conditions lead to decomposition of the compound. Therefore, close monitoring of the reaction using TLC was necessary to stop the reaction at monoprotected stage. Purification of the compound was also difficult due to the highly polar properties of fluorescein. Desired compounds were purified by employing flash chromatography with 5% MeOH/EtOAc as solvent. Final deprotection of the benzyl group was accomplished using standard hydrogenolysis conditions in THF. However, for the caged DABCYL derivative **3.28a**, hydrogenolysis conditions were not successful because the azo linkage underwent reduction. Removal of the benzyl group in DABCYL containing derivatives was accomplished using FeCl₃.

Synthesis of the QpHPFl ensemble (**3.39**) was initially attempted following the same route as for the FlpHPQ unit. The carbazole substituent was attached to the pHP moiety by an EDC coupling reaction between benzyl protected 5-acetylsalicylic acid (**3.27**) and 9H-carbazole-9-ethanol. However, attempts to brominate the α -position of the resulting acetophenone employing either CuBr₂ and phenyltrimethylammonium tribromide resulted in carbazole ring bromination. Therefore, carbazole was attached to the pHP nucleus after α -bromination of 5-acetylsalicylic acid (Scheme 3.6 *Results*). Subsequent S_N2 displacement of bromide by 5-

carboxyfluorescein gave the desired QpHPFl ensemble **3.39**. Purification of **3.39** was achieved by preparative thin layer chromatography.

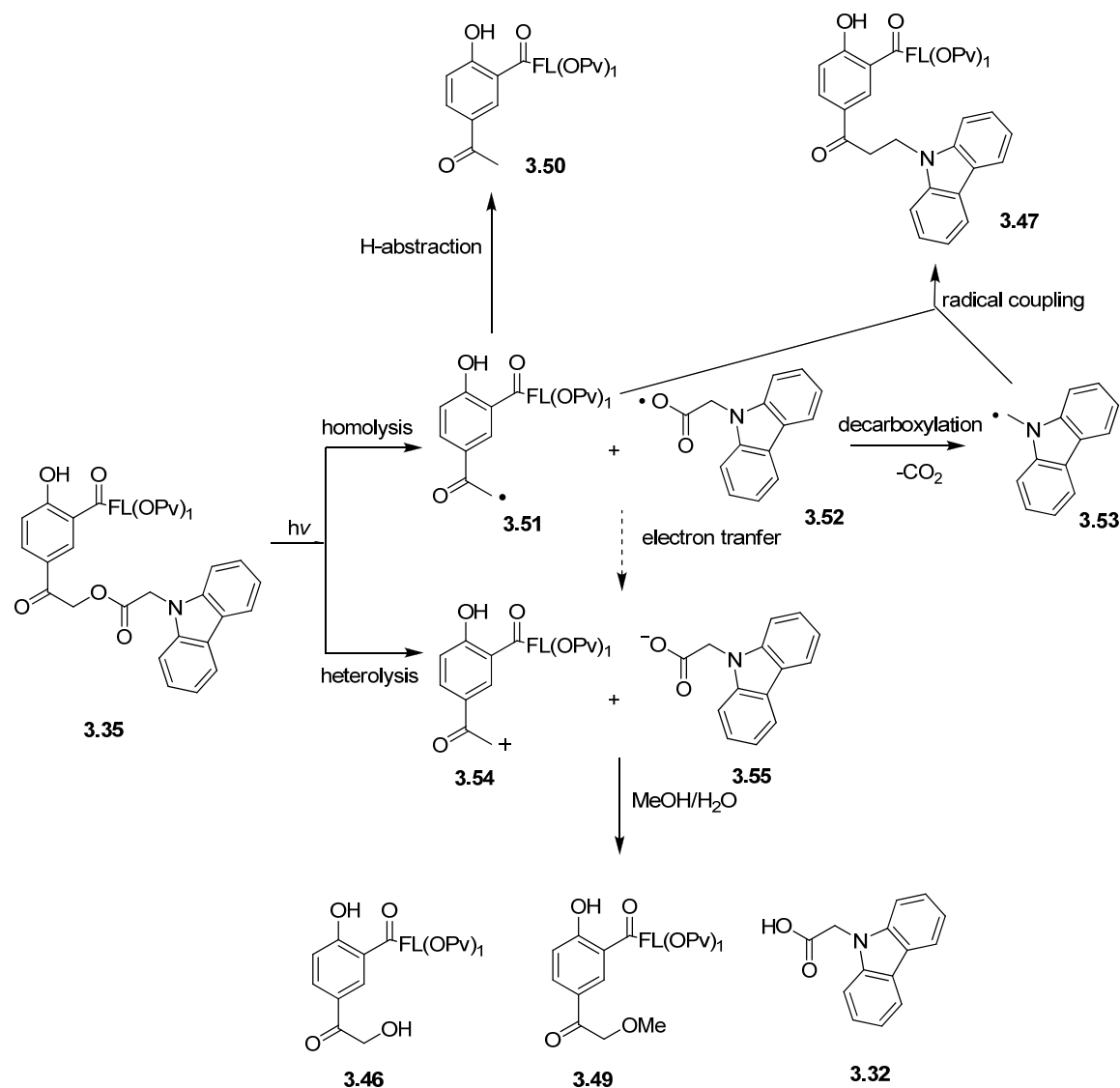
Photochemical studies of 3-[5-aminoFL(OPv)₂] pHP DABCYL (3.33) DABCYL derivative **3.33** was photo-inert at 300 nm even for prolonged exposure to irradiation in 10% D₂O/DMSO. Use of DMSO was necessary because **3.33** was insoluble in CD₃CN/D₂O. Previous studies done with cyano substituted pHP acetates discussed in this Dissertation (*Chapter 1*) and in work reported by Stensrud,⁵⁷ showed that other pHP derivatives undergo anticipated Favorskii rearrangements in aqueous DMSO. Work accomplished in this project and reported in *Chapter 2, Section 4* of this Dissertation shows that pHP photochemistry can take place in the presence of the fluorescein chromophore even though the latter is the stronger absorber in the wavelength region employed for the study. Therefore, lack of photorelease from **3.33** is more likely due to the properties of DABCYL component.

Photochemical cis-trans isomerization of azo compounds is a well studied phenomenon.⁵⁸ One possibility is that energy absorbed by the chromophore is simply used for cis-trans isomerization of DABCYL thereby shutting down pHP photorearrangement chemistry.

Photochemical Explorations of 3-[5-aminoFL(OPv)₁] pHP Carbazole-9-acetic acid (3.35). Photochemistry 3-[5-aminoFL(OPv)₁] pHP Carbazole-9-acetic acid (**3.35**) differed from other pHP derivatives. Although the compound was photoreactive, formation of the Favorskii products, i.e., the *p*-hydroxyphenylacetic acid and *p*-hydroxybenzyl alcohol types of products, was not observed. However, photorelease of carbazole did occur. Therefore, a mechanism other than the Favorskii rearrangement is operative in this pHP derivative.

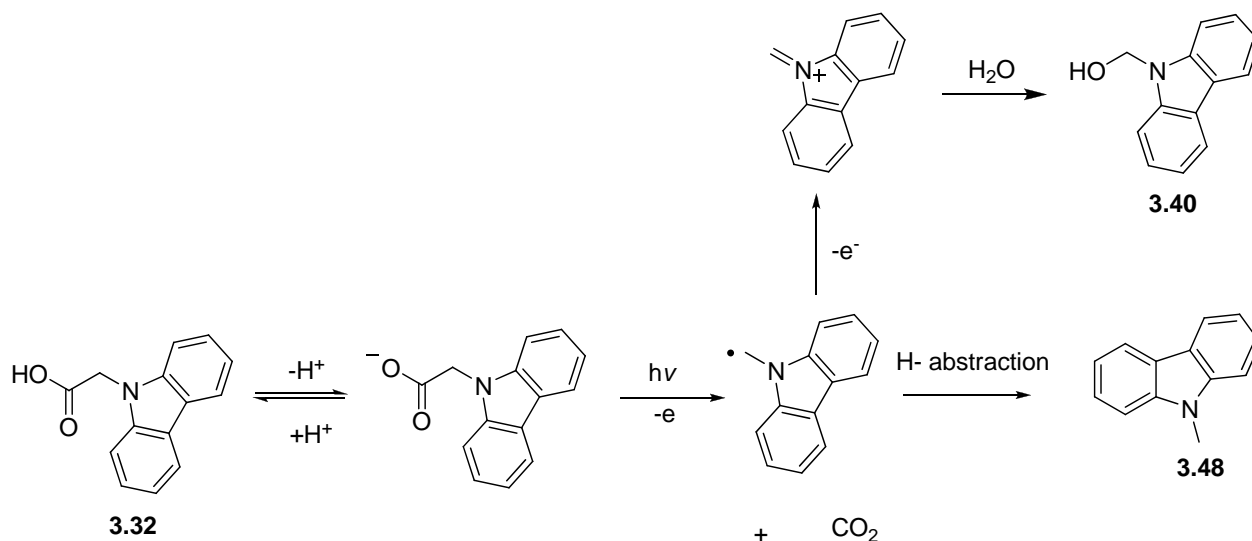
An array of photoproducts was observed in 20% pH 7.05 tris buffer/MeOH (*Results*, Scheme 3.12). From the pHP moiety, *p*-hydroxyphenacyl alcohol (**3.46**), *p*-hydroxyphenacyl methyl ether (**3.49**), and acetophenone (**3.50**) derivatives and from the carbazole component 9H-carbazole-9-acetic acid (**3.32**), 9H-carbazole-9-methanol (**3.40**), 9-methyl-9H-carbazole (**3.41**) were observed. In addition to these, a coupling product **3.47** was observed (Scheme 3.12 *Results*). Two viable mechanistic pathways for photorelease are heterolysis and homolysis of the carbon-oxygen ester bond connecting the pHP unit to the carbazole moiety.⁵⁹ Formation of the coupling product **3.47**, acetophenone **3.50**, and 9-methyl-9H-carbazole (**3.41**) suggest the heterolytic pathway. A plausible mechanism for the photorelease of 9H-carbazole-9-acetic acid (**3.32**) from **3.33** is illustrated in Scheme 3.14. Homolysis of the ester linkage will give rise to an acetophenone radical (**3.51**) and a carboxyl radical **3.52**. Decarboxylation of the carboxyl radical will generate methylene radical **3.53** that can couple with the acetophenone radical to give **3.47**. Electron exchange of the initial radicals **3.51** and **3.52** will give rise to a cation-anion pair, **3.54** and **3.55**, that can react with the solvents present to yield the observed products. H-abstraction by radical **3.51** generates the acetophenone derivative **3.50**. Pathways for the formation of carbazole derivatives **3.40** and **3.48** are illustrated in Scheme 3.15.

Scheme 3.14



Independent photochemical investigation of 9H-carbazole-9-acetic acid (**3.32**) (*Results*, Scheme 3.13) showed that formation of 9H-carbazole-9-methanol (**3.40**) and 9-methyl-9H-carbazole (**3.41**) is due to secondary photochemistry of 9H-carbazole-9-acetic acid. Decarboxylation of carboxylic acids is a well known phenomenon⁶⁰ and a plausible mechanism for the photochemistry of 9H-carbazole-9-acetic acid (**3.32**) is illustrated in Scheme 3.15.

Scheme 3.15



3-Carbomethoxy pHP carbazole-9-acetic acid (**3.43**) shows the same product distribution as observed for the photolysis **3.35** and **3.32** under identical conditions, suggesting that the photochemistry observed in these compounds is mainly dictated by the carbazole moiety and is independent of the presence of fluorescein.

Quantum efficiency (Φ) studies Quantum efficiencies of 0.02, 0.07, and 0.35 were measured for 3-[5-aminoFL(OPv)₁] pHP carbazole-9-acetic acid (**3.35**), 3-carbomethoxy pHP carbazole-9-acetic acid (**3.43**), and 3-carbomethoxy pHP GABA (**3.44**), respectively. Therefore, the decrease of Φ of **3.35** can be ascribed to effects from both the carbazole and fluorescein chromophores since 3-carbomethoxy pHP GABA, which lacks both of these moieties, showed the highest Φ and 3-carbomethoxy pHP carbazole-9-acetic acid, which contains only the carbazole group but not the fluorescein moiety, shows a Φ that is four times higher than that of **3.35**. Thus, to a first approximation, both carbazole and fluorescein participate in the dissipation of energy, absorbed

by the molecule and from carbazole more so than from fluorescein. However, it is necessary to note that 3-carbomethoxy pHP GABA follows the usual photo-Favorskii pathway while 3-[5-aminoFL(OPv)₁] pHP carbazole-9-acetic acid and 3-carbomethoxy pHP carbazole-9-acetic acid follow a different mechanism such as that illustrated in Scheme 3.14.

Combined photorelease and fluorescence studies of FlpHPQ and QpHPFl ensembles.

Neither the FlpHPQ or QpHPFl arrangements resulted in complete quenching of the fluorescence. However, a significant reduction of fluorescence was observed. The QpHPFl unit **3.39** showed a 20 fold decrease in fluorescence compared to the standard (5-carboxyfluorescein) whereas the FlpHPQ unit **3.35** showed only a 7 fold decrease indicating that the QpHPFl orientation is superior for quenching by this quencher. Molecular modeling calculations on **3.39** and **3.35** discussed in the *Results* section showed that the π -stacked conformation of **3.39** is more stable with an E_0 value of 15.5 kcal/mol than the π -stacked conformation of **3.35** with an $E_0 = 22.63$ kcal/mol, indicating that π -stacking is better in **3.39** which is in accordance with the observed higher quenching. The presence of two methylene groups in the carbazole component of **3.39** allows more flexibility which may be responsible for the observed greater π -stacking.

Fluorescence spectra obtained with increasing photolysis time showed the expected increase in fluorescence (Figures 3-12, 3-13 *Results*). However, the maximum fluorescence observed after complete photolysis was substantially less than that of standards for both **3.39** and **3.35**. The reason for this observation is not fully understood.

Future studies. This was a proof-of-concept investigation to explore the possibility of developing a caged fluorescent probe based on pHP photoremovable protecting groups and the results described here are a preliminary affirmation of this application for pHP protecting groups. Calculations of the fluorescence quantum yields (Φ_F) of the designed ensembles will be valuable in obtaining quantitative measures of the reactivation of fluorescence by photolysis. In **3.35** the complex mixture of photoproducts observed and lack of Favorskii rearrangement may be due to the photochemistry of carbazole-9-acetic acid. Incorporation of more methylene units, i.e., a longer tether, between the carbazole and the pHP moiety may result in a photo-Favorskii style rearrangement and cleaner overall reaction. Removal of the remaining pivalate group will also give rise to better fluorescence enhancement. This study was confined to fluorescein and carbazole fluorophore-quencher pair. Design of other fluorophore-quencher pairs where fluorescence is completely quenched prior to photolysis, is important for applicability of these systems in actual biological studies.

Conclusions. Newly designed pHP fluorophore-quencher ensembles in this study showed reduced fluorescence in the reactant form which can restore the fluorescence upon photolysis. Photolysis of 3-[5-aminoFL(OPv)₁] pHP carbazole-9-acetic acid (**3.35**) did not follow the photo-Favorskii rearrangement precedent observed with other pHP derivatives. The photorelease via a mechanistic pathway that involved homolysis seems more favorable. The quantum efficiencies of photorelease from the new pHP derivatives were relatively low which is likely due to the presence of two additional chromophores competing for light and possibly some quenching of the photochemistry.

Experimental

General methods: Melting points were conducted with open-ended capillary tubes using a non-calibrated melting point apparatus. Products of all reactions were assessed for purity using the following instrumental techniques: ^1H and ^{13}C were obtained using Bruker 400 Hz instrument unless otherwise stated. Exact masses were obtained using a triple quadrupole electrospray ionization mass spectrometer. UV-vis data were obtained using 1.5 mL quartz cuvettes on a Cary 100 spectrophotometer (Varian, Inc., Palo Alto, CA). Fluorescence data were acquired using a 10 mm quartz cell in Cary Eclipsed Fluorescence Spectrophotometer (Varian, Inc., Palo Alto, CA.). IR data were obtained with pressed potassium bromide (KBr) pellets. Product separation was achieved by flash chromatography using silica gel and gradient of hexanes/ethyl acetate as eluting solvents unless otherwise stated.

Photolysis studies were performed in a Rayonet RPR-100 photoreactor equipped with two or sixteen 16 W, 3000 Å lamps and a Merry-go-round apparatus. Quantum yield studies and product identification were achieved through UPLC or LC/MS/MS, triple quadrupole electro spray ionization mass spectrometric analysis. The instrument was equipped with a UV-vis dual wavelength detector set at 250 and 280 nm. The reservoirs used were as follows: A) 99% water, 1% acetonitrile, and 0.06% formic acid; B) 99% acetonitrile, 1% water, and 0.08% formic acid. The compounds were separated on a reverse-phase (C18, 5 μm mesh), 50 mm length column. Three injections of 5 μl - 100 μl were made with an automated sampler for each sample. The mobile phase gradient was optimized for compound separation and the flow rate was set at 200 $\mu\text{l}/\text{min}$. During data analysis, smoothing functions were used for

peak area determinations of the chromatographic peaks. Calibration curves were constructed for all compounds and photoproducts for quantification purposes.

Synthesis

2,2-Dimethyl-1,1'-(5-amino-3-oxospiro[isobenzofuran-1(3H),9'-(9H)xanthenes]-3',6'-diyl) ester propanoic acid (3.24) The general method of Hong *et al.*⁴⁶ was followed. 5-Aminofluorescein (1.0 g, 2.9 mmol) and Cs₂CO₃ (4.7g, 14.4 mmol) was dissolved in DMF and pivalic anhydride (1.25 ml, 5.8 mmol) was slowly added and the reaction mixture was stirred at room temperature until completion of reaction was observed by TLC (~2h). Water (100 ml) and EtOAc (100 ml) were added to the reaction mixture and EtOAc layer separated was washed several times with water. Further purification by column chromatography (2:2:1 hexane:CH₂Cl₂:EtOAc) provided 2,2-dimethyl-1,1'-(5-amino-3-oxospiro[isobenzofuran-1(3H),9'-(9H)xanthenes]-3',6'-diyl) ester propanoic acid (**3.24**) as a slight yellow solid (1.30 mg, 85%). mp, 190-193 °C. IR (KBr): 3473, 3386, 2974, 1751, 1610, 1490, 1419, 1325, 1155, 1116, 1072, 995, 891, 825, 765 cm⁻¹. ¹H NMR (400 MHz CDCl₃): δ 1.26 (s, 18H), 6.76 (dd, 1H), 6.81 (m, 5H), 7.02 (d, 2H), 7.20 (d, 1H). ¹³C NMR (100 MHz, CDCl₃): δ (ppm) 27.2, 39.1, 81.7, 110.1, 116.9, 117.5, 122.5, 124.6, 127.7, 129.0, 142.7, 148.4, 151.7, 152.4, 169.6, 171.2, 176.6. HRMS calculated for C₃₀H₂₉NO₇+ H= 516.2022, observed = 516.2021.

5-Acetyl-2-(phenylmethoxy)benzoic acid (3.25) The general method of Freché, *et al.*⁶¹ was followed. Methyl 5-acetylsalicylate (2.0 g, 10.30 mmol), benzyl bromide (1.08 ml, 10.30 mmol), and K₂CO₃ (3.56 g, 25.75 mmol) were stirred at 60 °C, in CH₃CN (50 ml) for 16 h. The resulting solution was evaporated to dryness, dissolved in water and extracted with ethyl acetate. The ethyl acetate layer was dried with anhydrous MgSO₄ and the solvent evaporated *in vacuo* to obtain methyl 5-acetyl-2-(phenylmethoxy)benzoate (2.90 g, 99%). 5-Acetyl-2-(phenylmethoxy)

benzoate was further hydrolyzed by the general method of Chen *et al.*⁶² 1 M NaOH (10 ml, 10.55 mmol) was added to a solution of 5-acetyl-2-(benzyloxy)benzoate (2.0g, 7.03 mmol) in 100 ml of dioxane and refluxed for 1 h. The resulting solution was concentrated by removal of solvent and 1 N HCl was added until the pH reached pH = 1 and extracted with EtOAc. The EtOAc layer was dried with anhydrous MgSO₄ and solvent removed to obtain 5-acetyl-2-(phenylmethoxy)benzoic acid (**3.25**) as a white solid in 100% yield (1.9 g) and was used without further purification. mp, 135-137 °C. IR (KBr): 3033, 1739, 1670, 1595, 1498, 1272, 979, 821 cm⁻¹. ¹H NMR (400 MHz CDCl₃): δ 2.61 (s, 2H), 5.37 (s, 2H), 7.19 (dd, 2H), 7.43 (m, 5H), 8.17 (dd, 1H), 8.71(d, 1H). ¹³C NMR (100 MHz, CDCl₃): δ (ppm) 26.5, 67.0, 113.3, 113.4, 118.1, 127.6, 127.7, 132.2, 134.1, 134.2, 160.9, 166.9, 196.1.

5-(5-Acetyl-2-(benzyloxy)benzamido)-3-oxo-3H-spiro[isobenzofuran-1,9'-xanthene]-3',6'-diyl bis(2,2-dimethylpropanoate) (3.26) 5-Acetyl-2-(phenylmethoxy)benzoic acid (**3.25**, 40 mg, 0.15 mmol) and EDC (29 mg, 0.15 mg) in THF were stirred at room temperature for 15 mins. Then **3.24** (32 mg, 0.06 mmol) was added and the stirring continued at 40 °C for 12 h. The solvent was evaporated *in vacuo* and to the resulting oil was added 20 ml H₂O/CH₂Cl₂. The CH₂Cl₂ layer extracted and washed with water and NaHCO₃, dried with anhydrous MgSO₄, and the solvent evaporated. The resulting solid was purified by column chromatography (2:2:1 hexane:CH₂Cl₂: EtOAc) to obtain 47 m g of 5-(5-acetyl-2-(benzyloxy)benzamido)-3-oxo-3H-spiro[isobenzofuran-1,9'-xanthene]-3',6'-diyl bis(2,2-dimethylpropanoate) (57%): mp, 278-280 °C. IR (KBr): 1766, 1749, 1681, 1600, 1417, 1336, 1253, 1244, 1157, 114, 1068, 993, 894, 605 cm⁻¹. ¹H NMR (400 MHz CDCl₃): δ 1.36 (s, 18H), 2.68(s, 2H), 5.33 (s, 2H), 6.75 (m, 4H), 6.95 (d, 1H), 7.03 (d, 2H), 7.27 (t, 1H), 7.56 (m, 5H), 7.97(s, 1H), 8.24 (dd, 2H), 8.94 (d,1H), 10.20 (s, 1H). ¹³C NMR (100 MHz, CDCl₃): δ (ppm) 23.8, 26.5, 39.1, 72.5, 81.4, 106.4, 107. 6, 110.1,

110.2, 112.8, 115.2, 116.2, 116.8, 117.5, 117.6, 120.6, 122.4, 124.3, 124.7, 126.6, 127.0, 128.9, 129.6, 130.2, 131.3, 134.0, 134.1, 140.0, 148.14, 148.2, 151.5, 151.6, 152.3, 153.5, 159.3, 168.6, 176.6, 196.5. HRMS calculated for $C_{46}H_{42}NO_{10} + H = 768.2809$, observed = 768.2832.

5-(2-(Benzyloxy)-5-(2-bromoacetyl)benzamido)-3-oxo-3H-spiro[isobenzofuran-1,9'-

xanthene]-3',6'-diyl bis(2,2-dimethylpropanoate) (3.27) The general method of Holman, *et al.*

⁶³ was followed. **3.26** (228 mg, 2.90 mmol) and phenyltrimethylammonium tribromide (111 mg, 2.90 mmol) in 3:1 CH_2Cl_2 : MeOH (20 ml) was stirred at room temperature for 16 h. The solvent was evaporated *in vacuo* and to the resulting oil was added 20 ml H_2O/CH_2Cl_2 and the CH_2Cl_2 layer extracted and washed with water five times, dried with anhydrous $MgSO_4$, and the solvent evaporated. The resulting solid was purified by column chromatography (2:2:1 hexane: CH_2Cl_2 : EtOAc) to obtain 5-(2-(benzyloxy)-5-(2-bromoacetyl)benzamido)-3-oxo-3H-spiro[isobenzofuran-1,9'-xanthene]-3',6'-diylbis(2,2-dimethylpropanoate) (175 mg, 70%): mp, 190-192 °C. IR (KBr): 3352, 2972, 1749, 1731, 1693, 1600, 1417, 1267, 115, 1114, 1068, 1027, 943, 827, 783, 470 cm^{-1} . ¹H NMR (400 MHz $CDCl_3$): δ 1.36 (s, 18H), 4.52 (s, 2H), 5.33 (s, 2H), 6.75 (m, 4H), 6.95 (m, 1H), 7.03 (d, 2H), 7.27 (m, 1H), 7.56 (m, 5H), 7.97 (s, 1H), 8.24 (dd, 2H), 8.94 (d, 1H), 10.20 (s, 1H). ¹³C NMR (100 MHz, $CDCl_3$): δ (ppm) 27.0, 30.9, 39.2, 72.7, 81.4, 110.3, 113.3, 115.2, 116.2, 117.7, 121.0, 124.4, 126.6, 127.0, 128.0, 128.9, 129.0, 129.6, 130.2, 133.9, 134.2, 139.9, 148.2, 151.5, 152.5, 160.4, 162.0, 168.6, 176.6, 189.7. HRMS calculated for $C_{46}H_{41}BrNO_{10} + H = 846.1913$, observed = 846.1912.

5-(2-(Benzyloxy)-5-(2-(4-((4-dimethylamino)phenyl)diazenyl)benzoyloxy)acetyl)benzamido)-3-oxo-3H-spiro[isobenzofuran-1,9'-xanthene]-3',6'-diyl bis(2,2-dimethylpropanoate). The general method of Hiyama, *et al.*⁶⁴ was applied. A mixture of **3.27** (56 mg, 0.06 mmol), DABCYL (18 mg, 0.06 mmol), and K_2CO_3 (22 mg, 0.15 mmol) in CH_3CN (5 ml) was stirred at

room temperature for 24 h. The solvent was evaporated, the resulting residue dissolved in water, and the water layer extracted with ethyl acetate three times. The compound was further purified by column chromatography (1:1 ethyl acetate: hexane) to yield the desired product, 5-(2-(benzyloxy)-5-(2-(4-((4-dimethylamino)phenyl)diazenyl)benzoyloxy)acetyl)benzamido)-3-oxo-3H-spiro[isobenzofuran-1,9'-xanthene]-3',6'-diylbis(2,2-dimethylpropanoate) (**3.28a**) as a orange-red solid (31 mg, 50%): mp,229-230 °C. IR (KBr): 2925, 1760, 1755, 1725, 1718, 1650, 1598, 1490, 1419, 1363, 1272, 1244, 1155, 1134, 945, 821, 490 cm⁻¹. ¹H NMR (400 MHz CDCl₃): δ 1.36 (s, 18H), 3.10 (s, 6H), 5.32 (s, 2H), 5.65 (s, 2H), 6.74 (m, 6H), 6.77 (d, 1H), 6.97 (s, 2H), 7.03 (d, 2H), 7.56 (m, 5H), 7.88 (m, 5H), 8.26 (d, 2H), 8.95 (d,1H), 10.17 (s, 1H). ¹³C NMR (100 MHz, CDCl₃): δ (ppm) 27.0, 30.9, 39.2, 40.3,66.5, 72.7, 81.4, 110.3, 114.4, 113.3, 115.2, 116.2, 117.7, 120.9,122.0, 124.4, 125.5, 126.6, 127.0, 128.3, 129.3, 129.3, 129.6, 130.2,131.0, 132.8, 133.8, 133.9, 140.0, 143.0,148.2, 151.5, 152.5, 152.9, 156.2, 160.4, 162.0, 165.7, 168.6, 176.6, 190.5.HRMS calculated for C₆₁H₅₅N₄O₁₂+ H= 1035.3816, observed = 1035.3807.

5-(5-(2-(2-(9H-cCarbazol-9-yl)acetoxo)acetyl)-2-(benzyloxy)benzamido)-3-oxo-3H-spiro[isobenzofuran-1,9'-xanthene]-3',6'-diyl bis(2,2-dimethylpropanoate) (3.28b) The same procedure as used for **3.28b** was followed to obtain the desired compound, 5-(5-(2-(2-(9H-carbazol-9-yl)acetoxo)acetyl)-2-(benzyloxy)benzamido)-3-oxo-3H-spiro[isobenzofuran-1,9'-xanthene]-3',6'-diyl bis(2,2-dimethylpropanoate) (99%) mp,229-230 °C. IR (KBr): 2927, 1757, 1749, 1700, 1676, 1650, 1602, 1541, 1490, 1458, 1384, 1325, 1155, 1114, 993, 896, 752 cm⁻¹. ¹H NMR (400 MHz CDCl₃): δ 1.36 (s, 18H), 5.25 (s, 2H), 5.31 (s, 2H), 5.46 (s, 2H), 6.76 (m, 4H), 6.94 (d, 1H), 7.03 (d, 2H), 7.23 (m, 2H), 7.46 (m, 6H), 7.56 (m, 5H), 7.94 (s, 1H), 8.09 (d,2H), 8.18 (d, 1H), 8.81 (s, 1H),10.11 (s, 1H). ¹³C NMR (100 MHz, CDCl₃): δ (ppm) 27.0, 30.9, 39.2, 44.4, 66.8, 72.6, 81.4, 108.5, 110.2, 113.2, 113.2, 115.2, 116.2, 117.7, 199.7, 120.4,

122.8, 123.2, 124.3, 126.0, 127.0, 127.8, 128.9, 129.0, 129.6, 130.3, 132.8, 133.8, 139.8, 140.5, 148.1, 151.51, 152.4, 160.4, 161.8, 168.2, 168.6, 176.6, 189.6. HRMS calculated for $C_{60}H_{51}N_2O_{12} + H = 991.3442$, observed = 991.3492

9H-Carbazole-9-acetic acid (3.32) The general method of Harima *et al.* was followed.⁶⁵ Sodium hydride (143 mg, 3.6 mmol) was slowly added to a solution of carbazole (500 mg, 3.0 mmol) in dry acetonitrile. After the bubbling of H_2 ceased, ethyl chloroacetate was added drop wise and heated to 80 °C. Solvent was removed and aqueous KOH in THF was added to the resulting mixture and heated at 60 °C. THF was removed *in vacuo* and the resulting solution was acidified and extracted in to EtOAc to give the desired compound, 9H-carbazole-9-acetic acid in 52% yield (352 mg) as a white solid and was used for subsequent synthesis without any further purification. mp, 200-202 °C. IR (KBr): 3049, 1718, 1596, 1485, 1404, 1367, 1325, 1238, 1209, 1153, 1120, 937, 754, 723, 626 cm^{-1} . 1H NMR (400 MHz $CDCl_3$): δ 5.04 (s, 2H), 7.25 (m, 4H), 7.45 (m, 2H), 8.11 (d, 2H). ^{13}C NMR (100 MHz, $CDCl_3$): δ (ppm) 44.0, 108.1, 120.0, 120.5, 123.2, 126.1, 140.3, 172.6.

5-(5-(2-(4-((4-(Dimethylamino)phenyl)diazanyl)benzoyloxy)acetyl)-2-hydroxybenzamido)-3-oxo-3H-spiro[isobenzofuran-1,9'-xanthene]-3',6'-diyl bis(2,2-dimethylpropanoate) (3-[5-aminoFL(OPv)₂] pHP DABCYL ,3.33) The general method by Jiang *et al.*⁶⁶ was followed. $FeCl_3$ (45 mg, 0.3 mmol) was added to a solution of **43.28a** (90 mg, 0.08 mmol) in CH_2Cl_2 and stirred at room temperature for 2 h. water was added to the resulting reaction mixture and water layer extracted three times (10 ml \times 3) with CH_2Cl_2 . Purification employing column chromatography (1:1 ethyl acetate: hexane) produced 5-(5-(2-(4-((4-(dimethylamino) phenyl) diazenyl) benzoyloxy)acetyl)-2-hydroxybenzamido)-3-oxo-3H-spiro[isobenzofuran-1,9'-xanthene]-3',6'-diyl bis(2,2-dimethylpropanoate) as a break red solid (30 mg, 52%) mp, 168-170 °C. IR

(KBr): 3292, 2925, 1760, 1755, 1725, 1718, 1650, 1598, 1490, 1419, 1363, 1272, 1244, 1155, 1134, 945, 821, 490 cm^{-1} . ^1H NMR (400 MHz CDCl_3): δ 1.36 (s, 18H), 3.10 (s, 6H), 5.65 (s, 2H), 6.74 (m, 6H), 6.77 (d, 1H), 6.97 (d, 2H), 7.03 (dd, 2H), 7.88 (m, 6H), 8.26(d, 1H), 8.59(s, 1H) 8.95(d,1H), 9.54 (s, 1H), 10.17(s, 1H). ^{13}C NMR (100 MHz, CDCl_3): δ (ppm) 27.0, 30.9, 39.2, 40.3,66.5, 72.7, 81.4, 110.3, 11.44, 113.3, 115.2, 116.2, 117.7, 120.9,122.0, 124.4, 125.5, 126.6, 127.0, 128.3, 129.3, 129.3, 129.6, 130.2,131.0, 132.8, 133.8, 133.9, 140.0, 143.0,148.2, 151.5, 152.5, 152.9, 156.2, 160.4, 162.0, 165.7, 168.6, 176.6, 190.5.HRMS calculated for $\text{C}_{54}\text{H}_{49}\text{N}_4\text{O}_{12} + \text{H} = 945.3347$, observed = 945.3345.

5-(5-(2-(2-(9H-Carbazol-9-yl)acetoxy)acetyl)-2-(benzyloxy)benzamido)-3'-hydroxy-3-oxo-3H-spiro[isobenzofuran-1,9'-xanthene]-6'-yl pivalate (3.34). A 250 mg quantity of **3.28b** (0.25 mmol) was added to 10 ml of 95% TFA in CH_2Cl_2 and stirred at room temperature. The reaction progress was monitored using TLC and the reaction was stopped when the TLC showed multiple spots near the baseline indicating the decomposition of the compound (~2h). Solvent removal and directed purification by column chromatography (5% MeOH / EtOAc) gave 5-(5-(2-(2-(9H-carbazol-9-yl)acetoxy)acetyl)-2-(benzyloxy)benzamido)-3'-hydroxy-3-oxo-3H-spiro[isobenzofuran-1,9'-xanthene]-6'-yl pivalate as yellow solid in 44% yield (100 mg): mp,222-224 $^{\circ}\text{C}$. IR (KBr): 3282, 1751, 1730, 1690, 1650, 1602, 1541, 1485, 1425, 1326, 1259, 1166, 1114, 993, 752, 723 cm^{-1} . ^1H NMR (400 MHz $\text{CO}_2(\text{CD})_3$): δ 1.36 (s, 9H), 5.43 (s, 4H), 5.55 (s, 2H), 6.67 (m, 4H), 6.84 (m, 2H), 7.13 (d, 2H), 7.23 (t, 2H), 7.46 (m, 6H), 7.63 (m, H), 8.12 (d, 1H), 8.40 (d,2H), 8.11 (d, 1H), 8.64 (s, 1H), 10.19 (s, 1H). ^{13}C NMR (100 MHz, $\text{CO}_2(\text{CD})_3$): δ (ppm) 27.0, 30.9, 39.2, 44.4, 66.8, 72.6, 81.4,108.5, 110.2, 113.2, 113.2, 115.2, 116.2, 117.7, 199.7, 120.4,122.8, 123.2, 124.3, 126.o, 127.0, 127.8, 128.9, 129.0, 129.6, 130.3,

132.8, 133.8, 139.8, 140.5, 148.1, 151.51, 152.4, 160.4, 161.8, 168.2, 168.6, 176.6, 189.6. HRMS calculated for $C_{55}H_{42}N_2O_{11} + H = 907.2867$, observed = 907.2889.

5-(5-(2-(2-(9H-Carbazol-9-yl)acetoxy)acetyl)-2-hydroxybenzamido)-3'-hydroxy-3-oxo-3H-spiro[isobenzofuran-1,9'-xanthene]-6'-yl pivalate, (3-5aminoFL(OPv)₁ pHP Carbazole-9-acetic acid, 3.35) Pd/C (10 mg, 10% by weight) was added to a solution of **3.34** (100 mg, 0.11 mmol) in THF and H₂ gas bubbled to it. The reaction was followed by TLC and was complete after 1.5 h. Compound **3.35** was further purified by column chromatography (5% MeOH / EtOAc) (85.5 mg, 95%) mp, 147-148 °C. IR (KBr): 3357, 2960, 1751, 1735, 1695, 1647, 1608, 1485, 1458, 1427, 1251, 1174, 1114, 993, 752, 723 cm⁻¹. ¹H NMR (400 MHz CO₂(CD)₃): δ 1.36 (s, 9H), 5.45 (s, 2H), 5.57 (s, 2H), 6.78 (m, 2H), 6.92 (d, 2H), 6.97 (d, 1H), 7.08 (m, 1H), 7.15 (m, 1H), 7.22 (t, 2H), 7.26 (d, 2H), 7.46 (m, 1H), 7.61 (d, 2H), 8.07 (m, 2H), 8.14 (d, 2H), 8.56 (d, 1H), 8.56 (s, 1H). ¹³C NMR (100 MHz, CO₂(CD)₃): δ (ppm) 27.0, 30.9, 39.2, 44.4, 67.8, 82.4, 103.3, 109.9, 111.1, 113.7, 117.0, 118.0, 118.6, 119.5, 120.3, 124.0, 125.4, 126.7, 128.4, 129.0, 130.1, 130.5, 134.7, 141.7, 249.4, 152.7, 153.1, 153.6, 160.5, 169.1, 16.2, 176.8, 190.5. HRMS calculated for $C_{48}H_{37}N_2O_{11} + H = 817.2398$, observed = 817.2367. UV (50% pH 7.5 buffer/MeOH) λ_{max} = 480 (ε = 6300), λ_{max} = 451 (ε = 7100), λ_{max} = 341 (ε = 2200), λ_{max} = 279 (ε = 14354)

5-(2-Bromoacetyl)-2-hydroxybenzoic acid (3.37) The same procedure as used for **3.27** was followed to obtain the desired compound, 5-(2-bromoacetyl)-2-hydroxybenzoic acid (**3.37**). Column chromatography was conducted using 5% MeOH/EtOAc as solvent. However, 20% of unreacted starting material was present and the next synthetic step was carried out with this mixture. ¹H NMR (400 MHz CO₂(CD)₃): δ 4.75 (d, 2H), 7.10 (d, 1H), 8.22 (d, 1H), 8.61 (d, 1H),

^{13}C NMR (100 MHz, $\text{CO}_2(\text{CD})_3$): δ (ppm) 32.6, 114.1, 131.2, 132.6, 136.5, 139.7, 166.81, 172.0, 190.0. HRMS calculated for $\text{C}_9\text{H}_6\text{O}_4\text{Br} + \text{H} = 256.9449$, observed = 256.9449.

2-(9H-Carbazol-9-yl)ethyl 5-(2-bromoacetyl)-2-hydroxybenzoate (3.38) The same procedure as used for **3.26** was followed at room temperature to obtain the desired compound 2-(9H-carbazol-9-yl)ethyl 5-(2-bromoacetyl)-2-hydroxybenzoate in 70% yield. mp, 169-170 $^\circ\text{C}$. IR (KBr): 3433, 1701, 1670, 1589, 1485, 1460, 1382, 1217, 1091, 1018, 796, 750, 725, 482 cm^{-1} . ^1H NMR (400 MHz CDCl_3): δ 4.21 (d, 2H), 4.83 (m, 4H), 7.00 (d, 1H), 7.27 (m, 2H), 7.49 (m, 4H), 7.80 (d, 1H), 8.31 (s, 2H), 11.04 (s, 1H). ^{13}C NMR (100 MHz, CDCl_3): δ (ppm) 41.5, 46.0, 63.9, 108.2, 118.0, 119.5, 120.8, 123.16, 125.8, 130.2, 135.9, 138.8, 165.9, 169.2, 188.8. HRMS calculated for $\text{C}_{23}\text{H}_{17}\text{NO}_4\text{Br} + \text{H} = 450.0341$ observed = 450.0354.

2-(3-((2-(9H-Carbazol-9-yl)ethoxy)carbonyl)-4-hydroxyphenyl)-2-oxoethyl 3',6'-dihydroxy-3-oxo-3H-spiro[isobenzofuran-1,9'-xanthene]-5-carboxylate, (3-[9-(2-hydroxyethyl) carbazole] pHP 5-carboxyFL ,3.39) The same procedure as used for **3.28** was followed to obtain the desired compound 2-(3-((2-(9H-carbazol-9-yl)ethoxy)carbonyl)-4-hydroxyphenyl)-2-oxoethyl 3',6'-dihydroxy-3-oxo-3H-spiro[isobenzofuran-1,9'-xanthene]-5-carboxylate in 32% yield as a yellow solid. Purification of the compound was achieved via preparative thin layer chromatography using 5% MeOH/ EtOAc as the eluting solvent. mp, 177-179 $^\circ\text{C}$. IR (KBr): 3413, 1762, 1733, 1710, 1602, 1452, 1384, 1209, 1078, 802, 752, 472 cm^{-1} . ^1H NMR (400 MHz $\text{CO}(\text{CD})_3$): δ 4.94 (m, 4H), 5.48 (s, 2H), 6.66 (d, 2H), 6.69 (m, 4H), 7.06 (d, 1H), 7.21 (d, 2H), 7.46 (m, 3H), 7.78 (d, 2H), 8.16 (m, 3H), 8.24 (d, 1H), 8.47 (d, 1H), 8.63 (s, 1H). ^{13}C NMR (100 MHz, $\text{CO}_2(\text{CD})_3$): δ (ppm) 58.8, 61.9, 64.6, 100.2, 106.8, 107.6, 109.6, 110.3, 115.9, 116.9, 118.0, 120.7, 122.5, 123.7, 125.4, 127.3, 128.6, 129.4, 132.7, 133.7, 138.3, 150.1, 155.0, 157.3, 162.0, 165.4, 166.9, 187.2. HRMS calculated for $\text{C}_{44}\text{H}_{30}\text{NO}_{11} + \text{H} = 748.1819$ observed =

748.1833. UV (20% pH 7.5 buffer/MeOH) $\lambda_{\max} = 492$ ($\epsilon = 7500$), $\lambda_{\max} = 320$ ($\epsilon = 7298$), $\lambda_{\max} = 280$ ($\epsilon = 16900$).

9H-Carbazole-9-methanol (3.40) This is a known compound.⁶⁷ The general method by Viktor *et al.*⁶⁷ was followed. A solution of carbazole (500mg, 3.0 mmol) and K_2CO_3 in 2 ml of ethanol was refluxed for 5 mins. Formaldehyde was added and refluxed for another 10 min. Water (10 ml) was added after solvent removal and extracted three times in to EtOAc (10 ml \times 3). EtOAc layers were combined, dried, and solvent evaporated. The resulting crude product was purified by recrystallization from toluene to obtain the desired, 9H-carbazole-9-methanol as a white needle-like crystals (230 mg, 40%) . mp, 137-138 $^{\circ}C$. 1H NMR (400 MHz CD_3CN): δ 4.25 (t, 1H), 5.80 (d, 1H), 7.24 (t, 2h) 7.49 (dd, 2H), 7.61 (d, 2H), 8.10 (d, 2H). ^{13}C NMR (100 MHz, CD_3CN): δ (ppm) 65.2, 109.2, 119.3, 122.8, 125.5, 139.6.

9-Methyl-9H-carbazole (3.41) This is a known compound.⁶⁸ The method reported by Sheh *et al.* was followed.⁶⁸ Carbazole (500 mg, 3.0 mmol) DABCO (33 mg, 0.3 mmol) and dimethyl carbonate (5 ml) in DMF was refluxed for 24 h. The reaction mixture was cooled to room temperature and EtOAc (50 ml) and water (50 ml) was added. The EtOAc layer was separated and washed with water (50 ml), 10% aqueous citric acid (2 \times 50 ml) and water (4 \times 50 ml) sequentially. The resulting crude product was purified by column chromatography (2:2:1 hexane/ CH_2Cl_2 /EtOAc) to obtain 190 mg of 9-methyl-9H-carbazole as a white solid (35%) mp, 75-76 $^{\circ}C$. 1H NMR (400 MHz CD_3CN): δ 3.86 (s, 3H), 7.22 (m, 2H), 7.48 (dd, 4h), 8.11 (d, 2H). ^{13}C NMR (100 MHz, CD_3CN): δ (ppm) 28.2, 108.4, 118.4, 119.8, 122.0, 125.4, 140.7

Methyl 5-(2-bromoacetyl)-2-hydroxybenzoate (3.42) The same procedure as used for **3.27** was followed to obtain the desired compound methyl 5-(2-bromoacetyl)-2-hydroxybenzoate in 97% yield. mp, 82-85 $^{\circ}C$. IR (KBr): 3070, 2952, 1710, 1676, 1589, 1490, 1444, 1392, 1305, 1257,

1218, 1186, 1093, 1027, 962, 835, 794, 669, 594, 435 cm^{-1} . ^1H NMR (400 MHz CDCl_3): δ 4.01 (s, 3H), 4.40 (s, 2H), 7.08 (dd, 2H) 8.12 (dd, 2H), 8.53 (d, 1H). ^{13}C NMR (100 MHz, CDCl_3): δ (ppm) 29.8, 52.8, 112.4, 118.5, 125.6, 130.8, 136.9, 165.8, 169.9, 189.3.

Methyl 5-(2-(2-(9H-carbazol-9-yl)acetoxy)acetyl)-2-hydroxybenzoate, (3-carbomethoxy pH P carbazole-9-acetic acid, 3.43) The general procedure as used for **3.28** was followed to obtain the desired compound methyl 5-(2-(2-(9H-carbazol-9-yl)acetoxy)acetyl)-2-hydroxy benzoate in 65% yield. mp, 154-155 $^{\circ}\text{C}$. IR (KBr): 3440, 2958, 2850, 2931, 2358, 2343, 1757, 1706, 1677, 1589, 1458, 1452, 1232, 1182, 800, 752, 721 cm^{-1} . ^1H NMR (400 MHz CDCl_3): δ 3.96 (s, 3H), 5.21 (s, 2H), 5.33 (s, 2H), 7.01 (d, 2H), 7.22 (t, 2H), 7.42 (d, 2H), 7.48 (t, 2H), 7.96 (dd, 2H) 8.10 (d, 2H), 8.35 (s, 1H). ^{13}C NMR (100 MHz, CDCl_3): δ (ppm) 44.5, 52.8, 66.5, 108.4, 112.3, 118.5, 119.8, 120.4, 123.2, 126.0, 130.9, 134.9, 140.5, 165.9, 168.2, 169.7, 189.2. HRMS calculated for $\text{C}_{24}\text{H}_{19}\text{NO}_6 + \text{Na} = 440.1110$; observed = 440.1129. UV (16% pH 7.5 buffer/MeOH) $\lambda_{\text{max}} = 336$ ($\epsilon = 2900$), $\lambda_{\text{max}} = 309$ ($\epsilon = 38008$), $\lambda_{\text{max}} = 290$ ($\epsilon = 13200$), $\lambda_{\text{max}} = 279$ ($\epsilon = 12400$), $\lambda_{\text{max}} = 258$ ($\epsilon = 15300$)

4-(2-(4-Hydroxy-3-(methoxycarbonyl)phenyl)-2-oxoethoxy)-4-oxobutan-1-aminium (3-carbomethoxy pH P GABA, 3.44). Methyl 5-(2-bromoacetyl)-2-hydroxybenzoate (**3.42**) (100 mg, 0.36 mmol), 4-(*tert*-butoxycarbonylamino)butanoic acid (^tBoc GABA, 89 mg, 0.44 mmol), and K_2CO_3 (126 mg, 0.9 mmol) in CH_3CN (10 ml) were stirred at room temperature for 24 h. The solvent was evaporated, the resulting residue dissolved in water, and the water layer extracted with ethyl acetate three times. The compound was further purified by column chromatography. The resulting 3-carbomethoxy pH P ^tBoc GABA was further, reacted with 10 ml of 50% TFA/ CH_2Cl_2 for 15 min at room temperature. Solvent was removed *in vacuo* and ethyl acetate (10 ml) and water (10 ml) were added to the residue and the water layer extracted, frozen and

lyophilized to remove water to yield 4-(2-(4-hydroxy-3-(methoxycarbonyl)phenyl)-2-oxoethoxy)-4-oxobutan-1-aminium (**3.44**) in 80% yield as an oil. IR : 3359, 2987, 2968, 2360, 2343, 1741, 1685, 1606, 1523, 1170, 1093, 1218, 792, 756 cm^{-1} . ^1H NMR (400 MHz $\text{CO}(\text{CD})_3$): δ (ppm) 2.17 (t, 2H), 2.67 (m, 2H), 3.91 (t, 2H), 4.05 (s, 3H), 5.47 (s, 2H), 7.10 (d, 1H), 8.15 (d, 1H), 8.50 (s, 1H). ^{13}C NMR (100 MHz, $\text{CO}(\text{CD})_3$): δ (ppm) 29.3, 39.5, 47.0, 53.3, 66.9, 113.4, 118.8, 127.0, 131.6, 135.9, 166.0, 170.6, 172.7, 191.2. The HRMS was calculated for $\text{C}_{14}\text{H}_{18}\text{NO}_6 = 296.1134$, observed = 296.1162. UV (16% pH 7.5 buffer/MeOH) $\lambda_{\text{max}} = 270$ ($\epsilon = 1800$), $\lambda_{\text{max}} = 309$ ($\epsilon = 500$).

5-(5-Acetyl-2-(benzyloxy)benzamido)-3'-hydroxy-3-oxo-3H-spiro[isobenzofuran-1,9'-xanthene]-6'-yl pivalate (3.45). A solution **3.26** (100 mg, 0.13 mmol) in 90% TFA in CH_2Cl_2 was stirred at room temperature for 3 h. The resulting mixture was concentrated and purified by column chromatography (5% MeOH /EtOAc) to yield 5-(5-acetyl-2-(benzyloxy)benzamido)-3'-hydroxy-3-oxo-3H-spiro[isobenzofuran-1,9'-xanthene]-6'-yl pivalate in 50% yield. mp, 173-175 $^\circ\text{C}$. IR (KBr): 3433, 2974, 1762, 1751, 1650, 1610, 1425, 1257, 1114, 993, 815, 763 cm^{-1} . ^1H NMR (400 MHz $\text{CO}(\text{CD})_3$): δ 1.29 (s, 9H), 2.62 (s, 3H), 5.51 (s, 2H), 5.33 (s, 2H), 6.68 (m, 4H), 6.93 (m, 2H), 7.00 (m, 2H), 7.48 (m, 5H), 7.71 (d, 2H), 8.54 (d, 1H), 8.72 (s, 1H). ^{13}C NMR (100 MHz, $\text{CO}(\text{CD})_3$): δ (ppm) 25.6, 26.3, 38.7, 71.7, 81.7, 102.4, 110.1, 110.3, 112.7, 113.3, 114.3, 116.3, 117.7, 117.9, 118.1, 118.2, 122.2, 124.4, 126.3, 126.4, 127.5, 128.7, 128.9, 129.0, 129.3, 130.8, 132.1, 133.4, 135.6, 140.4, 147.8, 151.7, 152.2, 152.7, 159.4, 162.8, 168.2, 175.9, 195.2. HRMS calculated for $\text{C}_{41}\text{H}_{34}\text{NO}_9 + \text{H} = 684.2233$ observed = 684.2224.

Photolysis studies

¹H NMR experiments: A sample of 10 mg of the relevant compound (**3.35**, **3.32**, or **3.43**) was dissolved in 1.5 ml of 20% D₂O/CD₃CN and photolyzed in a Pyrex NMR tube using a Rayonet photoreactor equipped with two 3000 Å bulbs and a merry-go-round apparatus. The reaction was followed using ¹H NMR every 10 min until the reaction was complete.

Quantum yield studies In a general experiment, about 10.00 mg of pHP derivative and 5.00 mg of caffeine (internal standard) was dissolved in 5 ml of 20% pH 7.5 Tris buffer/ MeOH and photolyzed in a quartz tube using 16 3000 Å lamps in a Rayonet RPR-100 photoreactor fitted with a Merry-go-round apparatus. Aliquots of 100 µl were removed every 60 seconds, diluted to 1.5 ml with the same solvent system, and the solution analyzed using UPLC. The quantum yield data are given in Table 3-4 in the Results section.

Combined photorelease and fluorescence studies of 3-[5aminoFL(OPv)₁] pHP Carbazole-9-acetic acid (3.35**).** Sample preparation and photolysis conditions were the same as those described under quantum yield studies. During photolysis at 10 min intervals fluorescence spectra were recorded and photolysis progress monitored via UPLC. Samples by fluorescence and by UPLC, Samples were taken by removal of 200 µl of reaction mixture at a given time and diluting to 5 ml in volumetric flasks with the same solvent. Fluorescence of **3.45** at the same concentration in the same solvent system was used as the standard.

Combined photorelease and fluorescence studies of 3-[9-(2-hydroxyethyl)carbazole] pHP 5-carboxyFL (3.39**)** Experiments were conducted according to the same procedure described for **3.35**. UPLC samples were prepared by removing 100 µl of sample and diluting up to 5.00 ml with same solvent. Fluorescence samples were prepared by diluting 600 µl of UPLC samples up to 10.00 ml with same solvent system. Fluorescence of 5-carboxyfluorescein under identical conditions were used as the standard.

References

- ¹ Givens, R. S.; Yousef, A. L. In *Dynamic Studies in Biology* Goeldner, M.; Givens, R. S. Eds.; Wiley-Vch, Weinheim, 2005; 55-75.
- ² Givens, R. S.; Jung, A.; Park, C.-H.; Weber, J.; Bartlett, W. *J. Am. Chem. Soc.* **1997**, *119*, 8369-8370.
- ³ Katz, L. C.; Dalva, M. B. *J. Neurosci. Methods* **1994**, *54*, 205-218.
- ⁴ Dalva, M. B.; Katz, L. C. *Science* **1994**, *265*, 255-258.
- ⁵ (a) Pirrung, M. C.; Shuey, S. W. *J. Org. Chem.* **1994**, *59*, 3890-3897. (b) Niu, L.; Wieboldt, R.; Ramesh, D.; Carpenter, B. K.; Hess, G. P. *Biochemistry* **1996**, *35*, 8136-8142.
- ⁶ Kandler, K.; Katz, I. C.; Kauer, J. A. *Nat. Neurosci.* **1998**, *1*, 119-123.
- ⁷ Givens, R. S.; Weber, J. F. W.; Conrad, P. G.; Orosz, G.; Donahue, S. L.; Thayer, S. A. *J. Am. Chem. Soc.* **2000**, *122*, 2687-2697.
- ⁸ Sul, J.-Y.; Orosz, G.; Givens, R. S.; Haydon, P. G. *Neuron Glia Biology* **2004**, *1*, 3-11.
- ⁹ Specht, A.; Loudwig, S.; Peng, L.; Goeldner, M. *Tetrahedron Lett.* **2002**, *43*, 8947-8950.
- ¹⁰ (a) Givens, R. S.; Park, C. H. *Tetrahedron Lett.* **1996**, *35*, 6259-6266. (b) Park, C.H.; Givens, R. S. *J. Am. Chem. Soc.* **1997**, *119*, 2453-2463.
- ¹¹ Geibel, S.; Barth, A.; Amslinger, S.; Jung, A. H.; Burzic, C.; Clarke, R. J.; Givens R. S.; Fendler, K. *Biophys. J.* **2000**, *79*, 1346-1357.
- ¹² Du, X.; Frei, H.; Kim, S.-H.; *J. Biol. Chem.* **2000**, *275*, 8492-8500.
- ¹³ Arabaci, G.; Guo, X.; Beebe, K. D.; Coggeshall, K. M.; Pet, D. *J. Am. Chem. Soc.* **1999**, *121*, 5085-5086.
- ¹⁴ Hunter, T. *Cell* **1995**, *80*, 225-236.
- ¹⁵ Zou, K.; Cheley, S.; Givens, R. S.; Bayley, H. *J. Am. Chem. Soc.* **2002**, *124*, 8820-8229.
- ¹⁶ (a) Salmon, E. D.; Leslie, R. J.; Saxton, W. M.; Karow, J. R. *J. Cell Biol.* **1984**, *99*, 2165-2174. (b) Gorbsky, G. J.; Borisy, G. G. *J. Cell Biol.* **1989**, *109*, 653-662.
- ¹⁷ Mitchison, T. J.; Sawin, K. E.; Theriot, J. A.; Gee, K.; Mallavarapu, A. Caged Fluorescent Probes. In *Methods of Enzymology*; Marriott, G. Eds.; Academic Press: New York, 1998; 291, pp 63-77.
- ¹⁸ Mitchison, T. J. *J. Cell Biol.* **1989**, *109*, 637-652.
- ¹⁹ Mitchison, T. J.; Sawin, K. S.; Theriot, J. A. In *Handbook of Cell Biology*; Celis, J. E., Eds.; Academic Press: New York, 1994; 2, pp 65-76.
- ²⁰ Baeyer, A. *ber. Dtsch. Chem. Ges.* **1871**, *4*, 555-558.
- ²¹ Haugland, R. P. *Handbook of Fluorescent Probes and Research Products*; Molecular Probes: Eugene, Origen, 2002.
- ²² Weber, G.; Teale, F. W. *J. Trans. Frady Soc.* **1958**, *54*, 640-648.
- ²³ Paekar, C. A.; Rees, W. T. *Analyst* **1960**, *58*, 581-600.
- ²⁴ (a) Weigele, M.; DeBernardo, S.; Leimgruber, W. *Biochem. Biophys. Res. Commun.* **1973**, *50*, 352-360. (b) Geisow, M. *J. Exp. Cell. Res.* **1984**, *150*, 29-35. (c) Carvell, M.; Robb, I. D.; Small, P. W. *Polymer* **1998**, *39*, 39-42.
- ²⁵ (a) Stein, S.; Böhlen, P.; Udenfriend, S. *Arch. Biochem. Biophys.* **1974**, *163*, 400-404. (b) Bridges, M. A.; McErlane, K. M.; Kwong, E.; Katz, S.; Applegarth, D. A. *Clin. Chim. Acta* **1986**, *157*, 73-85.
- ²⁶ Theriot, J. A.; Mitchison, T. J. *Nature*, **1991**, *352*, 126-132.
- ²⁷ Zhao, Y.; Zheng, Q.; Dakin, K.; Xu, K.; Martinez, M. L.; Li, W. *J. Am. Chem. Soc.* **2004**, *126*, 4653-4663.
- ²⁸ Ottl, J.; Gabriel, D.; Marriott, G. *Bioconjugate chem.* **1998**, *9*, 143-151.
- ²⁹ Kraft, G. A.; Sutton, R.; Cummings, T. R. *J. Am. Chem. Soc.* **1988**, *110*, 301-303.
- ³⁰ (a) Patchornik, A.; Amit, B.; Woodward, R. B. *J. Am. Chem. Soc.* **1970**, *92*, 6333-6335. (b) Amit, B.; Zehari, U.; Patchornik, A. *Isr. J. Chem.* **1974**, *12*, 103-113. (c) Pillai, W. N. R. *Synthesis* **1980**, 1-26. (d) Amit, B.; Zehari, U.; Patchornik, A. *J. Org. Chem.* **1974**, *39*, 192-196.
- ³¹ Zlokarnik, G.; Negulescu, P. A.; Knapp, T. E.; Mere, L.; Bures, N.; Feng, L.; Whitney, M.; Roemer, K.; Tsien, R. Y. *Science* **1998**, *279*, 84-88.
- ³² Furuta, T. In *Dynamic Studies in Biology* Goeldner, M.; Givens, R. S. Eds.; Wiley-Vch, Weinheim, 2005; pp 29-55.
- ³³ Fedoryak, O. D.; Dore, T. M. *Org. Lett.* **2002**, *4*, 3419-3422.
- ³⁴ Dore, T. M. In *Dynamic Studies in Biology* Givens, R. S., Goeldner, M., Eds.; Wiley-VCH, Weinheim, 2005; pp 435-457.

-
- ³⁵ Brown, E. B.; Shear, J. B.; Adams, S. R.; Ysien, R. Y.; Webb, W. W. *Biophys. J.* **1999**, *76*, 489-499.
- ³⁶ Guo, Y.; Chen, S.; Shety, P.; Zheng, G.; Lin, R.; Li, W. *Nature Methods* **2008**, *8*, 835-841.
- ³⁷ Brenner, S. *Genetics* **1974**, *77*, 71-94.
- ³⁸ Kosbayashi, T.; Urano, Y.; Kamiya, M.; Ueno, T.; Kojima, H.; Nagano, T. *J. Am. Chem. Soc.* **2007**, *129*, 6696-6697.
- ³⁹ de Silva, A. P.; Gunaratne, H. Q. N.; Gunnlaugsson, T.; Huxley, A. J. M.; McCoy, C. P.; Rademacher, J. T.; Rice, T. E. *Chem. Rev.* **1997**, *97*, 1515-1556.
- ⁴⁰ Kollmannsberger, M.; Rurack, K.; Resch-Genger, U.; Daub, J. *J. Phys. Chem. A* **1998**, *102*, 10211-10220.
- ⁴¹ Urano, Y.; Kamiya, M.; Kanda, K.; Ueno, T.; Hirose, K.; Nagano, T. *J. Am. Chem. Soc.* **2005**, *127*, 4888-4894.
- ⁴² Miura, T.; Urano, Y.; Tanaka, K.; Nagano, T.; Ohkubo, K.; Fukuzumi, S. *J. Am. Chem. Soc.* **2003**, *125*, 8666-8671.
- ⁴³ Tyagi, S.; Kramer, R. *Nature Biotechnol.* **1996**, *14*, 303-309.
- ⁴⁴ Cardullo, R. A.; Agrawal, S.; Flores, C.; Zamecnik, P. C.; Wolf, D. E. *Proc. Natl. Acad. Sci.* **1988**, *85*, 8790-8794.
- ⁴⁵ Kent, T.; Iezzi, R. Lignon Eye Institute, Wayne State University, Unpublished data, 2008.
- ⁴⁶ Kim, T. W.; Yoon, H. Y.; Park, J.; Kwon, O.; Jang, D.; Hong, J. *Org. Lett.* **2005**, *7*, 111-114.
- ⁴⁷ Wuts, P. G.; Green, T. W. *Greene's Protective Groups in Organic Synthesis*, 4, Wiley-Interscience, New Jersey, 2006; pp 250-253.
- ⁴⁸ SYBYL 8.0, The Tripos Associates, St. Louis, MO, 2008.
- ⁴⁹ Clark, M.; Cramer, R. D. III; Van Opdenbosch, N.; *J. Comput. Chem.* **1989**, *10*, 982-1012.
- ⁵⁰ Gasteiger, J.; Marsili, M. *Tetrahedron* **1980**, *36*, 3219-3228.
- ⁵¹ Johansson, M. K.; Cook, R. M. *Chem. Eur. J.* **2003**, *9*, 3466-3471.
- ⁵² Lakowicz, J. *Principles of Fluorescence Spectroscopy*, 2nd ed., Plenum, New York, 1999.
- ⁵³ Förster, T. *Ann. Phys.* **1948**, *2*, 55.
- ⁵⁴ Dexter, D. L. *J. Phys. Chem.* **1953**, *21*, 836.
- ⁵⁵ Marti, A.; Lockusch, S.; Stevens, N.; Ju, J.; Turro, N. J. *Acc. Chem. Res.* **2007**, *40*, 402-409.
- ⁵⁶ Hudgins, R. R.; Huand, F.; Gramlich, G.; Nau, W. M. *J. Am. Chem. Soc.* **2002**, *124*, 556.
- ⁵⁷ Stensrud, K. F. Ph D Dissertation 2008, Chemistry Department, University of Kansas
- ⁵⁸ Knoll, K. Photoisomerization of Azobenzenes in *CRC Handbook of Organic Photochemistry and Photobiology*; Horspool, W. M., Song, P. S., Eds.; CRC Press, Boca Ran, FL, 2004; pp 1-89
- ⁵⁹ (a)Klan, P.; Wirz, J. Chemistry of Excited Molecules in *Photochemistry of Organic Compounds*, Wiley: West Sussex, 2009; pp 227-452. (b)Decosta, D. P.; Pincock, J. A. *J. Am. Chem. Soc.* **1993**, *115*, 2180-2190.
- ⁶⁰ Wan, P.; Budac, D. Photodecarboxylation of Acids and Lactones in *CRC Handbook of Organic Photochemistry and Photobiology*; Horspool, W. M., Song, P. S., Eds.; CRC Press, Boca Ran, FL, 1995; pp 384-392.
- ⁶¹ Hawker, C. J.; Lee, R.; Freché, J. M. *J. Am. Chem. Soc.* **1991**, *113*, 4583-4588.
- ⁶² Tiny, S.; Hsei, I.; Chen, C. P. *Bioorg. Med. Chem.* **2006**, *14*, 6106-6119.
- ⁶³ Vaaquez-Martines, Y.; Ohri, R. V.; Kenyon, V.; Holman, T.; Sepulveda-Boza, S.; *Bioorg. Med. Chem.* **2007**, *23*, 7408-7425.
- ⁶⁴ Hiyama, T.; Fujita, M. *J. Org. Chem.* **1988**, *53*, 5405-5414.
- ⁶⁵ Oyama, Y.; Shimada, Y.; Kagawa, Y.; Yamada, Y.; Imae, I.; Komaguchi, K.; Harima, Y. *Tetrahedron Lett.* **2007**, *48*, 9167-9170.
- ⁶⁶ Huand, W.; Zhang, X.; Liu, H.; Shen, J.; Jiang, H. *Tetrahedron Lett.* **2005**, *46*, 5965-5967.
- ⁶⁷ Viktor, M.; Kada, R.; Lokaj, J. *Molbank* **2004**, M354. <http://www.mdpi.net/molbank/molbank2004/m0354.htm> (accessed Sep 25, 2009)
- ⁶⁸ Sheh, W.C.; Dells, S.; Bach, A.; Blacklock, J. T. *J. Org. Chem.* **2003**, *68*, 1954-1957.

**4.0 Applications of pHP Photochemistry as a Fluorous Separation Technique,
A Method of Separation for Product Isolation; a Proof-of-Concept Investigation**

Introduction

The *p*-Hydroxyphenacyl photoremovable protecting (pHP) group, although introduced only a decade ago, has shown great potential in biological studies. The appearance of the pHP group in several reviews is a testimony to the versatility of the chromophore.^{1,2,3} Several applications in biological studies⁴ were discussed in *Chapter 2, Section 3*. Here the combination of the pHP group photorelease capabilities with fluororous separation techniques provides yet another novel application of photochemistry crossing disciplinary boundaries.

Fluororous Chemistry

Fluororous chemistry is a relatively new technology. The first report of fluororous chemistry appeared in 1991 by Vogt and Kiem.⁵ The study used perfluorinated polyethers to immobilize catalysts. This was followed by Zhu's⁶ report of perfluorinated polyethers for azeotropic separations. However, these reports did not attract very much attention, until the first significant report of fluororous chemistry by Horvath and Rabai⁷ in 1994. The authors reported rhodium-catalyzed hydroformylation in organic and perfluorinated solvents which they termed "fluororous biphasic catalysis". In general, fluororous chemistry encompasses "the study of the structure, composition, properties, and reactions of highly fluorinated molecules, molecular fragments, materials and media".⁸

Recent interests in fluororous chemistry can be separated in to two categories, fluororous solvents and fluororous compounds. Fluororous solvents are generally highly fluorinated alkanes, ethers, or tertiary amines. These are colorless, high density, inert, and nonpolar liquids.⁸ Fluororous solvents are both hydrophobic and lipophobic due to their weak intermolecular forces⁹ and form

bilayers with organic and aqueous solvents at room temperature that become miscible at higher temperatures (~ 50 °C and above).¹⁰ A list of common fluorinated solvents is shown in table 4-1.¹⁰

Table 4-1. Some Representative Fluorinated Solvents¹⁰

Solvent	Formula	BP/ °C	MP/ °C	Common Name
Perfluorohexane	C ₆ F ₁₄	57.1	-87.1	FC-72
Perfluoro(methylcyclohexane)	C ₆ F ₁₁ CF ₃	76.1	-44.7	PFMC, PFMCH
Perfluorodecalin	C ₁₀ F ₁₈	142	-10	-
Perfluorotributylamine	C ₁₂ F ₂₇ N	178	-50	FC-43
Perfluoropolyether	CF ₃ [(OCF(CF ₃)CF ₂) _n - (OCF ₂) _m]OCF ₃	70	<-110	Galden HT70

Fluorinated molecules may contain a long perfluorinated alkyl chain that is referred to as a “fluorinated tag” or “fluorinated ponytail”.¹¹ A reactant, reagent or catalyst can be made fluorinated-like by simply appending a fluorinated tag. Therefore, a fluorinated molecule may have two domains, the fluorinated domain that controls the solubility of the molecule in fluorinated solvents and the organic domain that controls the reactivity of the molecule.⁹ Fluorinated compounds are categorized as “heavy fluorinated” and “light fluorinated” depending on the percentage of fluorine present. Compounds containing more than 60% fluorine by molecular weight are known as “heavy fluorinated” whereas compounds with less than 40% are referred to as “light fluorinated”.¹² The fluorinated tags generally have the formula, CF₃(CF₂)_{m-1}(CH₂)_n which is abbreviated as R_{fm}(CH₂)_n.

Applications of fluorinated chemistry can be broadly categorized into two sections, fluorinated separation techniques and fluorinated synthetic techniques

Fluorinated Separation Techniques

Fluorinated compounds show very high affinity toward fluorinated solvents, abiding the ‘like-dissolves-like’ concept,¹³ while organic molecules show very low affinities for fluorinated solvents when compared with organic solvents. Fluorinated separation techniques are developed based on

this selective solubility of fluorous compounds in fluorous solvents and are attractive since these provide a means of easy separation of fluorous compounds from other nonfluorous materials. Fluorous separation techniques can be classified according to three types : fluorous liquid-liquid extraction (F-LLE), fluorous solid-liquid extraction (F-SPE) and fluorous chromatography.

Fluorous liquid-liquid extraction is very similar to traditional liquid-liquid extraction, but one phase is replaced with a fluorous solvent and is referred to as the fluorous phase in analogy to organic/aqueous phase.⁹ As fluorous solvents are immiscible with both organic and aqueous solvents, three phase extractions are also possible. A diagram of a three phase F-LLE is shown in Figure 4-1. F-LLE was first introduced in Horvath and Rabai's much-cited publication⁷ and has been used quite extensively since, especially in the catalysis arena.

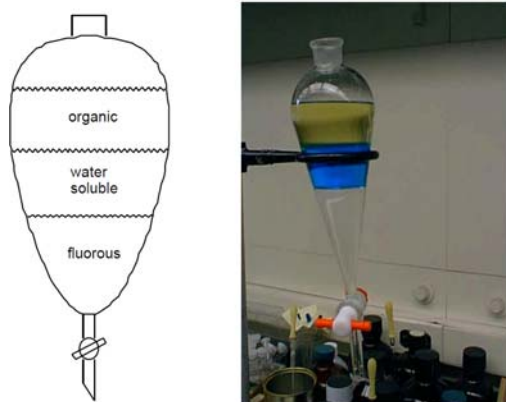


Figure 4-1. Illustration of a three phase liquid-liquid extraction. Reproduced with permission from Fluorous Inc.¹⁴

In general, F-LLE is used to separate desired organic compounds from fluorous reagents or catalysts and the separated product, in many cases, is pure enough to be taken to the next step in a synthesis. The fluorous reagent can also be recycled, if needed.¹⁴ F-LLE is most successful

for heavy fluorinated compounds and when, at its best, only one extraction is sufficient for clean product isolation. When multiple washings are necessary, loss of the desired organic product is comparatively minor due to low solubility of organic compounds in fluorinated solvents.

Fine tuning of the fluorinated solvent to overcome drawbacks of F-LLE with light fluorinated compounds has been exploited by several groups. To extract ureas into fluorocarbons, Castedo, *et al.* used perfluorocarboxylic acids as additives.¹⁵ The use of the nonvolatile amphiphilic compound, F-262 (2-perfluoro-ethyl-1,3-dimethylbutyl ether), to immobilize palladium catalyst was reported by Ryu and coworkers.¹⁶ Nagashima, *et al.*¹⁷ introduced a perfluorobutyl methyl ether (HFE-7100) as a fluorinated solvent which has a greater affinity for light fluorinated compounds. HFE-7100 is miscible with most organic solvents at room temperature but becomes immiscible with the addition >5% of water. The partition coefficients (p) for perfluorotriphenyl phosphine [$R_{6F}(CH_2)_2$] and simple triphenylphosphine were calculated in FC-72/organic and FC-72/5% H₂O in organic and HFE-7100/5% H₂O in organic solvent systems. A few selected data are shown in Table 4-2. Partition coefficients for perfluorotriphenylphosphine changed from 0.12 to 15.11 to 100 when the solvent systems used are FC-72/DMF and FC-72/5% H₂O in DMF and HFE-7100/5% H₂O in DMF, respectively. To overcome drawbacks of F-LLE with light fluorinated compounds, Crich, *et al.*¹⁸ also introduced a cooled, continuous extraction procedure.

Table 4-2. Partition Coefficients (p) for Triphenylphosphine and Perfluorotriphenylphosphine in Various Fluorinated/Organic Solvent Systems¹²

Solvent system	Compound	p
FC-72/DMF	perfluoroPPh ₃	0.12
FC-72/5% H ₂ O-DMF	PPh ₃	<0.02
FC-72/DMF	perfluoroPPh ₃	15.11
FC-72/5% H ₂ O-DMF	PPh ₃	<0.02
HFE-7100/5% H ₂ O-DMF	perfluoroPPh ₃	>100
HFE-7100/5% H ₂ O-DMF	PPh ₃	0.12

Increasing the fluorine content though desired for F-LLE can be problematic, since heavy fluorinated compounds tend to be less soluble in both fluorinated and organic solvents. This can be avoided by opting to use fluorinated solid-liquid extraction (F-SPE) which is more attuned to light fluorinated compounds. Thus the most popular fluorinated separation method used is F-SPE employing fluoro flash cartridges.¹⁹ The cartridges are filled with fluorinated reverse phase silica gel (silica bonded with $-\text{CH}_2\text{CH}_2\text{C}_8\text{F}_7$).¹⁴ In a general separation, the mixture of compounds comprised of both fluorinated and organic compounds is loaded on the cartridge and first eluted with a “fluorophobic” solvent, commonly 20% water/methanol, to obtain the organic portion. Then the cartridge is washed with a “fluorophilic” solvent (methanol) to obtain the fluorinated compounds. A schematic diagram of F-SPE is illustrated in Figure 4-2. F-SPE is essentially a filtration technique and can be automated quite readily.²⁰ The lack of the need for expensive fluorinated solvents is also attractive. The cartridges can be washed and reused multiple times.

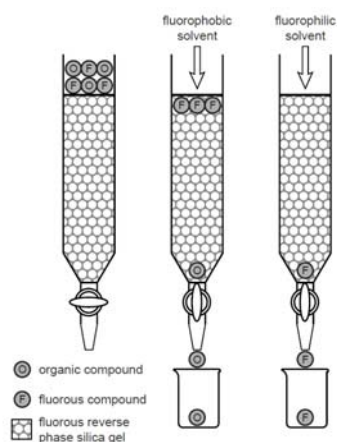


Figure 4-2. Solid phase extraction over fluorinated reverse phase silica gel. Reproduced with permission from Journal of Chemical Education.⁹

Fluorous chromatography is very similar to customary column or thin layer chromatography. An array of products including loose fluorous silica gel, fluorous TLC plates and fluorous HPLC columns are commercially available.¹⁴ Fluorous chromatography can be used to separate fluorous compounds based on their fluorous content. The first two methods described, F-LLE and F-SPE, are only used to separate fluorous material from nonfluorous material and do not differentiate among mixtures of several different fluorous compounds. General chromatographic methods can be used to separate fluorous compounds but fluorous chromatography is much more effective.¹⁴ Similar to F-SPE, fluorous chromatography does not require the use of fluorous solvents. An HPLC trace obtained from a separation of amines with different fluorine content is illustrated in Figure 4-3. The parent compounds, without any fluorous tag are essentially eluted with the solvent front, while a higher percentage of fluorophilic solvent is required in order to elute the highly fluorinated derivatives.

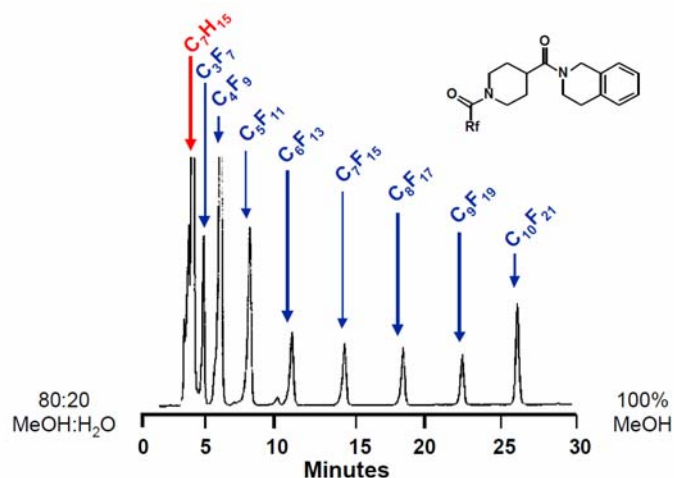


Figure 4-3. An HPLC trace illustrating a separation based on the fluorine content. Reproduced with permission from Fluorous Inc.¹⁴

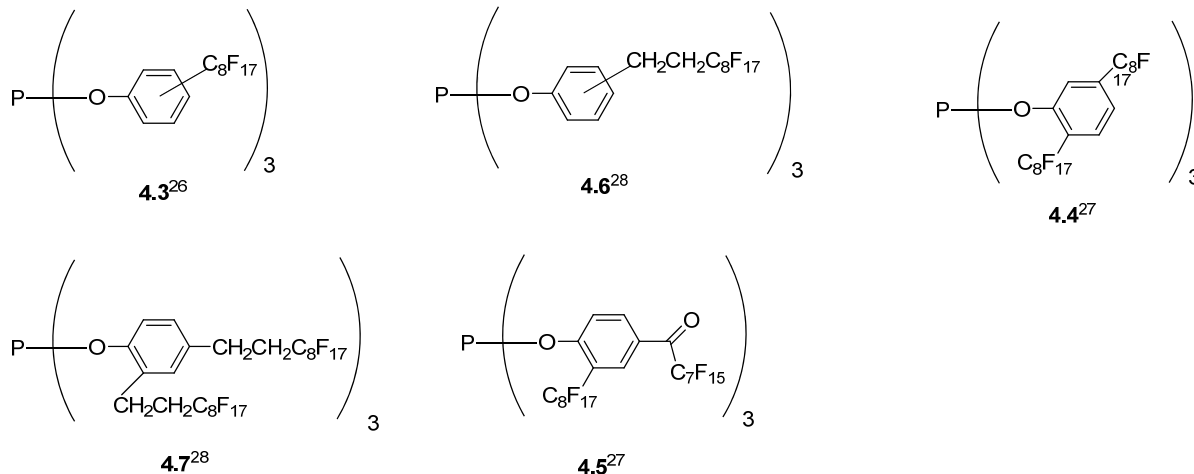
Fluorous Synthesis Techniques

Fluorous synthesis can be adapted to organic synthesis by simply substituting fluorous reagents for a typical organic reagent of the same overall structure. Catalysts, reactants, reagents and protecting groups have been made fluorous by attaching fluorous tags. Due to the chemical inertness of the fluorous tags, fluorous compounds can be exposed to almost any organic reaction conditions without any complications or damage to the fluorous tag.^{7,12} The electronic properties of the active site of the compound can be fine-tuned based on the number of CH₂ groups in the fluorous tag (R_{fm}(CH₂)_n). When *n* is large the organic domain of the compound can be insulated from the electron withdrawing effects of the fluorines. The presence of a short methylene chain or the absence of methylene groups altogether tend to increase the Lewis acidity of the reaction center.²¹

Compared to solid phase syntheses, fluorous syntheses have several advantages. The ability to conduct reactions under homogenous conditions, using either high temperature where fluorous and organic solvents become miscible or taking advantage of the solubility of many fluorous compounds in organic solvents.^{7,12} Rapid characterization of intermediates using traditional methods like NMR and MS, easy separation using either F-SPE or F-LLE, straight forward adaptations of literature procedures of traditional synthesis, and the capability to scale up reactions are several other advantages of fluorous compounds in synthesis.⁷

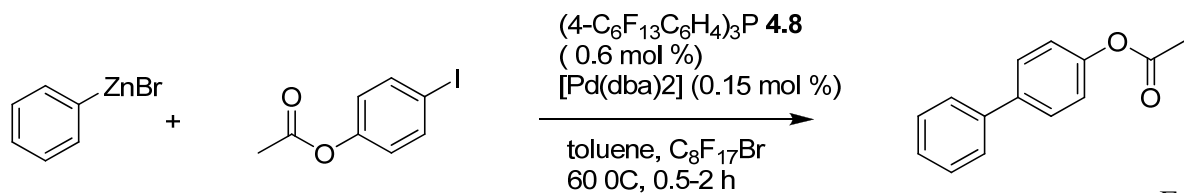
Fluorous catalysis has been one of the most pursued areas of fluorous chemistry and is essentially a combined phase separation and catalyst immobilization technique.²² The reactions are generally performed in biphasic media (fluorous/organic) and are termed fluorous biphasic catalysis (FBC)¹⁴ or a fluorous biphasic system (FBS).²² The reactions are performed at a higher

Scheme 4.1



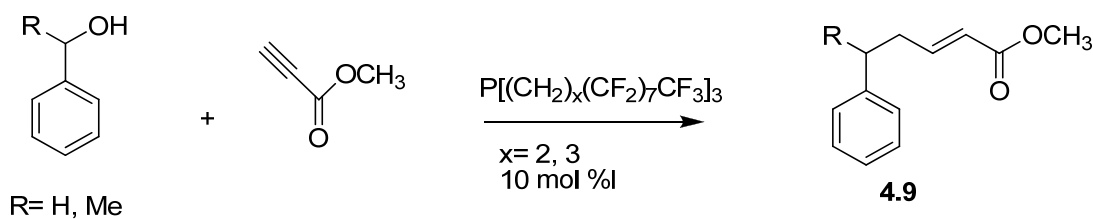
Fluorous rhodium catalysts have been explored for hydrogenation reactions as well. A fluorous analog of Wilkinson's catalyst ($\text{CIRh}(\text{P}(\text{R}_f)_3)_3$ where $\text{R}_f = \text{CH}_2\text{CH}_2\text{C}_6\text{F}_{13}$ was developed by Horvath *et al.*²⁹ and successfully used for the hydrogenation of a series of alkenes.

The use of fluorous tagged palladium catalysts has been demonstrated for well-known C-C coupling reactions like the Negishi reaction,³⁰ Heck reaction,³¹ Stille coupling,³² Suzuki coupling³³ and Sonogashira coupling.³⁴ As an example, a perfluoro derivative employed in the Negishi reaction is shown in equation 4.2. Betzemeier and Knochel³⁰ reported that the use of a Pd complex with perfluorinated phosphine ligands (**4.8**) in the Negishi reaction gave good yields of 87-99%. The catalyst could be reused four times without significant loss of efficiency with yields of 93, 91, 90, and 86% for consecutive runs when used in 1.5 mol % levels.



Eq. 4.2

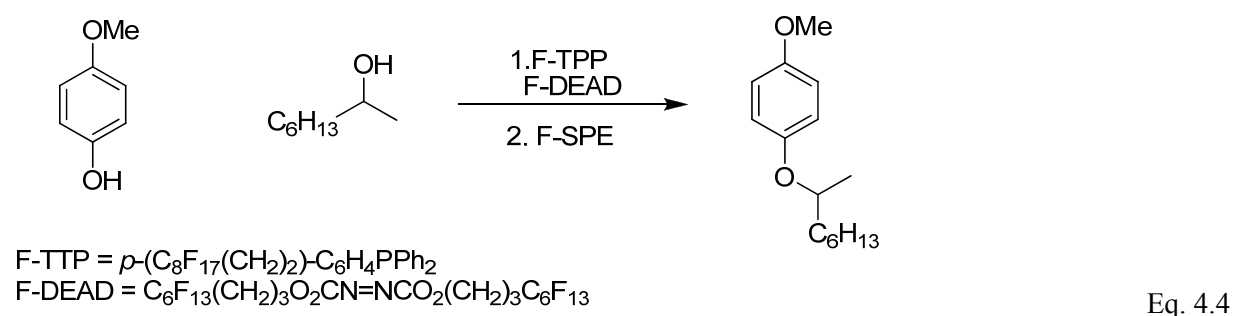
A major drawback related to FBC is the need to use fluoruous solvents. Fluoruous solvents are expensive and their environmental effects have been questioned.⁹ Recently, the thermomophic nature (temperature-dependent solubility)^{12,35,36} of fluoruous catalysts have been utilized to overcome this problem. Use of fluoruous catalysts that are soluble in organic solvents at higher temperatures limits the use of fluoruous solvents to only the separation process. The phosphine catalyzed addition of alcohols to propiolates is an example of a fluoruous thermomophic reaction.³⁵ Comparable yields of the product **4.9** were obtained with the use of either a fluoruous biphasic system (perfluoro(methylcyclohexane)/octane) or only an organic solvent (*n*-octane) (Equation 4.3).



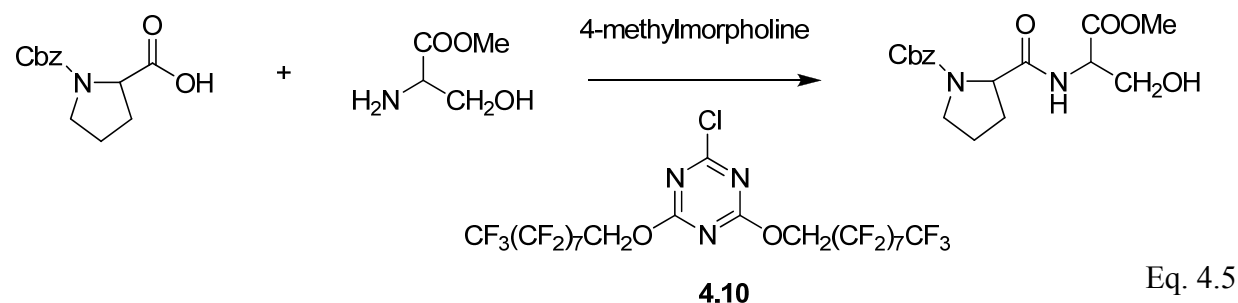
Eq. 4.3

Fluoruous reagents, reactants and protecting groups have also gained much attention. Fluoruous reagents are designed such that at the end of the reaction, only the fluoruous components, the starting reagent and its byproducts, remain in the fluoruous solvent, so that separation of the desired product becomes more readily feasible.⁹

Development of fluorous reagents has been focused in areas where use of traditional reagents becomes problematic due to separation difficulties.³⁶ Advances in developing fluorous Mitsunobu reagents³⁷ were pursued by Dandapani and Curran³⁸ to overcome the problems with isolation of the desired products from reagent derived byproducts. They synthesized the fluorous analogs of the Mitsunobu reagents, diethyl azodicarboxylate (DEAD) and triphenylphosphine, and isolated the pure product on 55% yield after a simple F-SPE separation (Equation 4.4). The reaction was run in THF at 60 °C.



Several fluorous condensation reagents have been developed for amide bond formation for the reaction of carboxylic acids with amines.^{39,40} Markowicz and Dembinski replaced the condensation reagent chlorodimethoxy-1,3,5-triazine with its perfluoro derivative **4.10** and employed it for peptide synthesis. A representative example is illustrated in equation 4.5.³⁹



In spite of their toxicity and separation issues, tin reagents are extensively used in reductive radical chemistry and cross-coupling reactions.³⁶ To overcome these drawbacks several groups have pursued the development of fluororous tin reagents. Fluororous tin hydrides,⁴¹ azides,⁴² oxides,⁴³ and allyl tin reagents^{19,44} have been created. The Stille reaction has also been carried out with fluororous tin reagents.⁴⁵ Some fluororous tin reagents, their uses and the methods of product purification are given in Table 4-3.

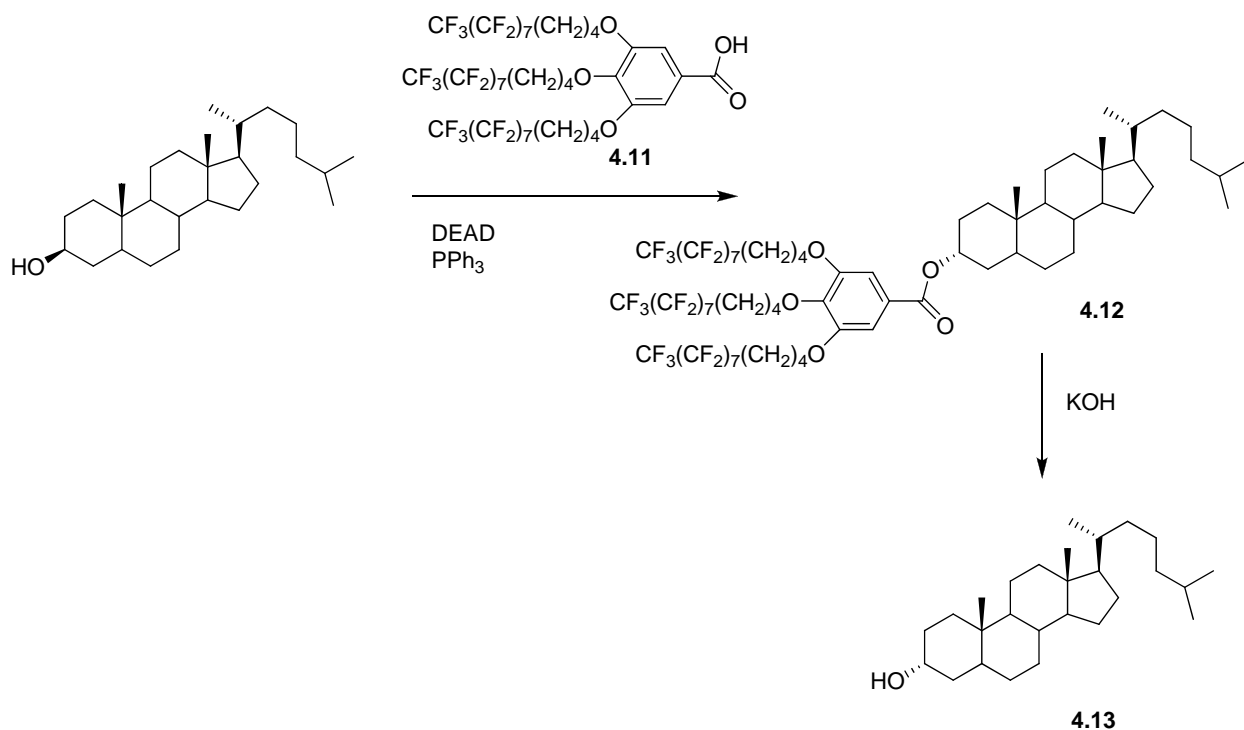
Table 4-3. Some Fluororous Tin Reagents, Their Applications, and Mode of Purification³⁶

Reagent	Applications	Purification method
$(R_fCH_2CH_2)_mSnMe_{3-m}H$	Reduction of alkyl halides, radical cyclization, Giese reaction	$R_f = C_6F_{13}, m = 3, F-LLE$ $R_f = C_{10}F_{21}, m = 1, F-SPE$
$(R_fCH_2CH_2CH_2)_3SnCH_2CH=CH_2$	Thermal allylation of aldehydes, Barber and Keck allylations	$R_f = C_6F_{13}, F-LLE$ $R_f = C_4F_9, F-SPE$
$(C_6F_{13}CH_2CH_2)_3SnN_3$	Synthesis of tetrazole	F-LLE
$(C_6F_{13}CH_2CH_2)_3SnAr$	Stille reaction	F-LLE
$[(C_6F_{13}CH_2CH_2)_2(Cl)Sn]_2O$	Trans esterification	F-LLE, F-SPE

Fluororous reactants are not very popular in synthesis as attempts to tag different reactants in a multistep synthesis and final removal of the tags from the desired product can be exhausting.⁹ If one were to use fluororous reagents in this context, one first must attach a fluororous tag to a reactant of interest to use it in a single step or multistep synthetic sequence. At the end of the reaction process, only the desired product should contain the fluororous tag so that the product can be isolated using fluororous separation techniques. Following separation, the fluororous tag must be removed to obtain the desired product. The use of a fluororous reagent was illustrated using the Mitsunobu reaction by Markowicz and Dembinski.⁴⁶ A fluororous tag is attached to the benzoic acid **4.11** and the reaction is carried out in the presence of diisopropyl azodicarboxylate (DIAD)

and triphenylphosphine in THF with no fluoruous solvent. The separation of the resulting ester **4.12** with the fluoruous tag was attempted by extraction using supercritical CO₂, by extraction with a fluoruous solvent (perfluorocyclohexane), and by recrystallization from 1:1 CHCl₃:MeOH independently. The recrystallization method gave the best results and free alcohol **4.13** was obtained in 94% yield after hydrolysis of the tagged ester. The perfluoro acid was recovered in 78% yield (Scheme 4.2).

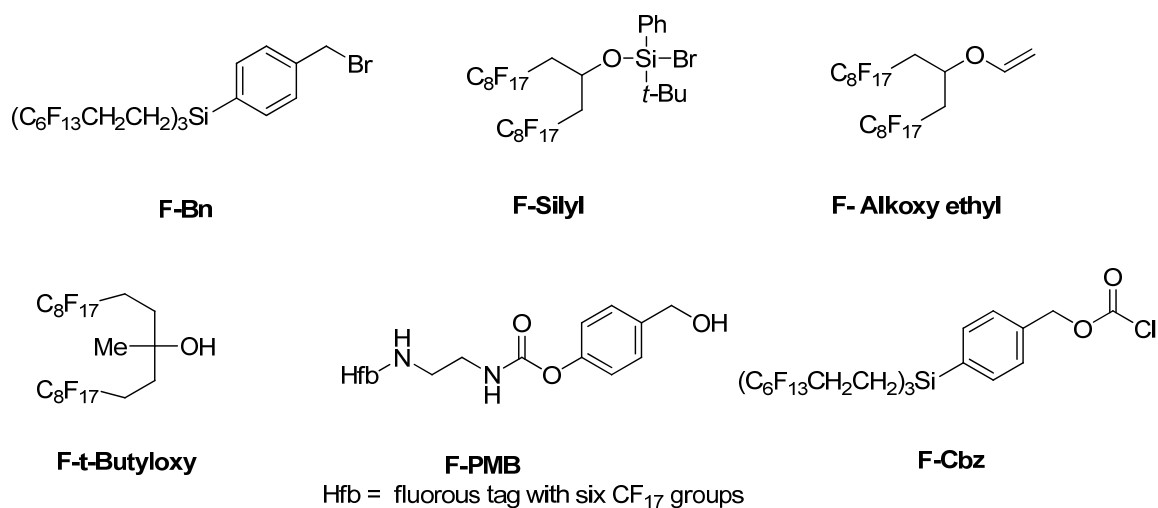
Scheme 4.2



Practitioners of fluoruous chemistry have also ventured into the arena of protecting group applications and an array of fluoruous protecting groups has been developed for various syntheses. Similar to other fluoruous applications, fluoruous protecting groups can be divided into “heavy” and “light” fluoruous protecting groups.¹² The protocols followed for attachment and removal of

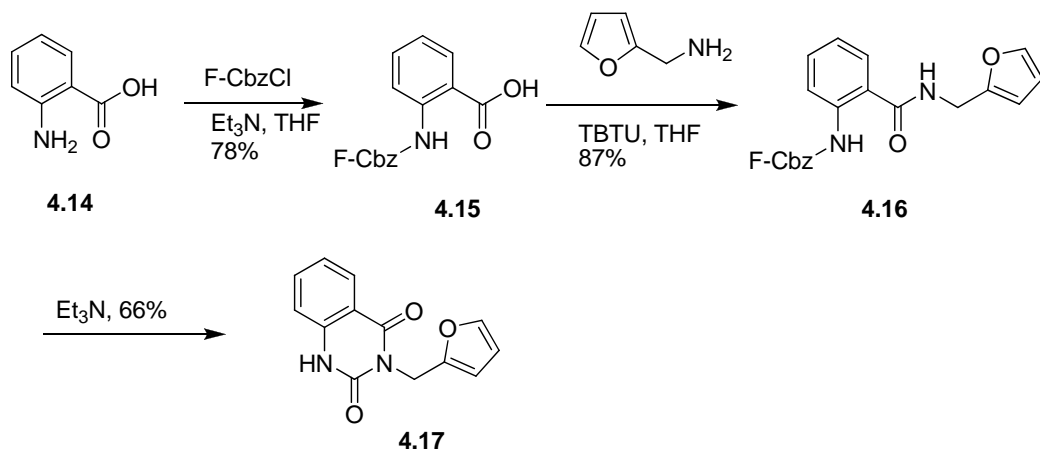
traditional protecting groups are generally applicable to fluorous protecting groups as well. Fluorous benzyl bromide,⁴⁷ fluorous alkoxyethyl chlorides,⁴⁸ fluorous vinyl ethers,⁴⁹ fluorous carbobenzyloxy chlorides (F-CbzCl),⁵⁰ fluorous *t*-butyl alcohol,⁵¹ and fluorous *p*-methoxybenzyl bromide⁵² are examples of heavy fluorous protecting groups (Scheme 4.3)

Scheme 4.3



As an example, Bannwarth and coworkers⁵⁰ developed the F-Cbz group and utilized it in the synthesis of quinazoline-2,4-diones (Scheme 4.4). F-Cbz protection of the amine group in anthranilic acid (**4.14**) was achieved with Et₃N in THF and F-Cbz amine protected acid (**4.15**) was separated by F-LLE (FC-72). Following the amidation of the carboxylic acid group of **4.15**, the resulting amide **4.16** was purified by F-LLE and the F-Cbz protecting group then removed with Et₃N to yield the quinazoline-2,4-dione (**4.17**). Purification of **4.17** was achieved by an F-LLE but now the compound was extracted into the ethyl acetate layer leaving the F-Cbz group in the fluorous layer.

Scheme 4.4



Analogous to scavengers⁵³ in solid phase synthesis, fluoros scavengers have also been constructed to remove excess reagents and/or reaction byproducts after a solution phase reaction. Heavy fluoros scavengers⁵⁴ did not find many applications due to their low solubility in organic solvents. However, light fluoros scavengers introduced in 2002 by Fluorous Technologies and Merck Research Laboratories have found many applications and have been used to isolate the desired product in good yield and high purity.^{55,56,57}

An interesting reaction setup called “Fluorous Triphasic Reactions” has been developed combining both fluoros separation techniques and fluoros synthesis. The fluoros triphasic reaction setup consists of two organic layers separated by a fluoros layer, restricting exchange between the two organic layers to compounds that can pass through the fluoros layer (Figure 4-4). As an example, the desired compound with a fluoros tag and other impurities are added to the left arm containing the organic layer, and reagents used for detagging the fluoros tag are added to the right arm also containing an organic layer. The fluoros compound on the left arm will migrate toward the organic layer in the right arm, leaving the impurities in the left arm organic phase. At the interface of the fluoros layer and the right arm organic layer, the

detagging reaction will take place and the desired product will partition into the right arm organic layer leaving the removed fluororous tag in the fluororous layer.^{9,14,58}

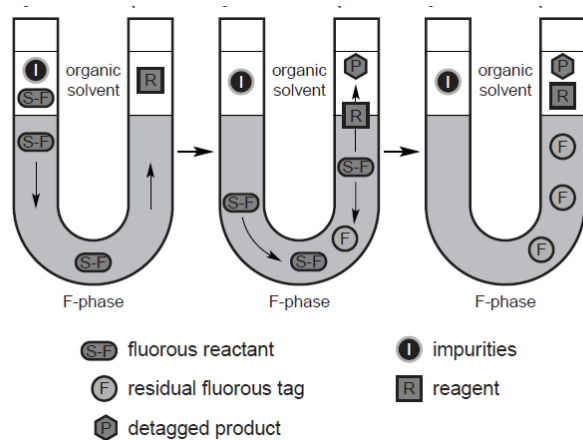


Figure 4-4. An example of a strategy for fluororous triphasic reaction with separation. Reproduced with permission from Journal of Chemical Education.⁹

Fluororous chemistry has found applications in many other areas of chemistry. Natural product synthesis,⁵⁹ combinatorial chemistry,⁶⁰ peptide,⁶¹ oligosaccharide⁶² and oligonucleotide⁶³ synthesis, and proteomics⁶⁴ are but a few examples. Fluororous carbohydrates have also been developed.⁶⁵ However, reports of the combination of fluororous chemistry with photochemistry are rare. In 2005 Evans and co-workers⁶⁶ reported the use of fluororous tags in a photoactivated hydrophilic/hydrophobic switch in amine-functionalized self-assembled monolayers (SAM).⁶⁷ A highly active amine surface (hydrophilic) is masked using *o*-nitrobenzyl photoremovable protecting group via a succinyl ester (hydrophobic). The *o*-nitrobenzyl group is tagged with a fluororous tag. Addition of fluororous tags have shown to produce more stable SAMs than analogous hydrocarbon chains.⁶⁸ When exposed to UV radiation (≈ 365 nm), the *o*-nitrobenzyl group was

removed, thus exposing the active amine function. Figure 4-5 illustrates this sequence and Figure 4-6 shows the actual structures of the hydrophobic moieties used in the study.

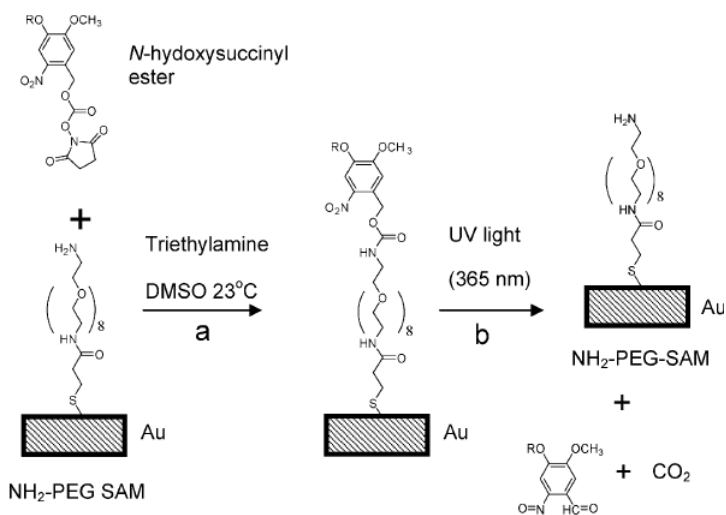


Figure 4-5. Schematic representation of synthesis of photocleavable surface and subsequent photodeprotection. Reproduced with permission from Langmuir⁶⁶

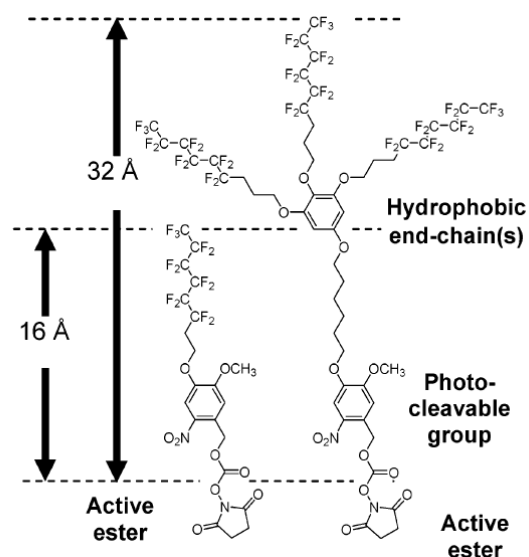


Figure 4-6. Molecular structures of the photoactive reagents used for masking the SAM surface. Reproduced with permission from Langmuir⁶⁶

Fluorous chemistry has come a long way in a very short time and branched into many areas of chemistry. Researchers in this field have tried to create fluorinated analogs for many traditional protocols. D. P. Curran, a major contributor to the development of fluorinated chemistry, acknowledge this as a development of a “parallel chemical universe”.⁸ Despite all the work and new applications reported for fluorinated chemistry, its full potential is far from being fully explored.

Statement of the Problem

Fluorous chemistry has grown enormously since its discovery a decade ago and has found applications in many areas of chemistry. Fluorous separation techniques have been developed and successfully used for product isolation, and fluorous analogs for almost every important synthetic reaction have been developed.¹² Yet reports of the coalescence of photochemistry with fluorous chemistry are few and far between.

The *p*-Hydroxyphenacyl chromophore (pHP), a novel, more efficient photoremovable protecting group (PPG), has shown great promise in many biological studies⁴ and has also been explored for solid phase synthesis and combinatorial chemistry.⁶⁹ From a synthetic organic chemist's perspective, the pHP may be viewed as an attractive protecting group, because the byproducts of the reaction do not compete for light nor do they undergo secondary photochemistry, making it possible to drive the photorelease to higher conversion without losing photoreaction efficiency or creating an undesirable mixture.

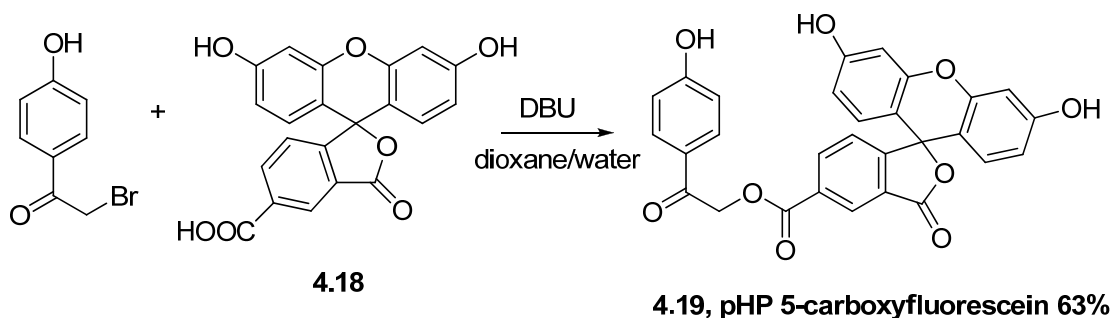
In this proof-of-concept study, the versatility of the pHP group, as a protecting group in synthetic organic chemistry, is extended by combining pHP photochemistry with fluorous separation techniques. The pHP moiety can be transformed into a fluorous reagent by simply attaching a fluorous tag to the chromophore. Use of light, "a traceless reagent," as the deprotecting agent also makes PPGs an attractive alternative to conventional protecting groups. The applicability of any protecting group will depend mainly on ease of protection, ease of removal, and ease of product isolation following deprotection. When a functionality is protected by a fluorous pHP, the presence of the fluorous tag makes the compound fluorophilic, rendering the possibility of utilizing fluorous separation techniques for product isolation in the initial

protecting step and any other subsequent steps prior to deprotection. But more importantly, the ease of product isolation upon deprotection can be greatly enhanced by employing a fluorous pHP. Once deprotected using light, only the photoproducts of the chromophore and starting material (if any is left) will carry the fluorous tag, allowing the convenient isolation of the desired compound using the fluorous separation techniques.

Results

Preliminary Studies

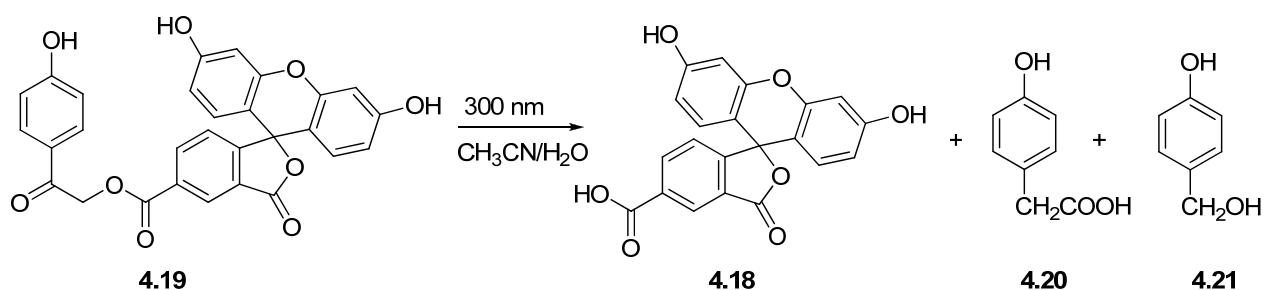
For preliminary studies and to test the potential of the release of fluorescein from the *p*-hydroxyphenacyl photoprotecting group, pHP 5-carboxyfluorescein (**4.19**) was synthesized and its photochemistry explored. The synthesis of pHP 5-carboxyfluorescein was achieved by the reaction between pHP bromide (pHP Br) and 5-carboxyfluorescein (**4.18**) in the presence of DBU (Equation 4.6) in 63% yield. The UV-Vis spectrum of pHP 5-carboxyfluorescein in 10% water/methanol, shows two absorption bands, one at 499 nm with a shoulder at 470 nm, the other at 279 nm. The latter is due to the absorbance of the pHP chromophore while the one at higher wavelength is due to the absorbance of the 5-carboxyfluorescein chromophore. The fluorescence spectrum of pHP 5-carboxy fluorescein ester is similar to that of 5-carboxylfluorecein with an emission maximum at 521 nm (excitation wavelength 485 nm). pHP 5-carboxyfluorescein is not soluble in water but is soluble in polar organic solvents like methanol, acetone and ethyl acetate.



Eq. 4.6

The photolysis of **4.19** was investigated using both ^1H NMR and UPLC analyses. The NMR experiments were performed by photolyzing the samples in a Pyrex NMR tube. A 10 mg sample of **4.19** was dissolved in 1.5 ml of 1:1 $\text{CD}_3\text{CN}/\text{D}_2\text{O}$ and photolyzed in a Rayonet

photoreactor equipped with a merry-go-round apparatus and two 3000 Å lamps. The sample was then irradiated and ^1H NMR spectra recorded at 10 min intervals. The release of 5-carboxyfluorescein (**4.18**) took place smoothly along with the formation of the rearranged *p*-hydroxyphenylacetic acid (**4.20**) as the major and *p*-hydroxybenzyl alcohol (**4.21**) as the minor photoproducts (Equation 4.7). The identities of these products were confirmed by spiking the ^1H NMR sample with authentic samples. Photolysis studies analyzed by UPLC were performed using the same photoreactor setup described above. However, the solvent system for photolysis was replaced by 1:1 $\text{CH}_3\text{CN}:\text{H}_2\text{O}$, and the irradiations were carried out in 5 ml quartz tubes. 100 μl aliquots were removed every 10 min and diluted up to 1 ml with water prior to analysis.



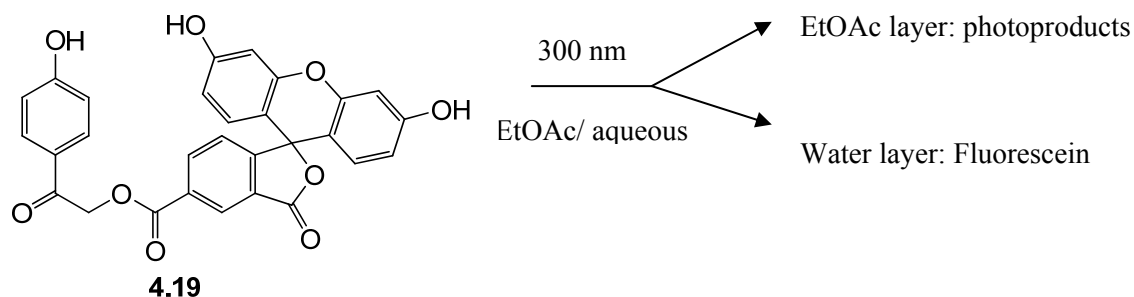
Eq. 4.7

To investigate photolysis in biphasic media, photolysis experiments were conducted in EtOAc/ammonium acetate buffer (pH 7.04). The selection of pH 7.04 buffer was based on properties of both fluorescein and the pHP chromophore. Depending on the solvent and the pH of the solution, fluorescein can exist in two forms, the fluorescent quinone form and the non-fluorescent lactone form.⁷⁰ The fluorescent quinone form is only present at pH 6.5 or higher with maximum fluorescence at pH 9.⁷⁰ Previous work done by Givens *et.al.*⁷¹ has shown that the efficiency of photorelease by the pHP photoprotecting group decreases at higher pH with best

efficiency in water at pH ~ 7 . Therefore, pH 7 buffer was chosen to obtain fluorescein in its fluorescent form without compromising the efficiency of photorelease.

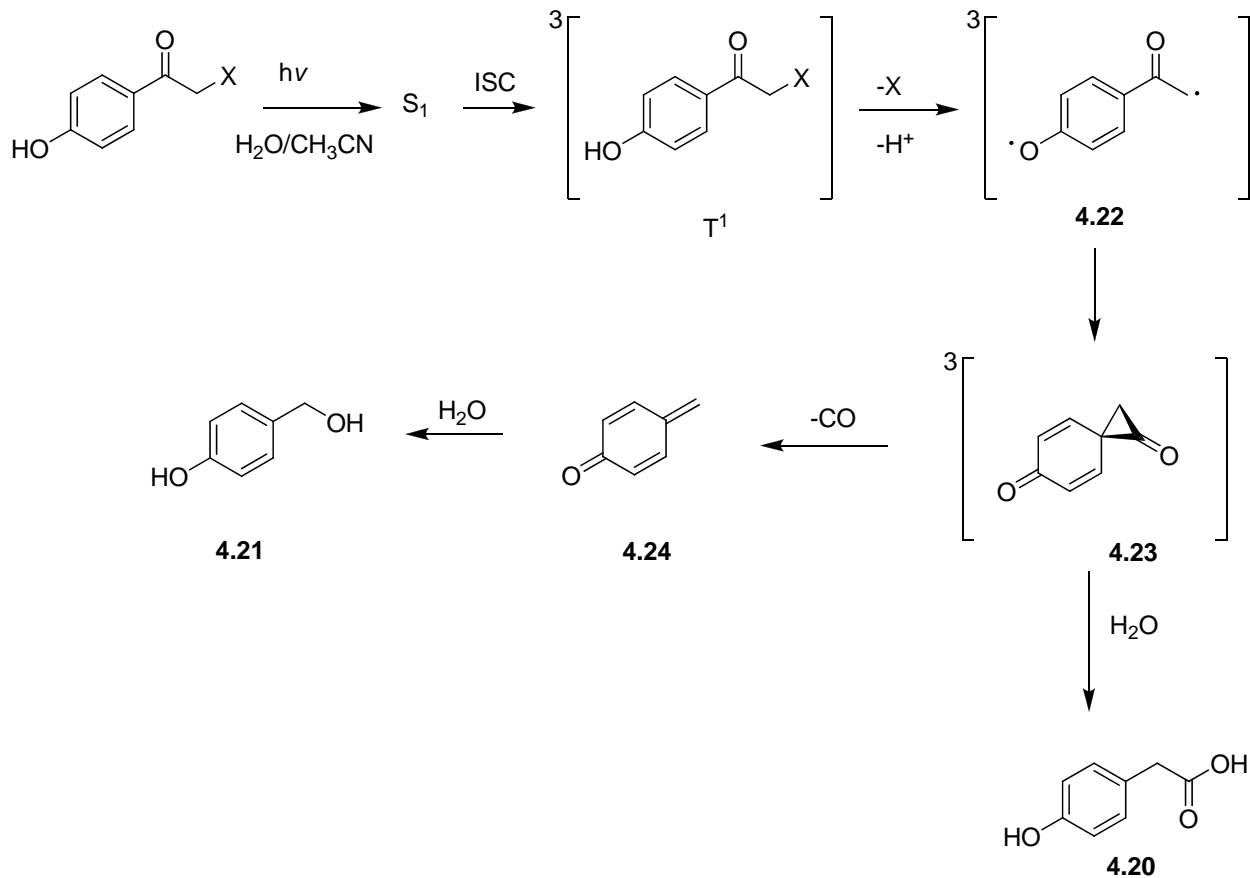
When **4.19** was photolyzed in biphasic EtOAc/aqueous buffer (pH 7.04), the EtOAc layer appeared slightly yellow in color before photolysis, while the aqueous layer was colorless. Under a UV lamp the EtOAc layer showed a slight fluorescent glow compared to no fluorescence in the aqueous layer. However, upon photolysis the aqueous layer become yellow and, under a UV lamp, showed a very prominent fluorescent glow characteristic of fluorescein dyes. The color of the EtOAc layer remained unchanged. The photolysis was quantitatively followed using UPLC and fluorescence spectroscopy for each layer at 30 min intervals. Upon photolysis of **4.19** in the biphasic EtOAc/aqueous buffer (pH 7.04), the fluorescence in the H₂O layer increased drastically. However the fluorescence of the EtOAc layer also increased, but to a lesser extent. UPLC analysis showed that the released 5-carboxy fluorescein had equilibrated between both layers but was preferentially concentrated in the aqueous layer. As expected, the remaining pHP 5-carboxyfluorescein (**4.19**) and the photoproducts **4.20** and **4.21** remained in the EtOAc layer (Scheme 4.5). The reaction was complete in 7 h.

Scheme 4.5



Photolysis studies of **4.19** qualitatively demonstrated that fluorescein can be quantitatively photoreleased and that photolysis in biphasic media produces the known photochemical products expected from a photo-Favorskii rearrangement⁷² of *p*-hydroxyphenacyl esters, as described in the *Introduction* section of *Chapter 1*. The most recent mechanism put forward by Givens and coworkers⁷³ for the photo-Favorskii rearrangement is illustrated in Scheme 4.6. Upon initial excitation to the singlet excited state, **4.19** will undergo rapid intersystem crossing to the triplet state, from which a triplet biradical (**4.22**) is generated with the loss of a proton and fluorescein-5-carboxylate (the conjugate base of **4.18**). The triplet biradical relaxes to the strained spirodienedione (**4.23**), the Favorskii intermediate, which either undergoes hydrolysis with water to give rise to the major Favorskii photoproduct, *p*-hydroxyphenylacetic acid (**4.20**) or undergoes decarbonylation to form a quinone methide intermediate (**4.24**), which subsequently reacts with water to generate the minor photoproduct, *p*-hydroxybenzyl alcohol (**4.21**).

Scheme 4.6



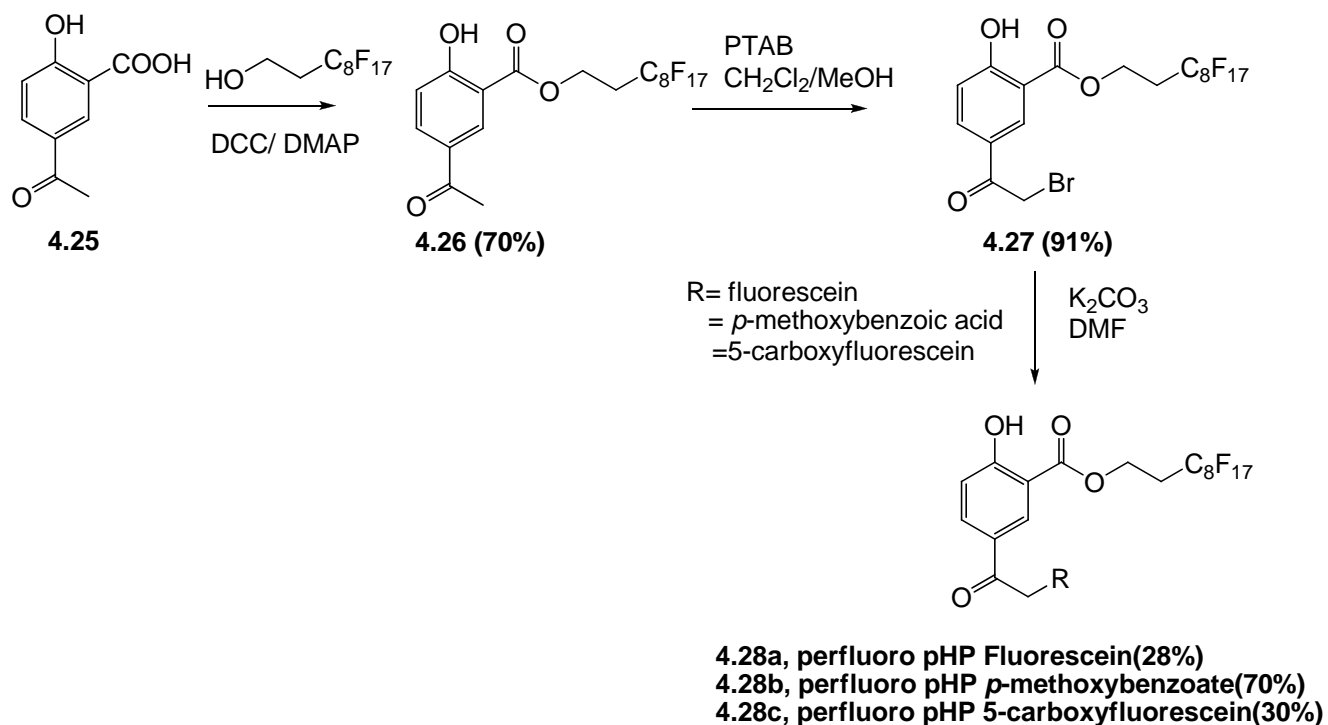
Fluorous chemistry

Synthetic Route

An eight carbon fluorous ponytail²³ was attached to the carboxylic acid group of the readily available 5-acetylsalicylic acid (4.25) providing a fluorous “handle” for enhancing the solubility of a pHP photoremovable protecting group in fluorous media. The DCC coupling reaction between 5-acetylsalicylic acid and 1H,1H,2H,2H-perfluoro-1-decanol gave the perfluoro ester 4.26 in 70% yield. Fluorous silica gel, i.e., silica containing long perfluoro alkyl chains (fluorous chains),¹⁴ was used for separation of the synthesis intermediate 4.26 from the

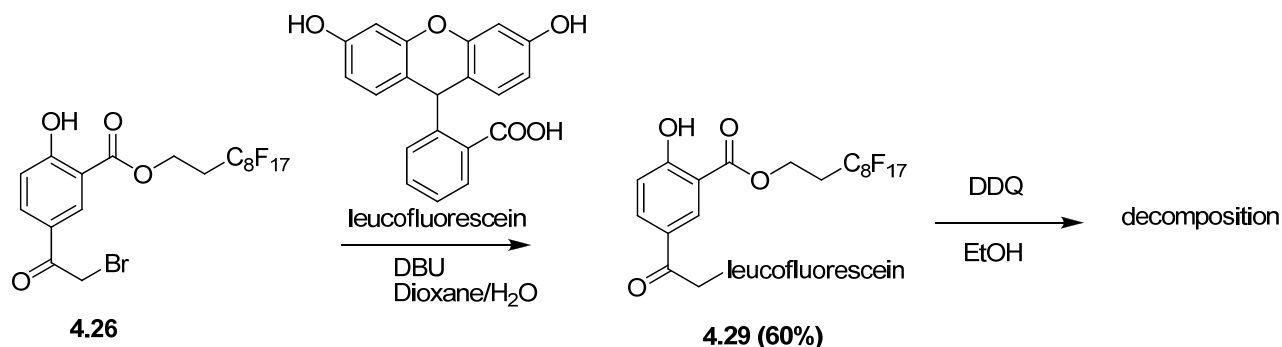
byproducts. The fluorosilica gel was packed in a 2 cm × 30 cm column and the products eluted using 1:1 hexane:EtOAc. The column was conditioned for reuse by eluting with acetone (~ 100 ml) to remove residues from the synthesis mixture. α - Bromination of **4.26** was achieved by reaction with phenyltrimethylammonium tribromide (PTAB) in 91% yield. *p*-Methoxybenzoic acid, fluorescein, and 5-carboxyfluorescein were caged via an S_N2 reaction of the free acids with perfluoro pHP Br **4.27** in the presence of K₂CO₃ (Scheme 4.7).

Scheme 4.7



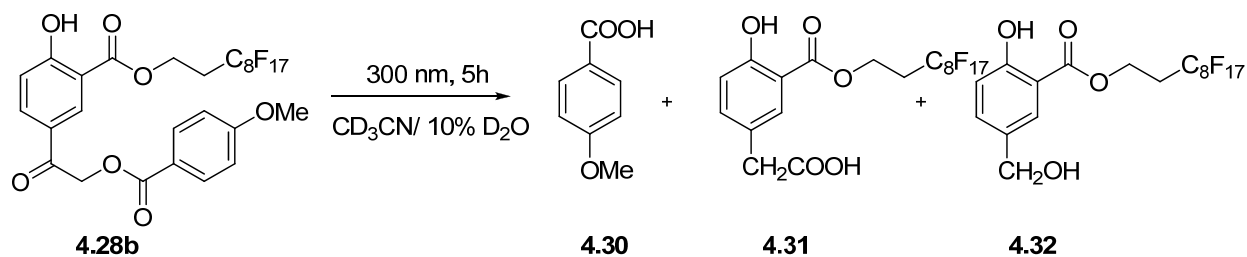
Due to the lower yield of the route shown in Scheme 4.7, synthesis of perfluoro pHP fluorescein (**4.28a**) was also attempted by the reaction between perfluoro pHP Br (**4.27**) and leucofluorescein. However, attempts to oxidize **4.29** with DDQ resulted in the decomposition of the starting material (Scheme 4.8).

Scheme 4.8



Due to difficulties with the synthesis and purification of perfluoro pHP fluorescein derivatives, perfluoro pHP *p*-methoxybenzoate was also examined as the model for studies for the separations using fluorous techniques.

Photolysis studies of Perfluoro pHP *p*-methoxybenzoate (4.28b)



Eq. 4.8

Initial photolysis studies of **4.8b** were performed in 10% D₂O/CD₃CN in Pyrex NMR tubes using the same photoreactor set up described under photochemical studies of pHP 5-carboxyfluorescein. ¹H NMR spectra taken at 1 h intervals revealed released *p*-methoxybenzoic acid (**4.30**) along with the two fluorous substituted pHP photoproducts, *p*-hydroxyphenylacetic acid derivative **4.31** and *p*-hydroxybenzyl alcohol derivative **4.32** (Equation 4.8). NMR spectra

at $t = 0$ h and $t = 6$ h are illustrated in Figure 4-7. Two new peaks were observed at 3.6 ppm, assigned to **4.31**, and at 4.7 ppm, assigned to **4.32**

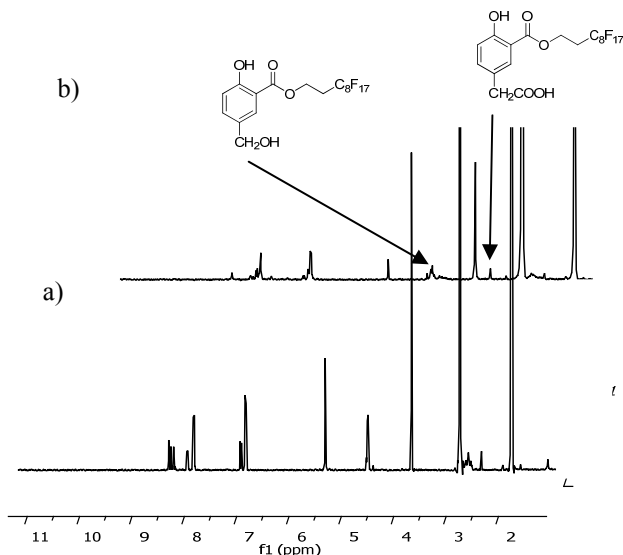
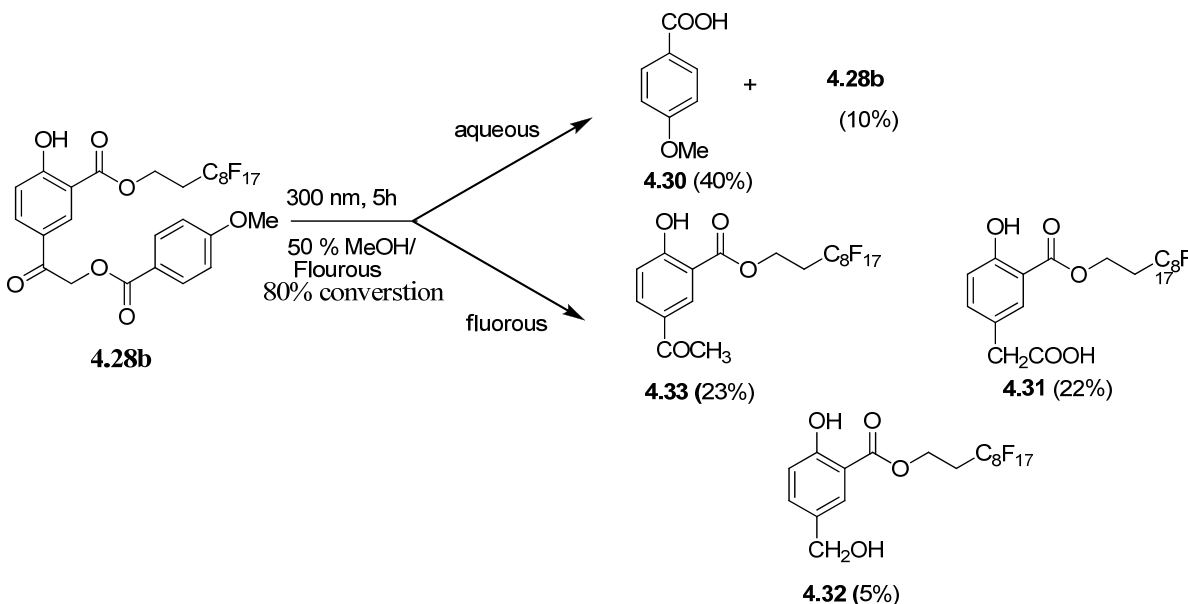


Figure 4-7. ^1H NMR spectra of the photolysis of **4.28b** in 10% $\text{D}_2\text{O}:\text{CD}_3\text{CN}$ at a) $t = 0$ h b) $t = 6$ h.

The fluoruous solvent selected for study was methyl nonafluorobutyl ether ($\text{CF}_3(\text{CF}_2)_3\text{OCH}_3$) because of its known ability to dissolve light fluoruous compounds, i.e., those compounds containing short fluoruous chains, and the favorable partition coefficients with many aqueous organic solvents.¹⁷ Perfluoro pHP *p*-methoxybenzoate (**4.28b**) was partly soluble in methyl nonafluorobutyl ether, but attempts to carry out the photolysis in this fluoruous solvent failed as evidenced by the observation that the compound remained unchanged upon prolonged exposure to light (300 nm, 16 lamps, 24 h). The photolysis of **4.28b** could be carried out in 50% $\text{MeOH}/\text{CF}_3(\text{CF}_2)_3\text{OCH}_3$. A solution of 10 mg of **4.28b** was dissolved in a solution of 2 ml of MeOH and 2 ml of $\text{CF}_3(\text{CF}_2)_3\text{OCH}_3$ and photolyzed in a 5 ml quartz tube for 2 h. Following photolysis, water was added, the layers separated, and each was analyzed by NMR. The starting

material conversion was *ca.* 80%. The aqueous layer contained *p*-methoxybenzoic acid and unreacted starting material, **4.28b**, while the fluorous layer contained all the photoproducts possessing the fluorous tag (Scheme 4.9).

Scheme 4.9



Products were identified using ^1H NMR spectra. Spiking experiments were performed for identification of **4.30** and **4.33** as authentic samples were available. It is noteworthy that perfluoro *p*-hydroxyacetophenone **4.33** was not observed when the photolysis was performed in $\text{D}_2\text{O}/\text{CD}_3\text{CN}$ (Figure 4-7, Equation 4.8). The two Favorskii products, **4.31** and **4.32**, were identified by comparing chemical shifts from photolysis studies of **4.28b** in $\text{D}_2\text{O}/\text{CD}_3\text{CN}$.

Photolysis studies of perfluoro pHP Fluorescein (**4.28a**)

Photolysis studies of **4.28a** were performed in two phase solutions of EtOAc and aqueous buffer (pH 7.04). The reaction was followed by monitoring the fluorescence emission

from each layer as a function of the photolysis time. In a typical experiment 10 mg of **4.28a** was dissolved in 2 ml of EtOAc, transferred to a 5 ml quartz tube, and 2 ml of aqueous buffer (pH 7.04) was added. Samples for fluorescence measurements were prepared by removing 100 μ l from both layers at 10 min intervals and diluting to 10 ml. The initial fluorescence observed in the EtOAc layer decreased with time during irradiation, whereas the fluorescence of the water layer increased upon photolysis. Fluorescence spectra are illustrated in Figure 4-8a-d. Photolysis in a two-phase mixture of methyl nonafluorobutyl ether and aqueous buffer (pH 7.04) medium resulted in no reaction.

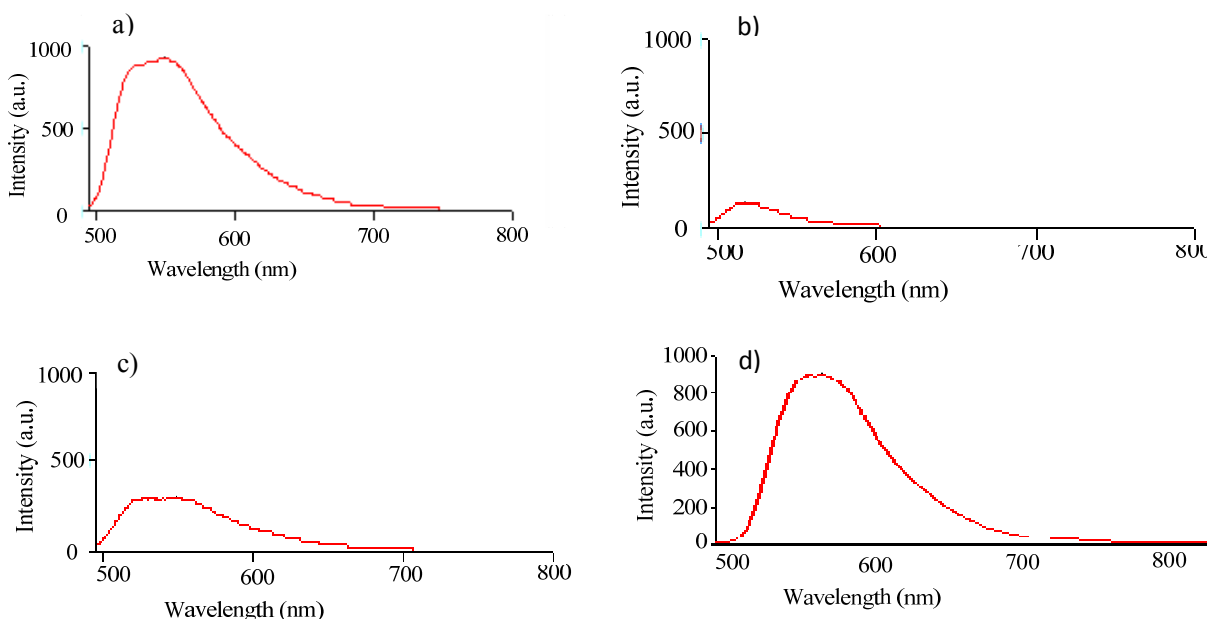


Figure 4-8. Fluorescence spectra ($\lambda_{\text{ex}} = 487$, $\lambda_{\text{em}} = 517$, Conc. 4.8×10^{-6} M) of the fluorescence emission from samples of **4.28a** subjected to photolysis in EtOAc/buffer (pH 7.04): a) EtOAc layer $t = 0$ min b) H₂O layer $t = 0$ min c) EtOAc layer $t = 10$ min d) H₂O layer $t = 10$ min.

Product separation using fluoros SPE and liquid-liquid extraction

In general, photolysis were carried out in 12% H₂O/CH₃CN in a Rayonet photoreactor equipped with 2×3000 Å lamps and a merry-go-round apparatus in 5 ml quartz tubes.

Following photolysis for 2 h, fluoruous solid phase extraction (F-SPE)^{74,8} and liquid-liquid extraction¹⁷ were employed to isolate the leaving group (*p*-methoxybenzoic acid, fluorescein, or 5-carboxyfluorescein) from the fluoruous photoproducts. F-SPE was performed using F-SPE cartridges packed with silica with a perfluorooctylethylsilyl (Si (CH₂)₂C₈F₁₇) bonded phase.¹⁴ After photolysis, solvent was evaporated, the residue was dissolved in DMF, and loaded on to the F-SPE cartridge. Separation was achieved using a mixture of 80:20 MeOH/H₂O as the fluorophobic solvent and MeOH as the fluorophilic solvent.

Liquid-liquid extraction was performed using methyl nonafluorobutyl ether and water. After photolysis, solvents were evaporated and water (5 ml) was added. The solution was extracted with methyl nonafluorobutyl ether (3 × 5 ml). The amount of leaving group isolated in each method is given in Table 4-4. The yield of each compound present in each layer was quantified using analytical UPLC. Working curves were constructed for all three perfluoro PHP derivatives and the leaving groups for quantification purposes.

Table 4-4. Percentage of Leaving Group Recovered After Separating from Other Photoproducts Employing F-SPE and Liquid-Liquid Extraction Following Photolysis

Compound	F-SPE		Extraction	
	Organic	Aqueous	Fluorous	Aqueous
4.28a (fluorescein)	0%	80%	0%	100%
4.28b (<i>p</i> -methoxybenzoic acid)	0%	90%	0%	95%
4.28c (5-carboxyfluorescein)	0%	92%	0%	95%

The fluorescence of each layer was also measured after the separation was carried out by both techniques. If the separation techniques were as successful as observed for the UPLC analysis, fluorescence should only be observed in the fluorophobic layer. In fact, when separation of the leaving group was achieved using F-SPE, fluorescence was observed only in

the MeOH/H₂O fraction, i.e., the fluorophobic solvent. Fluorescence spectra of both MeOH/H₂O and MeOH layers following the F-SPE separation of the photolysis mixture of **4.28c** are illustrated in Figure 4-9.

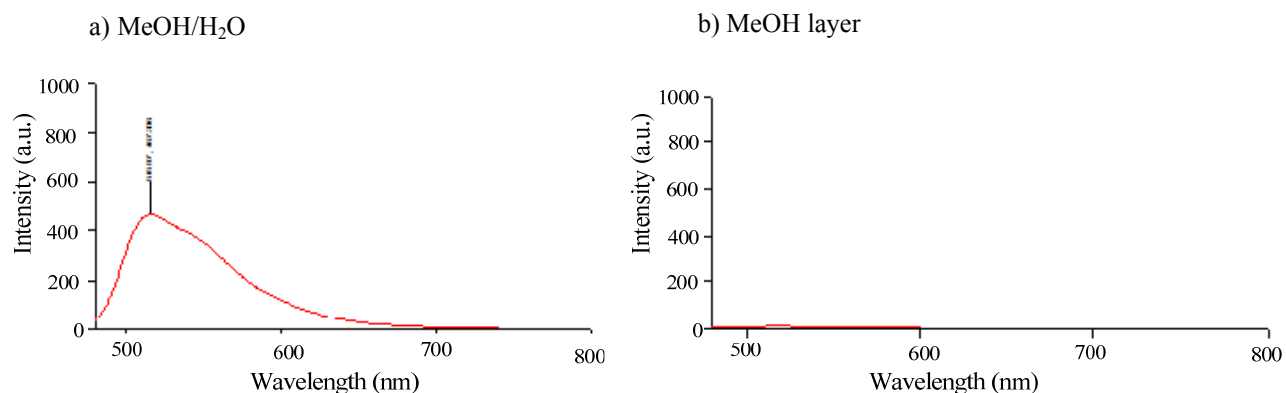


Figure 4-9: Fluorescence spectra of the fluorophobic and fluorophilic fractions obtained from the separation of the photolysis mixture of **4.28c** using F-SPE ($\lambda_{\text{ex}} = 485$, $\lambda_{\text{em}} = 515$, Conc. 2.2×10^{-6} M): a) MeOH/H₂O layer b) MeOH layer.

When the method of separation was liquid-liquid extraction, fluorescence was observed only in the aqueous layer. The fluorescence spectra of fluorous layer and the aqueous layer after the separation of the photolysis mixture of **4.28c** are shown in Figure 4-10.

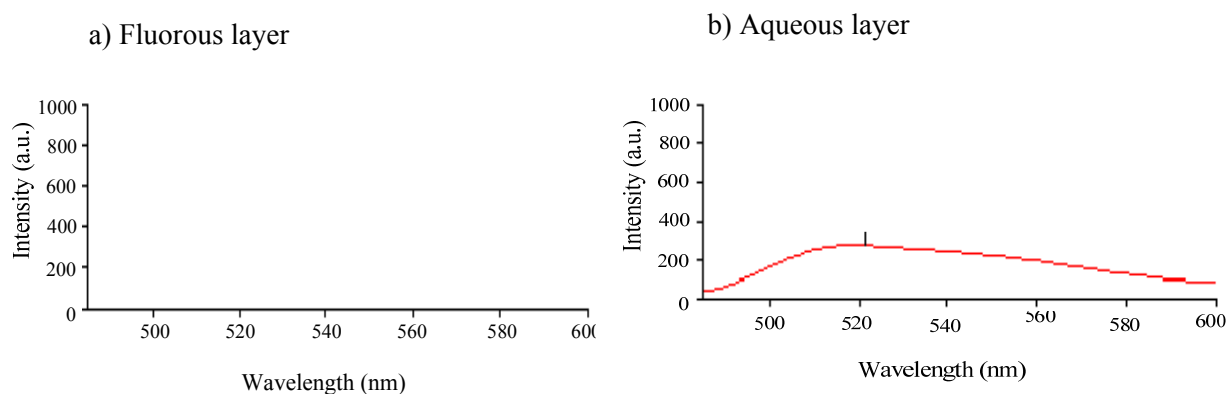


Figure 4-10: Fluorescence spectra of the fluorophobic and fluorophilic layers obtained from the separation of the photolysis mixture of **4.28c** using liquid-liquid extraction ($\lambda_{\text{ex}} = 485$, $\lambda_{\text{em}} = 521$, Conc. 2.2×10^{-6}): a) fluorous layer and b) water layer

Discussion

Preliminary studies. The leaving group employed in this study is fluorescein, a highly light absorbing chromophore. Therefore, to investigate whether fluorescein would interfere with pHP photochemistry some preliminary studies using pHP 5-carboxyfluorescein were necessary. Synthesis of pHP 5-carboxyfluorescein (**4.19**) was straightforward via a base activated S_N2 displacement reaction between pHP Br and 5-carboxyfluorescein. Use of H₂O/dioxane solvent mixtures for the reaction were required due to the solubility properties of 5-carboxyfluorescein. Purification of the final product using silica gel chromatography was difficult owing to the high polarity of pHP 5-carboxyfluorescein. Therefore, the use of polar solvent systems like CH₂Cl₂/MeOH was needed. Photorelease of 5-carboxyfluorescein took place smoothly. In accordance with other pHP derivatives,⁷⁵ the photoproducts formed when pHP 5-carboxyfluorescein was photolyzed in aqueous acetonitrile were 4-hydroxyphenylacetic acid (major) and 4-hydroxybenzyl alcohol (minor, 5%). Photolysis studies performed in EtOAc/pH 7.05 buffer showed that pHP photochemistry can be conducted in biphasic media without complications. In an ideal situation, the released 5-carboxyfluorescein should diffuse into the aqueous layer, leaving the photoproducts and any remaining starting material in the EtOAc layer. However the HPLC studies showed that released 5-carboxyfluorescein equilibrates into both layers with preferential solubility in the aqueous layer. This drawback could be avoided if EtOAc were replaced with a fluorinated solvent and employing fluorinated pHP derivatives, assuming that the photochemistry of the pHP chromophore is unchanged under these new conditions.

Fluorous Chemistry

Synthetic approaches. The synthesis of all three fluorous pHP derivatives began with the basic unit of 5-acetylsalicylic acid (**4.25**). The use of 5-acetylsalicylic acid is appealing as it gives two handles, one via the carboxylic acid group and the other via the acetyl group, which can be manipulated separately. It is also commercially available, inexpensive and biologically benign. An eight carbon fluorous chain was chosen as the fluorous tag (or ponytail), and the attachment of this tag to the pHP moiety was achieved via a DCC coupling reaction. One common drawback of DCC coupling reactions is the difficulty of the removal of the dicyclohexylurea byproduct.⁷⁶ However, in this synthesis the desired fluorous ester product **4.26** is fluorophilic so it could be easily isolated in 70% yield using fluorous column chromatography by employing traditional solvents like hexane/EtOAc. The fluorous silica gel was reused multiple times after washing with acetone. The fluorous ester **4.26** could also be isolated using traditional silica gel column chromatography, but this was more tedious and required several repetitive column chromatographic separations to obtain the pure compound. α -Bromination of the acetophenone functional group on **4.26** was achieved using phenyltrimethyl ammonium tribromide in 91% yield. The final construction of the fluorous pHP caged compounds was accomplished by an S_N2 displacement of bromide from **4.27** in the presence of K_2CO_3 in DMF by the eventual photoremovable leaving groups, such as fluorescein, 4-methoxybenzoic acid and 5-carboxyfluorescein. The final products were isolated using F-SPE cartridges.

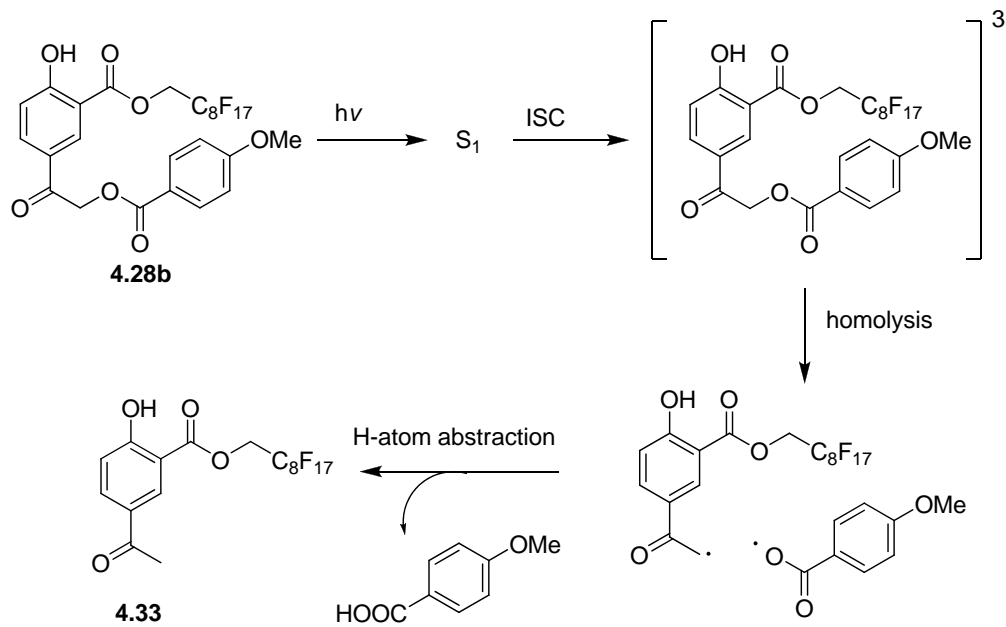
Solubility properties fluorous pHP derivatives. The percentages of fluorine present by molecular weight in the synthesized pHP derivatives are, 32%, 39%, 30% for **4.28a**, **4.28b** and **4.28c**, respectively. Thus the fluorous pHP derivatives belong in the “light fluorous” category

(*Introduction*). Light fluoruous species are more desirable than heavy fluoruous compounds because they are more soluble in organic solvents and do not require the use of fluoruous solvents for synthesis or separation.¹² However, light fluoruous compounds are not very amenable to separation by fluoruous liquid-liquid extraction (F-LLE). The fluoruous solvent selected for this study is methyl nonafluorobutyl ether (CF₃(CF₂)₃OCH₃), a solvent known to be better for dissolving light fluoruous compounds (Table 4-2, *Introduction*).¹⁷ However, of the three pHP derivatives studied, only perfluoro pHP *p*-methoxybenzoate (**4.28b**) was even partially soluble in the fluoruous solvent whereas the two fluorescein derivatives were insoluble. This lack of solubility in fluoruous solvent can be attributed to the highly polar nature of the fluorescein moiety. All three pHP derivatives were soluble in polar organic solvents such as ethyl acetate, methanol, and acetonitrile.

Photochemical studies of perfluoro pHP *p*-methoxybenzoate (4.28b): The outcome of the photolysis of **4.28b** in 10% D₂O/CD₃CN was consistent with other pHP derivatives. Upon photolysis, formation of the two prototypical photoproducts, 4-hydroxyphenylacetic acid **4.31**, and 4-hydroxybenzyl alcohol **4.32**, was observed with the release of 4-methoxybenzoic acid. However, perfluoro pHP *p*-methoxybenzoate (**4.28b**) was photostable in methyl nonafluorobutyl ether (CF₃ (CF₂)₃OCH₃) even after prolonged exposure to light (300 nm, 24h). The absence of any photoactivity in the fluoruous solvent was not entirely unanticipated since pHP derivatives are generally known to undergo photolysis best in aqueous or polar protic solvents.⁷⁷ Therefore, attempts to perform the photolysis in aqueous/fluoruous biphasic media were abandoned at this point and the photolysis were conducted in an aqueous MeOH/fluoruous biphasic mixtures. Under these conditions, the perfluoro pHP *p*-methoxybenzoate (**4.28b**) initially resides in the MeOH

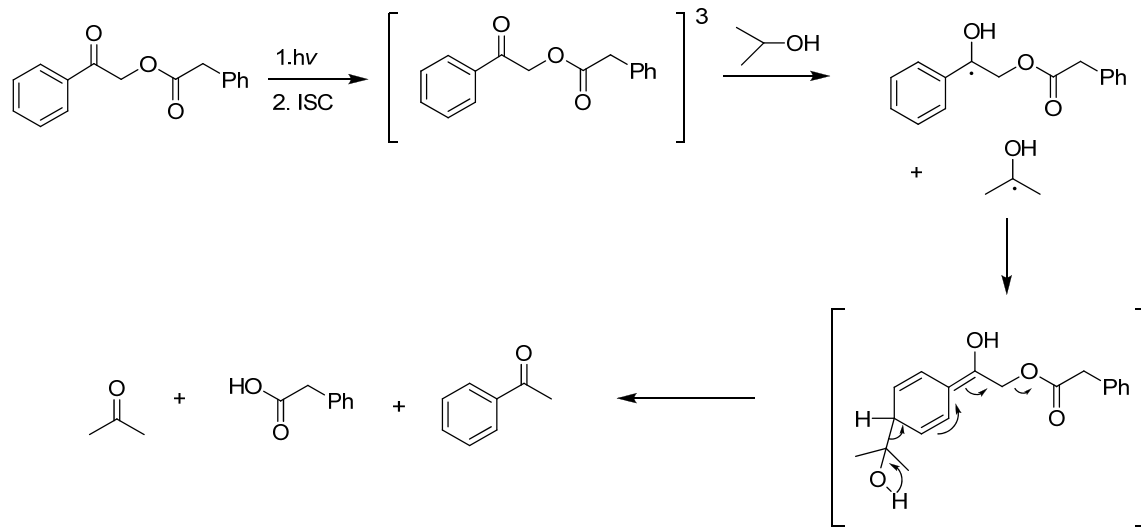
layer. Once photolyzed, the photoproducts that contain the fluoruous tag, i.e. **4.31** and **4.32**, diffuse into the fluoruous layer leaving behind the 4-methoxybenzoic acid in the MeOH layer. Thus, photolysis in aqueous MeOH/fluoruous biphasic media could be carried out successfully and, as anticipated, the fluoruous layer contained the photoproducts of the pHP chromophore while the aqueous layer contained only the released *p*-methoxybenzoic acid and unreacted starting material. It should be noted that **4.31** and **4.32** have 48% and 50% fluorine by weight and are leaning towards heavy fluoruous derivatives. The conversion in this reaction was 80% (Scheme 4.9 in *Results*). The photoproducts observed were perfluoro 4-hydroxyphenylacetic acid (**4.31**), perfluoro 4-hydroxybenzyl alcohol (**4.32**), and perfluoro 4-hydroxyacetophenone (**4.33**). Formation of **4.33** cannot be explained from the photo-Favorskii rearrangement mechanism as illustrated in Scheme 4.6 (*Results*). Also, formation of 4-hydroxyacetophenone was not observed in studies employing H₂O/CH₃CN. However, there is precedence for formation of **4.33** in pHP photochemistry.^{78,79} A possible pathway is the homolysis of the CH₂-O bond between the pHP chromophore and the leaving group followed by subsequent H-atom abstraction to produce **4.33** (Scheme 4.10) as discussed in *Chapter 2, Section three*.

Scheme 4.10



However, Falvey *et al.*⁷⁸ has proposed a different mechanism for the acetophenone formation from phenacyl benzoates in which H-atom transfer to the carbonyl carbon occurs prior to CH₂-O bond cleavage. The authors' proposal is supported by the observation that the quantum efficiency of photorelease increases in the presence of H-atom donors like 2-propanol (Scheme 4.11).

Scheme 4.11



Photolysis studies of perfluoro pHP Fluorescein (4.7a). Photolysis studies of perfluoro pHP fluorescein (4.28a) were performed in EtOAc and pH 7.04 buffer biphasic media and the fluorescence of each layer was recorded to determine the distribution of the fluorescein component throughout photolysis. Ideally, before photolysis the fluorescence should be confined to the EtOAc layer and perfluoro pHP fluorescein should remain in that layer. After complete conversion, fluorescence should be observed only in the aqueous layer since the released fluorescein should diffuse to the aqueous layer. However, there was a slight fluorescence observed in the water layer prior to the photolysis (Figure 4-8b *Results*). This is most likely due to the equilibration of partially soluble perfluoro pHP fluorescein between both layers. Upon photolysis a significant increase in the fluorescence of the aqueous layer was observed accompanied by a decrease in fluorescence of the EtOAc layer. However, fluorescence in the EtOAc layer did not completely disappear (Figure 4-8c *Results*). This might be due to unreacted starting material or possibly the equilibration of released fluorescein between both layers as shown in preliminary studies using pHP 5-carboxyfluorescein.

Leaving group isolation using fluoruous SPE (F-SPE) and liquid-liquid extraction (F-LLE).

The concept of performing the photolysis in biphasic media is very attractive as products can be isolated simply by separating the two layers after the photolysis. Unfortunately, work done in this study shows that the pHP chromophore is photoinactive in fluoruous solvents and, when the photolysis is performed in aqueous/organic biphasic media, the released leaving group tends to equilibrate between both layers. This led us to look into another approach. In general pHP photochemistry is at its best when water or water/acetonitrile is used as the solvent. Use of solvents like EtOAc and MeOH resulted in a mixture of photoproducts and slower photorelease. Therefore, a rational approach would be to conduct the photolysis in aqueous CH₃CN and employ fluoruous separation techniques for product isolation. Thus, for all three perfluoro pHP derivatives, photolysis was performed in 12% H₂O/CH₃CN and the leaving group separated using F-LLE and F-SPE. The leaving group was isolated in 80%-100% yield employing both techniques. The percentage of leaving group isolated is illustrated in Table 4-4 in the *Results* section. It is important to note that according to UPLC analysis there is no significant presence of the unreacted starting material or the photoproducts in the aqueous or organic layers and no presence of leaving group in the fluoruous solvent for both techniques. This is also supported by the lack of fluorescence in the MeOH layer in F-SPE (Figure 4-9 in *Results*) and lack of fluorescence in fluoruous layer in F-LLE (Figure 4-10 in *Results*) in the study employing perfluoro pHP 5-carboxyfluorescein. Interestingly, for the three pHP derivatives investigated in this study, the amount of leaving group recovered from F-LLE, the technique that is unfavorable for light fluoruous compounds, is higher than the amount isolated using F-SPE. This can be attributed to the high fluorophobic nature of the leaving groups employed in this study.

Future studies. This was a proof-of-concept investigation that demonstrated fluororous chemistry and pHP photochemistry can be used in conjunction with each other to arrive at a more convenient, yet effective, separation technique. Although this study was confined to the carboxylate group as the leaving group, it can easily be extended to the other pHP compatible leaving groups, making it worthwhile to explore the full potential of the new approach. Further extensions would include the synthesis of libraries of compounds employing the combination of pHP photochemistry with fluororous separations chemistry discussed here and investigate full investigation of the applicability of this novel approach toward automation in library separation methodologies.

Conclusion This project clearly demonstrated that the combination of pHP photochemistry and fluororous separation methodology is a viable concept. Attaching a fluororous tag can be achieved easily using 5-acetylsalicylic acid as a platform and, once the pHP tag has been attached, all separations of the desired products and reagents can be achieved conveniently via fluororous separation techniques. The fluororous tag did not interfere with the photochemistry of the pHP group except as noted. The finding that the photoreaction was inoperative in the fluororous media could, itself, also be advantageous in other circumstances. Fluorescein, a highly fluorescent chromophore, could be photoreleased from the pHP moiety without complication and product isolation could still be achieved successfully by both F-SPE and F-LLE following the photolysis.

Experimental

General Methods. Melting points were conducted with open end capillary tubes using a non-calibrated melting point apparatus. Products of all reactions were assessed for purity using the following instrumental techniques: ^1H , ^{13}C , and ^{19}F NMR (internal standard trifluoroacetic acid, $\delta = -76.55$ ppm) were obtained using a Bruker 400 HZ instrument unless otherwise stated. Exact masses were obtained using a triple quadrupole electrospray ionization mass spectrometer. UV/Vis data was obtained using 1.5 ml quartz cuvettes on a Cary 100 spectrophotometer (Varian, Inc., Palo Alto, CA). Fluorescence data were acquired using a 10 mm quartz cell using a Cary Eclipsed Fluorescence spectrophotometer (Varian, Inc., Palo Alto, CA.). IR data were obtained with pressed potassium bromide (KBr) pellets. Product separation was achieved by flash chromatography using silica gel and gradient hexanes/ethyl acetate as the eluting solvents unless otherwise stated. F-SPE cartridges (size 5g, 10 ml tube packed with silica containing a perfluorooctylethylsilyl bonded phase) and fluorosilica gel were obtained from Fluorous Technologies, Inc. The cartridges were washed with 1 ml of DMF and preconditioned with 20% $\text{H}_2\text{O}/\text{MeOH}$ before initial use. Photolysis studies were performed in a Rayonet RPR-100 photoreactor equipped with two 16 W, 3000 Å lamps and a merry-go-round apparatus. Photoproduct identification was achieved through UPLC (Waters Acquity) analysis equipped with UV-Vis detection of a dual wavelength detector set at 250 and 280 nm. The reservoirs used were as follows: A) 99% water, 1% acetonitrile, and 0.06% formic acid. B) 99% acetonitrile, 1% water, and 0.08% formic acid. The column was a reverse-phase (C18), 5 μm mesh, and 50 mm in length. Injections of 5 μl were made with an automated sampler for each run for a total of 3 injections per vial. A

mobile phase gradient was utilized to optimize compound separation. The flow rate was set at 200 μ l/min. During data analysis smoothing functions were used for peak area determinations of the chromatographic peaks. Calibration curves were constructed for each product for product quantifications for each separation protocol using caffeine or biphenyl as the internal standards.

2-(4-Hydroxyphenyl)-2-oxoethyl- 3',6'-dihydroxy-3-oxo-3H-spiro[isobenzofuran-1,9'-xanthene]-5-carboxylate (pHP 5-carboxyfluorescein, 4.19) DBU (0.041 ml, 0.26 mmol) was added to a solution of α -bromo-4-hydroxyacetophenone (170 mg, 0.52 mmol) and 5-carboxyfluorescein (100 mg, 0.26 mmol) in 50% dioxane water and stirred for 24 h. The solvent was evaporated from the resulting yellow solution and the residue dissolved in water and extracted in to EtOAc and purified by column chromatography starting with 1:1 hexane/EtOAc then 100% EtOAc and finally 1:1 $\text{CH}_2\text{Cl}_2/\text{MeOH}$, to obtain 2-(4-hydroxyphenyl)-2-oxoethyl- 3',6'-dihydroxy-3-oxo-3H-spiro[isobenzofuran-1,9'-xanthene]-5-carboxylate (**4.19**) in 63% yield: mp =181-183 $^\circ\text{C}$. ^1H NMR (400 MHz $(\text{CD}_3)_2\text{CO}$): δ 5.45 (s, 2H), 6.64 (m, 2H), 6.66 (m, 2H), 6.90 (m, 2H), 7.47 (d, 1H), 7.98 (d, 2H), 8.44 (d, 1H), 8.59 (s, 1H). ^{13}C NMR (100 MHz, $(\text{CD}_3)_2\text{CO}$): δ (ppm) 66.9, 102.5, 110.0, 112.6, 114.9, 115.1, 115.4, 155.5, 124.7, 125.9, 126.4, 127.7, 129.5, 1130.3, 1130.4, 131.8, 131.9, 135.9, 152.4, 157.2, 159.6, 162.6, 164.4, 167.6, 189.8. IR (KBr): 3392, 1733, 1726, 1718, 1706, 1604, 1550, 1508, 1500, 1450. UV (10% water/methanol) $\lambda_{\text{max}} = 279$ ($\epsilon = 34200$), $\lambda_{\text{max}} = 498$ ($\epsilon = 36800$). HRMS calculated for $\text{C}_{19}\text{H}_{12}\text{F}_{17}\text{O}_4 = 627.0464$, observed = 627.0433.

3,3,4,4,5,5,6,6,7,7,8,8,9,9,10,10,10-heptadecafluorodecyl 5-acetyl-2-hydroxybenzoate (4.26)

The general method of Shelkov *et al.*⁸⁰ was followed. To a solution of 5-acetylsalicylic acid (1.0 g, 5.51 mmol), DCC (1.90 g, 9.22 mmol) and DMAP (0.112g, 0.92 mmol) in CH₂Cl₂ 1H,1H,2H,2H-perfluoro-1-decanol (2.14 g, 4.62 mmol) was added and stirred for 24 h. The solid obtained upon evaporation of the solvent was dissolved in ethyl acetate and filtered through celite and purified using fluorosilica gel (1:1 hexane/EtOAc) to obtain the desired product, 1H,1H,2H,2H-perfluorodecyl 5-acetyl-2-hydroxybenzoate (**4.26**) (2.0 g, 70 %): mp = 92-93 °C. ¹H NMR (400 MHz CDCl₃): δ 2.74 (s, 3H), 2.80 (m, 2H), 4.87 (s, 2H), 7.19 (d, 1H), 8.24 (d, 1H), 8.61 (s, 1H), 11.14 (s, 1H). ¹³C NMR (100 MHz, CDCl₃): δ (ppm) 26.2, 30.6, 57.6, 111.5, 118.2, 129.2, 131.4, 135.8, 169.4, 169.2, 195.7. ¹⁹F NMR (400 MHz CDCl₃): δ (ppm) -126.0, -123.3, -122.6, -121.8, -121.5, -113.4, -113.3, 133.3, -80.7. IR (KBr): 3392, 1679, 1589, 1244, 1201, 1149, 794. HRMS calculated for M+ H, C₃₈H₂₂O₉F₁₇ = 957.0993, observed = 957.0963.

3,3,4,4,5,5,6,6,7,7,8,8,9,9,10,10,10-heptadecafluorodecyl 5-(2-bromoacetyl)-2-hydroxy benzoate (perfluoro pHP Br, 4.27)

The general method of Holman, *et al.*⁸¹ was followed. phenyl trimethyl ammonium tribromide (0.36 g, 0.95 mmol) was added to **4.6** (0.5 g, 0.8 mmol) dissolved in 20 ml of 25% MeOH/ CH₂Cl₂ and stirred for 72 h at room temperature. Solvent was evaporated and resulting solid residue dissolved in CH₂Cl₂ and washed five times with water to obtain relatively pure 3,3,4,4,5,5,6,6,7,7,8,8,9,9,10,10,10-heptadecafluorodecyl 5-(2-bromoacetyl)-2-hydroxy benzoate (**4.27**) as a white solid (0.51 mg, 91%) and was used without any further purification: mp=73-74 °C. ¹H NMR (400 MHz CDCl₃): δ 2.80 (m, 2H), 4.49 (s, 2H), 4.88 (t, 2H), 7.21 (d, 2H), 8.25 (d, 2H), 8.66 (s, 1H), 11.24 (s, 1H). ¹³C NMR (100 MHz, CDCl₃): δ (ppm) 25.1, 29.2, 56.7, 111.9, 117.2, 127.8, 134.9, 138.5, 167.8, 168.0, 187.2. ¹⁹F

NMR (400 MHz CDCl₃): δ (ppm) -126.0, -123.3, -122.6, -121.8, -121.5, -113.4, -113.3, 133.3, -80.7. IR (KBr): 3413, 1679, 1589, 1350, 1240, 1203, 1147, 794, 659

3,3,4,4,5,5,6,6,7,7,8,8,9,9,10,10,10-heptafluorodecyl 2-hydroxy-5-(2-(2-(6-hydroxy-3-oxo-3H-xanthen-9-yl)benzoyloxy)acetyl)benzoate (perfluoro pHP fluorescein, 4.28a) The general method of Hiyama, *et al.*⁸² was applied. Solid K₂CO₃ (0.117 g) was added to a solution of fluorescein (0.094 g, 0.28 mmol) in DMF and stirred for 15 min. Perfluoro pHP bromide **4.7** (0.200 mg, 0.28 mmol) was added to the reaction mixture and stirred overnight. Water (100 ml) and ethyl acetate (100 ml) were added and the ethyl acetate layer was extracted and washed five times with water to remove DMF. The solvent was evaporated in vacuo and the residue was purified by F-SPE using fluoros cartridge to obtain 3,3,4,4,5,5,6,6,7,7,8,8,9,9,10,10,10-heptafluorodecyl 2-hydroxy-5-(2-(2-(6-hydroxy-3-oxo-3H-xanthen-9-yl)benzoyloxy)acetyl)benzoate (**4.28a**) as an orange solid (28 %): mp=130-132 °C. ¹H NMR (400 MHz, CD₃COCD₃): δ 2.96 (m, 2H), 4.84 (t, 2H), 5.37 (s, 2H), 6.56 (d, 1H), 6.84 (d, 1H), 8.42 (s, 1H). ¹³C NMR (100 MHz, CD₃CO): δ (ppm) 31.9, 58.0, 66.6, 70.4, 104.0, 105.1, 117.0, 112.6, 115.5, 119.5, 119.8, 126.0, 127.5, 127.8, 128.10, 1229.2, 123.0, 130.1, 130.3, 130.5, 131.0, 133.3, 134.7, 135.3, 136.4, 145.2, 160.3, 160.5, 164.1, 188.7, 189.6. ¹⁹F NMR (400 MHz CD₃COCD₃): δ (ppm) -126.0, -123.3, -122.6, -121.8, -121.5, -113.4, -113.3, 133.3, -80.7. IR(KBr): 3458, 1728, 1714, 1693, 1681, 1614, 1589, 1504, 1299, 1103, 1983, 993. UV (10% water/methanol) λ_{\max} = 270 (ϵ = 14000), λ_{\max} = 312 (ϵ = 8300) λ_{\max} = 502 (ϵ = 15700) HRMS calculated for M + H, C₃₈H₂₂O₉F₁₇ = 957.0993, observed = 957.0963.

3,3,4,4,5,5,6,6,7,7,8,8,9,9,10,10,10-heptafluorodecyl 2-hydroxy-5-(2-(4-methoxybenzoyloxy)acetyl)benzoate (perfluoro pHP p-methoxybenzoate, 4.28b) The same procedure as used

for **4.28a** was followed yielding 3,3,4,4,5,5,6,6,7,7,8,8,9,9,10,10,10-heptadecafluorodecyl 2-hydroxy-5-(2-(4-methoxy benzoyl oxy)acetyl)benzoate (**4.28b**) in 2 h (70 %). mp=98-100 °C. ¹H NMR (400 MHz (CD)₃CO): δ 2.91 (m, 2H), 3.90 (s, 3H), 4.81 (m, 2H), 5.62 (s, 2H), 7.05 (d, 2H), 7.15 (d, 1H), 8.05 (d, 2H), 8.23 (d, 1H), 8.59(s, 1H) ¹³C NMR (100 MHz, (CD)₃CO): δ (ppm) 55.0, 65.9,112.3, 113.8, 117.9, 121.9, 126.5, 130.7, 131.5, 131.6, 135.3, 163.8, 165.0, 165.2, 168.7, 190.2. ¹⁹F NMR (400 MHz CD₃COCD₃): δ (ppm) -126.0, -123.3, -122.6, -121.8, -121.5, -113.4, -113.3, 133.3, -80.7. IR (KBr): 3433, 1718, 1697, 1683, 1604, 1589, 1307, 1286, 1251, 1211, 1095, 981, 802,700. UV (10% water/methanol) λ_{max} = 266 (ε = 4040), λ_{max} = 308 (ε = 970). HRMS calculated for M+ H, C₂₇H₁₇O₇F₁₇Na = 799.0601, observed = 799.0579.

2-(3-((3,3,4,4,5,5,6,6,7,7,8,8,9,9,10,10,10-heptadecafluorodecyloxy)carbonyl)-4-hydroxyphenyl)-2-oxoethyl-3',6'-dihydroxy-3-oxo-3H-spiro[isobenzofuran-1,9'-xanthene]-5-carboxylate (perfluoro pHP 5-carboxyfluorescein, 4.28c) The same procedure as used for **4.28a** was followed yielding 3,3,4,4,5,5,6,6,7,7,8,8,9,9,10,10,10-heptadecafluorodecyl 2-hydroxy-5-(2-(4-methoxy benzoyloxy)acetyl)benzoate (**4.8c**) in 2 h (30 %). mp=229-230 °C. ¹H NMR (400 MHz (CD)₂CO): δ 2.91 (m, 4H), 4.81 (m, 2H), 5.81 (s, 2H), 6.66 (m, 2H), 6.75 (m, 4H), 7.17 (d, 1H), 7.48 (d, 1H), 8.30(m, 1H),8.44(d, 1H), 4.59(m, 2h) ¹³C NMR (100 MHz, (CD)₂CO): δ (ppm) 35.3, 57.9, 66.9, 83.3, 102.5, 109.9, 112.6, 112.4, 118.2, 124.8, 125.9, 126.3, 127.7, 129.4, 130.9, 131.7, 135.4, 136.0, 152.4, 157.3, 159.8, 162.0, 164.3, 165.4, 167.6, 168.9, 189.6. ¹⁹F NMR (400 MHz CD₃COCD₃): δ (ppm) -126.0, -123.3, -122.6, -121.8, -121.5, -113.4, -113.3, 133.3, -80.7. IR (KBr): 3413, 3390, 1735, 1679, 1589, 1242, 1172, 1116, 891, 850, 796, UV (10% water/methanol) λ_{max} = 269 (ε = 18596), λ_{max} = 310 (ε = 8200) λ_{max} = 459 (ε = 143000),

$\lambda_{\text{max}} = 487$ ($\epsilon = 14500$). HRMS calculated for $M^+ H$, $C_{40}H_{22}O_{11}F_{17} = 1001.0891$, observed = 1001.0892.

Photolysis studies

Photolysis studies of pHP 5-carboxyfluorescein (4.19): 1H NMR experiments: 5 mg of pHP 5-carboxyfluorescein was dissolved in 1.5 ml of 20% D_2O/CD_3CN and photolyzed in a Pyrex NMR tube using a Rayonet photoreactor equipped with two 3000 Å bulbs and a merry-go-round apparatus. The reaction was followed using 1H NMR every 10 min until the reaction was complete.

Photolysis in EtOAc/buffer (pH 7.5) biphasic media: pHP 5-carboxyfluorescein (7 mg) was dissolved in 2 ml of EtOAc and 2 ml of buffer solution was added to it. Photolysis was performed in this biphasic medium in a 5 ml quartz tube and both phases were subjected to UPLC and fluorescence analysis every 30 min. UPLC samples were prepared by removing 100 μ l of sample and diluting up to 1.00 ml with water. Caffeine and biphenyl was added as standards for the aqueous and organic layers respectively. Fluorescence samples were prepared by diluting 100 μ l of sample up to 10.00 ml with water (Scheme 2).

Photolysis studies of perfluoro pHP derivatives

1H NMR experiments and experiments in biphasic media were performed using the same protocol as used for pHP 5-carboxyfluorescein (Figures 4-7 and 4-8 *Results* section)

Photolysis studies for exploring the fluororous separation techniques: In a typical experiment compounds **4.28a-4.28c** were dissolved in 5 ml of 12% H_2O/CH_3CN and photolyzed for 2 h

which resulted in complete conversion. The resulting mixture was separated using F-SPE cartridges or by liquid-liquid extraction

F-SPE: after solvent was evaporated from the photolyzed solution the mixture was dissolved in 0.5 ml DMF and loaded in to the F-SPE cartridge under vacuum. The cartridge was then flushed with 20% H₂O /MeOH 8 ml × 3 (the fluorophobic solvent) to separate the leaving group from the fluorous products. Next the F-SPE cartridge was flushed with 8 ml × 3 MeOH (the fluorophilic solvent) to separate the photoproducts containing the fluorous tag. Each layer was analyzed by UPLC and fluorescence spectrum recorded. Samples for UPLC and fluorescence studies were prepared as described under photolysis studies for pHP 5-carboxyfluorescein. The fluorescence spectra for both fractions after separation for perfluoro pHP 5-carboxyfluorescein (**4.28c**) are illustrated in Figure 4-9 in *Results* section The cartridge was washed with 8 ml of acetone and air dried before reuse.

Liquid-Liquid Extraction: Flowing photolysis, the solvent was removed and 5 ml of methyl nonafluorobutyl ether was added and the solution was extracted 3 times with water (5 ml). Each layer was analyzed by UPLC and its fluorescence spectra recorded. Fluorescence spectra for both layers after separation for **4.28c** are shown in Figure 4-10 *Results* section. Samples for UPLC and fluorescence spectra were prepared as described under photolysis studies for pHP 5-carboxyfluorescein

References

- ¹ Pelliccioli, A. P.; Wirz, *Photochem. Photobiol. Sci.* **2002**, *1*, 441-458.
- ² Bochet, C. G.; *J. Chem. Soc. PerkinTrans.* **2002**, *1*, 125-142.
- ³ Adams, S. R.; Tsein, R. Y.; *Annu. Rev. Physiol.* **1993**, *55*, 755-84.
- ⁴ Givens, R. S.; Yousef, A. L. In *Dynamic Studies in Biology* Goeldner, M.; Givens, R. S. Eds.; Wiley-Vch, Weinheim, 2005; 55-75
- ⁵ Vogt, M. Ph.D. Thesis, Rheinisch-Westfälischen Technischen Hochschule, Aachen, Germany, 1991.
- ⁶ Zhu, D. W. *Synthesis* **1993**, 953-954.
- ⁷(a) Horvath, I. T.; Rabai, J. *Science* **1994**, *266*, 72-75. (b) Horvath, I. T.; Rabai, J. Fluorous Multiphase Systems. US Patent 5,463,082, Oct 1995.
- ⁸ Gladysz, J. A.; Curran, D. P. *Tetrahedron* **2002**, *58*, 3823-3825.
- ⁹ Ubeda, M. A.; Dembinski, R. *J. Chem. Educ.* **2006**, *83*, 84-92.
- ¹⁰ Barthel-Rosa, L. P.; Gladysz, J. A. *Coord. Chem. Rev.* **1999**, *190*, 587-605.
- ¹¹ Zhang, W. *Chem. Rev.* **2004**, *104*, 2531-2556.
- ¹² *Handbook of Fluorous Chemistry*; Gladysz, J. A., Curran, D.P., Horváth, I. T., Eds.; Wiley-VCH: Weinheim, Germany, 2004; pp 1-595.
- ¹³ Atkins, P.; Jones, L. *Chemical Principles: The Quest for Insight*; 4; Macmillan: New York; 2007, 309-356.
- ¹⁴ Fluorous Technologies, Inc. Home Page. <http://fluorous.com/fspe.php> (accessed Jul 1, 2009)
- ¹⁵ Pardo, J.; Cobas, A.; Guitian, E.; Castedo, L. *Org. Lett.* **2001**, *3*, 3711-3714.
- ¹⁶ Fukuyama, T.; Arial, M.; Matsubara, H.; Ryu, I. *J. Org. Chem.* **2004**, *69*, 8105-8107.
- ¹⁷ Yu, S. M.; Curran, D. P.; Nagashima, T. *Org. Lett.* **2005**, *7*, 3677-3680.
- ¹⁸ Crich, D.; Hao, X.; Lucas, M. *Tetrahedron* **1999**, *55*, 14261-14268
- ¹⁹ Curran, D. P.; Hadida, S.; He, M. *J. Org. Chem.* **1997**, *62*, 6714- 6715.
- ²⁰ Park, G.; Ko, K.; Zakharova, A.; Pohl, N. L. *J. Fluorine Chem.* **2008**, *129*, 978-982.
- ²¹ Jiao, H.; Le Stang, S.; Soos, T.; Meier, R.; Kowski, K.; Rademacher, P.; Jafarpour, L.; Hamard, J. B.; Nolan, S. P.; Gladysz, J. A. *J. Am. Chem. Soc.* **2002**, *124*, 1516-1523
- ²² Shen, M.; Cai, C.; Yi, W. *J. Heterocycl. Chem.* **2009**, *46*, 796-799.
- ²³ Horvath, T. *Accounts Chem. Res.* **1998**, *31*, 641-650
- ²⁴ Dobbs, A. P.; Kimberly, M. R. *J. Fluorine Chem.* **2002**, *118*, 3-17.
- ²⁵ Frohning, C. D.; Kohlpainther, C. W. In *Applied Homogeneous Catalysis with Organometallic Compounds* Cornils, B.; Herrmann, W. A., Eds.; Weinheim, **1996**, Vol 1, pp. 27-104.
- ²⁶ Mathivet, T.; Monflier, E.; Castanet, Y.; Mortreux, A.; Couturier, J. L. *Tetrahedron Lett.* **1998**, *39*, 9411-9414
- ²⁷ Mathivet, T.; Monflier, E.; Castanet, Y.; Mortreux, A.; Couturier, J. L. *Tetrahedron Lett.* **1999**, *40*, 3885-3888.
- ²⁸ Mathivet, T.; Monflier, E.; Castanet, Y.; Mortreux, A.; Couturier, J. L. *Tetrahedron* **2002**, *58*, 3877-3888.
- ²⁹ Rutherford, D.; Juliette, J.; Horvath, I. T.; Gladysz, J. A. *Catalysis Today*, **1998**, *42*, 381-388
- ³⁰ Betzemeier, B.; Knochel, P. *Angew. Chem.* **1997**, *109*, 2736-2738.
- ³¹ Moineau, J.; Pozzi, G.; Quici, S.; Sinou, D. *Tetrahedron Lett.* **1999**, *40*, 7683-7686.
- ³² Schneider, S.; Bannwarth, W. *Angew. Chem.* **2000**, *112*, 4293-4295.
- ³³ Schneider, S.; Bannwarth, W. *Hev. Chim. Acta.* **2002**, *112*, 4007-4014
- ³⁴ Market, C.; Bannwarth, W. *Hev. Chim. Acta.* **2002**, *85*, 1877-1882
- ³⁵ (a)Wende, M.; Gladysz, J. A. *J. Am. Chem. Soc.* **2003**, *125*, 5861-5872. (b) Wende, M.; Meier, R.; Gladysz, J. A. *J. Am. Chem. Soc.* **2001**, *123*, 11490-11491.
- ³⁶ Dandapani, S. *QSAR Comb. Sci.* **2006**, *25*, 681-688.
- ³⁷ a) Mitsunobu, O. *Synthesis* **1981**, 1- 28. (b) Hughes, D. L. *Org. React.* **1993**, *42*, 335-656. (c) Wisniewski, K.; Koldziejczyk, A. S.; Falkiewicz, B. *J. Pept. Sci.* **1998**, *4*, 1-14. (d) Hughes, D. L. *Org. Prep. Proced. Int.* **1996**,

28, 127-164

- ³⁸ Dandapani, S.; Curran, D. P. *J. Org. Chem.* **2004**, *69*, 8751-8757
- ³⁹ Markowicz, M. W.; Dembinski, R. *Synthesis* **2004**, 80-86.
- ⁴⁰ Palomo, C.; Aizpurua, J. M.; Loinaz, I.; Fernandez-Berridi, M. J.; Irusta, L. *Org. Lett.* **2001**, *3*, 2361-2364.
- ⁴¹ a) Curran, D. P.; Hadida, S. *J. Am. Chem. Soc.* **1996**, *118*, 2531-2532. (b) Curran, D. P.; Hadida, S.; Kim, S.; Luo, Z. *J. Am. Chem. Soc.* **1999**, *121*, 6607-6615.
- ⁴² Curran, D. P.; Hadida, S.; Kim, S. Y. *Tetrahedron* **1999**, *55*, 8997-9006.
- ⁴³ a) Bucher, B.; Curran, D. P. *Tetrahedron Lett.* **2000**, *41*, 9617-9621. b) Otera, J. *Acc. Chem. Res.* **2004**, *37*, 288-296.
- ⁴⁴ a) Curran, D. P.; Luo, Z. *Degegenkolb, P. Bioorg. Med. Chem. Lett.* **1998**, *8*, 2403-2408 (b) Ryu, I.; Kreimerman, S.; Niguma, T.; Minakata, S.; Komatsu, M.; Luo, Z.; Curran, D. P. *Tetrahedron Lett.* **2001**, *42*, 947-950.
- ⁴⁵ a) Curran, D. P.; Hoshino, M. *J. Org. Chem.* **1996**, *61*, 6480-6481. (b) Hoshino, M.; Degenkolb, M.; Curran, D. P. *J. Org. Chem.* **1997**, *62*, 8341. (c) Osswald, T.; Schneider, S.; Wang, S.; Bannwarth, W. *Tetrahedron Lett.* **2001**, *42*, 2965-2967
- ⁴⁶ Markowicz, M. W.; Dembinski, R. *Org. Lett.* **2002**, *4*, 3785-3787.
- ⁴⁷ Curran, D. P.; Ferritto, R.; Hua, Y. *Tetrahedron Lett.* **1998**, *39*, 4937-4940.
- ⁴⁸ Rover, S.; Wipe, P. *Tetrahedron Lett.* **1999**, *39*, 5667-5670.
- ⁴⁹ Wipe, P.; Reeves, J. *Tetrahedron Lett.* **1999**, *39*, 5139-5142.
- ⁵⁰ Schwinn, D.; Bannwarth, W. *Helv. Chim. Acta.* **2002**, *85*, 255-264
- ⁵¹ Prado, J.; Cobse, A.; Guitian, E.; Castedo, L. *Org. Lett.* **2001**, *3*, 3711-3714.
- ⁵² Mizuno, M.; Goto, K.; Miura, D.; Hosaka, T.; Inazu, T. *Chem. Commun.* **2003**, 972-973.
- ⁵³ Booth, J. R.; Hodges, J. *J. Am. Chem. Soc.* **1997**, *119*, 4882-4886.
- ⁵⁴ a) Curran, D. P. *Org. Chem.* **1996**, *9*, 75-80. (b) Curran, D. P.; Hoshino, M. *J. Org. Chem.* **1996**, *61*, 6480-6486.
- ⁵⁵ Zhang, W.; Curran, D. P.; Chen, C. H. *Tetrahedron* **2002**, *58*, 3871-3875
- ⁵⁶ Zhang, W.; Chen, C. H.; Nagashima, T. *Tetrahedron Lett.* **2002**, *44*, 2065-2068.
- ⁵⁷ a) Lindsley, C. W.; Zhao, Z.; Leister, W. H. *Tetrahedron Lett.* **2002**, *43*, 4225-4228. (b) Lindsley, C. W.; Zhao, Z.; Leister, W. H.; Strauss, K. A. *Tetrahedron Lett.* **2002**, *43*, 6319-6323.
- ⁵⁸ Nakamura, H.; Linclau, B.; Curran, D. P. *J. Am. Chem. Soc.* **2001**, *123*, 10119-10120.
- ⁵⁹ Kojima, M.; Nakamura, Y.; Nakamura, A.; Takeuchi, S. *Tetrahedron Lett.* **2009**, *50*, 939-942.
- ⁶⁰ Werner, S.; Nielsen, S. D.; Wipf, P.; Turner, D. M.; Chamners, P. G.; Geib, S. J.; Curran, D. P.; Zhang, W. *J. Comb. Chem.* **2009**, *11*, 452-459.
- ⁶¹ Filippov, D. V.; Zoelen, D. J.; Oldfield, S. P.; Overkleeft, H. S.; Grijthout, J. W.; van der Marel, G. A.; van Boom, J. H. *Tetrahedron Lett.* **2002**, *43*, 7809-7812.
- ⁶² Seeberger, P. H. *Chem. Commun.* **2003**, 1115-1121.
- ⁶³ Pearson, W. H.; Berry, D. A.; Stoy, P.; Jung, K. Y.; Sercel, A. D. *J. Org. Chem.* **2005**, *70*, 7114-7122.
- ⁶⁴ Brittain, S. M.; Ficarro, S. B.; Brock, A.; Peters, E. C. *Nat. Biotechnol.* **2005**, *23*, 463-468.
- ⁶⁵ Ko, K. S.; Jaipuri, F. A.; Pohl, N. *J. Am. Chem. Soc.* **2005**, *127*, 13162-13163.
- ⁶⁶ Critchley, K.; Jeyadevan, J. P.; Fukushima, H.; Ishida, M.; Shimoda, T.; Bushby, R. J.; Evans, S. D. *Langmuir* **2005**, *21*, 4554-4561.
- ⁶⁷ Laibinis, P. E.; Whitesides, G. M. *J. Am. Chem. Soc.* **1992**, *114*, 1990-1995.
- ⁶⁸ Fukushima, H.; Seki, S.; Nishikawa, T.; Tamada, K.; Abe, K.; Colorado, R. J.; Graupe, M.; Shmakova, O. E.; Lee, T. R. *J. Phys. Chem. B* **2000**, *104*, 7417-7424.
- ⁶⁹ Sharong, Y. University of Kansas, KS. Unpublished data, 2007
- ⁷⁰ Mitchison, T. J.; Sawin, K. E.; Theriot, J. A.; Gee, K.; Mallavarapu, A. Caged Fluorescent Probes In *Methods in Enzymology*, Marriott, G. Eds.; Academic Press: New York, 1998; Vol. 291, 63-77.

-
- ⁷¹ Stensrud, F. K.; Heger, D.; Sebej, P.; Wirz, J.; Givens, R. S. *Photochem. Photobiol. Sci.* **2008**, *7*, 614-624.
- ⁷² Givens, R. S.; Weber, J. F. W.; Conrad, P. G., II; Orose, G.; Donahaue, S. L.; Thayer, S. A. *J. Am. Chem. Soc.* **2000**, *122*, 2687-2697 and references therein
- ⁷³ Givens, R. S.; Heger, D.; Hellrung, B.; Kamdzhilov, Y.; Mac, M.; Conrad, p. G., II; Cope, E.; Lee, J. I.; Mata-Segreda, J. F.; Schowen, R. L.; Wirz, J. *J. Am. Chem. Soc.* **2008**, *130*, 3307-3309.
- ⁷⁴ Zhang, W.; Curran, D.P. *Tetrahedron.* **2006**, *62*, 11837-11685.
- ⁷⁵ a) Stensrud, F. K.; Heger, D.; Sebej, P.; Wirz, J.; Givens, R. S. *Photochem. Photobiol. Sci.* **2008**, *7*, 614-624. (b) Stensrud, K.; Kandler, K.; Noh, J.; Wirz, J.; Heger, D.; Givens, R.S. *J. Org. Chem.* **2009**, *74*, 5219-5227
- ⁷⁶ March, J. *Advanced Organic Chemistry*, 4th ed.; John Wiley and Sons, New York, 2004; pp 395-396.
- ⁷⁷ Ma, C.; Kwok, W. M.; Chan, W. S.; Du, Y.; Kan, J. T. W.; Toy, P. K.; Phillips, D. L. *J. Am. Chem. Soc.* **2006**, *128*, 2558-2570
- ⁷⁸ Falvey, D> E.; Banerjee, A. *J. Am. Chem. Soc.* **1998**, *120*, 2965-2966.
- ⁷⁹ Yousef, A. Dissertation 2005, Chemistry Department, University of Kansas.
- ⁸⁰ Shelkov, R.; Nahamang, M.; Melman, A. *Org. Biomol. Chem.* **2004**, *2*, 397-401
- ⁸¹ Vasquez-Martines, Y.; Ohri, R.V.; Kenyon, V.; Holman, T.; Sepulveda-Boza, S. *Bioorg. Med. Chem.* **2007**, *23*, 7408-7425.
- ⁸² Hiyama, T.; Fujita, M. *J. Org. Chem.* **1988**, *53*, 5405-5414